



HAL
open science

Evolution of a novel left-right asymmetry in *Drosophila* *pachea*

Bénédicte Lefèvre

► **To cite this version:**

Bénédicte Lefèvre. Evolution of a novel left-right asymmetry in *Drosophila pachea*. Agricultural sciences. Université Paris Cité, 2021. English. NNT : 2021UNIP7025 . tel-03519510

HAL Id: tel-03519510

<https://theses.hal.science/tel-03519510>

Submitted on 10 Jan 2022

HAL is a multi-disciplinary open access archive for the deposit and dissemination of scientific research documents, whether they are published or not. The documents may come from teaching and research institutions in France or abroad, or from public or private research centers.

L'archive ouverte pluridisciplinaire **HAL**, est destinée au dépôt et à la diffusion de documents scientifiques de niveau recherche, publiés ou non, émanant des établissements d'enseignement et de recherche français ou étrangers, des laboratoires publics ou privés.

Evolution of a novel left-right asymmetry in *Drosophila pachea*

Par Bénédicte Lefèvre



Thèse de doctorat de Génétique

dirigée par Alexis Lalouette et co-encadrée par Michael Lang

Présentée et soutenue publiquement à Paris le 12 janvier 2021

devant un jury composé de :

Sylvie Rétaux, directrice de recherche, CNRS, présidente du jury

Benjamin Prud'homme, directeur de recherche, CNRS, rapporteur

Magali Suzanne, directrice de recherche, CNRS, rapporteur

Alexis Lalouette, maître de conférence, Université de Paris, directeur de thèse

Michael Lang, chercheur, CNRS, membre invité, co-encadrant

Except where otherwise noted, this work is licensed under
<https://creativecommons.org/licenses/by-nc-nd/3.0/fr/>



Titre : Evolution d'une nouvelle asymétrie latérale chez *Drosophila pachea*

Résumé :

La plupart des animaux possèdent divers organes latéralement asymétriques. Cependant, les processus génétiques et cellulaires sous-jacents qui conduisent à ces asymétries restent flous. Nous étudions le rôle et le développement d'une asymétrie gauche-droite en utilisant *Drosophila pachea* comme nouvelle espèce modèle. Chez cette espèce, les mâles ont une paire de lobes génitaux asymétriques, le lobe gauche étant 1,5 fois plus long que le droit.

Les lobes stabilisent le complexe génital formé entre la femelle et le mâle pendant la copulation. Nous avons étudié leur rôle avant la copulation et avons découvert que la longueur du lobe gauche, mais pas nécessairement celle du lobe droit, affecte les chances du mâle de copuler. La morphologie de ce caractère sexuel primaire peut donc affecter le succès reproductif, via la transmission des signaux de cour ou en facilitant l'établissement des contacts génitaux entre le mâle et la femelle au début de la copulation.

La caractérisation du développement des lobes a révélé que les lobes croissent entre 24 h et 36 h après la formation du puparium (APF) pour atteindre environ 410 et 220 cellules dans les lobes gauche et droit respectivement. Cependant, aucune différence de taux mitotiqueLa plupart des animaux possèdent divers organes latéralement asymétriques. Cependant, les processus génétiques et cellulaires sous-jacents qui conduisent à ces asymétries restent flous. Nous étudions le rôle et le développement d'une asymétrie gauche-droite en utilisant *Drosophila pachea* comme nouvelle espèce modèle. Chez cette espèce, les mâles ont une paire de lobes génitaux asymétriques, le lobe gauche étant 1,5 fois plus long que le droit n'a été détectée entre le lobe gauche et le lobe droit au cours du développement par marquage immuno-fluorescent, indiquant un éventuel recrutement de cellules à partir des tissus voisins. La croissance des lobesLa plupart des animaux possèdent divers organes latéralement asymétriques. Cependant, les processus génétiques et cellulaires sous-jacents qui conduisent à ces asymétries restent flous. Nous étudions le rôle et le développement d'une asymétrie gauche-droite en utilisant *Drosophila pachea* comme nouvelle espèce modèle. Chez cette espèce, les mâles ont une paire de lobes génitaux asymétriques, le lobe gauche étant 1,5 fois plus long que le droit. En comparant les durées du développement pupal chez diverses espèces de drosophiles, nous avons découvert que les premières 0 à 55 h APF sont assez bien conservées entre espèces. Ainsi, l'établissement de l'asymétrie génitale chez *D. pachea* n'est probablement pas affectée par un changement global du déroulement du développement pupal par rapport aux autres espèces.

Nous avons mis au point une souche transgénique de *D. pachea* exprimant un marqueur membranaire fluorescent, une DE-cadhérine tronquée et fusionnée à une protéine fluorescente verte (Green Fluorescent Protein, GFP), pour marquer chaque cellule et suivre la dynamique du développement asymétrique des lobes. La microscopie *in vivo* a révélé que le lobe gauche interagit physiquement avec les tissus environnants à la périphérie des pièces génitales. La croissance asymétrique dépend donc vraisemblablement de processus intrinsèques aux pièces génitales, mais aussi d'interactions tissu-tissu particulières dans le contexte de la rotation des genitalia. Ainsi, un processus développemental asymétrique conservé, la rotation des pièces génitales, aurait pu être co-optée au cours de l'évolution pour dériver une nouvelle structure asymétrique.

En conclusion, ma thèse de doctorat traite du pourquoi, par la fonction, et du comment, par le développement, de l'évolution de cette nouvelle asymétrie latérale chez *D. pachea*. Par la combinaison de diverses approches biologiques, mon projet a permis d'étudier l'asymétrie droite-gauche des lobes génitaux de *D. pachea* à différentes échelles biologiques : chez les individus adultes, au niveau tissulaire via l'analyse de la dynamique du développement des primordia génitaux, mais aussi au niveau cellulaire avec l'analyse de la croissance cellulaire à l'intérieur des lobes en formation. De plus, nous avons établi *D. pachea* comme un nouveau modèle en biologie du développement et généré un nouvel outil bio-technologique pour l'imagerie *in vivo* et l'analyse fonctionnelle. Cette avancée ouvre la porte à un large panel de recherches futures.

Mots clefs :

Evo-Devo ; asymétrie gauche-droite ; morphogenèse ; cour ; *Drosophila pachea* ; genitalia mâle ; système génital.

Title: Evolution of a novel left-right asymmetry in *Drosophila pachea*

Abstract:

Most animals have various left-right asymmetric organs. However, the underlying genetic and cellular changes leading to these asymmetries during evolution remain unclear. We study the role and the development of morphological left-right asymmetry using *Drosophila pachea* as a new model system. Males of this species have a pair of asymmetric genital lobes with the left lobe being 1.5 times longer compared to the right lobe.

It was previously found that the lobes stabilize the genital complex of the female and the male during copulation. In my thesis, I investigated their role during pre-copulatory events and found that left lobe length, but not necessarily right lobe length, affects the male chance to copulate. The morphology of this primary sexual trait may thus affect reproductive success by mediating courtship signals or by facilitating the establishment of genital contacts at the onset of copulation.

The characterization of lobe development revealed that lobes grow between 24 h and 36 h after puparium formation (APF) to about 410 and 220 cells at the left and right lobe, respectively. However, no differences in mitotic rates were detected at various time points of development by immuno-fluorescence staining, indicating a possible recruitment of cells from the neighboring tissues. Lobe growth occurs while male genitalia rotate clockwise during pupal development between 25 h and 40 h APF. In a *D. pachea* mutant with variable left lobe length, this rotation occurs 6 h earlier compared to wild-type stocks, indicating that the correct temporal coupling of genitalia rotation and lobe growth are required for proper asymmetry establishment. By comparing the pupal development timing of various other *Drosophila* species, we found out that the relative timing of the first developmental period from 0 to 55 h after puparium formation is well conserved across species. Since this period encompasses lobe development, the genital asymmetry establishment in *D. pachea* is probably not affected through a global shift of developmental timing in this species.

We developed transgenic *D. pachea* expressing a fluorescent membrane marker, a truncated DE-cadherin fused to a GFP, to monitor *in vivo* the dynamics of the development of asymmetric lobes. Live-imaging of developing genitalia revealed that the left lobe interacts physically with the surrounding tissue. Asymmetric growth thus likely depends on intrinsic asymmetric cellular growth processes inside the genitalia, but also on a particular tissue-tissue interaction in the context of the rotating tissue. This might indicate that a conserved

asymmetric developmental process, the genitalia rotation, may have been co-opted during evolution to derive a novel asymmetric structure.

Altogether, my PhD thesis is related to how (developmental processes), and why (behavioral function), this novel left-right asymmetry evolved in *D. pachea*, and to how asymmetric tissue size is determined during development. My project aims to combine diverse approaches to work on different biological scales, including adult individuals, dynamics of the complex genital primordia during development, but also cellular growth dynamics within the forming lobes. In addition, we established *D. pachea* as a new model in developmental biology and generate a new tool for live-imaging and functional analysis, and open a door for a large panel of future research.

Keywords:

Evo-Devo ; left-right asymmetry ; morphogenesis ; courtship ; *Drosophila pachea* ; male genitalia ; genital system.

Am not I
A fly like thee?
Or art not thou
A man like me?

William Blake, *The Fly*,
Songs of Experience, 1794

Résumé

Le règne animal présente une incroyable diversité en termes de morphologies (Carroll 2005). Comment les métazoaires se développent-ils à partir d'un embryon d'une cellule en un organisme constitué d'une multitude de cellules différenciées et de tissus aux formes et aux fonctions complexes ? Leur développement résulte de l'action coordonnée d'un nombre limité de gènes, et les variations de formes entre espèces résultent de variations dans les programmes développementaux à l'origine de ces formes (Carroll 2005). Aussi, parmi la variété de formes qui apparaissent dans la nature, celles des organes génitaux sont particulièrement importantes car elles sont impliquées dans la reproduction (Schilthuizen 2015). En particulier, chez les espèces à fécondation interne, le transfert des spermatozoïdes du mâle à la femelle se fait généralement par l'établissement d'un complexe entre les pièces génitales mâles et femelles. Une modification de leur forme peut conduire à l'altération de ce complexe, et donc, à l'altération du succès de la copulation (Huber, Sinclair, and Schmitt 2007, Huber 2010, Schilthuizen 2013, Schilthuizen 2015). Ainsi, l'évolution de nouvelles formes d'organes génitaux est à l'intersection de ces deux questions : comment le développement change-t-il au cours de l'évolution pour dériver de nouvelles structures et en quoi ces nouvelles structures affectent-elles le succès reproducteur ?

Des caractères propres aux individus d'une espèce, les pièces génitales sont ceux qui évoluent le plus rapidement et présentent donc le plus de variabilité morphologique, y compris entre espèces étroitement apparentées (Eberhard 1985, Eberhard 2010a, Schilthuizen 2015). Au sein de certains groupes d'espèces, celles-ci ne semblent d'ailleurs différer que par la morphologie de leurs pièces génitales (Perkin 2007, Schilthuizen 2015). Aussi, cette diversité de structures génitales a été utilisée par les taxonomistes pour différencier les espèces, conduisant à l'accumulation d'une quantité importante de données sur la morphologie et l'évolution des structures génitales (Eberhard 2010a, Schilthuizen 2015). Traditionnellement, les caractères sexuels sont classés comme primaires ou secondaires, respectivement selon qu'ils soient directement utilisés dans le transfert de gamètes ou qu'ils diffèrent simplement entre femelles et mâles et soient liés à la reproduction (Darwin 1859). Ainsi, il est accepté que la sélection sexuelle des caractères sexuels primaires s'opère généralement pendant ou après la copulation alors que celle des caractères sexuels secondaires s'opère essentiellement pendant la cour (Eberhard 1985, Eberhard 1994).

Femelles et mâles adoptent généralement différentes stratégies reproductives (Bateman 1948, Leonard and Córdoba-Aguilar 2010, Schilthuizen 2015). Il a été proposé que cette différence repose sur la différence de descendance potentielle entre mâles et femelles, liée à

la différence de production de gamètes (Bateman 1948). Les mâles produisant généralement beaucoup de gamètes de petite taille, pourraient générer plus de descendants que les femelles, qui produisent un nombre beaucoup plus limité de gamètes de grande taille (Bateman 1948). Plusieurs mécanismes de sélection sexuelle ont été proposés pour expliquer l'évolution rapide des organes génitaux, tels que la compétition intra-sexuelle ou le choix pré-copulatoire (Bateman 1948). La compétition intra-sexuelle a été traditionnellement pensée comme une compétition entre mâles pour une femelle (Bateman 1948), bien que la compétition entre femelles pour un mâle existe également (Leonard and Córdoba-Aguilar 2010). De même, le choix copulatoire a été traditionnellement pensé comme un choix du mâle par la femelle (Bateman 1948), de même, l'inverse existe également (Bonduriansky 2001 Edward and Chapman 2012). De manière générale, la sélection sexuelle implique un conflit sexuel dès que les stratégies reproductives diffèrent entre femelles et mâles (Kokko and Jennions 2014).

Parmi la variété de formes présentes dans la nature, les asymétries gauche-droite sont extrêmement répandues (Levin, Klar, and Ramsdell 2016). Chez les bilatériens, la morphologie externe apparaît généralement symétrique par rapport au plan défini par les axes antéro-postérieur et dorso-ventral. Ainsi, les côtés droit et gauche de l'organisme constituent globalement une image en miroir l'un de l'autre. Cependant, la plupart des animaux possèdent des organes asymétriques, aussi bien dans leur positionnement par rapport à l'axe médian, tels le cœur ou l'estomac situés du côté gauche, ou le foie, du côté droit, chez l'humain, ou dans leur forme, tels le cœur dont les cavités sont asymétriques, ou les poumons, constitués de deux lobes du côté droit et de trois lobes du côté gauche (Lebreton et al. 2018, Blum and Ott 2018, Levin, Klar, and Ramsdell 2016, Palmer 2016, Coutelis et al. 2014, Schilthuisen and Gravendeel 2012, Spéder and Noselli 2007). L'étude des processus à l'origine du développement de structures asymétriques a révélé l'existence d'une grande variété de mécanismes entre les espèces. Parmi eux, MyoID semble être un facteur clé, à la fois chez les vertébrés et les invertébrés, via son interaction avec les jonctions adhérentes, le cytosquelette d'actine, la voie de polarité cellulaire planaire (PCP) et la mort cellulaire régulée par la voie Jun kinase (Chougule et al. 2020, Tingler et al. 2018, Juan et al. 2018, Yuan and Brueckner 2018, Lebreton et al. 2018, González-Morales et al. 2015, Petzoldt et al. 2012, Benitez et al. 2010, Suzanne et al. 2010). Concernant les pièces génitales, des asymétries gauche-droite ont évolué à plusieurs reprises, au sein de divers phyla, et en particulier chez les insectes (Huber, Sinclair, and Schmitt 2007, Huber 2010, Schilthuisen 2013, Schilthuisen 2015). Cependant, au sein des drosophiles, groupe qui compte plus de 1500 espèces (Bächli, Bernhard, and Godknecht 2020), des asymétries gauche-droite affectant les pièces génitales n'ont été détectées que chez les mâles dans seulement onze espèces différentes, dont trois du groupe nannoptera (Acurio

et al. 2019). Plusieurs mécanismes ont été proposé pour expliquer l'évolution de structures génitales asymétriques, dont la co-évolution antagoniste entre mâles et femelles ou l'évolution du fait d'un choix de la femelle pour des structures mâles asymétriques (Huber 2010).

Le groupe *nannoptera* compte quatre espèces de drosophiles cactophiles vivant dans le désert du Sonora (Mexique) et en Amérique centrale (Markow and O'Grady 2007, Lang et al. 2014) : *D. pachea* (Patterson and Wheeler 1942), *D. wassermani* (Pitnick and Heed 1994), *D. acanthoptera* et *D. nannoptera* (Wheeler 1949). Parmi ces espèces, les mâles *D. pachea* et *D. acanthoptera* présentent une asymétrie gauche-droite au niveau distal du phallus (Vilela, Bächli, et al. 1990, Acurio et al. 2019). De plus, les mâles *D. pachea* possèdent également une paire de lobes épandriaux asymétriques dont le gauche est 1,5 fois plus long que le droit (Pitnick and Heed 1994, Lang and Orgogozo 2012, Lang et al. 2014, Rhebergen et al. 2016, Acurio et al. 2019), et les mâles *D. wassermani*, une paire de plaques anales asymétrique dont la gauche est élargie par rapport à la droite (Pitnick and Heed 1994, Lang and Orgogozo 2012 Acurio et al. 2019). Il est intéressant de noter que chez ces deux espèces, l'asymétrie est due à un élargissement de la structure du côté gauche par rapport au côté droit. En plus de ces asymétries morphologiques, *D. pachea* et *D. nannoptera* adoptent des positions copulatoires asymétriques, le mâle étant décalé vers la droite par rapport à l'axe médian de la femelle (Lang and Orgogozo 2012, Rhebergen et al. 2016, Acurio et al. 2019). Chez *D. pachea*, il a été montré que l'asymétrie des lobes permet de stabiliser le complexe des pièces génitales mâles et femelle pendant la copulation, ainsi que leur position de copulation asymétrique (Rhebergen et al. 2016). Aussi, les espèces du groupe *nannoptera* produisent des spermatozoïdes particulièrement longs. Si *D. acanthoptera* et *D. wassermani* produisent respectivement des spermatozoïdes de 5,83 mm et 4,52 mm de long, ceux produits par *D. nannoptera* et *D. pachea* peuvent être qualifiés de géants avec des longueurs de 15,74 mm et 16,53 mm respectivement (Pitnick and Heed 1994). Il a été proposé que les positions copulatoires asymétriques aient évolué chez *D. nannoptera* et *D. pachea* permettant potentiellement une optimisation de transfert de gamètes du mâle vers la femelle pendant la copulation (Acurio et al. 2019). Les lobes génitaux asymétriques des mâles *D. pachea* ont donc pu être sélectionnés au cours de l'évolution du fait de leur rôle pendant la copulation. Cependant, d'autres mécanismes de sélection ne sont pas à exclure, notamment, si les lobes génitaux des mâles affectent les événements pré-copulatoire.

Chez les drosophiles, la plupart des structures adultes se développent au stade pupal, pendant la métamorphose, à partir de structures appelées disques imaginaux. Les pièces génitales mâles et femelles se développent à partir du disque génital, qui est le seul disque imaginal n'étant pas apparié et étant situé en position médiale (Estrada, Casares, and Sánchez-Herrero

2003). Cette structure contient trois primordia : celui dérivé du 8^{ème} segment abdominal donne les structures génitales femelles, celui dérivé du 9^{ème} segment abdominal, les structures génitales mâles, et celui dérivé du 10^{ème} segment abdominal, les plaques anales (Estrada, Casares, and Sánchez-Herrero 2003, Sánchez and Guerrero 2001). Chez les femelles, le 9^{ème} segment abdominal est réduit, alors que cette réduction affecte le 8^{ème} segment abdominal chez les mâles (Estrada, Casares, and Sánchez-Herrero 2003, Sánchez and Guerrero 2001). De plus, chez les mâles, un autre processus développemental asymétrique, la rotation des génitalia, a lieu de manière concomitante au développement des pièces génitales. Pendant ce processus conservé chez les mouches, les pièces génitales mâles effectuent une rotation de 360 ° dans le sens des aiguilles d’une montre (Spéder, Ádám, and Noselli 2006, Suzanne et al. 2010). Il a été montré que la direction de cette rotation est dirigée par la myosine MyoID (Spéder, Ádám, and Noselli 2006). Aussi, le 8^{ème} segment abdominal est impliqué dans le déroulement de cet événement, notamment du fait d’apoptoses et de mouvements cellulaires asymétriques nécessaires à la rotation du 9^{ème} segment abdominal (Suzanne et al. 2010, Sato et al. 2015)

Dans ce contexte, nous avons utilisé les lobes génitaux asymétriques de *D. pachea* comme modèle pour étudier le pourquoi, en termes de fonction, et le comment, en termes de développement, de l’évolution de cette structure asymétrique. Les objectifs de cette thèse étaient donc les suivants. Tout d’abord, concernant la fonction des lobes génitaux des mâles *D. pachea*, si celle-ci a été caractérisée pendant la copulation, ces structures peuvent aussi avoir évolué du fait d’autres fonctions pendant les événements pré-copulatoires. Nous avons testé si les lobes affectent le succès copulatoire des mâles via un choix des femelles. Deuxièmement, concernant le développement des lobes, nous avons dans un premier temps examiné la possibilité que leur développement soit affecté par un changement global dans le déroulement du développement pupal. Enfin, nous avons caractérisé la croissance des lobes dans le contexte de la rotation des pièces génitales. Pour ce faire, nous avons développé des *D. pachea* transgéniques exprimant un marqueur membranaire fluorescent, ce qui constitue un nouvel outil génétique dans cette espèce.

Si la forme sauvage des lobes génitaux des mâles *D. pachea* est asymétrique, le lobe gauche étant 1,5 fois plus long que le lobe droit, une forme dans laquelle les mâles présentent deux lobes symétriques courts a été identifiée au sein d’un des stocks de laboratoire (Lang and Orgogozo 2012). Les mâles présentant ces lobes génitaux courts ont été sélectionnés et croisés de manière à générer un stock, appelé stock de sélection, dans lequel les mâles présentent un lobe droit de longueur similaire à ceux des mâles sauvages, et un lobe gauche de longueur variable. Pour tester l’influence de l’asymétrie des lobes, déterminée par la longueur du lobe

gauche, sur les chances du mâle de copuler, nous avons mené des expériences d'accouplement compétitif au cours desquels une femelle était mise en présence de deux mâles différant par la longueur de leur lobe gauche. Nous avons ainsi mené 104 expériences au cours desquelles les deux mâles ont fait la cour à la femelle. La durée de la cour, des séquences de léchage (l'un des comportements stéréotypés de la cour chez les drosophiles, prépondérant chez les mâles *D. pachea*), et la longueur des lobes génitaux des mâles ont été mesurés. L'analyse a révélé que la longueur du lobe génital gauche du mâle et la vigueur de la cour, estimée à partir du comportement de léchage, affectent significativement le succès copulatoire, conférant un avantage au mâle. Pour tester la possibilité que la longueur du lobe soit associée à d'autres caractères pouvant affecter la cour et que nous n'aurions pas détecté, nous avons mené 53 expériences supplémentaires dans lesquelles les deux mâles présentaient un lobe gauche amputé à divers degrés par micro-chirurgie. Dans ces expériences, un effet plus faible, non-significatif, de la longueur du lobe gauche a été observé sur les chances du mâle d'engager une copulation. La morphologie de ce trait sexuel primaire peut donc affecter le succès de la reproduction pendant la cour. Les lobes génitaux asymétriques des mâles *D. pachea* ont ainsi pu être sélectionnés au cours de l'évolution de par leur rôle pendant la copulation, mais aussi de par leur action pendant la cour. Cependant, la manière dont la longueur du lobe gauche affecte la cour, éventuellement via une modulation du chant du mâle ou via l'émission de phéromones, ainsi que celle dont il est détecté par la femelle restent à caractériser. Par ailleurs, notre étude a révélé que la durée globale de la cour augmente lorsque les deux mâles font simultanément la cour à la femelle, par rapport à la situation où un seul des deux mâles montre ce genre de comportement. Cette différence pourrait refléter la compétition entre les deux mâles pour la femelle. De plus, un écart apparaît entre les périodes reproductives des mâles et des femelles, ce qui pourrait constituer un mécanisme de réduction de la consanguinité entre mâles et femelles d'une même fratrie. Cette étude a donné lieu à un article, en révision auprès de BMC Evolutionary Biology (Lefèvre et al. 2020).

Le deuxième objectif de ma thèse était de déterminer si le développement des lobe génitaux asymétriques des mâles *D. pachea* était dû à un changement global du déroulement du développement pupal par rapport à celui d'espèces drosophiles dont les mâles ont des genitalia symétriques. Pour cela, la caractérisation du déroulement du stage pupal a été réalisée chez *D. pachea*, mais aussi chez les espèces étroitement apparentées *D. nannoptera* et *D. acanthoptera* d'après la caractérisation du développement pupal établie chez l'espèce modèle *D. melanogaster* par Bainbridge and Bownes 1981. La comparaison du déroulement du développement pupal de *D. pachea*, *D. acanthoptera* et *D. nannoptera* avec celles d'autres

d'espèces drosophiles a révélé que la chronologie du début du développement pupal, de 0 h après formation du puparium (after puparium formation, APF) à 50 h APF est conservée entre les espèces (stades 1 à 7). La croissance des lobes de *D. pachea* se produit entre 24 h APF et 36 h APF, ce processus asymétrique ne se produit donc pas dans un contexte développemental global affecté par un changement majeur de chronologie par rapport aux espèces présentant des génitalia symétriques. De plus, la conservation de la chronologie du développement pupal des stades 1 à 7 (0 h APF à 55 h APF) pourrait indiquer l'existence de contraintes développementales au cours de cette période.

Aussi, *D. pachea* vit dans le désert de Sonora, dans des cavités formées sur les zones en décomposition du cactus Senita. Cet environnement présente d'importantes variations de température, pouvant aller jusqu'à 35 degrés d'amplitude (Gibbs, Perkins, and Markow 2003). L'effet de la température sur le déroulement du développement pupal a été testé en comparant celui-ci chez des mouches élevées à 25 °C ou 29 °C. La comparaison a révélé que la température n'affecte pas la durée globale du développement pupal chez *D. pachea*, contrairement à d'autres espèces pour lesquelles l'augmentation de la température entraîne une accélération du développement (David and Clavel 1966, Powsner 1935, James and Partridge 1995). Ceci pourrait indiquer l'existence d'un mécanisme tamponnant l'effet de température sur le développement chez *D. pachea*, préservant son déroulement de variations chronologiques induites par la température ambiante. Cependant, la nature ainsi que le mode d'action d'un tel mécanisme reste à découvrir, tout comme, de façon plus générale, la manière dont *D. pachea* parvient à survivre à des températures extrêmes.

La comparaison des durées de développement global et de celles des stades embryonnaire, larvaires et pupal parmi une variété d'espèces a révélé des variations interspécifiques qui augmentent avec la distance phylogénétique entre les espèces. Cependant, les facteurs génétiques et biochimiques potentiellement responsables de ces variations, ainsi que leur importance biologique, restent à étudier. En outre, ces travaux ont permis d'établir une description exhaustive du développement de *D. pachea* dans les conditions de laboratoire, potentiellement utile pour la caractérisation future de tout processus développemental d'intérêt dans cette espèce.

Enfin, le dernier objectif de ma thèse était de caractériser les mécanismes intrinsèques de croissance à l'origine du développement des lobes génitaux asymétriques de *D. pachea*. Pour ce faire, nous avons utilisé deux approches différentes : le marquage par immunofluorescence de tissus génitaux fixés à différents moments du développement et l'imagerie *in vivo* du développement génital à l'aide de souches transgéniques exprimant un marqueur

membranaire, la cadhérine épidermale de drosophile (DE-cad) fusionnée à une protéine fluorescente verte (Green Fluorescent Protein, GFP), que nous avons développés.

La génération de transgéniques chez *D. pachea* ouvre la voie au développement d'un vaste panel d'outils génétiques dans cette espèce pour de futures recherches. En outre, les stocks établis exprimant la DE-cad::GFP seront utiles pour approfondir l'étude des mécanismes de croissance asymétrique des lobes, ainsi que pour tout type d'étude développementale nécessitant l'expression *in vivo* d'un marqueur membranaire fluorescent.

Concernant la croissance des lobes, notre caractérisation a révélé que celle-ci n'est pas due à un groupe de cellules à la périphérie ou à l'extrémité des lobes, mais qu'elle se produit par un mécanisme de "croissance en masse" via des cellules distribuées tout au sein du tissu (Irvine and Shraiman 2017). Une telle croissance pourrait être déclenchée par un gradient de morphogène stimulant la division cellulaire, comme c'est le cas avec *Dpp* dans les disques des ailes (Irvine and Shraiman 2017), cependant, l'implication possible d'un tel gradient morphogène dans le développement des lobes reste à élucider. Les lobes gauche et droit atteignent environ 410 et 220 cellules respectivement, mais aucune différence dans le taux mitotique n'a été détectée entre les deux lobes. Ainsi, leur asymétrie pourrait résulter du recrutement de cellules à partir du tissu voisin de l'épandrium ou du tissu alentour. Le changement de forme des cellules et l'orientation éventuelle de la division cellulaire, ainsi que les événements d'apoptose, pourraient également affecter la croissance asymétrique des lobes. Ces comportements cellulaires restent à caractériser en détail pour comprendre de façon plus approfondie les mécanismes qui sous-tendent la croissance asymétrique des lobes.

Aussi, la croissance lobaire se produit entre 24 h APF et 36 h APF, ce qui correspond à la première moitié de la rotation des pièces génitales mâles. Cette rotation a lieu environ 6 heures plus tôt chez les mâles du stock de sélection, dont le lobe gauche présente une longueur variable par rapport à ceux du stock sauvage dont le lobe gauche est typiquement long. Ce décalage indique vraisemblablement un lien fonctionnel entre ces deux processus développementaux. Ainsi, la rotation des genitalia mâles pourrait avoir été co-optée au cours de l'évolution pour dériver les lobes génitaux asymétriques chez *D. pachea*. De plus, lors de la croissance des lobes, des interactions tissu-tissu semblent avoir lieu entre le tissu du lobe en développement et le tissu environnant. Ces interactions restent à caractériser, en particulier l'origine des deux tissus en interaction, ainsi que la force et la nature de l'interaction. Cette interaction pourrait résulter de processus mettant en jeu des changements d'adhésion cellulaire ou des défauts d'apoptose. Enfin, il serait intéressant d'étudier les forces mécaniques déclenchées par ces interactions dans le contexte de la rotation des pièces génitales, ainsi que

leurs conséquences probables sur la morphologie des lobes.

Enfin, la comparaison du développement des structures génitales mâles de *D. pachea* et des espèces étroitement apparentées *D. acanthoptera* et *D. nannopectera* a révélé l'existence de différences morphologiques entre espèces dès 24 h APF, au début de la croissance des lobes de *D. pachea*. Les changements de morphologie affectant les pièces génitales sont donc initiés précocément, pendant cette période. Le changement de leur développement, relativement à ceux des deux espèces soeurs de *D. pachea*, est donc probablement initié à 24 h APF ou antérieurement. La détermination de la croissance des lobes chez *D. pachea* reste donc à être caractérisée pour permettre l'identification des facteurs développementaux dérivant de nouvelles formes génitales.

Pour conclure, les différents objectifs de ma thèse ont permis d'apporter de nouveaux éléments quant à l'évolution et au développement des lobes génitaux asymétriques chez *D. pachea*.

Remerciements

J'ai découvert le travail de l'équipe de Virginie, et en particulier celui de Michael sur les pièces génitales asymétriques chez *Drosophila patchea* lorsque j'étais en troisième année de licence et que je faisais mes recherches pour trouver mon stage de master 1. A l'époque, j'étais déjà très intéressée par la génétique et les drosophiles, et je voulais que ces deux composantes soient au cœur de mon stage de master 2 et idéalement, par la suite, d'une thèse. Séduite par l'originalité de leurs recherches, j'ai donc contacté Virginie et Michael dans l'espoir de réaliser mon stage de master 2 avec eux, avant même d'avoir fini ma licence.

Je tiens tout d'abord à remercier Michael Lang, pour ces quatre années à travailler avec toi. Je suis très honorée d'être ta première thésarde et je n'aurais pas pu rêver meilleur encadrant pour m'accompagner sur ce parcours parfois difficile mais extrêmement stimulant qu'est le doctorat. Merci pour tout ce que tu as pu m'apprendre, pour ta gentillesse et ta disponibilité, quelque soit le moment. J'espère un jour avoir ton sens du détail.

Un grand merci également à Virginie Courtier-Orgogozo pour m'avoir accueillie au sein de son équipe. Merci pour ta bienveillance, ta gentillesse, ainsi que pour ton intérêt et ta curiosité pour une incroyable variété de sujets, de la colle des mouches au comportement des rats domestiques, qui m'a permis d'en apprendre plus sur beaucoup de choses.

Un merci particulier à Alexis Lalouette d'avoir accepté d'être mon directeur de thèse, et pour son aide par rapport à toute la partie administrative de celle-ci.

Merci à tous les membres de l'équipe, passés et présents, de contribuer à l'ambiance chaleureuse de l'équipe et pour toutes les discussions stimulantes, qu'elles soient scientifiques ou non : merci à Flora Borne, Jean David, Marine Delvigne, Medhi Hamdani, Rob Kulathinal, Alexis Matamoro-Vidal, Manon Monier, Olga Nagy, Isabelle Nuez, Alexandre Peluffo, Stéphane Prigent, Aurélie Surtel et Josué Vidal. Un grand merci également à Josué Vidal pour son travail avec Michael qui a permis l'amélioration du protocole de transformation des lignées germinales, ainsi qu'à Aurélie Surtel pour son aide dans l'entretien des stocks de mouches et lors des sessions d'injections des embryons, et à Olga Nagy et Orestis Faklaris de la plateforme ImagoSeine pour la mise au point du montage des pièces génitales marquées par immuno-fluorescence.

Merci à Magali Suzanne et Benjamin Prud'homme pour avoir accepté d'évaluer mon travail en faisant partie de mon jury en tant que rapporteurs, ainsi qu'à Sylvie Rétaux, en tant qu'examinatrice.

Merci à Véronique Brodu et Jean-Michel Gibert d'avoir suivi l'avancement de mon projet au sein de mon Comité de Suivi. Merci pour votre bienveillance et votre enthousiasme, ainsi que pour les discussions et questionnements constructifs que vous m'avez apporté.

Je n'aurais pas pu faire cette thèse sans financements. Merci à l'Ecole doctorale BioSorbonne Paris Cité pour avoir financé mes trois ans de doctorat, ainsi qu'au Labex Who Am I? pour m'avoir attribué un financement complémentaire de trois mois¹. Merci à Michael et Virginie d'avoir financé un dernier mois, me permettant de terminer ma thèse bien plus sereinement.

Merci à la plateforme ImagoSeine ainsi qu'à tous les membres de l'équipe d'imagerie photonique pour l'aide qu'ils m'ont apporté concernant l'imagerie et le traitement des données de microscopie. Pour leur soutien concernant les tâches administratives liées à l'Institut, merci à Martine Malet, Lindsay Polienor, Isabelle Ladegaillerie et Christine Bénichou ; pour celles liées à l'école doctorale, merci à Johanna Lévy et Déborah Débost. Pour leur accueil toujours souriant au magasin, merci à Jonathan Lopez et Norry Baouz. Pour la préparation des milieux, merci à Romain Servouze.

Pour m'avoir permis d'évoluer dans un cadre de travail stimulant et chaleureux, merci à l'Institut Jacques Monod et à son directeur Michel Werner. Un merci particulier aux équipes voisines, pour les discussions constructives en pièce à mouche ou autour d'un repas ou d'un café : merci à Marina Antunes, Isabelle Becam, Eva Beaumale, Antoine Guichet, Nicolas Joly, Jean-Antoine Lepsant, Maëlys Loh, Samia Miled, Sylvia Nkombo Nkoula, Anne Plessis, Amina Zemouri, et tous ceux que je n'ai pas cité ici. Un grand merci également à Rosine Haguenaer-Tsapis pour l'énergie que tu consacres au programme "Apprentis-chercheurs" auquel j'ai pu participer deux fois avec grand plaisir.

Pour ses conseils éclairés tout au long de mon cursus universitaire, dont le meilleur conseil que l'on m'ait donné pendant celui-ci ("Si ça te plaît, alors fonce !"), pour tout ce qu'elle m'a appris et pour m'avoir fait découvrir ces fascinantes petites bêtes que sont les Drosophiles, merci à Stéphanie Le Bras. Pour m'avoir permis de réaliser des stages qui ont été décisifs dans la construction de mon projet professionnel ainsi que pour ma culture scientifique, merci à Benoît Martin et Gabriel Dieuset, merci à Roland Le Borgne et Stéphanie Le Bras, merci à Claude Prigent, merci à Arnaud Echard et Kerstin Klinkert.

Enfin, je ne serais pas arrivée là sans le soutien de mes amis et de ma famille. Commençons d'abord par les amis. Pour votre soutien et votre présence à mes côtés dans les bons et les

¹"Initiatives d'excellence", Idex ANR-18-IDEX-0001 ; ANR du Labex Who Am I?: ANR-11-LABX-0071

moins bons moments, pour votre enthousiasme quant à mes mouches (même si cela vous semble parfois farfelu), pour tous les fous rires, merci à Agathe et Juliette, merci à Sophie, Carole et Mathieu, merci à Perrine, Marie J et Marie C, et Pauline.

Merci à ma belle-famille, à Isabelle, qui nous manque, et à Joël ; à Anne-Sophie, Rémy et Gabin ; à Jeanine.

Merci à ma famille, ma maman, Dominique, pour m'avoir donné le sens du travail et du dépassement de soi ; ma marraine, Yvette, pour ton soutien et tes encouragements indéfectibles, et ma grand-mère, Madeleine, qui se serait intéressée aux mouches, j'en suis sûre.

Enfin, merci à Amélie d'être à mes côtés tous les jours depuis bientôt dix ans, de croire en moi et d'illuminer ma vie. Merci d'avoir supporté mon obsession des drosophiles, surtout ces derniers temps. Je n'y serais pas arrivée sans toi.

Table des matières - Table of contents

Résumé	10
Remerciements	18
Table of figures	25
Table of tables	27
Abbréviations	28
1 Introduction	30
1.1 Evolutionary developmental biology and reproduction	30
1.2 General principles of tissue growth and genitalia development in <i>Drosophila</i> .	30
1.2.1 General mechanisms of tissue growth	30
1.2.2 Genitalia development in <i>Drosophila</i> species	32
1.3 Left-right asymmetries: types, development and evolution	33
1.3.1 Different types of left-right asymmetries	33
1.3.2 Left-right asymmetry establishment and evolution	34
1.3.3 Left-right asymmetries in <i>Drosophila</i> and their developmental basis .	36
1.4 Genital diversity, sexual selection mechanisms, and asymmetric genitalia in insects	38
1.4.1 Genital diversity	38
1.4.2 Sexual selection mechanisms	39
1.4.3 Primary sexual characters as courtship devices	41
1.4.4 Evolution of asymmetric genitalia in insects	42
1.5 <i>Drosophila pachea</i> and the <i>Drosophila nannoptera</i> species group	42
1.5.1 Ecology of the species from the nannoptera group	42
1.5.2 Sperm gigantism in nannoptera species	44
1.5.3 Left-right asymmetric male genitalia and mating position in species of the nannoptera group	44
1.6 Objectives	47
2 Material and Methods	48
2.1 <i>Drosophila</i> husbandry	48
2.2 Mate competition assay	50

2.2.1	Collection and phenotyping of virgin adults for competitive matings	50
2.2.2	Lobe surgery	50
2.2.3	Competitive mating assay	51
2.2.4	Adult dissections and imaging	54
2.2.5	Analysis of courtship and copulation behaviors	55
2.2.6	Data usage in mate competition assay	59
2.2.7	Statistical analysis in mate competition assay	59
2.3	Developmental timing characterization	60
2.3.1	Cohort synchronisation of embryos, larvae and pupae	60
2.3.2	Time lapse recording of embryonic development	62
2.3.3	Dissection and imaging of larvae	62
2.3.4	Determination of developmental pupal stages in <i>D. pachea</i>	63
2.3.5	Characterisation of rotation timing of <i>D. pachea</i> male genitalia on freshly dissected samples	64
2.3.6	Immuno-staining of male genitalia during pupal development	65
2.4	Molecular methods used to clone a PiggyBac plasmid containing a DE-cadherin fused to a Green Fluorescent Protein	67
2.4.1	Cloning strategy	67
2.4.2	Sequence alignment	69
2.4.3	RNA extraction and retro-transcription from <i>D. melanogaster</i> T7 stock	69
2.4.4	Amplification of DNA fragments by PCR	70
2.4.5	DNA fragment purification	70
2.4.6	Plasmid linearization	71
2.4.7	Gibson assembly and bacterial transformation	71
2.4.8	Plasmid purification and evaluation of transformation products	72
2.5	Development of transgenic <i>D. pachea</i> expressing DE-cad::GFP for live imaging	72
2.5.1	Germline transformation in <i>D. pachea</i>	72
2.5.2	Identification of transgenic <i>D. pachea</i> flies and stock establishment	74
2.5.3	Insertion site localisation of the transgene	74
2.5.4	Live-imaging microscopy of developing genitalia	75
2.5.5	Statistical analysis and figure assembly	76
3	Do asymmetric male genital lobes play a role in pre-copulatory events?	77
3.1	Results	77
3.1.1	Genital lobe lengths differ between <i>D. pachea</i> stocks	77

3.1.2	Male genital left lobe length, male courtship and failed copulation attempts have an effect on copulation success	79
3.1.3	Courtship duration increases when two males court a female simultaneously	83
3.1.4	Lobe length is not associated with the amount of ejaculate in female sperm storage organs	84
3.2	Discussion	85
3.2.1	Left lobe length affects the chance of a male to copulate	85
3.2.2	Male intra-sexual competition is potentially reflected by male courtship intensity	85
3.2.3	Potential female benefits gained from mate-choice for males with long left lobes	86
3.2.4	Age of reproductive activities appear to be non-overlapping in sibling males and females	88
4	Timing of development in <i>Drosophila pachea</i>	90
4.1	Results	90
4.1.1	Durations of <i>Drosophila pachea</i> embryonic and larval development . .	90
4.1.2	The timing of pupal development is conserved up to the pharate adult stage between <i>D. pachea</i> and various <i>Drosophila</i> species	92
4.1.3	The relative timing of pupal stages of <i>D. pachea</i> varies between 25°C and 29°C, whereas the total duration does not	95
4.2	Discussion	97
4.2.1	Conserved overall developmental progress during early pupal stages .	97
4.2.2	The duration of development varies among <i>Drosophila</i> species	97
5	Generation of transgenic <i>D. pachea</i> expressing DE-cad::GFP, a membrane marker	103
5.1	Results	103
5.1.1	The <i>D. pachea shotgun</i> homolog shares conserved functional domains with <i>D. melanogaster</i>	103
5.1.2	Design of the truncated DE-cad::GFP to mark the cell membranes and reduce off-target phenotypes	105
5.1.3	Transgenic <i>D. pachea</i> stocks	106
5.1.4	The DE-cad::GFP is inserted inside putative intergenic regions in four different <i>D. pachea</i> stocks	108

5.1.5	GFP expression in DE-cad::GFP <i>Drosophila pachea</i> is localized at cell membranes	109
5.2	Discussion	111
5.2.1	The truncated DE-cad::GFP encoded by the transgene localizes at cell membranes in transgenic <i>D. pachea</i>	111
5.2.2	Generation of transgenic <i>D. pachea</i> , a promising new genetic tool . .	111
6	How is <i>D. pachea</i> male genital lobe asymmetry established during development?	113
6.1	Results	113
6.1.1	Asymmetric <i>Drosophila pachea</i> lobe growth occurs between 24 h APF and 36 h APF	113
6.1.2	Differences in male genitalia morphology appear from 24 h APF between <i>D. pachea</i> and <i>D. nanoptera</i>	117
6.1.3	Genitalia rotation takes place between 24 h APF and 45 h APF in wild-type <i>Drosophila pachea</i> whereas it happens about 6 h earlier in a mutant stock	118
6.1.4	The speed of genitalia rotation peaks at 35 h APF, which approximately corresponds to 225° of rotation	123
6.1.5	Live-imaging of developing genitalia reveals possible tissue-tissue interactions and tissue deformation during genitalia rotation	124
6.2	Discussion	129
6.2.1	The left-right asymmetric tissue growth does not appear to depend on cell division differences in the left and right lobes	129
6.2.2	Premature genitalia rotation in the selection stock is associated with a variable left lobe length of <i>D. pachea</i>	130
6.2.3	The developing lobes appear to interact with surrounding non-rotating tissue during the first half of the genitalia rotation	131
7	Conclusions	134
	Bibliography	137
	Annexes	150
	Oligonucleotides	150
	PiggyBac plasmid maps	151
	Article Manuscript	164

Table of figures

1	<i>Drosophila packea</i> habitat.	43
2	<i>Drosophila packea</i> male morphology.	45
3	Pairwise lobe length differences of males used in the competition mating experiments.	52
4	Camera set-up for recording mating behavior in <i>D. packea</i>	53
5	Ejaculate filling levels in female spermathecae.	55
6	Courtship and copulation duration in competition mating experiments (first part).	56
6	Courtship and copulation duration in competition mating experiments (second part).	57
7	Mouth hook morphology at different larval instars.	62
8	Dissection strategy to characterise genitalia rotation timing in <i>D. packea</i> . . .	64
9	Mounting of dissected genitalia from <i>D. packea</i> males.	66
10	Cloning strategy to produce a PiggyBac plasmid containing a truncated DE-cad fused to GFP.	68
11	Mounting of pupae for live-imaging of male genitalia morphogenesis and rotation. .	76
12	<i>Drosophila packea</i> male genital lobes.	78
13	Genital lobe lengths differ between <i>D. packea</i> stocks.	79
14	Courtship durations and relative courtship activity.	81
15	Failed copulation attempts compared to female age.	82
16	Courtship duration increases with female age.	83
17	Duration of the embryonic and larval developmental stages in <i>D. packea</i> and <i>D. melanogaster</i>	91
18	<i>D. packea</i> , <i>D. nanoptera</i> , and <i>D. acanthoptera</i> flies display differences in eye and body pigmentation.	93
19	Timing of the pupal development in <i>D. packea</i> , <i>D. nanoptera</i> , <i>D. acanthoptera</i> , <i>D. melanogaster</i> and <i>D. guttifera</i> at 25°C.	94
20	Progress of pupal development in <i>D. packea</i> at 25°C and 29°C.	96
21	Embryo-to-adult duration in various <i>Drosophila</i> species raised at 25°C. . . .	98
22	Durations of the embryonic development in various <i>Drosophila</i> species at 22°C - 25°C.	99
23	Annotation of the <i>shg</i> gene encoding the DE-Cadherin in <i>D. melanogaster</i> and <i>D. packea</i>	104

24	Simplified map of the DE-cad::GFP PiggyBac plasmid.	106
25	Localisation of the transgene insertion site in four <i>D. pachea</i> stocks.	109
26	GFP fluorescence localizes at cell membranes in <i>D. pachea</i> DE-cad::GFP stocks.	110
27	Immuno-fluorescent staining of developing genitalia at various developmental time points in the wild-type stock 1698.01.	114
28	Quantification of the number of nuclei per lobe at various developmental time points in the 1698.01 wild-type stock.	115
29	Proportion of mitotic cells in <i>D. pachea</i> male genital lobes at various developmental time points.	116
30	Immuno-fluorescent staining of <i>D. pachea</i> , <i>D. acanthoptera</i> and <i>D. nannopectera</i> developing genitalia at various developmental time points.	119
31	Characterization of the genitalia rotation timing on fixed samples from selection stock and wild-type stock 1698.01.	120
32	Characterization of genitalia rotation timing measured on dissected samples from stock 1698.01 and extrapolated from live-imaging analysis of the DE-cad::GFP transgenic stocks.	122
33	Genitalia rotation velocity in DE-cad::GFP male pupae.	123
34	Time-lapse imaging of developing asymmetric genital lobes during genitalia rotation in transgenic DE-cad::GFP <i>D. pachea</i>	125
35	Three dimensional reconstruction of developing male genitalia in <i>D. pachea</i> (first part).	126
35	Three dimensional reconstruction of developing male genitalia in <i>D. pachea</i> (second part).	127
36	Hypothetical model explaining the functional link between genitalia rotation and left-right lobe asymmetry establishment.	132

Table of tables

1	<i>Drosophila</i> stock resources.	49
2	Courtship duration, male licking behavior and copulation duration in trials where both males courted the female.	58
3	Competition mating trials used for courtship analysis.	59
4	Genital lobe lengths in <i>D. pachea</i> stocks.	79
5	Bradley–Terry model examining the effects of left lobe length, sum licking duration, number of licking sequences and failed mounting attempts on copulation success.	82
6	Bradley–Terry model examining the effects of left lobe length, sum licking duration, and number of licking sequences on copulation success.	83
7	Linear model, examining the effects of lobe length, sum licking duration, copulation duration and age on spermathecae filling levels.	84
8	Morphological markers used to examine the developmental stage of pupae, adapted from Bainbridge and Bownes (1981).	93
9	Embryo-to-adult developmental duration in various <i>Drosophila</i> species.	100
10	Duration of the embryonic development in various <i>Drosophila</i> species.	101
11	Conservation of <i>shg</i> sequence coding for functional domains between <i>D. melanogaster</i> and <i>D. pachea</i>	105
12	<i>D. pachea</i> germline transformation efficiency.	106
13	Crosses and stocks with transgenic <i>D. pachea</i> , carrying DE-cad::GFP (first part).	107
13	Crosses and stocks with transgenic <i>D. pachea</i> , carrying DE-cad::GFP (second part).	108
14	Parameters of the logistic curves describing lobe growth.	117
15	Parameters of the logistic regression models describing genitalia rotation in the wild-type and in the selection stock.	121

Abbreviations

1698.01: *D. pachea* stock 15090-**1698.01**

1698.01_14.2: *D. pachea* stock 15090-**1698.01_14.2**

1698.02: *D. pachea* stock 15090-**1698.02**

7-DHC: **7-des**hydrocholesterol

acan: *D. acanthoptera* stock 15090-1693.00

act5C: **actin 5C**

APF: **a**fter **p**uparium formation

BM: **B**radley-**T**erry model

bp: **b**ase **p**air

BSA: **b**ovine serum **a**lbumine

cDNA: **c**omplementary **D**esoxyribo**N**ucleic **A**cid

CDS: **c**oding sequence

DAAM: **D**ishevelled **A**ssociated **A**ctivator of **M**orphogenesis

DAPI: 4'-**d**iamidino-2-**p**henylindole

DE-cad: **D**rosophila **E**pidermal **c**adherin

DMHF: **d**imethyl-**h**ydantoin formaldehyde

DNA: **D**esoxyribo**N**ucleic **A**cid

DPP: **d**ecapentaplegic

dsx: **d**oublesex

EDTA: **e**thylenedi**a**minet**e**tetraacetic **a**cid

FA: **F**luctuating **A**symmetry

GFP: **g**reen **f**luorescent **p**rotein

LB: **L**ysogeny **B**roth

nan00: *D. nannoptera* stock 15090-1692.00

nan12: *D. nanoptera* stock 15090-1692.12

PBS buffer: phosphate-buffered saline buffer

PCC: Planar Cell-shape Chirality

PCP pathway: Planar Cell Polarity pathway

PCR: polymerase chain reaction

PFA: paraformaldehyde

RFP: red fluorescent protein

RNA: RiboNucleid Acid

SD: Standard Deviation

shg: *shotgun*

SOC: Super Optimal Broth Catabolite repression medium

T7: *D. melanogaster* stock Tuscon 14021-0231.7

TAE buffer: Tris Acetate EDTA buffer

TNT buffer: Tris-NaCl-tween buffer

UTR: untranslated region

1 Introduction

1.1 Evolutionary developmental biology and reproduction.

The animal kingdom presents a high diversity of shapes that are established during development through the coordinated action of a limited number of genes (Carroll 2005). In evolutionary developmental biology, or evo-devo, the developmental basis underlying shape establishment and their changes during evolution is examined (Carroll 2005). The major question is, how developmental processes and underlying molecular and genetic pathways change during evolution to give rise to changes, losses and gains of morphological characters.

However, evolution involves reproduction of individuals and among the variety of shapes observed in animals, genitalia are particularly important as they directly affect reproductive success (Schilthuizen 2015). Species with internal fertilization transfer sperm from the male to the female via an intromittent phallus into the female inner reproductive organs. A change in genitalia shapes may thus affect the efficiency of gamete transfer and fertilization success (Huber, Sinclair, and Schmitt 2007, Huber 2010, Schilthuizen 2013, Schilthuizen 2015). Genital shape and usage change quickly during evolution and are object to selection based on sexual conflicts between and males and females when reproductive strategies differ (Kokko and Jennions 2014).

Here, we study how genitalia shape evolves and evaluate the impact of genital shape differences on reproductive success. For this, we focus our attention on a particularly interesting left-right asymmetry in a pair of external male genital lobes of the species *Drosophila patchea* as a model.

1.2 General principles of tissue growth and genitalia development in *Drosophila*

1.2.1 General mechanisms of tissue growth

The development of adults, composed of a huge number of cells (about one thousand cells in *C. elegans* (Sulston et al. 1983) and about 10^{13} cells in humans (Bianconi et al. 2013)) must be precisely coordinated to finally reproduce similar adult body plans with complex organs or tissues (Lecuit and Mahadevan 2017, Lecuit and Lenne 2007, Nelson et al. 2005).

At cellular scale, the range of behaviors influencing tissue shape is limited: cells can divide, die, grow, migrate or change their shape (Lecuit and Lenne 2007). However, in tissues cells have physical interactions with their neighbors due to complexes, which enables the built-up of diverse and complex tissues. These complexes ensure the tissue cohesion and allow the transmission of mechanical forces between neighbouring cells. Cadherin are involved in these structures. These are transmembrane proteins that are in interaction with α -catenin, β -catenin and actomyosin cytoskeleton in the cytoplasmic compartment (Lecuit 2010, Oda et al. 1994). The interaction between the adhesion complexes and the cytoskeleton has been shown to be involved in various developmental processes such as gastrulation or morphogenesis (LeGoff and Lecuit 2016). Furthermore, the Hippo signalling pathway was revealed to be a key element in the integration of both biomechanical and biochemical signals (Sun and Irvine 2016, Irvine and Shraiman 2017). Tissue stretching has been found to stimulate cell proliferation whereas this process is inhibited by tissue compression (Irvine and Shraiman 2017), both *in vitro* in different cell types (Streichan et al. 2014, Eder, Aegerter, and Basler 2017, LeGoff and Lecuit 2016), and *in vivo* in drosophila ovaries (Wang and Riechmann 2007). In both cases, the tension information is integrated by cells via the Hippo pathway that potentially interacts on biochemical pathways regulating growth (Irvine and Shraiman 2017).

Tissue growth can result either from "boundary growth", where the growth is due to cells at the periphery of the tissue, or from "bulk growth" with proliferating cells being randomly located throughout the tissue (Irvine and Shraiman 2017). Various examples indicate that these two modes correlate with the stiffness of the tissue. Hard tissue usually growth by boundary growth whereas soft tissue grows through bulk growth (Cowin 2004). The most common mechanisms of growth are related to cell division. This potentially involves specific orientations of the division axis along the tissue axis, cell competition between adjacent cell populations that display different biological properties, or cell movements and shape changes, such as cell intercalation (Lecuit and Le Goff 2007, Taniguchi et al. 2011). The regulation of cell divisions and cell apoptosis throughout a tissue is known to be regulated by morphogen gradients: a signalling molecule that will diffuse throughout a tissue and creates a concentration gradient with increasing distance from the source cells. This can specify diverse cell fates in function of the morphogen concentration. For example, the *D. melanogaster* wing disc is a flat epithelium, in which tissue growth depends on non-linear gradients of morphogens, such as decapentaplegic (Dpp) (Rogulja and Irvine 2005, Kicheva et al. 2007, Irvine and Shraiman 2017). Cells in this tissue are exposed to different levels of Dpp, which then determine diverse cell fates and also differently promote cell division

(Rogulja and Irvine 2005, Kicheva et al. 2007, Irvine and Shraiman 2017) or apoptosis via the Jun kinase pathway (Adachi-Yamada et al. 1999, Adachi-Yamada et al. 1999). Similarly, apoptosis triggered by Jun kinase pathway at limits of the Dpp gradient has been found to play an essential role in the folding of the leg imaginal disc (Manjón, Sánchez-Herrero, and Suzanne 2007, Monier et al. 2015). The tissue folding is triggered by tensions induced in a Myosin II-dependent manner by these apoptotic cells, in which adherens junction components, such as DE-cad, α -catenin and β -catenin, accumulate at the apical surface of the dying cell (Monier et al. 2015).

Altogether, the growth and the shaping of a tissue depends on the coordination of cell behaviors through chemical and physical signals. These events have been well characterised in model species such as *Drosophila melanogaster*. The characterization of growth and shaping mechanisms in other *Drosophila* species, such as *Drosophila pachea* would potentially shed light on changes in developmental pathways underlying changes in morphology.

1.2.2 Genitalia development in *Drosophila* species

In *Drosophila* species, most of the adult organs are formed from structures called imaginal discs, that finally replace most of the larval tissue during metamorphosis. The genitalia of both males and females derive from the genital disc, which is the only unpaired and medially located imaginal disc (Estrada, Casares, and Sánchez-Herrero 2003). The genital disc is complex and encompasses three primordia: the 8th abdominal segment, which gives rise to genitalia in females, the 9th abdominal segment from which male genitalia develop, and the anal primordium that derives from the 10th abdominal segment (Estrada, Casares, and Sánchez-Herrero 2003, Sánchez and Guerrero 2001). Thus genital discs have the potential to derive either male or female structures (Estrada, Casares, and Sánchez-Herrero 2003, Sánchez and Guerrero 2001). In females, the 9th abdominal segment gets largely reduced, such as the 8th abdominal segments in males (Estrada, Casares, and Sánchez-Herrero 2003, Sánchez and Guerrero 2001). Nonetheless, the 8th segment is known to have important developmental functions during male genitalia development (Suzanne et al. 2010, Sato et al. 2015). The proper development of male and female genitalia rely on sex determination genes, and in particular the *doublesex* (*Dsx*) pathway. The sex-specific splicing of *Dsx* leads to the differential activation of the Hedgehog, Decapentaplegic and Wingless signalling pathways. In females, this leads to the development of the female primordia and the anal primordia. In males, it is the male primordia and the anal primordia that develop respectively (Sánchez and Guerrero 2001, Estrada, Casares, and Sánchez-Herrero 2003).

In male *Drosophila*, an asymmetric developmental process affecting genitalia occurs during the pupal stage. The male genitalia undergo a 360° clockwise rotation during development. This process affects the entire male terminalia, including male genitalia, spermiducts, gut and anal plate (Spéder and Noselli 2007). This process is explained in detail part 1.3.3, page 36, and was found to rely on an interplay of non-conventional type I myosins with apoptosis and tissue movement of the 7th and 8th abdominal segment (Spéder, Ádám, and Noselli 2006, Suzanne et al. 2010, Sato et al. 2015).

It would be interesting to investigate what developmental changes in genitalia development occurs to derive different genital shapes. Such a study have been recently conducted to unravel how female ovipositor length increased in *D. suzukii*, compared to *D. melanogaster* females (Green et al. 2019). Furthermore, as male genitalia development occurs in the context of genitalia rotation in *Drosophila* species, it would be interesting to investigate if this asymmetric rotation process may impact genital shape. In particular, it could potentially account for the evolution of asymmetric genital shapes.

1.3 Left-right asymmetries: types, development and evolution

1.3.1 Different types of left-right asymmetries

Asymmetric shapes are widespread in the animal kingdom and arise at different biological scales, ranging from molecules to cells, tissues and organs (Lebreton et al. 2018, Blum and Ott 2018, Levin, Klar, and Ramsdell 2016, Coutelis et al. 2014, Schilthuisen and Gravendeel 2012, Spéder and Noselli 2007). In bilaterians, the body plan of organisms is characterised by three main axis: the antero-posterior axis (or cranio-caudal axis), from the head to the tail ; the dorso-ventral axis, from the back to the belly side (rachis to viscera); and the left-right axis, which is defined relatively to the midplane formed by the antero-posterior axis and the dorso-ventral axis. The default-state development of bilaterians is expected to be symmetric and left-right asymmetry occurs through so-called "symmetry breaking" events (Palmer 2004). Many examples of left-right asymmetries are found in animal species and can affect morphology and/or positioning of organs (Blum and Ott 2018, Palmer 2016). In humans, the heart, the stomach and the spleen present shape and position asymmetries. The paired left and right lungs display different numbers of lobes (Blum and Ott 2018). The left-right asymmetries can also be rotational, related to a coiling, a looping or the rotation of a structure in either clockwise (or dextral) or counter-clockwise (sinistral) direction (Palmer 2016, Schilthuisen et al. 2007). Different kinds of left-right asymmetries are usually

distinguished: fluctuating asymmetries, anti-symmetries and directional asymmetries.

Fluctuating asymmetries are slight (random) variations from symmetry of characters that in average are symmetric (Ludwig 1932, Møller 1993). These asymmetries potentially develop due to stress factors, such as extreme temperature, toxic compounds, pathogens, or malnutrition. Genetic factor may also play a role, such as inbreeding, deleterious alleles, or mutations. The heritability of fluctuating asymmetry is variable and depends on the factor that disturbs development (Møller 1993).

Antisymmetries correspond to asymmetric characters that can be found in a sinistral or dextral form in a same species, such as the coiling direction of shells in some snail species, the side of valve attachment in diverse mussel species or for example the enlarged claw of fiddler crabs and lobsters (reviewed by Palmer 2005). The individual direction of antisymmetry is generally determined by random or external environmental stimuli that affect the development of the asymmetric structure. Thus, direction of these asymmetry is generally not inherited across generations (Palmer 2005, Palmer 2004).

Directional asymmetries are asymmetric characters that are found in only one of the sinistral or dextral form within a species, also called fixed asymmetry. The asymmetries and their direction are genetically inherited (Palmer 2004).

1.3.2 Left-right asymmetry establishment and evolution

Brown and Wolpert (1990) proposed a model to explain the development of left-right asymmetric structure, the so-called "F molecule model". This model relies on chiral molecules that could trigger cell asymmetry and underlies left-right asymmetric development by the establishment of asymmetric morphogen gradients (Brown and Wolpert 1990). Five years later, the work of Levin et al. (1995) on chick embryos reported the left-right asymmetric expression of the TGF- β family member and Nodal related gene *c-NR1* to affect heart asymmetry. However, the genetic and developmental basis of left-right asymmetries remained a puzzling question for decades as diverse bilaterian lineages revealed the existence of distinct pathways underlying left-right asymmetric development (Spéder and Noselli 2007, Coutelis et al. 2014). For example, Nodal dependent establishment of asymmetry has been found in numerous deuterostome species (such as vertebrates) and in some lophotrochozoan species (for example molluscs), but is probably absent in ecdysozoan species (such as arthropods) (Namigai, Kenny, and Shimeld 2014).

In most of deuterostomes, left-right asymmetry of most of asymmetric organs depends on developmental processes in developmental organizing centers of early embryos (reviewed in Coutelis et al. 2014). These structures are constituted of a transient mono-layer of epithelium like-cells containing a cavity (Spéder and Noselli 2007, Vandenberg and Levin 2013, Coutelis et al. 2014) and are located at the ventral side of the embryo during gastrulation.

In mouse, cells of this mono-layer are polarized by the Planar Cell Polarity (PCP) pathway and due to actin remodelling, leading the same orientation of cell cilia along the structure (Song et al. 2010, Antic et al. 2010). The unidirectional movement or tilting of these cilia then creates a leftward flow of extra embryonic fluid, leading to a reinforcement of Nodal signalling in the surrounding tissue at the left side of the node. Nodal then activates a positive feedback loop as well as the expression of two TGF- β family members Lefty1, Lefty2 and the transcription factor Pitx2. Lefty1 and Lefty2 are competitors of Nodal and reduce its diffusion to the right side of the embryo. The expression of Pitx2 on the left side of the lateral plate mesoderm will then lead to the morphogenesis of left-sided organs (Coutelis et al. 2014, Spéder and Noselli 2007). However, the way how Pitx2 induces morphogenesis is not totally understood. It has been shown in various species that the Nodal-Pitx2 pathway can affect extracellular matrix remodeling, cell adhesion and cell movements as well as other signalling pathways such as the Wnt pathway (reviewed by Grimes and Burdine 2017).

Ion pumps ($H^+/K^+ - ATPase$, $H^+ - V - ATPase$, $Na^+/K^+ - ATPase$) may also play a role in left-right asymmetry establishment of vertebrates. In chicken, xenopus and zebrafish they have been found to be asymmetrically located (Levin et al. 2002, Spéder and Noselli 2007, Coutelis et al. 2014) in early embryos before gastrulation and Nodal flow are established. It is proposed that their asymmetric distribution potentially leads to a pH gradient in the cells, that may lead to left-right asymmetric signalling and to left-right asymmetric development (Levin et al. 2002, Spéder and Noselli 2007, Coutelis et al. 2014). Also, formin was reported to act on spindle orientation and asymmetric cell division during spiral cleavage of the pond snail *Lymnaea stagnalis*, which determines sinistral or dextral chirality types. Formin also affects left-right asymmetry establishment in xenopus (Davison et al. 2016). Likewise, the Nodal/Pitx2 genes are also found to be asymmetrically expressed in snails at the 8-cell embryonic stage and were also shown to regulate chirality via the same cellular mechanisms. As in snails, in *C. elegans*, the left-right asymmetry is established by twisting of the mitotic spindle before the 8-cell embryonic stage (Naganathan et al. 2014, Coutelis et al. 2014, Spéder, Ádám, and Noselli 2006). *D. melanogaster* display several left-right asymmetric morphological characters, in various organs. These characters as well as their developmental basis have been particularly investigated and MyoID appears to direct the asymmetry of

most of the left-right asymmetric organs (see next part a detailed description of left-right asymmetry as well as the mechanisms underlying them in the next part).

Among the different mechanisms involved in left-right asymmetry development, MyoID appears to be a conserved key factor, both in vertebrates and invertebrates, by interacting with adherens junctions, the actin cytoskeleton, the PCP pathway and cell death regulated by the Jun kinase pathway (Chougule et al. 2020, Tingler et al. 2018, Juan et al. 2018, Yuan and Brueckner 2018, Lebreton et al. 2018, González-Morales et al. 2015, Petzoldt et al. 2012, Benitez et al. 2010, Suzanne et al. 2010). Left-right asymmetry have been proposed to be an ancestral feature of animals and cells, based on conserved cellular components, such as actin cytoskeleton and associated proteins or ion pumps, and that the Nodal flow mechanisms appeared later during evolution in complement to pre-existing ancestral mechanisms (Coutelis et al. 2014, Namigai, Kenny, and Shimeld 2014). Furthermore, it has been shown that additionally to its evolutionary conserved role in left-right asymmetric establishment, MyoID is also able to induce *de novo* left-right asymmetries when ectopically expressed in some tissues, indicating that some tissues have the potential to derive left-right asymmetry but lack the expression of a determinant component (Lebreton et al. 2018).

1.3.3 Left-right asymmetries in *Drosophila* and their developmental basis

Several left-right asymmetries have been reported in *D. melanogaster*: the clockwise looping of the embryonic and of the adult hindgut (Hozumi et al. 2006, Spéder and Noselli 2007, Coutelis et al. 2008, Géminard et al. 2014), the 360° clockwise rotation of male terminalia (Spéder, Ádám, and Noselli 2006), the looping of the testis (Stern 1941a, Stern 1941b), the positioning of the Malpighian tubules (Chintapalli et al. 2012), and the asymmetrically located Fas2 in the brain (Pascual et al. 2004). Interestingly, these asymmetric developmental processes occurs at different periods and in an independent manner (Coutelis et al. 2008, Géminard et al. 2014). Among those asymmetries, the embryonic hindgut looping and the male genitalia rotation has been the most investigated ones for now (Spéder and Noselli 2007, Coutelis et al. 2008, Géminard et al. 2014).

The embryonic gut asymmetry relies on several, independent looping and twisting events. The gut is constituted of three parts, foregut, the hindgut and the midgut. The first looping event occurs during embryogenesis, from the 13th to the 17th stage and is due to cell shape changes leading to a 90° right twist of the hindgut in the portion joining the midgut (reviewed in Spéder and Noselli 2007, Coutelis et al. 2008 and Géminard et al. 2014). The asymmetry

of the embryonic hindgut relies on a transient left-right asymmetry organizer constituted of cells polarized by the Planar Cell Polarity pathway. The atypical cadherin *dachsous* triggers left-right asymmetry in these cells in a non-autonomous way, by interacting with MyoID (González-Morales et al. 2015). Furthermore, the actin cytoskeleton is involved in the establishment of the correct left-right asymmetry of the embryonic hind gut (Hozumi et al. 2006). Then, several independent twisting events then take place in the different compartments of the gut, resulting in a completely asymmetric gut (reviewed by Géminard et al. 2014). During metamorphosis, most the embryonic and then larval gut is degraded and the adult gut develops from precursor cells. However, the mechanisms of its asymmetric development and maintenance through epithelium turn-over needs further investigation.

Malpighian tubules are a pair of bifurcated tubes important for toxic compounds clearing. These structures are connected to the midgut at its junction with the hindgut and asymmetrically positioned, the left pair being located in a posterior way relatively to the midgut connection, and the right pair, in anterior way (Chintapalli et al. 2012, Géminard et al. 2014). Furthermore, a transcriptomic analysis realised by Chintapalli et al. (2012) has revealed asymmetric gene expression.

The Fas2 body located in the fly brain is another left-right asymmetric structure found in *D. melanogaster*. This is a fascilin 2 positive tissue found next to the mushroom body. This structure was found to be located in the right hemisphere in 92 % of the flies, whereas the remaining 8% has two bodies, displaying a symmetrical position in both hemispheres (Pascual et al. 2004). The presence of these symmetric pair of asymmetric bodies is associated with long term memory dysfunction (Pascual et al. 2004).

The male genitalia rotation constitute another model of left-right asymmetry that has been particularly studied. In Dipterans, male genitalia rotation ranging from 0 to 180° was found in various species of the Muscomorpha group and a male genitalia rotation of 360° was found in cyclorrhaphan flies, to which *Drosophila* species belong (Suzanne et al. 2010). Furthermore, the 360°clockwise rotation of *D. melanogaster* results from the addition of two 180° "half-rotations" of the anterior and posterior compartment of the 8th abdominal segment (Suzanne et al. 2010). Thus, it has been proposed that the evolution of male genitalia rotation occurred in two steps, first with the development of a 180°clockwise rotation (observed in mosquitos) and then with a duplication of this process (Suzanne et al. 2010). It has been shown that the rotation direction is driven by the non conventional class I myosin, MyoID (Spéder, Ádám, and Noselli 2006). *Drosophila melanogaster* has three class I myosin genes, *Myo31DF*, *Myo61F* and *Myo95E*, that encode actin-based motor proteins: MyoID, MyoIC

and MyoIB, respectively (Petzoldt et al. 2012). The MyoID expression is controlled by the homeotic gene Abdominal-B (Coutelis et al. 2013). Interestingly, MyoID mutants display a 360° counter-clockwise rotation direction (Spéder, Ádám, and Noselli 2006, Petzoldt et al. 2012), due to MyoIC function (Petzoldt et al. 2012). The expression of MyoID and MyoIC is regulated by the homeotic gene Abdominal-B (Coutelis et al. 2013). Genitalia rotation depends on apoptosis of cells at the borders of the anterior and posterior compartment of the 8th abdominal segment, triggered by the Jun kinase pathway and activated in a dynamic and asymmetric manner (Benitez et al. 2010, Suzanne et al. 2010). Collective chiral cell behaviors, such as left-right asymmetric intercalation and unidirectional cell movement (Sato et al. 2015) are also involved in this process. As for embryonic hindgut looping, MyoID has been found to underlie the correct direction of its left-right asymmetry (Hozumi et al. 2006, Okumura et al. 2015). Also, Spéder, Ádám, and Noselli 2006 found out that the counter-clockwise rotation observed in In MyoID mutants was due to another non-conventional myosin, MyoIC.

In addition to genitalia rotation, males also display asymmetrical, clockwise twisted testis. It has been shown that the attachment of the testis to the vas deferens is essential both for the coiling and for its direction definition (Stern 1941a, Stern 1941b). As for genitalia rotation and embryonic hindgut looping, MyoID mutants display an inversion of the coiling direction of the testes (Hozumi et al. 2006).

Interestingly, three out of four species from the nanoptera group, *D. pachea*, *D. wassermani* and *D. acanthoptera* display asymmetric male genitalia (see part 1.5.3, 44 for more details) (Acurio et al. 2019), constituting good models to investigate both the development and the evolution of external left-right asymmetric structures.

1.4 Genital diversity, sexual selection mechanisms, and asymmetric genitalia in insects²

1.4.1 Genital diversity

Across animals with internal fertilization, genitalia are usually the most rapidly evolving organs, leading to a high diversity in genitalia morphology (Eberhard 1985, Eberhard 2010b, Schilthuizen 2015). Furthermore, this diversity among genital structures has been used by taxonomists to differentiate species, in particular closely related species that sometimes look

²The following introduction part is adapted from our article Lefèvre et al. 2020.

very similar in their overall morphology (Perkin 2007, Eberhard 2010b, Schilthuisen 2015). This has led to the accumulation of an important amount of data on genitalia morphology and evolution (Eberhard 2010a, Eberhard 2010b, Schilthuisen 2015).

1.4.2 Sexual selection mechanisms

Traditionally, sexual traits are categorized as primary or secondary (Darwin 1859). Genital structures are considered “primary” when they are directly used for the transfer of gametes during copulation or when they contribute to the complexing of female and male copulatory organs (Eberhard 1985, Ghiselin 2010). Other traits that differ between sexes and that are linked to reproduction are considered “secondary” sexual traits. For primary sexual traits, sexual selection is traditionally thought to act during or after copulation (Eberhard 1985, Eberhard 1994), while secondary sexual traits can be involved in pre-copulatory mate-choice via visual, auditory or chemical long range signalling (Andersson 1982, Schantz et al. 1989, Hill 1991, Norris 1993, Petrie 1994, Hasselquist, Bensch, and Schantz 1996, Welch, Semlitsch, and Gerhardt 1998, Birch 1970, Sreng 1993). Several hypotheses have been proposed that could explain this rapid morphological evolution, mostly based on sexual selection or which includes all inheritance constraints linked to reproduction.

The first hypothesis regarding this rapid morphological evolution of genitalia was the so-called "lock and key" hypothesis (Dufour 1844). This hypothesis proposes that males and females of a same species have specific genital shapes that match in the manner of a lock (female genitalia) and a key (male intromittent organ), thereby preventing interbreeding and providing an isolation mechanism between closely related species (Dobzhansky 1937). This hypothesis seems applicable in some particular cases but it has fallen in disuse as increasing evidences have shown that in most species female genitalia do not work as a specific lock to match specifically with male genitalia of the same species (Eberhard 2010a). The pleiotropy hypothesis, proposed by Mayr 1963, states that genes underlying genitalia development might be selected by natural selection on some of their multiple (pleiotropic) functions in various other organs or characters. This then affects genitalia development, leading to their fast evolution as a sort of "hitchhiking". However, the weakness of this hypothesis is the lack of evidences explaining why pleiotropic effects would be concentrated on genitalia more than on any other structure (Eberhard 2010b).

Bateman (1948) has proposed that males and females exhibit different reproduction strategies due to higher energy costs of larger female gametes compared to smaller and more abun-

dant male gametes, the so called Bateman's principle. It implies male-male intra-sexual mate-competition for siring the limited female gametes. In turn, females may optimize reproduction by choosing males that confer survival and fecundity benefits to her and to the offspring. This dynamics has been formalized into genetic models (Fisher 1930, Lande 1981) involving female preferences for particular male characters and male mate competition, and can contribute to the rapid evolution of female preferences and male sexual attributes. Male courtship is well known as a behaviour to attract females before copulation begins, but has also been reported to occur during or even after copulation (Eberhard 1991, Eberhard 1994). It is thought to be a widespread and key aspect of copulation in the cryptic female choice scenario, where males stimulate the female to utilize his own sperm (Eberhard 1985, Thornhill 1983). A variety of insect species were reported where males have evolved elaborated male genital structures that are used during copulation to stimulate the female through tapping or other physical stimuli (Eberhard 1991, Eberhard 1994). Evidences have also been found for male mate-choice and female intra-sexual selection (Bonduriansky 2001, Leonard and Córdoba-Aguilar 2010, Edward and Chapman 2012), showing that traditional sex-roles can vary between and within species. The notion of culture in the sense of learned behaviors that are transmitted among successive generations may also matter as it can affect female mating preferences *Drosophila melanogaster* (Danchin et al. 2018).

In a more general context, sexual selection implies a sexual conflict whenever male and female reproductive fitness strategies differ (Kokko and Jennions 2014). Moreover, sexual conflict exists in conditions of anisogamy, when gamete sizes differ between sexes, but also in conditions of isogamy, when they are of similar size among sexes (Matsuda and Abrams 1999). This indicates that anisogamy is not necessary a pre-requisite for sexual conflict (Kokko and Jennions 2014). Several hypotheses propose that the evolution of genitalia is based on sexual selection and a consequence of sexual conflict between males and females at different levels of reproduction, including competition of sperm from different males inside the female (sperm competition) (Birkhead and Pizzari 2002), female controlled storage and usage of sperm to fertilize eggs (cryptic female choice) (Eberhard 1985, Thornhill 1983, Eberhard 2010a), or sexually antagonistic co-evolution of aggressive and defensive morphologies and/or behaviors between male and female to control fertilization decisions (Arnqvist 1998, Chapman et al. 2003). The evolution of sexual characters, either primary or secondary, is therefore complex as it may depend on a combination of various mechanisms acting both on males and females, at different periods from courtship to fertilization processes. To get a more complete understanding of the evolution of a sexual characters, it is thus important to investigate its role during mating at different stages, ranging from courtship to fertilization.

1.4.3 Primary sexual characters as courtship devices

Secondary sexual characters play a role in courtship events by definition. However, primary genitalia, that are involved in gamete transfer, could also be possibly involved in pre-copulatory mate choice. Supposing that a particular male genital trait-variance enhances or favours female fecundity, it might become preferred by the female during pre-copulatory courtship or at the moment of genitalia coupling (Polak and Rashed 2010, Grieshop and Polak 2012, Bertin and Fairbairn 2005). This preference could rely on direct benefits to reduce energy investment or predation risk caused by unsuccessful copulation attempts, or on indirect male genetic quality to be inherited into the offspring generation. Several examples of primary genitalia used in pre-copulatory courtship signalling are known in vertebrates. For example, male and female genital display, swelling, or coloration changes are associated with sexual activity (Ploog and MacLean 1963, Wickler 1966, Miller 2010). Penile display was also observed in lizards (Bohme 1983) and Human penis size was found to influence attractiveness of men to women (Mautz et al. 2013). In diverse mammalian species, females have also evolved external and visible structures that resemble male genitals, a phenomenon called andromimicry (Miller 2010, Estes 1991, Muller and Wrangham 2002). These structures are likely used in visual signalling and it is possible that the male analogous parts may also do. Furthermore, females of some live-bearing fish species were reported to prefer to mate with males with large gonopodia (Kahn, Mautz, and Jennions 2010, Langerhans, Layman, and DeWitt 2005). These mentioned cases involve visual stimuli and large genital organs. Only a few studies examined the roles of primary genitalia in invertebrates during courtship or at the onset of copulation, before phallus intromission is achieved (Polak and Rashed 2010, Grieshop and Polak 2012, Bertin and Fairbairn 2005, Moreno-Garcia and Cordero 2008, Michiels 1998). Longer male external genitalia of the water strider *Aquarius remigis* were associated with mating success (Bertin and Fairbairn 2005). In addition, male genital spine morphology of *Drosophila bipectinata* and *Drosophila ananassae* were reported to evolve in response to direct competition among males for securing mates in a so called "scramble competition" scenario (Polak and Rashed 2010, Grieshop and Polak 2012). However, the general role of primary sexual traits in establishing copulation or their role during courtship appears to an overlooked aspect that needs further investigation.

1.4.4 Evolution of asymmetric genitalia in insects

In animals, asymmetric genitalia have evolved multiple times independently and were proposed to have evolved in response to sexual selection via diverse mechanisms, including antagonistic co-evolution of males and females and/or cryptic female choice (Huber, Sinclair, and Schmitt 2007, Schilthuizen 2013, Schilthuizen 2015). Huber (2010) proposed that the origin of genital asymmetry in insects might be due to evolutionary changes in the mating position, from an ancestral "female-above" position to derived "male-above" position, observed in most insect species. In insects, sperm transfer via intromittent male organs (phallus) evolved from a spermatophore transfer in which the male deposits sperm bags from below into the female's gonopore. This is still observed in many lineages, such as crickets or mantids (Alexander 1964, Alexander, Marshall, and Cooley 1997, Schilthuizen 2015). The evolution from external to internal fertilization might be related to the colonization of terrestrial environments (Schilthuizen 2015, Eberhard 1985). The change in mating posture from female-above to male-above was likely driven by sexual selection and implies a gain of control of the male over the copulatory process. The change in mating position also implies mechanical stress on the female and male genital structures during copulation, that need to couple despite being used in a derived copulation posture. Morphological asymmetry could thus have evolved in diverse species to optimize genital coupling and to compensate a possible mismatch (Huber 2010). Alternatively, left and right sides of genitalia could have evolved to adopt different functions or one-side might got reduced (Huber 2010). However, some investigations remain to be pursued to test Huber's hypothesis, such as testing if the asymmetric state of male genitalia might be under sexual selection by female choice. Also, the described changes in mating position evolved throughout the past 200 million years and are difficult to trace with extant species.

1.5 *Drosophila pachea* and the *Drosophila nanoptera* species group

1.5.1 Ecology of the species from the nanoptera group

To date, more than 1500 species have been described in the genus *Drosophila* (Bächli, Bernhard, and Godknecht 2020). Being species rich, different *Drosophila* species have been grouped into so called "species groups", that contain closely related monophyletic groups of species (Throckmorton 1975). Among them, four species belong to the nanoptera group (Markow and O'Grady 2007): *D. pachea* (Patterson and Wheeler 1942), *D. wassermani*

(Pitnick and Heed 1994), *D. acanthoptera* and *D. nannopectera* (Wheeler 1949). These species live in central America and in Mexico and diverged in the last 3 to 6 million years (Lang et al. 2014). The nannopectera group species are particularly interesting from an evolutionary and ecological point of view to study the causes of ecological specialisation as they exclusively live on columnar cacti of the genera *Stenocereus* and *Pachycereus* (Heed 1982, Fogleman and Danielson 2001, Hernández-Hernández et al. 2011, Copetti et al. 2017). In particular, *D. packea* is an obligate specialist of the senita cactus, *Lophocereus schottii*, that is endemic to the Sonora desert (figure 1). This dependence to the senita cactus relies on a particular Δ^7 -sterol, the lathosterol, produced by this plant (Heed and Kircher 1965 ; Lang et al. 2012) and is due to a few missense mutations in the coding region of the *neverland* gene (*nvd*) (Lang et al. 2012). In insects, the Neverland enzyme converts dietary cholesterol into 7-dehydrocholesterol (7-DHC) as the first metabolic step in the ecdysone hormone synthesis pathway. (Lang et al. 2012). Ecdysone and 20-hydroxy-ecdysone are involved in various developmental processes in arthropods, including major developmental transitions, such as molting or metamorphosis (Huang, Warren, and Gilbert 2008, Ashburner et al. 1989). The mutations in the *D. packea neverland* gene rendered the species dependent on the senita cactus because the Neverland enzyme could only convert cactus derived lathosterol but not cholesterol as precursor for the ecdysone synthesis pathway. In the laboratory, *D. packea* food is supplemented with 7-DHC in order to raise this species.



Figure 1 – *Drosophila packea* habitat.

The Sonora desert area in which *D. packea* live is highlighted in orange. The location of the collection sites for 1698.01 (plus symbol) and 1698.02 (cross symbol) stocks are indicated (see Material and Methods for more details). Scale bar corresponds to 500 km. The map has been extracted from Google maps.

1.5.2 Sperm gigantism in nanoptera species

Among the four described species, *D. acanthoptera* and *D. wassermani* produce medium length sperm (5.83 mm and 4.52 mm, respectively) whereas *D. pachea* and *D. nanoptera* produce giant sperm (16.53 mm and 15.74 mm, respectively) (Pitnick and Markow 1994a). For comparison purposes, the model species *D. melanogaster* produce short sperm of about 1.84 mm long (Amitin and Pitnick 2007), and from 108 *Drosophila* species investigated by Joly, Korol, and Nevo (2004), only 8 species revealed sperm longer than 10 mm. The increase of sperm size that occurred in *D. pachea* has several implications on development and reproductive strategies. In this species, females reach sexual maturity 4 days after emerging, whereas males need 14 days to become fertile (Pitnick 1993). This period of 14 days coincides with the development time needed for the testis to reach its final size (Pitnick and Markow 1994b). The production of giant sperm also implied an increased energy cost of the sperm production compared to species that produce short sperm (Pitnick, Markow, and Spicer 1995). In addition to producing sperm that is about seven times the length of the entire fly (Pitnick and Markow 1994b), *D. pachea* males produce much less sperm compared to most of other *Drosophila* species (Pitnick and Markow 1994b). During a copulation, males transfer only a part of their sperm, and apparently partition it among several females through mating. In average, only 44 ± 6 sperm are transferred to the female per copulation, versus 4000 to 6000 in *D. melanogaster* (Pitnick and Markow 1994b). In addition, *D. pachea*, *D. wassermani* and *D. acanthoptera* females store sperm exclusively in their spermathecae in contrary to 110 other investigated *Drosophila* species that store it in both spermathecae and/or in the seminal receptacle (Pitnick, Marrow, and Spicer 1999). *D. pachea* females have been shown to remate more frequently than females of the three other nanoptera species (1.4 times more often than *D. wassermani*, 1.9 times more often than *D. nanoptera* and 2.1 times more often than *D. acanthoptera*), and several mates are needed to fill up their spermathecae (Pitnick and Markow 1994b). Altogether, these different features can biased the operational sex-ratio, and it has been shown that this ratio is female-biased in *D. pachea* (Pitnick 1993).

1.5.3 Left-right asymmetric male genitalia and mating position in species of the nanoptera group

Asymmetric genitalia have independently evolved multiple times in insects, still they present rather the exception than the rule in the genus *Drosophila*, where asymmetries have

only been described in 11 species (Acurio et al. 2019). However, distinct asymmetries have been identified in the male genitalia of nannoptera group species (Lang et al. 2014, Acurio et al. 2019). *D. acanthoptera* has an asymmetrically twisted phallus. *D. pachea* has an asymmetric phallus and two asymmetric external male genital lobes with the left lobe being longer compared to the right lobe (figure 2) (Pitnick and Heed 1994, Lang and Orgogozo 2012, Lang et al. 2014, Acurio et al. 2019). *D. wassermani* males have concave/convex shaped anal plates, with an enlarged left anal plate (Pitnick and Heed 1994, Lang et al. 2014). Only *D. nannoptera* reveals symmetric male genitalia (Acurio et al. 2019).

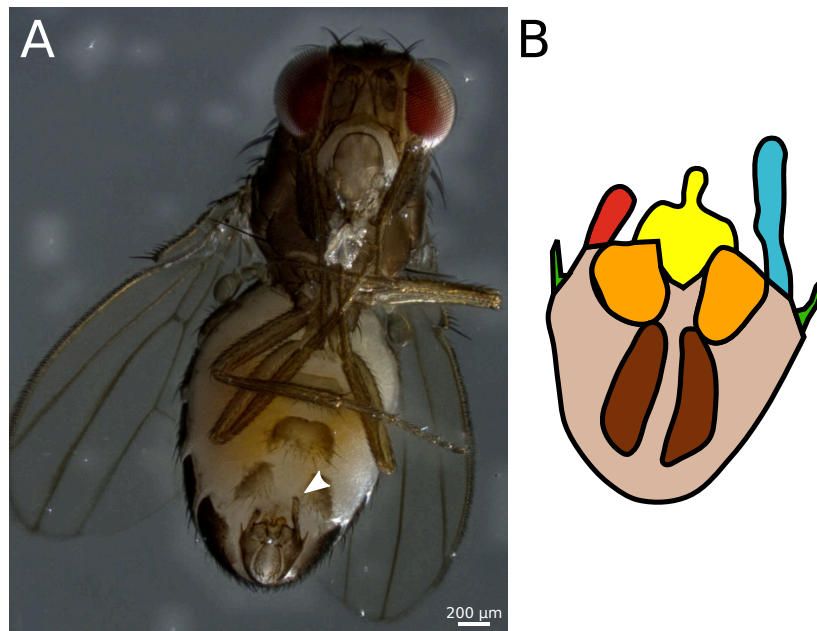


Figure 2 – *Drosophila pachea* male morphology.

A: male *D. pachea* in ventral view (adapted from Lefèvre et al. 2020). The tip of the left lobe is indicated by a white arrowhead. B: Scheme of the outer male genital structure, based on the picture shown in A, showing: left lobe (blue), right lobe (red), anal plates (dark brown), claspers (orange), phallus (yellow), spines (green), and epandrium (light brown).

Copulation postures have been investigated in *D. pachea*, *D. acanthoptera* and *D. nannoptera*. In *D. pachea*, males adopt a right-sided copulation posture with the male being located 6°-8° towards the right side of the female antero-posterior midline (Lang and Orgogozo 2012, Rhebergen et al. 2016, Acurio et al. 2019). In *D. nannoptera*, males tilt-down towards the female's right side during copulation (Acurio et al. 2019). In contrast, *D. acanthoptera* males adopt a classical, symmetrical copulation posture (Acurio et al. 2019) as observed in most *Drosophila* species. In *D. pachea*, the complex of female and male genitalia is asymmetric and the ovipositor is twisted during copulation (Rhebergen et al. 2016). Right-sided mating postures and morphological asymmetries may have evolved repeatedly in the nannoptera

species, since *D. acanthoptera* has an asymmetric phallus and mates in a symmetric position, whereas *D. nannoptera* has symmetric genitalia but copulates in a right-tilted mating posture (Acurio et al. 2019).

Due to its location at the very poster tip of the fly, both at pupal and adult stages, the left-right asymmetric lobes of *D. pachea* are easy to observe and to modify by surgery (Rhebergen et al. 2016), which make of this structure an unique model to investigate the function and development of asymmetric male genitalia. Furthermore, the host lab has identified some males in a lab stock that displayed short left lobes (Lang and Orgogozo 2012). These males revealed to have difficulties to establish a stable mating complex (Lang and Orgogozo 2012). To further investigate the relationship between genitalia morphology and mating posture, Rhebergen et al. (2016) modified the lobes of males, either removing bristles with an ablation laser or by surgically modifying the tip of the lobes, to observe the consequences on the mating postures. Males with modified lobes tended to tilt-down on the female's right side during copulation, similar to *D. nannoptera* wild-type flies. Their study revealed that the asymmetric genital lobes of males *D. pachea* function as a grasping device to stabilize the male-female genitalia complex during copulation. However, the asymmetric lobes may also have a role in pre-copulatory events or at the very beginning of copulation.

1.6 Objectives

During my thesis, I had three main objectives regarding the evolution and development of left-right asymmetric genital lobes of *Drosophila pachea*:

1. Do the the asymmetric genital lobe of males *D. pachea* play a role during pre-copulatory events? My first objective was to test this potential role of lobe asymmetry during courtship and at the onset of copulation, before the complex of female and male genitalia is fully established. To do so, I conducted competitive mating experiments with one female and two males differing in their left lobe length. Asymmetric lobes have been previously shown to stabilize the male-female genitalia complex during copulation (Rhebergen et al. 2016), however, this structure may also affect the male chance to copulate, and thus, might have been favored during evolution due to a pre-copulatory function.
2. Is the development of asymmetric genital lobe due to an overall timing change in the pupal development compared to those of species with symmetric genitalia? My second objective was to characterise the overall developmental timing in *Drosophila pachea* and to compare the relative duration of developmental stages between species. This work also aimed to give an exhaustive description of *D. pachea* development under laboratory conditions for future characterisation of any developmental process of interest.
3. How do the genital lobes develop and what are the differences leading to a short right lobe and a long left lobe? My third objective was to characterise lobe growth process and to investigate how left-right asymmetry is established during the development at the tissue level. To unravel intrinsic growth mechanisms of the lobes, I characterised lobe growth on fixed tissue and quantified the number of nuclei and of mitotic cells per lobe throughout their development. I also monitored this developmental process by time-lapse imaging with transgenic *D. pachea* stocks expressing a truncated DE-cadherin (DE-cad) fused to a Green Fluorescent Protein (GFP) as a membrane marker that I developed. This approach allowed to monitor both lobe growth dynamics and the interplay between lobe tissues and surrounding tissues in the context of genitalia rotation. Furthermore, the development of DE-cad::GFP *D. pachea* stocks raised the possibility of further investigations to decipher in more details the growth mechanisms underlying lobe asymmetry.

2 Material and Methods

2.1 *Drosophila* husbandry

Different *Drosophila pachea* stocks are available in the lab. The stocks 15090-1698.01 and 15090-1698.02 (hereinafter referred to as 1698.01 and 1698.02), were retrieved from the *Drosophila* Species Stock Center at UC San Diego (now the National *Drosophila* Species Stock Center, College of Agriculture and Life Science, Cornell University, USA) (Table 1). Stock 1698.01 originated from multiple females of wild *D. pachea* flies, collected in 1997 at the Organ pipe cactus National Monument in Arizona. Stock 1698.02 was a multi-females stock collected in Bahia de Kino in Sonora in 1996 (figure 1, page 43).

In the laboratory, several inbred lines were established from these two stocks before I started my thesis. Stock 1698.01_14.2 was generated from stock 1698.01 by 11 successive single pair crosses to reduce heterozygosity (Table 1). This stock was used for germline transformation to establish transgenic *D. pachea*. Less genetic variations between individuals was thought to improve genotyping of these flies and to decrease phenotypic variation among individuals. In stock 1698.01, males have asymmetric external genital lobes, such as observed in wild males *D. pachea* (see part 3.1.1, page 77) (Lefèvre 2017, Lefèvre et al. 2020). However, in stock 1698.02, about 10% of males with seemingly symmetric lobes were observed (Lang and Orgogozo 2012, Lefèvre 2017, Lefèvre et al. 2020). A selection stock, Sym222G (hereinafter referred to as "selection stock"), had been established to increase the proportion of males with short left lobes. To do so, three males of stock 1698.02 with apparently symmetric genital lobes were crossed with three to four sibling virgin females. Such crosses were repeated with progeny individuals for a total of 36 generations. Then, selection was continued for another 14 generations by removing males with asymmetric lobes from the resulting stock (table 1). The resulting stock revealed males with variable left lobe lengths (see part 3.1.1, page 77).

Two sister species of *D. pachea* were used in the characterization of developmental duration and in immuno-fluorescent staining procedures to examine developing genitalia: *Drosophila nannoptera* and *Drosophila acanthoptera* (Lang et al. 2014). The *D. nannoptera* stocks 15090-1692.00 and 15090-1692.12 (hereinafter referred to as nan00 and nan12, respectively) were retrieved from the *Drosophila* Species Stock Center at UC San Diego, as well as the *D. acanthoptera* stock 15090-1693.00 (hereinafter referred to as acan) (Table 1). Stocks nan00 and nan12 originated from multiple females of wild *D. nannoptera* flies, collected in 1992 respectively at Oxacana and Pueabla, Mexico. Stock acan originated from multiple females

of wild *D. acanthoptera* flies, collected in 1976 in Oaxaca, Mexico (Table 1).

The *D. melanogaster* stock 14021-0231.7, named hereinafter stock T7, (Drosophila Synthetic Population Resource, formerly maintained by the Tucson Drosophila Species Stock Center, ref. 14021-0231.7) was used to amplify the partial coding sequence of the *shotgun* gene (see part 2.4.1, page 67). The *D. melanogaster* stock BDSC_60584 in which the endogenous DE-cad was fused to GFP developed by Huang et al. (2009) and maintained by Bloomington Stock center was used as a reference to optimize time-lapse microscopy.

stock number	species	source	collection locality or parental stock	establishment date
15090-1698.01	<i>D. pachea</i>	Drosophila Species Stock Center	USA, Arizona, Organ Pipe Cactus National Monument	1997
15090-1698.02	<i>D. pachea</i>	Drosophila Species Stock Center	Mexico, Sonora, Bahia de Kino	1996
1698.01_14.2	<i>D. pachea</i>	Established in the Courtier-Orgogozo lab	15090-1698.01	2016-2017
selection stock	<i>D. pachea</i>	Established in the Courtier-Orgogozo lab	15090-1698.02	2011-2016
15090-1692.00	<i>D. nanoptera</i>	Drosophila Species Stock Center	Oaxaca, Mexico	1992
15090-1692.12	<i>D. nanoptera</i>	Drosophila Species Stock Center	Puebla, Mexico	1992
15090-1693.00	<i>D. acanthoptera</i>	Drosophila Species Stock Center	Oaxaca, Mexico	1976
14021-0231.7	<i>D. melanogaster</i>	Drosophila Species Stock Center	Ken-ting, Taiwan	1968
BDSB_60584	<i>D. melanogaster</i>	Bloomington Stock Center	–	2009

Table 1 – *Drosophila* stock resources.

Drosophila pachea flies were maintained in 25 x 95 mm plastic vials (Dutscher) containing about 10 mL of standard Drosophila medium, which was composed of 60 g/L of brewer’s yeast, 66.6 g/L of cornmeal, 8.6 g/L of agar, 5 g/L of methyl-4-hydroxybenzoate and 2.5% v/v ethanol. As *D. pachea* is dependent on $\Delta 7$ -sterols for proper development (Heed and Kircher 1965 ; Lang et al. 2012 ; Warren et al. 2001), we mixed 40 μ L of 5 mg/mL of 7-dehydrocholesterol (7DHC) (Sigma) dissolved in ethanol into the food with a spatula (standard *D. pachea* food). A piece of 1 cm x 4 cm paper sheet (BenchGuard) was added to each vial as a support for pupae. For behavioral assays, stocks were kept at 25°C at a 12 h light:12 h dark photoperiodic cycle with a 30 min transition from light (1080 lm) to dark (0 lm) and from dark to light. Alternatively, flies were raised at 27°C or 29°C in

order to accelerate development. Flies were transferred into fresh food vials at least once a week (on Fridays), or twice a week (Mondays and Fridays) during periods of stock amplification. *Drosophila nanoptera*, *Drosophila acanthoptera* and *D. melanogaster* were maintained in similar conditions as for *D. pachea* flies, except that 7-DHC was not added to the fly medium.

2.2 Mate competition assay³

2.2.1 Collection and phenotyping of virgin adults for competitive matings

Freshly emerged virgin flies of 0-1 day after hatching from pupae were CO₂-anaesthetized once a day and examined on a CO₂ pad (INJECT+MATIC Sleeper) under a stereomicroscope Stemi 2000 (Zeiss). Flies were sorted according to their sex into fresh vials to collect cohorts of virgin and sexually immature adults. Males and females were kept separately until reaching sexual maturity, at about 14 days for males and 4 days for females at 25°C (Pitnick 1993). This allowed us to use virgin individuals in each mating experiments to avoid learning effects due to multiple matings (Pitnick and Markow 1994b). We had previously observed that males kept in community with other males are less likely to perform courtship. Therefore, males were anaesthetised on the CO₂-pad, sorted according to lobe morphology, and isolated into single vials at least two days before each mating experiment took place.

2.2.2 Lobe surgery

Genital lobe surgery was done on 5-6 day-old adult male *D. pachea* of the selection stock following Rhebergen et al. (2016). Males were anesthetized on a CO₂ pad (INJECT+MATIC sleeper) under a stereo-microscope (Zeiss Stemi 2000) and then further immobilized with a small copper wire, which was slightly pressed onto the male abdomen. The left epandrial lobe was shortened at various lengths with micro dissection scissors (SuperFine Vannas Scissors, World Precision Instruments). Flies were let to recover for at least 7 days or until reaching sexual maturity on standard *D. pachea* food at 25°C in groups. No mortality was observed in males that underwent lobe surgery, similar to what was observed by Rhebergen et al. (2016). Partially amputated lobes ranged in length from lacking at least their most distal tip to more reduced stumps whose length approximated the corresponding right lobe. We shortened the

³The following Material and Methods parts related to mate competition assay are reproduced and eventually adapted from our manuscript Lefèvre et al. (2020).

left lobes of both males by making wounds and amputation sections of similar sizes in order to be able to neglect possible effects of the caused wound on the male's chance to achieve a copulation. Both amputated males also lacked the bristles at most distal tip of the left lobe, which may be possibly involved in male courtship or copulation performance.

2.2.3 Competitive mating assay

A single virgin female of wild-type stock 1698.01 or 1698.02 was introduced with two sibling males of the selection stock that visually differed in lobe length when inspected with a binocular microscope. This selection was done to increase the average pairwise difference of lobe lengths between the two males (figure 3). Males used in our experiments were 14 to 49 days old, and females were 6 to 27 days old. Specimens were introduced into a white, cylindrical mating cell with a diameter of 20 mm, a depth of 4 mm and a transparent 1 mm Plexiglas top-cover. In 16 trials, mating cells were concave with a diameter of 20 mm and a depth of 4 mm at the center. A detailed scheme of the mating cells is shown in figure 4. Flies were transferred without CO₂ anaesthesia using a fly aspirator: a 7 mm diameter silicone tube closed at the tip with cotton and a 1000 μ L wide bore (3 mm) micro-tip. Movie recordings were started as soon as the chamber was immediately put under the camera (see below).

All mating trials were carried out inside a temperature and humidity controlled climate chamber at $25\text{ }^{\circ}\text{C} \pm 0.1\text{ }^{\circ}\text{C}$ and $80\% \pm 5\%$ or $60\% \pm 5\%$ (trials 1-15) humidity. We used digital cameras MIRAZOOM MZ902 (OWL) or DigiMicro Profi (DNT) to record copulation and courtship behaviour. The MIRAZOOM MZ902 (OWL) camera was mounted on a modified microscope stand (191348, Conrad) equipped with a 8-cm LED white light illumination ring (EBAE-COB-Cover, YM E-Bright) and a platform to hold four individual cylindrical mating cells (figure 4). Experiment 16 was filmed with the OWL camera and a concave shaped mating cell that was put on a flat plastic cover on top of the microscope stand. For trials 1-15, we used concave shaped mating cells that were put onto the stand of the DigiMicro Profi (DNT) camera. Data was acquired with the programs Cheese (version 3.18.1) (<https://wiki.gnome.org/Apps/Cheese>) or Gucvview Gtk UVC (version 0.9.9) (trials 1-15) on an ubuntu linux operating system in webm or mkv format. Up to four trials were recorded in a single movie, which was split after recording and converted into mp4 format with Avidemux 2.6 (<http://www.avidemux.org/>) to obtain a single movie per experiment.

We waited for a copulation to take place between one of the males and the female. The

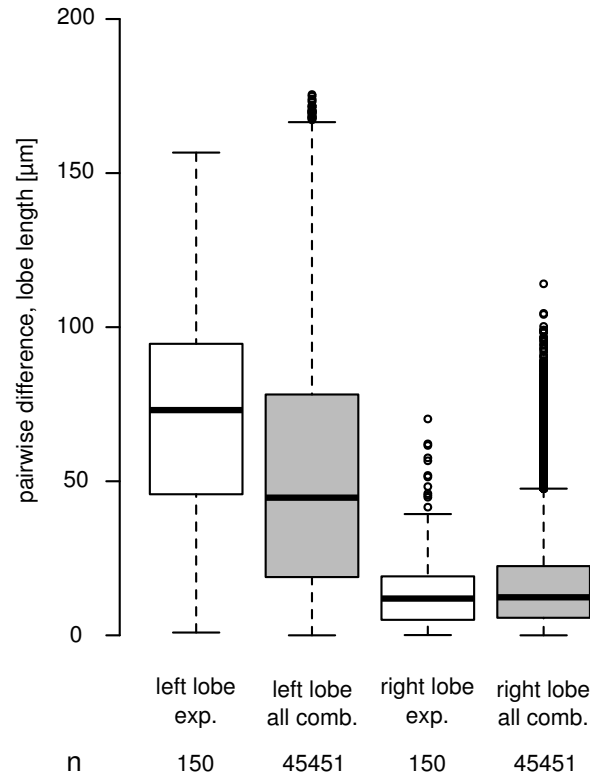


Figure 3 – Pairwise lobe length differences of males used in the competition mating experiments.

The lobe length pairwise length differences of selected pairs in our competition mating experiments (exp., white boxplots) compared to randomly assigned lobe length differences (random comp., grey boxplots).

mating cell was shortly recovered from the climate chamber at about 5-10 min after copulation start and the non-copulating male was isolated from the cell with an aspirator and transferred into a 2 mL reaction tube filled with 70% ethanol. The copulating male and the female were isolated from the mating cell after copulation had ended and were also isolated into single 2 mL reaction tubes filled with 70% ethanol. Optionally, the female was kept alive for 12-24 h in a vial containing 5-10 mL grape juice agar (24 gr/L agar, 26 gr/L sucrose, 120 mg/L Tegosept, 20% v/v grape juice, and 1.5% v/v ethanol). The presence of eggs on the plate was systematically checked but never observed. Females were finally sacrificed to prepare spermathecae.

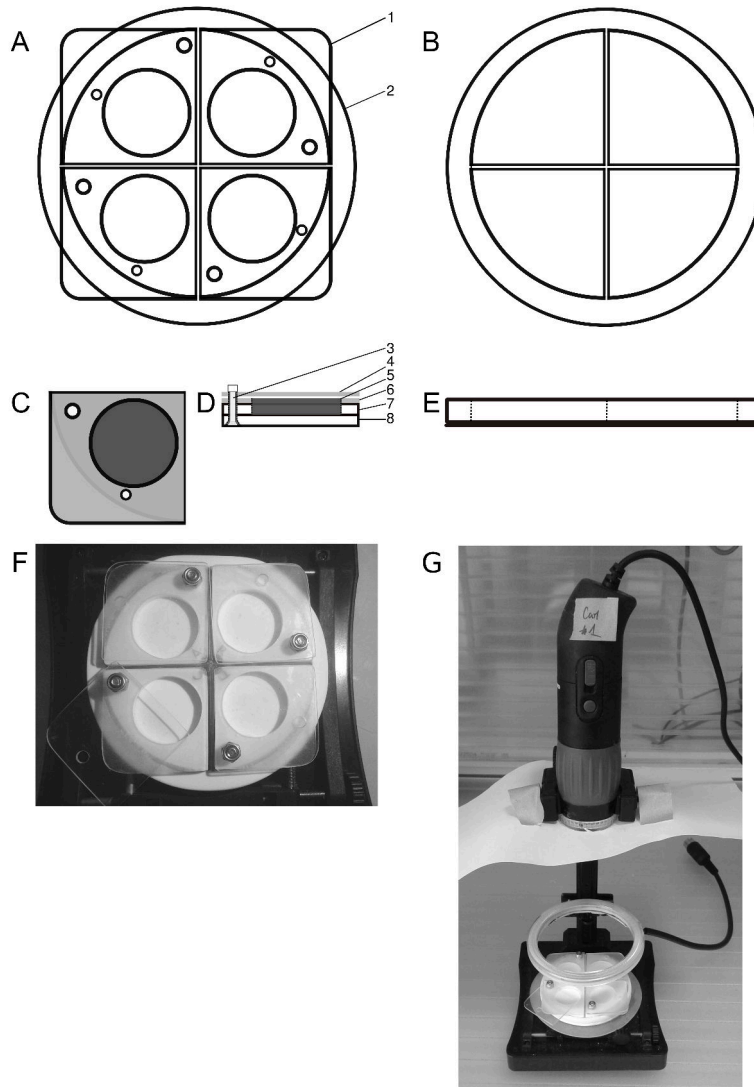


Figure 4 – Camera set-up for recording mating behavior in *D. pachea*.

A) Schematic drawing of 4 mating cells (1) arranged on a round support (2); B) The round support has an inner diameter of 62 mm and is cross-divided (1 mm plexiglas) to hold four individual mating cells; C) The round mating cell support in lateral view. It consists of a Plexiglas ring of 5 mm, an outer diameter of 70 mm and an inner diameter of 60 mm. It is glued to a 1 mm thick Plexiglas bottom layer. Dashed lines indicate the inner edge of the Plexiglas ring and the 1 mm cross division. D) the mating cell is a 30 mm quadrant (top view). A 3 mm screw (3) holds a transparent top cover (4), which has 3 mm bore for the screw and a 2 mm bore to introduce flies. E) The mating cell in lateral view shows the layer construction: it is assembled with a 3 mm screw (3) that holds the 1 mm thick transparent Plexiglas cover (4) on top of a 7 mm thick plastic unit with the cylindrical 20 mm x 4 mm inside of the mating cell (5). It consists of a 1 mm transparent Plexiglas layer (6) that serves as a handle and has an inner bore of 20 mm, a 3 mm thick white Plexiglas layer (7) with the inner bore, and a 3 mm thick white Plexiglas bottom layer (8). F) The assembled mating cell device with 4 mating cells and the support mounted on a microscope stand (191348, Conrad). G) The mating cell device mounted on the microscope stand and equipped with a LED white light 3-12 V, 8-cm illumination ring (EB-AE-COB-Cover, YM E-Bright) and a camera (MIRAZOOM MZ902, OWL).

2.2.4 Adult dissections and imaging

Adults were dissected in water with forceps (Forceps Dumont #5, Fine Science Tool) inside a transparent 25 mm round dissection dish under a stereo-microscope (Zeiss Stemi 2000). Male genitalia were isolated by piercing the abdomen with the forceps between the genital arch and the A6 abdominal segment and thereby separating the genitalia from the abdomen. We also dissected the left anterior leg of each male. Female spermathecae were recovered after opening the ventral abdomen with forceps and removal of the gut and ovaries. The spermathecae were isolated and separated according to left and right sides and immediately examined using a microscope (see below). All dissected tissues were stored in 200 μ L storage solution (glycerol : acetate : ethanol ; 1:1:3) at 4°C.

For imaging, male genitalia were transferred into a dissection dish filled with pure glycerol and examined with a VHX2000 (Keyence) microscope equipped with a 100-1000x VH-Z100W (Keyence) zoom objective at 300-400 fold magnification. Genitalia were oriented to be visible in posterior view. The left and right lateral spines, as well as the dorsal edge of the genital arch were aligned to be visible in the same focal plane. In some preparations, the genital arch broke and lobes were aligned without adjusting the position of the dorsal genital arch. The experiment was discarded from analysis in cases where lobes could not be aligned. Male lobe lengths were measured on acquired images as the distance between the base of each lateral spine and the tip of each lobe using ImageJ version 1.50d (<https://imagej.nih.gov/ij>). Male legs were put on a flat glycerol surface with the inner side of the tibia facing to the camera. Legs were imaged at 200 fold magnification with the VHX 2000 microscope (Keyence) as described above.

We prepared the female paired sperm storage organs (spermathecae) at 12 h - 24 h after copulation and examined the presence of ejaculate. *D. pachea* has giant sperm (Pitnick and Markow 1994a), which makes direct sperm counts difficult. Therefore, we determined an apparent average spermathecae filling level per female based on visual inspection, similar to Jefferson (1977). Female spermathecae were arranged on the bottom of the transparent plastic dissection dish, filled with water. Images were acquired using transmission light in lateral view with the Keyence VHX2000 microscope at 400-500 fold magnification. Ejaculate was directly visible inside the transparent spermathecae. Ejaculate filling levels were annotated for each spermatheca separately to match three different categories: 0, 1/6 or 1/3 of its total volume. Then, the average filling level for both spermathecae was calculated for each female (figure 5).

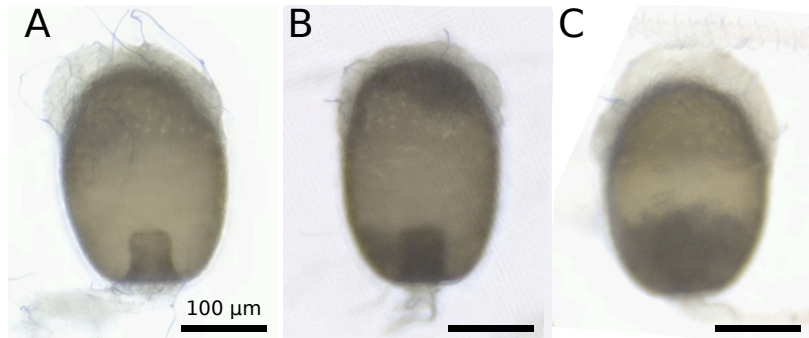


Figure 5 – Ejaculate filling levels in female spermathecae.

Ejaculate is directly visible in the female spermathecae: A: empty spermatheca, B: 1/6 filled spermatheca and C: 1/3 filled spermatheca. Scale bar: 100 μm .

2.2.5 Analysis of courtship and copulation behaviors

Videos were analysed with the OpenShot Video Editor software, version 1.4.3 (<https://www.openshot.org>) to annotate the relative timing of courtship and copulation in our experiments (Figure 6). Data was manually entered into spreadsheets. We annotated the beginning of male courtship as the start of at least three consecutive male courtship behaviours according to Spieth (1952), such as male touching the female abdomen with the forelegs, wing vibration, male following the female, and male “licking”. The latter behavior was estimated as the periods that one male spent with the head being close to the female ovipositor and following it, which was often accompanied by the male proboscis (mouth-parts) touching the female oviscapit or the bottom of the mating cell next to it.

We estimated licking behavior throughout courtship of each male in 158 trials where both males courted the female simultaneously. This data was used to approximate male courtship vigor (figure 6). We calculated the sum duration of all licking events per male and trial and the number of licking sequences. However, this behavior could not be quantified in 7 trials because the males changed positions very fast so that they could not be unambiguously distinguished. In all analysed trials, licking behaviour was observed throughout *D. pachea* courtship from shortly after courtship start to the start of copulation. Both males reached at least once the licking position in all trials (figure 6). This indicates that the female had physical contact with the proboscis of both males before copulation started.

The beginning of copulation was defined as the moment when the male mounted the female abdomen. However, we only scored a copulation start if the male also settled into an invariant copulation posture. Upon mounting, the male moves its abdomen tip forth and

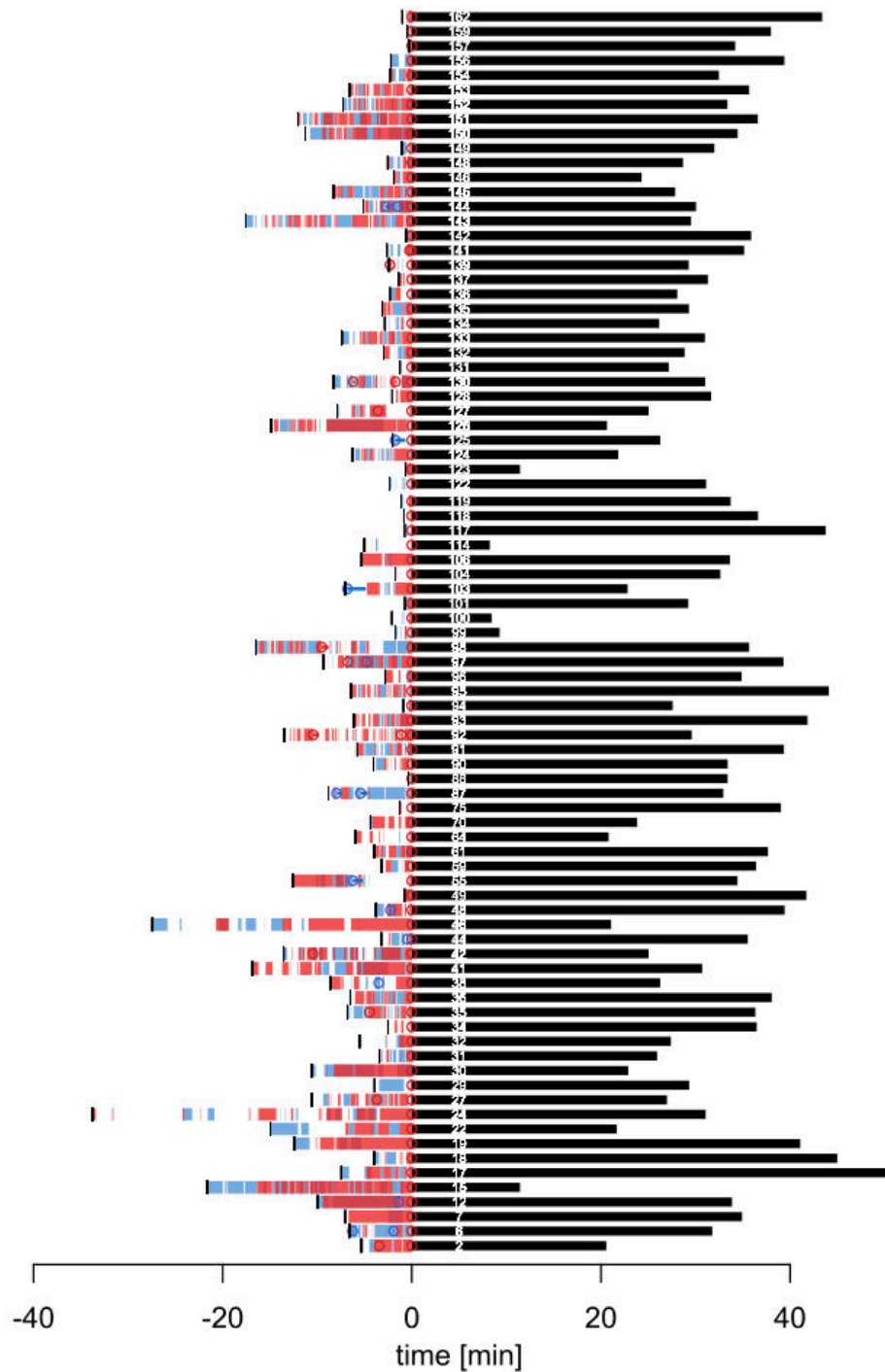


Figure 6 – Courtship and copulation duration in competition mating experiments (continued on following page).

The black dash indicates courtship start, segments indicate licking periods, open circles mark mounting events and horizontal bars indicate the durations of failed mounting attempts of the copulating male (red) and the non-copulating male (blue). The black bar indicates copulation duration and the number refers to the trial (mating ID).

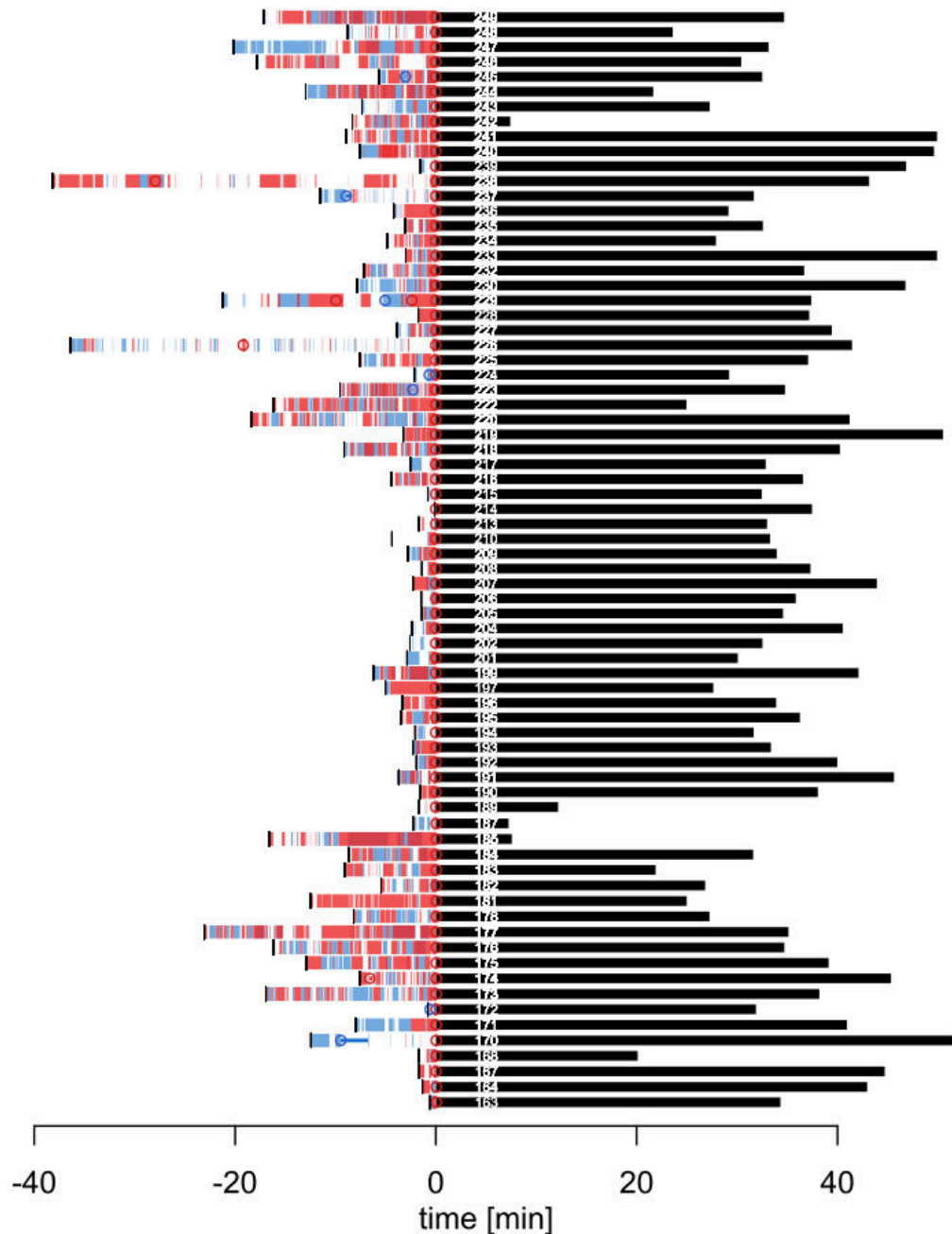


Figure 6 – Courtship and copulation duration in competition mating experiments (continued from previous page).

The black dash indicates courtship start, segments indicate licking periods, open circles mark mounting events and horizontal bars indicate the durations of failed mounting attempts of the copulating male (red) and the non-copulating male (blue). The black bar indicates copulation duration and the number refers to the trial (mating ID).

back along the female oviscapt. This behavior lasts for up to about three minutes and during this time the male grasps the female wings and abdomen with its legs. This behavior was previously described as settling period and ends with a characteristic right-sided, invariant copulation posture (Lang and Orgogozo 2012, Rhebergen et al. 2016, Acurio et al. 2019). Any copulation that ended within the first minutes after mounting without settling was considered to be a “failed mounting attempt”. The end of copulation was considered as the moment when male and female genitalia were separated and the male had completely descended with the forelegs from the female abdomen.

Movie-recording failed during copulation of 5 trials. With exclusion of these trials, a copulation duration of 31.75 ± 7.81 min ($N = 76$, mean \pm standard deviation) was estimated in trials with non-lobe modified males and females of stock 1698.01, of 26.89 ± 7.50 min ($N = 72$, mean \pm standard deviation) in trials non-lobe modified males and females of stock 1698.02, and of 33.44 ± 7.20 min ($N = 60$, mean \pm standard deviation) in trials with lobe modified males and females of stock 1698.01 (table 2). These durations were similar to previous analyses of *D. pachea* copulation durations (Jefferson 1977, Pitnick and Markow 1994b, Lang and Orgogozo 2012, Rhebergen et al. 2016). We observed that copulation ended upon isolation of the non-copulating male in 3/76 trials with females of stock 1698.01 and in 4/76 copulations with females of stock 1698.02. This resulted into premature copulation end but had little impact on average copulation duration estimates when comparing mean and median values.

female	male	n	total courtship duration [min]		sum licking duration [min]		no. of licking sequence		copulation duration [min]	
			median	range	median	range	median	range	median	range
1698.01	non copulating sel. lobe length	47	3.23	0.30-33.80	0.63	0.02-7.68	4	1-22	—	—
	copulating sel. lobe length	47			1.00	0.10-12.53	3	1-29	32.84	10.13-49.21
1698.02	non copulating sel. lobe length	57	6.30	0.74-23.10	1.58	0.04-14.24	5	1-36	—	—
	copulating sel. lobe length	57			2.80	0.14-14.58	5	1-35	27.70	2.72-50.21
1698.01	non copulating modif. lobe length	54	7.20	0.12-38.18	1.28	0.02-12.22	7	1-64	—	—
	copulating modif. lobe length	54			1.84	0.10-14.92	6.5	1-34	33.05	3.45-49.23

Table 2 – Courtship duration, male licking behavior and copulation duration in trials where both males courted the female. Males with non modified lobes: sel. lobe length ; males with surgically modified lobes: modif. lobe length.

2.2.6 Data usage in mate competition assay

Our aim was to compare at least 50 trials, where both males courted the female simultaneously and where copulation was observed. In total, we carried out 98 and 89 trials with females of stocks 1698.01 and 1698.02, respectively (table 3). Then, we performed another 62 trials with males that underwent surgical manipulation of the left lobe and females of stock 1698.01. In total, we removed 36 trials from the analysis because either copulation was not observed until 1 h after recording started (21 trials), flies escaped, got injured or died inside the mating cell (4 trials) or the dissections of male genitalia failed (11 trials). We thus annotated 152 trials with unmodified males and 61 trials with males that had undergone genital surgery. Among those, we observed that both males courted the female simultaneously in 111 and 54 trials, respectively.

female stock	male stock	lobe surgery	number of experiments					
			total	included	excluded*		male courtship	
					no copulation /no courtship	other	one	both
1698.01	selection stock	no	98	76	16/4	2	25	51
1698.02	selection stock	no	89	76	4/0	9	16	60
1698.01	selection stock	yes	62	61	1/0	0	7	54

Table 3 – Competition mating trials used for courtship analysis.

*Experiment excluded when at least one fly escaped, died, or was injured, the movie recording or data storage failed, or the genitalia dissection failed.

2.2.7 Statistical analysis in mate competition assay

Data analysis was performed in R version 3.6 (Core Team 2014). Male copulation success was evaluated with a Bradley Terry Model (Bradley and Terry 1952) (BM) using the R package BradleyTerry2 (Turner, Firth, et al. 2012). We incorporated data from trials where both males courted the female into a list with three objects: 1) the data frame “contest” with the pairings of males, a trial ID and a factor indicating trials with males that had modified left genital lobes, 2) a data frame with trial-specific variables “conditions”, containing data for female age, female stock, courtship duration and a factor indicating which male initiated courtship, 3) a data frame with male-specific predictor variables “male_predictors”, with left and right genital lobe lengths, male tibia length, sum licking duration, number of licking

sequences and occurrences of failed mounting attempts (Lefèvre et al. 2020). We developed the statistical model by evaluating the effect of different variables on copulation success and by comparing the impact of variables in pairwise comparisons of nested models, using Chi-square tests with the generic `anova()` function (Turner, Firth, et al. 2012). This required a complete dataset without missing data, so that we removed 19 trials with missing values of the experiment with non-modified males (left lobe length: 2 trials, right lobe length: 2 trials, licking behavior and/or failed mounting attempts: 7 trials, tibia length: 8 trials) and one trial of the experiment with lobe-modified males (no information on tibia length). In total, we considered 92 trials with non lobe-modified males and 53 trials with lobe-modified males. We tested trial specific variables in interaction with all male-specific variables, but only found an interaction of female age with failed mounting attempts in the dataset with non lobe-modified males. We also tested for interactions between male specific predictor variables but did not find any. The best fitting model for the dataset with unmodified males was: $\text{copulation success} \sim \text{sum licking duration} + \text{number of licking sequences} + \text{left_lobe length} + \text{failed mounting attempt} \times \text{female age}$; and for the trials with lobe modified males: $\text{copulation success} \sim \text{sum licking duration} + \text{number of licking sequences} + \text{left lobe length}$. The male specific variables tibia length (body size approximation) and right lobe length were excluded from the final model because they had no significant impact on copulation success.

Spermathecae filling levels were evaluated with a linear model (R statistical environment) using the `lm()` function: $\text{spermatheca filling level} \sim \text{left lobe length} + \text{right lobe length} + \text{sum licking duration} + \text{Number of licking sequences} + \text{copulation duration} + \text{female age} + \text{male age}$, and significance of each variable was evaluated with an F-test using `anova()`.

2.3 Developmental timing characterization

2.3.1 Cohort synchronisation of embryos, larvae and pupae

The different stages of the life cycle of *D. pachea* were considered to be similar to those of *D. melanogaster*. Eggs are laid by adult females after fecundation. Larvae will hatched from embryo and will undergo three molts and three larval stages are considered that correspond to each instar: L1, L2 and L3. During the L3 wandering stage, larvae will come out from the nutritional medium, stop feeding and crawl around, probably to find a site for pupa formation. Pupae will give rise to adult flies. In contrast to *D. melanogaster* adults that become fertile within minutes or hours after emerging, *D. pachea adults* need 4 days (females) to 14 days (males) to become fertile (Jefferson 1977, Pitnick and Markow 1994b).

We synchronised the developmental stage of *Drosophila* individuals at various stages from embryos to pupae. Those cohorts were used to characterise the developmental progress of *D. pachea* with increased reproducibility. In addition, cohorts of early embryos of stock 1698.01_14.2 were used in germline transformation procedures to generate transgenic *D. pachea* stocks (see part 2.5.1, page 72). For collection of embryo cohorts, about 250-500 adult flies were transferred into a 9 x 6 cm plastic cylinder, closed by a net on the top and by a 5.5 cm diameter pertri-dish lid at the bottom. The petri-dish contained grape juice agar (24.0 g/L agar, 26.4 g/L saccharose, 20% grape juice, 50% distilled water, 12% Tegosept [1.1 g/mL in ethanol] (Dutscher), 4% 7-DHC (Sigma) and 50-200 μ L fresh baker's yeast as food source and egg laying substrate on top (yeast - grape juice agar plates, food plates). Female flies were let to lay eggs on the food plates, which were exchanged every 1-2 hours. Eggs (embryos) were retrieved from food plates by filtering the yeast paste through a 100 μ m nylon mesh (BS, Falcon 352360). The chorion of embryos was removed by a 90 sec incubation of the filter in 1.3% bleach (BEC Javel) under constant agitation until about half of the embryos were floating at the surface of the bleach bath. Embryos were extensively rinsed with tap water for at least 30 sec. Dechorionated embryos were aligned on a flat piece (20 mm x 10 mm x 5 mm) of 2% agar and were then gently lifted with a cover slip coated with Tesa glue. For this, the glue from about 1 m of a double sided tape (50 cm double-sided transparent tesafilm, Tesa) was dissolved overnight in 25 mL n-heptane (Merck). About 15 μ L of dissolved glue was transferred onto the cover slip to make a 3-mm wide stripe at one edge. The solvent was let to evaporate for about 2 min. For germline transformation, embryos were let to dry for 5 min to decrease their water content. This drying time was eventually adjusted in function of air humidity. Embryos were finally covered with 40 μ L of Voltalef 10S halocarbon oil (VWR) to avoid desiccation, and maintained and observed at 25°C until larvae hatched.

Cohorts of synchronised larvae were collected from food plates (see above), on which females were allowed to lay eggs for about 2 h. The plates were kept at 25°C until larvae hatched. Larvae were retrieved from the yeast paste with a fine forceps (Dumont #5, Fine Science Tool) or by filtering the yeast surface through a nylon mesh (see above).

Cohorts of synchronised pupae were obtained by collecting white pupae (see below) with a wet brush directly from *D. pachea* stock vials (Bainbridge and Bownes 1981). Individuals were placed onto moist Kimtech tissue (Kimberly-Clark) and put into a 5 cm diameter petri dish. Petri dishes with pupae were kept at 25°C inside plastic boxes, which also contained wet tissue paper.

2.3.2 Time lapse recording of embryonic development

To investigate the duration of the embryonic development in *D. pachea*, a cohort of embryos was collected after a period of 1 h of egg laying (see above), using adults of the 1698.01 stock. Live-imaging was carried out inside a temperature and humidity controlled chamber at $25^{\circ}\text{C} \pm 0.1^{\circ}\text{C}$ and $80\% \pm 1\%$ humidity after approximately 10 min of embryo preparation (see part 2.3.1, page 60). Thus, embryos had a maximum age difference of 70 min. Time lapse acquisition was performed at 1 image/7.5 sec for 36 h with a digital camera (Conrad 9-Megapixel USB digital microscope camera), using the program Cheese (version 3.18.1) on a computer with an ubuntu 16.04 linux operation system. Movies were assembled with avconv (libav-tools). Out of 28 embryos monitored, 12 pursued their development until hatching (43%). The determination of the overall embryonic development was determined based on these individuals, while the others were excluded from consideration. The duration of the embryonic development was measured as the time between the beginning of the recording and the hatching of the larva from the embryo.

2.3.3 Dissection and imaging of larvae

Vials with synchronised cohorts of larvae (see part 2.3.1, page 60) were examined once a day for about 10 days until all larvae had turned into pupae. Optionally, larvae were collected with fine forceps (Dumont #5, Fine Science Tool) and stored frozen at -20°C for later dissection. The instar stage of each dissected individual was determined based on larval tooth morphology (Strasburger 1935) (figure 7).

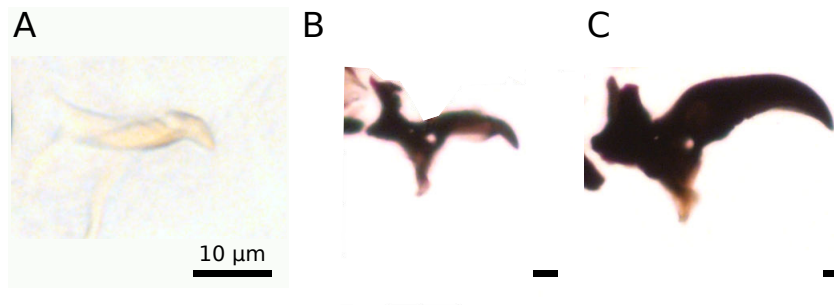


Figure 7 – Mouth hook morphology at the different larval instar.

Larval mouth hook from A: first, B: second, and C: third larval instar in *Drosophila pachea*. The scale bar is 10 μm .

For this, mouth parts were mounted in 20 μ L dimethyl-hydantoin formaldehyde (DMHF) medium (Entomopraxis) beneath a cover slip, which was gently pressed against the microscope slide to orient larval teeth in a flat, lateral orientation to the microscope objective. Larval teeth were imaged at 100 or 400 fold magnification in bright field illumination using the microscope IX83 (Olympus).

2.3.4 Determination of developmental pupal stages in *D. pachea*

To precisely characterise the duration of the puparium formation, we monitored nine pupariating larvae by time-lapse imaging. As larvae move before pupa formation, it was not possible to mount them in an immobile way. Instead, larvae at the third instar stage and third instar wandering stage were collected from stock 1698.01 and transferred into *D. pachea* standard medium (see part 2.1, page 48), inside a 5 cm diameter petri-dish, containing a piece of 1 cm x 4 cm paper sheet (BenchGuard). The dish was then placed into an open plastic box with moist paper in which larvae were free to move. Time-lapse acquisition was launched as previously described (see part 2.3.2, page 62). The duration of the white puparium stage was measured from the moment when the larva had everted the anterior spiracles and stopped moving up to the moment when the pupal case became gradually brown. White puparium stage lasts for about 102 min in *D. pachea* at 25°C. Thus, white pupae mark the very beginning of the puparium formation and collected cohorts at this stage had a maximum age difference of about 102 min (see part 2.3.1, page 60).

Developmental progress of synchronized pupa cohorts (see part 2.3.1, page 60) was examined at various time points using a stereomicroscope VisiScope SZB series 200 (VWR) and developmental stages were determined at various time points by eye according to Bainbridge and Bownes (1981). Alternatively, the development of pupae was recorded by time-lapse imaging (see part 2.3.2, page 62). For this, the anterior part of the pupal case was removed, letting the head and the anterior part of the thorax visible. Pupae were observed from 50 h after puparium formation (APF) until adults emerged. Image acquisition was done at 25°C \pm 0.1°C and 80% \pm 1% humidity in a controlled climate chamber, using VLC media player software, version 3.0, taking one picture every 13:02 min:sec for about 115 h. The results from both approaches were very similar for *D. pachea* and *D. nannoptera*, indicating that the removal of the anterior part of the pupal case did not disturb pupal development.

2.3.5 Characterisation of rotation timing of *D. pachea* male genitalia on freshly dissected samples

The characterization of the timing of genitalia rotation was done by dissection of pupae from synchronized cohorts (see part 2.3.1, page 60) at various time-points during pupal development between 16 h APF and 48 h APF. The posterior part of the pupa was dissected in a dissection dish filled with water, and the abdominal tissues were removed by gently flushing the pupal tissues of the posterior part of the pupa with a P20 or P200 pipetter (figure 8). Male genitalia are relatively compact tissues compared to other pupal tissues and stayed connected to the pupal epidermis. The genitalia were then visible under a stereomicroscope. Pictures were taken from the posterior part of the sample with a light microscope VHX2000 (Keyence) (figure 8). The rotation angle was measured using ImageJ software, version 1.50d (Schneider, Rasband, and Eliceiri 2012), as the angle between the ventrally located tip of the legs and the mid-point of the anal plates that are part of the rotating tissue (figure 8).

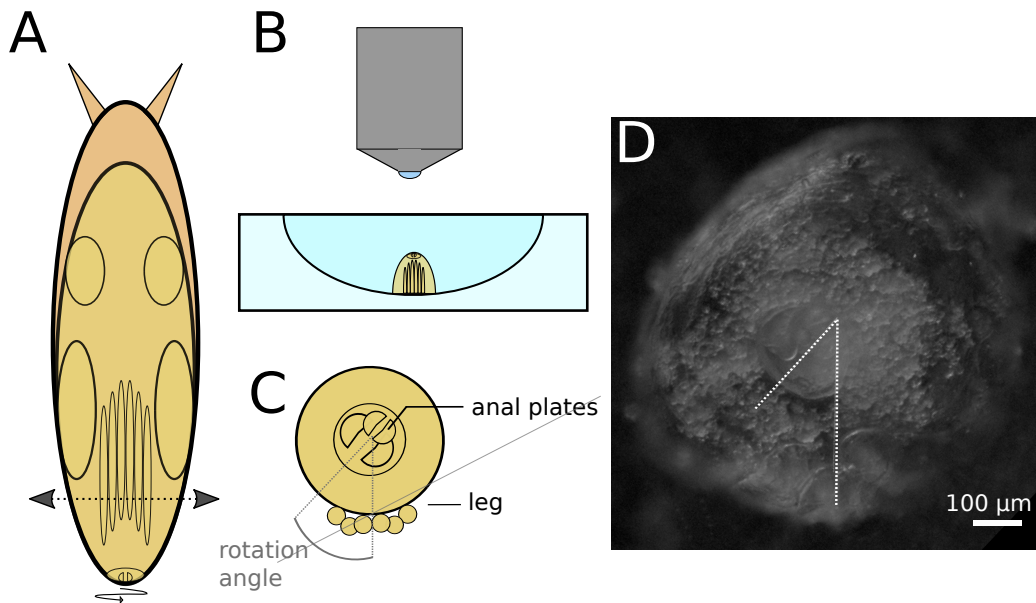


Figure 8 – Dissection strategy to characterise genitalia rotation timing in *D. pachea*.

A: Scheme of a pupa, separation of pupal tissue is indicated by the grey arrow. B: Dissected posterior part of a male pupa positioned upside down inside a dissection well for microscope imaging. C: Rotation angle measured as the angle between the ventrally located legs and the mid-point of the anal plates. D: Image of male terminalia dissected at 26 h APF, the rotation angle is indicated by white dotted lines.

2.3.6 Immuno-staining of male genitalia during pupal development

For characterization of the timing of asymmetric genital lobe development and to investigate the distribution and the rate of mitotic cells throughout the developing lobes in males *D. pachea*, I dissected 87 pupae from the wild-type stock 1698.01 and 107 pupae from the selection stock at various time points during development, ranging from 16 h APF to 46 h APF (see part 2.3.1, page 60, for details on synchronization). The posterior part of the pupa was dissected in a dissection dish filled with cold phosphate-buffered saline buffer (PBS ; 137 mM NaCl, 1.7 mM KCl, 8 mM Na₂HPO₄ pH = 7.4) and the abdominal tissue was removed as mentioned above (see part 2.3.5, page 64) by gently flushing PBS into the posterior part of the pupa with a P20 pipetter. However, here I kept flushing until the genitalia finally detached from the pupal skin. Samples were kept in PBS on ice for about 15 min until the dissection of 5 to 10 male genitalia was achieved. Tissues were fixed for 20 min in 500 μ L of 4% paraformaldehyde (PFA) (Sigma-Aldrich), diluted in PBS at room temperature. Incubation was carried out inside 5x15 mm (diameter x height) plastic baskets (parts of a 1.5 mL Eppendorf reaction tube) with a 100 μ m nylon mesh glued to the bottom. Baskets were placed into a well of a 24 well micro-titer dish. Liquid exchange was then achieved by transferring the basket with the genital samples into different wells. In total, samples underwent three incubations (washes) for 5 min in PBS with 0.1% Tween 20 (PBT) to stop the fixation and remove the PFA. Then, two washes were carried out in Tris-NaCl-Tween buffer (TNT ; 0.1 M Tris-HCl, 0.3 M NaCl pH = 7.4 with 0.5% Triton X-100). After that, samples were incubated for 1-2 h in bovine serum albumine (BSA, Sigma-Aldrich) diluted in TNT at 0.5 mg/mL to block possible unspecific epitopes. Then, samples incubated overnight at 4°C in rabbit anti-PhosphoHistone H3 antibody (ThermoFisher, #701258), at a dilution of 1:200 in TNT. Samples underwent four washes in 500 μ L TNT for 10 min at room temperature, followed by 1 h incubation at room temperature in the dark in TNT with a 1:200 dilution of the secondary antibody donkey anti-rabbit-A488 (ThermoFisher, #SA5-10038). Then, samples were transferred into TNT containing 0.25 μ g/mL of 4'6-diamidino-2-phenylindole (DAPI) (Sigma-Aldrich) and incubated for 15 min to stain nuclei. Finally, samples were washed three times for 5 min in TNT and an additional incubation was done in PBS before mounting because TNT precipitation had been previously observed in the mounting medium.

To mount the stained developing genitalia, we followed the advice of the imagoSeine platform to mount large and complex tissues (personal communication with Orestis Faklaris). Two spacer coverslips (Menzel-Gläser) were glued on a slide (ThermoScientific) that formed a 5-mm gap between them. The gap was filled with Vectashield H-1000 mounting medium

(Vector Laboratories) (Figure 9). The samples were first transferred into the edge of a coverslip 1.5 H (Marienfeld) together with a 10-20 μL drop of PBS using a P20 pipetter. PBS was absorbed with kimtech foil (Kimberly-Clark). Under these conditions, most of the samples got stuck to the coverslip surface in the correct orientation of the tissue with respect to the view of the microscope objective. Finally, samples were transferred into the mounting medium by orienting the coverslip onto the prepared slide (Figure 9). The assembled slide with coverslip was finally sealed with nail polish.

Samples were examined with a DMI8 inverted microscope (Leica) equipped with a spinning disc confocal head CSU-W1 (Yokogawa Corporation of America) and controlled by MetaMorph software (Molecular Devices), located at the ImagoSeine platform at the Institut Jacques Monod. Standard acquisition parameters were: GFP fluorescence was detected after illumination of the samples with a 488 nm laser set at 40% intensity, with an exposition of 200-400 ms, used with a 500-530 nm emission filter. DAPI fluorescence was detected after illumination of the samples with a 405 nm laser, set at 40% intensity, with 200-250 ms exposition.

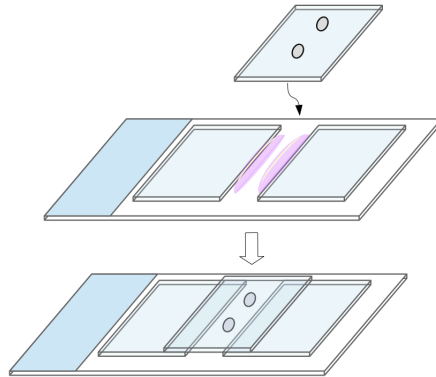


Figure 9 – Mounting of dissected genitalia from *D. pachea* males.

A slide with two spacer coverslips and a 5 mm gap in between, filled with mounting medium. Dissected samples were oriented on a coverslip and then the cover slip was put onto the prepared slide as shown by the black arrow.

2.4 Molecular methods used to clone a PiggyBac plasmid containing a DE-cadherin fused to a Green Fluorescent Protein

2.4.1 Cloning strategy

To develop PiggyBac plasmid containing fluorescent membrane marker, we proposed the following cloning strategy.

First, we modified a act-Histone H3::GFP PiggyBac plasmid available in the lab, which is a modified version of pBac[3xP3-EGFP afm] vector (Horn and Wimmer 2000) (figure 10A). This PiggyBac germline transformation vector contains a 3xP3-RFP transformation marker to screen for transgenic individuals (Horn and Wimmer 2000). The RFP marker is transcribed in the adult eyes due to an artificial *eyeless* promoter (Horn and Wimmer 2000). The PiggyBac elements enable to insert this vector randomly into the *D. pachea* genome using the PiggyBac transposase system (Handler et al. 1998, Handler and Harrell 1999). The aim was to produce a plasmid containing the act5C promoter, followed by a unique XhoI restriction site and the downstream eGFP coding sequence (figure 10B). This plasmid would be a useful tool to fuse any coding sequence of interest with GFP and to ubiquitously express this construct with the act5C promoter. We digested the act5C-H2::GFP plasmid (figure 10A) with NdeI and purified the backbone. Three sequences, annotated F1, F2 and F3, with respective lengths of 515, 1715 and 2267 bp, were amplified by PCR (see part 2.4.4, page 70) from the initial plasmid in order to derive the plasmid shown in figure 10B by Gibson assembly (Gibson et al. 2009). Primers F1_F and F1_R, F2_F and F2_R, F3_F and F3_R, used to amplify fragment 1, 2 and 3 respectively are shown in the annex (see annex 6.2.3, page 150). Primers were designed to be overlapping for at least 15 bp for each consecutive fragment in order to increase Gibson assembly efficiency and the primers F1_R and F2_F were used to add an XhoI restriction site enabling the later insertion of the *shg* coding sequence (see the annex, page 150).

Second, we prepared a partial coding sequence of the *shg* locus, encoding *D. melanogaster* DE-cadherin domains into the cloning plasmid vector pGEM-TEasy plasmid (Promega). The *shg* coding portion was also surrounded by two XhoI sites for subcloning it into the act5C-GFP PiggyBac vector (figure 10B). To clone the partial coding sequence of the *shg* gene, two DNA fragments were amplified by PCR (see part 2.4.4, page 70) from *shg* cDNA of *D. melanogaster* T7 (figure 10C). Fragment_4 was 1627 bp long and encoded the *D. melanogaster shg* 5' UTR and two initial cadherin repeats that are majorly cleaved as a

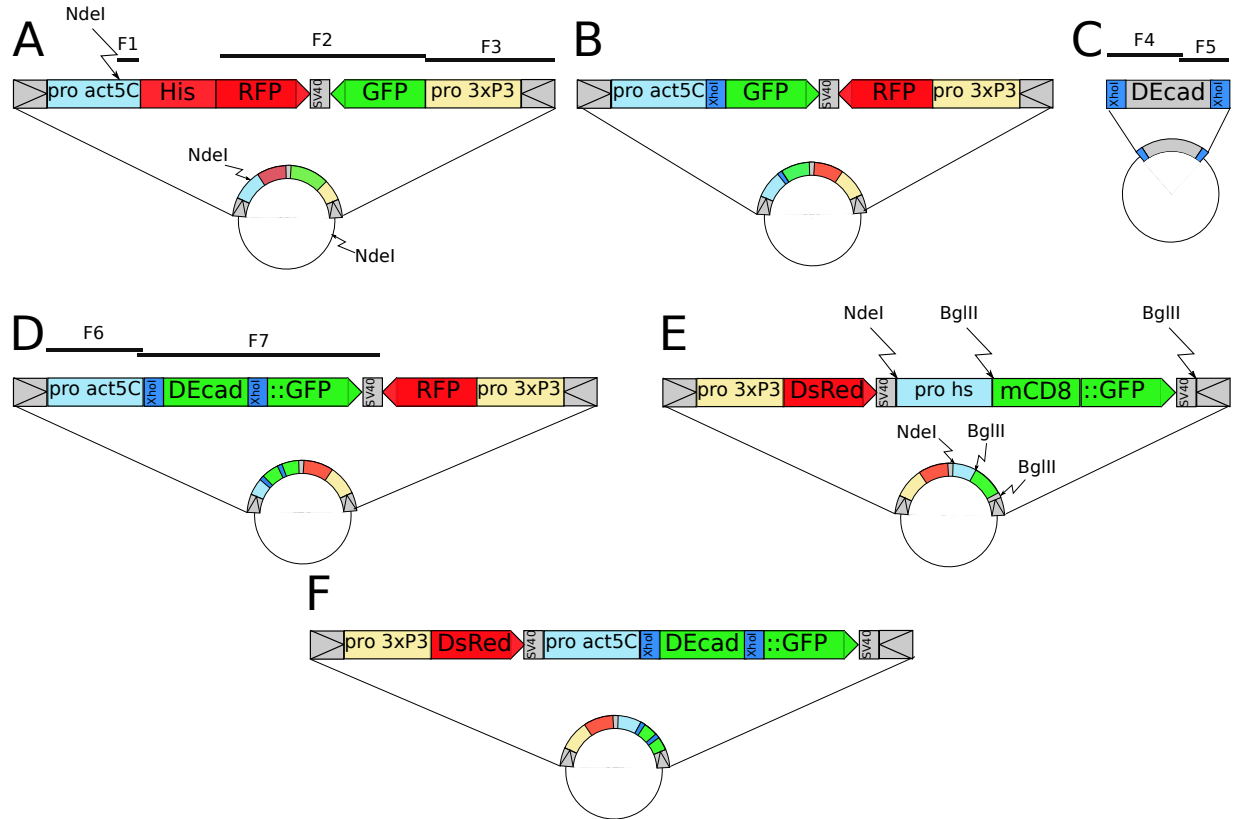


Figure 10 – Cloning strategy to produce a PiggyBac plasmid containing a truncated DE-cad fused to GFP.

Schemes of the different plasmids we used in our cloning strategy are shown. Grey boxes containing arrows indicate the PiggyBac left and right arms. The different sequences of interest are indicated in colored boxes. Promoters are indicated by the abbreviation "pro". Restriction sites used in the cloning experiments are shown as well as amplified DNA fragments. Each of these plasmids display a ColE1 replication origin and an Ampicillin resistance gene.

DE-cad specific pro-peptide (corresponding to the first exon and the 276 first nucleotides of the second exon). Fragment_5 was 342 pb long and contained the DE-cad trans-membrane domain and a part of the cytoplasmic domain, but lacking the β -Catenin binding domain (corresponding to nucleotides 5865 - 6179 ; Huber et al. 2001; Pacquelet and Rørth 2005). Fragments 4 and 5 were amplified with primers F4_F/F4_R, and F5_F/F5_R respectively (annex). Primer F4_F and F5_R were used to add the XhoI restriction sites mentioned above. Fragment 4 was inserted upstream of fragment 5 by Gibson cloning (Gibson et al. 2009) into pGEM-TEasy vector, which was linearized with the restriction enzyme NdeI . The structure of the predicted truncated DE-cad encoded by our construct is shown in figure 10D.

Our two plasmids shown in figure 10B and C were digested with XhoI, the truncated *shg* DNA fragment was purified and ligated into the linearized act5C-XhoI-GFP plasmid, giving

the act5C-DE-cad::GFP/3xP3-RFP construct, shown in figure 10D. However, the resulting clone act-DE-cad::GFP revealed variable lengths in some preparations due to partial loss of the eGFP and RFP coding sequences.

We therefore re-amplified the act5C-shg::GFP portion of this plasmid in two fragments. Fragment F6 of 2619 bp with primers F6_F and F6_R, and fragments F7 of 2995 bp with primers F7_F and F7_R (figure 10D ; primers shown in the annex) were then cloned by Gibson Assembly into a new PiggyBac backbone pBAC-DSRed-15xQUAS_TATA-mcd8-GFP-SV40. This plasmid was derived from the pBAC-ECFP-15xQUAS_TATA-mcd8-GFP-SV40 (Addgene 104878, gift from Christopher Potter) where the 3xP3-ECFP integration reporter gene was replaced by DsRed. The pBAC-DSRed-15xQUAS_TATA-mcd8-GFP-SV40 plasmid was linearized with NdeI and BglII (New England Biolabs) (figure 10E) to release the mcd8-GFP portion and to integrate fragments 6 and 7, containing the act5C-shg::GFP portion. The resulting plasmid, named hereinafter DE-cad::GFP PiggyBac plasmid (figure 10F), was 11003 bp long and revealed to be stable in subsequent plasmid preparations.

The detailed map of the different plasmids used as well as the final plasmid and their putative sequences are shown in the annex, page 151.

2.4.2 Sequence alignment

All deoxyribonucleic acid (DNA) sequences used in the cloning experiment were analysed using Geneious software (Biomatters, version R6.06). Alignments were done with the Geneious global alignment, with a gap open penalty of 12 and gap extension penalty of 3, and refined manually.

2.4.3 RNA extraction and retro-transcription from *D. melanogaster* T7 stock

Ribonucleic acid (RNA) was extracted from a pool of 5 females and 5 males from the *D. melanogaster* wild-type stock T7 in order to reverse-transcribe RNA into complementary DNA (cDNA) and to amplify fragments of the *shotgun* gene by polymerase chain reaction (PCR). The RNA extraction and purification was carried out using the Nucleospin RNA minikit (Macherey-Nagel) following the manual's instructions. The elution was done in a volume of 60 μ L and the RNA concentration was measured with a DS-11 Series Spectrophotometer/Fluorometer (DeNovix). The reverse transcription reaction was carried out with the SuperScript III First-Strand Synthesis System (ThermoFisher), 5 μ gr total RNA, 1.2 μ M

oligonucleotide m_DE-cad_3'UTR_R , and 0.4 mM dNTP (each) in 25 μ L reaction volume. The RNA template and the primer were heated for 5 min at 65°C and then rapidly chilled on ice for 1 min. The SuperScript III First-Strand Synthesis System (ThermoFisher) mix was prepared following supplier's instructions. A total of 25 μ L reaction mix were added to 25 μ L containing 5 μ g RNA and the reaction was carried out at 55°C for 2 h. The cDNA was stored at -20°C.

2.4.4 Amplification of DNA fragments by PCR

The amplification of DNA , described in part 2.4.1, page 67, was done by polymerase chain reaction (PCR) (Mullis et al. 1986). The primers used were optionally compatible with Gibson assembly (shown in the annex) and were designed either using Geneious (Biomatters, version R6.6) or NEBuilder tool (New England Biolabs, version 2.2.7) and produced by GATC (Eurofins). Annealing temperature and oligo compatibility were assessed using PerlPrimer software (Source Forge, version 1.1.21). PCR reactions were carried out in 35 μ with 7 units Phusion Taq polymerase (New England Biolabs), in 1x high fidelity buffer (New England Biolabs), 3-300 ng DNA template, 0.3 mM dNTPs (each) and 0.7 μ M of forward and reverse primer. The PCR program was composed of 1 cycle of 20 sec at 98°C, followed by 35 cycles of: 10 sec at 98°C, 30 sec an empirically derived annealing temperature suitable for each primer pair, and 1 min at 72°C for fragment extension/kb of amplified DNA, followed by a single final extension step of 7 min at 72°C.

2.4.5 DNA fragment purification

PCR products and restriction digestion fragments were isolated and purified from 1% agarose gels after migration in Tris Acetate EDTA buffer (TAE) for 45-90 min at 50 V. For this, the sides of the gel with a small portion of the sample well were cut and stained for 15 min 5 μ L ClearSight DNA stain (BioAtlas) in 100 mL TAE and under agitation. stained parts of the gel were examined on a UV-desk (Transilluminator, Sigma-Aldrich) and a notch was introduced to mark the location of the DNA fragment of interest. The gel was reassembled and a band was cut out of the non-stained gel that corresponded to the locations of the notches in the stained parts. DNA was then purified from the agarose band using the Gel and PCR Clean Up kit (Macherey-Nagel). Concentration of the purified product was determined using a DS-11 Series Spectrophotometer/Fluorometer (DeNovix). Purified DNA was then used for cloning or sequencing.

2.4.6 Plasmid linearization

The act-GFP PiggyBac plasmid and the 3Xp3-DsRed/hs-mCD8::GFP plasmids (see part 2.4.1, page 67, for more details) were linearized with restriction enzymes NdeI and BglII (ThermoScientific). Digestions were done with 1 μ g plasmid DNA, in 50 μ L reaction volume containing fast digest buffer (ThermoScientific) and 10 to 20 units restriction enzyme. Reactions were carried out overnight at 37°C. Digested plasmids were dephosphorylated by addition of 1 μ L Fast Alkaline Phosphatase (ThermoFisher) and further incubation at 37°C for 10 min. Dephosphorylation lowered the ability of self-circularization of the plasmid in downstream cloning procedures. In addition, linearized plasmid was purified from agarose gels as described above to exclude remains of non-digested plasmid.

2.4.7 Gibson assembly and bacterial transformation

Molecular cloning of plasmids was done following the one-step isothermal DNA assembly protocol from Gibson et al. (2009). PCR amplified DNA fragments were mixed at equimolar ratio with 100 ng of linearized and dephosphorylated plasmid in a 5.00 μ L pre-mix on ice. This pre-mix was then added to 15.00 μ L of Gibson mix, 0.5 units Phusion Taq (New England Biolabs), 80 units Taq ligase (New England Biolabs), 0.08 units T5 exonuclease (New England Biolabs), 10 mM Tris-HCl pH 7.5, 10 mM MgCl₂, 0.2 mM of dNTPs (each), 10 mM DTT, 5 g/L PEG-8000 and 1 mM NAD. This mix was incubated for 10 min at 37°C for partial digestion of the DNA by the T5 exonuclease, followed by 3 h incubation at 50°C for ligation and DNA repair. As a control, we carried out reactions that only contained the linearized and dephosphorylated plasmid.

One microliter of this mix was added to 25 μ L of NE10- β cells (New England Biolabs) and kept on ice for 30 min. Chemical transformation was accomplished via a 30 sec heatshock at 42°C, followed by a 2 min incubation on ice. Cells were then mixed with 500 μ L of Super Optimal Broth (SOC ; composed of 2 % tryptone, 0.5 % yeast extract, 10 mM NaCl, 2.5 mM KCl, 10 mM MgCl₂, 10 mM MgSO₄ and 20 mM glucose) and incubated for 1 h at 37°C and 220 rpm. The transformation culture was plated on three plates of Lysogeny Broth (LB) containing 100 μ g/mL Ampicillin by spreading 50, 100 and 350 μ L. Colonies were let to grow overnight at 37°C.

2.4.8 Plasmid purification and evaluation of transformation products

Single colonies were isolated with a 10 μ L pipette tip and grown overnight in 4 mL LB containing 50 μ g/mL Ampicillin , at 37°C and 220 rpm.

Glycerinated stocks were prepared by mixing 812 μ L grown culture medium with 187 μ L 80% glycerol (15% final glycerol concentration). Stocks were stored at -80°C. The rest of the culture was used to isolate the plasmid with the E.Z.N.A minikit I (Omega), following the supplier's instructions. Elution was done in 100 μ L elution buffer and DNA concentrations were measured with a DS-11 Series Spectrophotometer/Fluorometer (DeNovix).

The correct assembly of plasmids was tested by examination of DNA fragment lengths of restriction digested plasmids by gel electrophoresis (see above). Digested DNA was run on a 0.8% agarose gel. Plasmid clones were further evaluated by Sanger sequencing if the length of the digested DNA fragment matched the predicted lengths. Sanger sequencing was carried out on 100 ng supercoiled plasmid DNA by Eurogene TAGC with sequencing primers (annex). Finally, bacterial clones were amplified for 2-3 h 4 mL LB with 50 μ g/mL of Ampicillin (LB-Amp) at 37°C and 220 rpm. The pre-culture was then added to 300 mL LB-Amp and incubated overnight at 37°C and 220 rpm. Plasmid was purified from the grown culture using the NucleoBond Xtra Maxi Plus kit (Macherey-Nagel) following the supplier's instructions and eluted in 1 mL. DNA concentrations were examined with a DS-11 Series Spectrophotometer/Fluorometer (DeNovix).

2.5 Development of transgenic *D. pachea* expressing DE-cad::GFP for live imaging

2.5.1 Germline transformation in *D. pachea*

The inbred stock 1698.01_14.2 (see part 2.1, page 48) was used to produce transgenic *D. pachea* using the PiggyBac transposase approach (Handler et al. 1998 ; Handler and Harrell 1999 ; Handler and Harrell 2001). This method relies on the injection of a mix of two plasmids: a PiggyBac plasmid that contains a sequence of interest flanked by two specific repeat regions of a transposable element, and a helper plasmid that contains the corresponding transposase gene under control of a heatshock promoter (Handler et al. 1998). The transposase recognizes the specific repeated regions in the PiggyBac plasmid, leading to insertion of the sequence of interest into the genome of the injected cells at nearly random

locations (Handler et al. 1998).

The injection mix was prepared on ice and contained 100 ng/ μ L of helper plasmid (Handler et al. 1998), 100 ng/ μ L act5C-DE-cad::GFP PiggyBac plasmid (see part 2.4.1, page 67) and 1X Cas9 buffer (NEB). This mix was stored at -20°C between two injection sessions. Injection needles (1 mm diameter boro-silicate needles, GBF100-50-10, WPI) were prepared in the lab with a P1000 (Sutter) needle puller with the following parameters: heating: 458; velocity: 80; delay: 200; pressure: 500. Three microliters of the injection mix were loaded with a microloader tip (Eppendorf) into the injection needle before mounting it onto a micromanipulator 056530 (Leitz) and connecting it to a micro-injector Femtojet 4 (Eppendorf). Needles were opened by gently ripping it along the coverslip edge.

The injection procedure for *D. pachea* was previously optimized by Josu  Vidal and Michael Lang based on Spradling and Rubin (1982). Cohorts of synchronized embryos were collected as previously described in part 2.3.1, page 60. To optimize germline transformation of embryos, it is essential to inject the plasmid mix into early embryos at the syncytial blastoderm stage, before cell membranes form (Spradling and Rubin 1982). As this process takes place about 2-3 h after egg laying in *D. pachea*, the synchronized cohorts were obtained from 2-h incubation of egg laying plates, so most of the embryos were not yet cellularized when the plasmid injection was done. Embryos were prepared as described in part 2.3.1, page 60. The coverslip with aligned embryos was glued onto a slide (ThermoScientific). To avoid embryo disruption during plasmid mix injection, embryos were let to dry on air for 5 min. This drying time was eventually adjusted with respect to air humidity. The drying was stopped by covering embryos with 40 μ L (2 drops) 10S Voltalef oil (VWR). The injection needle and the prepared embryos were mounted onto a Leica DM LS light microscope (Leica). Embryos were then injected with approximately 1 nL injection mix into their posterior part, where the future pole of cells will form that constitute the germline of the organism. Embryos were kept at 25°C until hatching.

Larvae hatched from injected embryos were transferred into 2.5 mL of potato starch (Mousseline, Nestl ) with 10 μ L of 7-DHC [5 mg/mL in ethanol] and topped with a little amount of fresh yeast paste, using closed forceps (Forceps Dumont #5, Fine Science Tool). The petri-dish containing the larvae was then closed with a self-made 2 cm plastic cylinder (tinkered or 3D printed) with a 100 μ m nylon mesh glued on the top. Individuals were kept at 25°C until adults hatched.

2.5.2 Identification of transgenic *D. pachea* flies and stock establishment

Adults, hatched from injected embryos, were individually crossed with three or four virgin flies of the opposite sex from the 1698.01_14.2 stock. Female and male progeny from these crosses were counted and screened by eye, using a stereo-microscope (Zeiss Stemi 2000) equipped with fluorescent lamp (CoolLED pE-300). Transgenic adults were detectable by the red fluorescent eyes due to the 3xP3-DsRed integration marker (see part 2.4.1, page 67)(Handler and Harrell 2001). Transgenic individuals were crossed with three or four virgin flies of the opposite sex from the 1698.01_14.2 stock to constitute an individual stock. The progeny of these crosses were then crossed together and non-fluorescent flies were removed before reaching sexual maturity in the subsequent generations.

2.5.3 Insertion site localisation of the transgene

We used inverse PCR (see 2.4.4, page 70) to locate the insertion site of the transgene in some of the generated *D. pachea* transgenic stocks (see part 2.4.1, page 67, and part 2.5.1, page 72). Two pairs of nested PCR primers (annex), were designed inside one PiggyBac repeat sequence (left arm) of the plasmid used to transform the flies: #11_InvPCR_F1 and #11_InvPCR_R1, and #11_InvPCR_F2 and #11_InvPCR_R2.

The genomic DNA from 5 males and 5 females was extracted using DNeasy Blood and Tissue kit (Qiagen), as previously described in part 2.4.1, page 67. Genomic DNA was digested either using XbaI or XbaI and SpeI (New England Biolabs) as both of these enzymes yield compatible cohesive restriction-site overhangs. XbaI and SpeI also cut inside the plasmid at about 200 bp and 480 bp distance to the end of the left arm. The digestion was done overnight at 37°C with 1.0 µg genomic DNA in a volume of 50 µL, CutSmart buffer and 25 units restriction enzyme without exceeding 2.5% of final glycerol concentrations. Digested genomic DNA was purified with the PCR clean-up kit (Macherey-Nagel) following the supplier's instructions. The genomic DNA concentration was measured with a DS-11 Series Spectrophotometer/Fluorometer (DeNovix). Digestion efficiency was assessed by running native and digested samples in a 0.8% agarose gel containing ClearSight DNA stain (BioAtlas) for 45 min at 50 V.

Self-ligation of the digested DNA occurs at low DNA concentrations. We used DNA dilutions of 0.5 - 1 ng/µL, which was found to be optimal for our experimental purposes based on test ligations with serial dilutions of digested DNA. The diluted samples were heated for

5 min at 65°C and then rapidly chilled on ice before addition of ligation buffer and 3 units T4 DNA ligase (New England Biolabs) in a final reaction volume of 20 µL. Reactions were then incubated overnight at 16°C.

Two consecutive PCR reactions were done on each ligation mix, as described in part 2.4.4, page 70. The first PCR reaction was done with primers #11_InvPCR_F1 and #11_InvPCR_R1 (annex) and a second one was done with 1 µL on these PCR products and with primers #11_InvPCR_F2 and #11_InvPCR_R2. PCR products were then purified and sequenced by Eurofins TAGC with either #11_InvPCR_F1 or #11_InvPCR_F2 primers. The insertion site was identified in the *D. pachea* genome assembly (Lang and Courtier, in preparation) by local BLAST (Altschul et al. 1990) using the DNA sequence result as a query.

2.5.4 Live-imaging microscopy of developing genitalia

The *in vivo* monitoring of genitalia morphogenesis and genitalia rotation was done on synchronised pupae (see part 2.3.1, page 60) from DE-cad::GFP stocks (9_E1M1, 9_D2F1, 9_A3F1, 9_G3F1), from 20 h APF up to 48 h APF. Pupae were oriented with posterior part facing upwards in modeling clay (Play-Doh) in a dissection dish and the posterior part of the pupal case was removed with forceps (Forceps Dumont #5, Fine Science Tool).

A circular POC-R2 Cell Cultivation System (PECON) was combined with a 32 mm diameter round coverslip (0.17 mm ± 0.01 mm thick, ThermoScientific) and 1.5 mL of 1% agarose gel was casted onto the coverslip (Figure 5). After solidification, a wet rolled-up kimtech foil (Kimberly-Clark) was placed on the peripheric surface of the agarose gel to keep it wet as long as possible and to avoid the dehydration of the gel. In addition, a 5 cm petri dish bottom part was added on top of the circular POC-R2 Cell Cultivation System (PECON), to prevent humidity decrease. Holes of size of a pupae were introduced into the gel using a P1000 pipet tip (VWR) and were filled with water in order to evacuate the air. Pupae with removed posterior pupal case were finally gently placed into the holes with the posterior extremity touching the coverslip (Figure 11).

Mounted samples were imaged at the ImagoSeine platform with a DMI8 inverted microscope (Leica) equipped with a spinning-disc head CSU-W1 (Yokogawa Corporation of America) and controlled by MetaMorph software (Molecular Devices). The 488 nm laser was used with a 500 nm - 550 nm emission filter and set at 75% intensity and 650 ms exposure time. Images were taken every 30 min for 17-23 hours. Of 52 pupae used in experiments with the DMI8 microscope, 29 survived until adult flies pupae (56% survival). Alternatively,

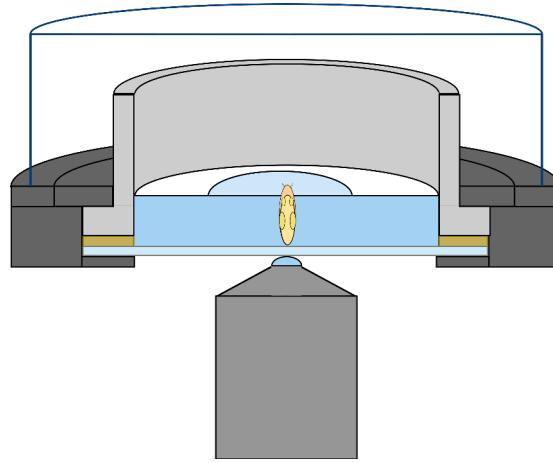


Figure 11 – Mounting of pupae for live-imaging of male genitalia morphogenesis and rotation.

A circular POC-R2 Cell Cultivation System (grey parts) with a round coverslip (light blue) and a circular joint (orange). The agarose gel was casted inside this support (blue), and pupae with removed pupal case at the posterior part was placed in it, posterior part in contact with the coverslip. A wet Kimtech tissue (white) was placed on top of the the agarose gel (white) and the cell was covered with a 5 cm petri dish bottom part (dark blue). Imaging was performed with inverted microscopes (objective represented).

samples were imaged on the platform with a LSM980 spectral Airyscan 2 inverted confocal microscope (Zeiss) controlled by ZenBlue software (Zeiss). The 488 nm laser was set at 4% intensity and acquisition was balanced between speed and resolution on ZenBlue software. Images were taken every 30 min for 24.5 hours.

Microscopy images were analysed using ImageJ software (NIH, version 1.52p). Three dimensional reconstructions of developing genitalia and the quantitative analysis of the signal was carried out with Imaris software (Oxford Instruments, version 8.4.1) available at the ImagoSeine platform.

2.5.5 Statistical analysis and figure assembly

Data has been entered manually in spreadsheets and saved in .csv format to be easily imported in R. All the data analysis and statistical analysis were performed in R version 3.6 (Core Team 2014). Figures were exported from R in .svg format. All figures were assembled using InkScape vectorial picture editor software, version 0.91 r13725.

3 Do asymmetric male genital lobes play a role in pre-copulatory events?

One of the main objective of my thesis was to test if the male asymmetric genital lobes in *D. pachea* have a pre-copulatory function (see the part 1.6 "Objectives", page 47). It is known that in *D. pachea*, males adopt an asymmetric, right-sided, mating position during copulation (Lang and Orgogozo 2012, Rhebergen et al. 2016, Acurio et al. 2019) and previous work in the lab has shown that lobes work as a grasping device to stabilize direct contacts of male and female genitalia during copulation (Rhebergen et al. 2016). The evolution of asymmetric lobes might therefore be related to their role during copulation. However, asymmetric lobes could also have been selected through other functions related to reproduction, such as courtship or contact mediation between female and male genitalia upon mounting but before intromission of the phallus is fully achieved. In this context, we tested if the asymmetric genital lobes of *D. pachea* may affect the chance of a male to engage into copulation with a female.

The results presented in this chapter mainly reproduce our submitted manuscript, B. Lefèvre, D. Catté, V. Courtier-Orgogozo, M. Lang, Male genital lobe morphology affects the chance to copulate in *Drosophila pachea*, 2020, under revision in BMC Evolutionary Biology (Lefèvre et al. 2020).

3.1 Results

3.1.1 Genital lobe lengths differ between *D. pachea* stocks

In our laboratory stock 1698.01, *D. pachea* males display a characteristic left-right size asymmetry of genital lobes with the left lobe being consistently larger than the right lobe (figure 12A and C, figure 13A, table 4). Similarly, in stock 1698.02, most males reveal larger left lobes, but a few individuals are observed with particularly small lobes that are rather symmetric in length (figure 12B and D, figure 13B). Males with short lobe lengths had been previously selected and crossed with sibling females for 50 generations (see part 2.1, page 48 for more details). The resulting stock was named selection stock and used in our experiments. We observed an increased variance of left lobe length in males of the selection stock compared to the source stock 1698.02 (Levene's test: selection stock/1698.02: $DF = 1/147$, $F = 11.506$, $P = 0.0008913$) (figure 13C). In contrast, the right lobe length differed only marginally among stocks (table 4) and the variances of right lobe lengths were not significantly different (Levene's test, $DF = 1/147$, $F = 0.5164$, $P = 0.4735$).



Figure 12 – *Drosophila pachea* male genital lobes.

A: Male of stock 1698.02 in ventral view and with asymmetric lobes. B: Male of the selection stock with apparently symmetric lobes. The scale bars correspond to 200 μm . C: Posterior view of a dissected male terminalia of stock 1698.02 with asymmetric lobes. D: Posterior view of a dissected male terminalia of the selection stock; the scale bars correspond to 100 μm , dots indicate lobe length measurement points.

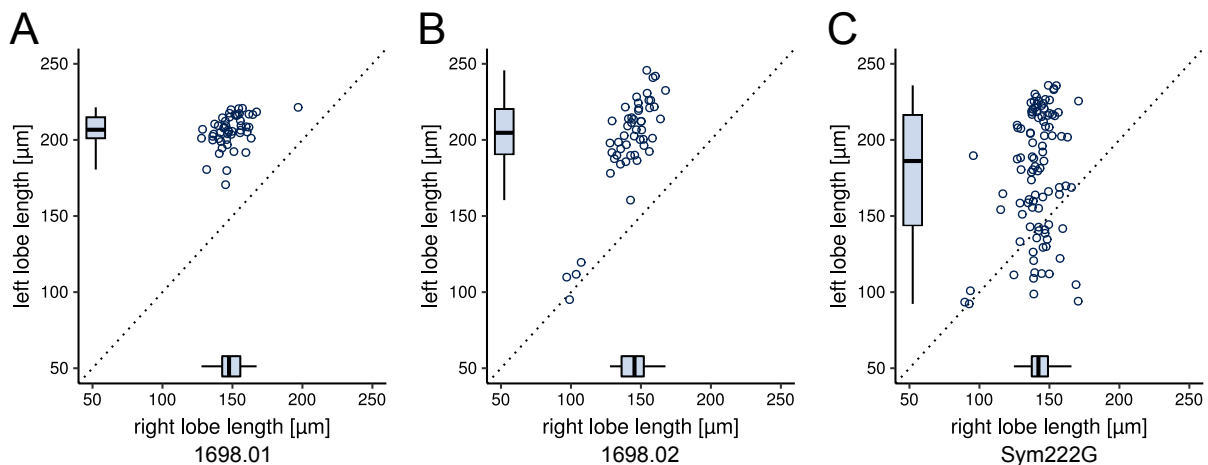


Figure 13 – Genital lobe lengths differ between *D. packea* stocks.

Lengths of the left and right epandrial lobe lobes are presented for A: stock 1698.01, B: stock 1698.02, and C: selection stock. Each point represents one male. The variance of left lobe length is increased in the selection stock compared to the source stock 1698.02 (Levene’s test: selection stock/1698.02: DF = 1/147, F = 11.506, P = 0.0009), while the variance of the right lobe length were not significantly different (Levene’s test, DF = 1/147, F = 0.5164, P = 0.4735)

stock	left lobe [μm] median (95% confidence interval)	right lobe [μm] median (95% confidence interval)	n
1698.01	206.7 (169.7 - 215.4)	147.6 (145.4 - 153.1)	50
1698.02	204.7 (190.5 - 209.2)	145.4 (138.6 - 146.4)	50
selection stock	186.1 (171.8 - 185.0)	142.2 (138.7 - 144.2)	99

Table 4 – Genital lobe lengths in *D. packea* stocks.

3.1.2 Male genital left lobe length, male courtship and failed copulation attempts have an effect on copulation success

We performed a mate competition assay (see part 2.2, page 50) with two males and a single female to test if differences in genital lobe length and courtship behavior may influence the chance of a male to copulate first with a single female. This first engagement into copulation will be referred to as “copulation success”. We filmed courtship and copulation behavior of two males of the selection stock and a single female of stock 1698.01 or 1698.02. We annotated 111 trials where both males simultaneously courted the female (see part 2.2, page 50) (51 and 60 trials with females of stocks 1698.01 or 1698.02, respectively). In particular, we waited for a first copulation to occur, then isolated the non-copulating male and finally the other two specimen once the first copulation had ended. Then, we dissected the genitalia of both males

to determine lobe lengths. We examined 54 additional trials with two courting males from the selection stock that had partially amputated left lobes and females of stock 1698.01. This was done to test if other characters might co-vary with left lobe length and could potentially also have an effect on copulation success. We shortened the left lobes of both males in order to be able to neglect possible effects of the caused wound. The relative courtship activity or vigor of the two males in each trial was compared by quantifying periods that each male spent touching the female ovipositor or the ground next to it with the proboscis (mouth-parts), hereafter referred to as “licking behavior” (see part 2.2, page 50). We counted the sum duration of these periods (sum licking duration) and the number of licking periods (number of licking sequences). A copulation was considered to take place, once a male had mounted the female abdomen and achieved to settle into an invariant copulation position (see part 2.2, page 50).

In the majority of trials (130/165), the first mounting attempt of a male resulted in a stable copulation. We did not observe any male behavior that could indicate an attempt of the non-copulating male to directly usurp the female as observed for *D. ananassae* or *D. bipectinata* (Polak and Rashed 2010, Grieshop and Polak 2012). However, in 35 trials, a total of 51 failed mounting attempts were observed (see part 2.2.6, page 59). These were not proportionally higher among trials with lobe amputated males (9 failed mounting attempts in 7/54 trials 13%) compared to unmodified males (42 failed mounting attempts in 28/111 trials 25%). Thus, the partial lobe amputation probably did not decrease the ability of a male to mount a female. Only 15/51 failed mounting attempts lasted 8 seconds or longer. Among those, the non-mounted male continued to court the female in 10/15 attempts. However, this was also observed in 131/165 successful mounting attempts and these proportions are not significantly different (X^2 -test, $X^2 : 1.4852$, $df = 1$, $P = 0.2230$). Altogether, mounting failure was not found to be significantly associated with the courtship activity of the other male.

Different variables were tested to have an effect on male copulation success by using a Bradley Terry Model (Bradley and Terry 1952) (see part 2.2.7, page 59). In trials with unmodified males, copulation success was positively associated with left lobe length and the sum licking duration of the males during courtship (table 5). The effect of sum licking duration is illustrated when comparing the ratio of sum licking duration and total courtship duration between the copulating and the non-copulating male (figure 14A). This ratio was higher in the copulating male compared to the non-copulating male. Copulation success was negatively associated with the number of licking sequences and with the number of failed mounting attempts (table 5). In particular, we identified a positive interaction of failed mounting at-

tempts and female age, indicating that the negative effect of failed mounting attempts is pronounced in young females but not in older females. However, this difference turned out to be based on three outlier observations when comparing the number of failed mounting attempts of either male over female age (figure 15). Therefore, more observations are required to evaluate this interaction and the effect of failed mounting attempts on copulation success.

In trials with males that underwent lobe surgery, left lobe length was not significantly associated with copulation success (table 6), although a similar positive effect was detected. Thus, we cannot exclude the possibility that left lobe length co-varies with yet another unknown selected trait that reveals an advantage for the male to copulate. Similarly, a non-significant negative effect of the number of licking events on copulation success was observed with those males (table 6) but a positive significant effect of sum licking duration.

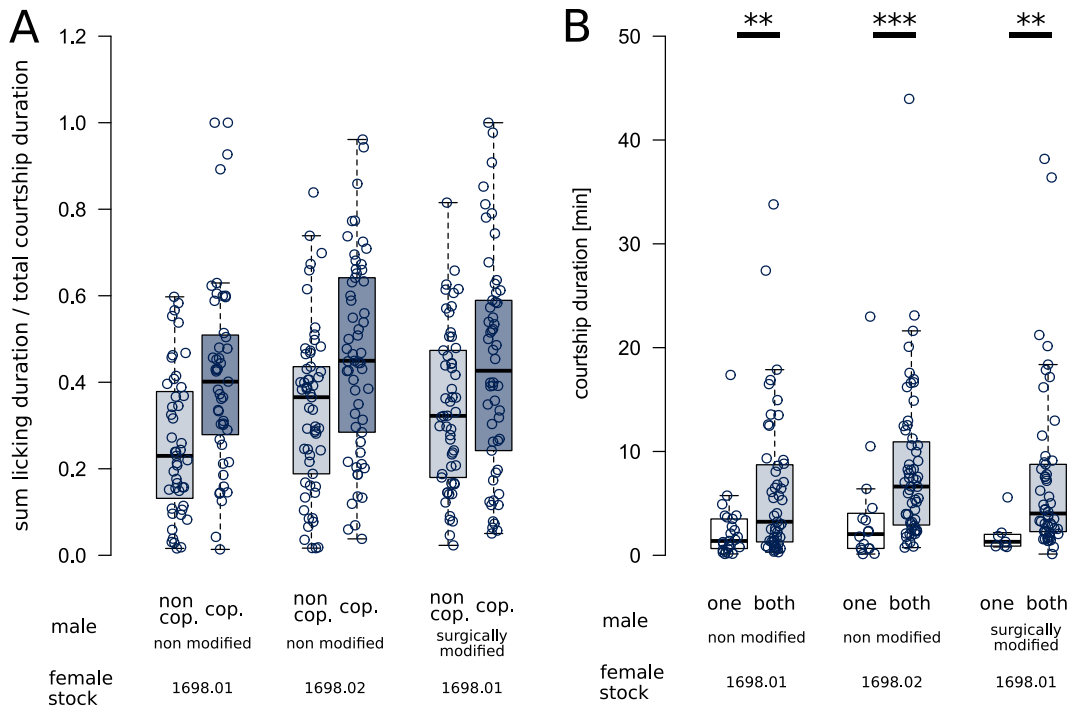


Figure 14 – Courtship durations and relative courtship activity.

A: The ratio of sum licking duration and total courtship duration in each trial shows that the copulating male (cop., dark blue box-plots) had a higher average sum licking duration compared to the non-copulating male (non cop., clear blue box-plots). Each point represents one male. B: The total courtship duration was shorter in trials with only one male displaying courtship signs (one, white box-plots) compared to trials with both males courting simultaneously (both, blue box-plots). Horizontal bars indicate pairwise comparisons with P-values $** < 0.01$ or $*** < 0.001$, Mann-Whitney-Wilcoxon test. Each point represents one mating experiment.

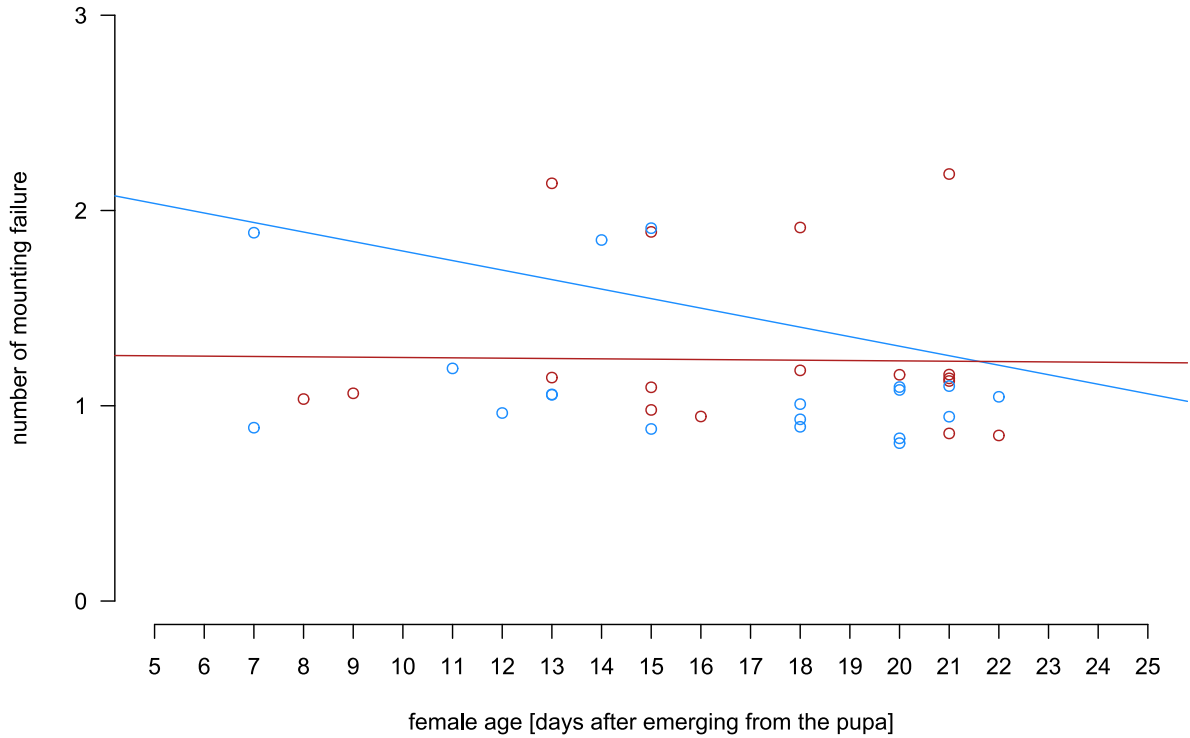


Figure 15 – Failed copulation attempts compared to female age.

Failed copulation attempts of the non copulating male (blue circles) and the copulating male (red circles) with linear regression lines (non copulating males: $r^2 = 0.019694$, $y = -0.04872x + 2.2795$, blue line, and copulating males: $r^2 = 0.00029967$, $y = -0.001731x + 1.2643$, red line).

variable	estimate	standard error	z value	P ($> z $)
sum licking duration	1.224514	0.334856	3.657	0.0003
number of licking sequences	-0.259216	0.127859	-2.027	0.0426
left lobe	0.007471	0.003582	2.086	0.0370
failed mounting attempts	-4.493660	1.834694	-2.449	0.0143
female age	NA	NA	NA	NA
failed mounting attempts x female age	0.295355	0.119397	2.474	0.01337

Table 5 – Bradley–Terry model examining the effects of left lobe length, sum licking duration, number of licking sequences and failed mounting attempts on copulation success. 92 trials with non-lobe modified males. The main effect for “female age” cannot be estimated in the Bradley-Terry (BT) model because it is specific to each trial and not to each male. Estimates highlighted in bold are significant.

variable	estimate	standard error	z value	P ($> z $)
sum licking duration	0.561757	0.256917	2.187	0.0288
number of licking sequences	-0.176035	0.090341	-1.949	0.0513
left lobe	0.009199	0.005090	1.807	0.0707

Table 6 – Bradley–Terry model examining the effects of left lobe length, sum licking duration, and number of licking sequences on copulation success.

53 trials with males that had surgically modified left genital lobes. Estimates highlighted in bold are significant.

3.1.3 Courtship duration increases when two males court a female simultaneously

Regardless of the stock for the female used, courtship duration appeared to be longer when both males courted the female simultaneously compared to trials where only one male courted (Mann-Whitney-Wilcoxon test, $W = 1906.5$, $N = 48/165$, $P = 4.7 \times 10^{-8}$) (figure 14B). We also observed that courtship duration was strikingly increased in females that were older than 11 days (after emerging from the pupa) compared to younger females (figure 16) (Mann-Whitney test, $W = 660$, $N_{\text{females younger than 12 days}}/N_{\text{females older than 11 days}} = 33/132$, $P = 6.333 \times 10^{-10}$). Thus, older females may be less likely to copulate and may also discriminate less between males based on failed mounting attempts (see previous part).

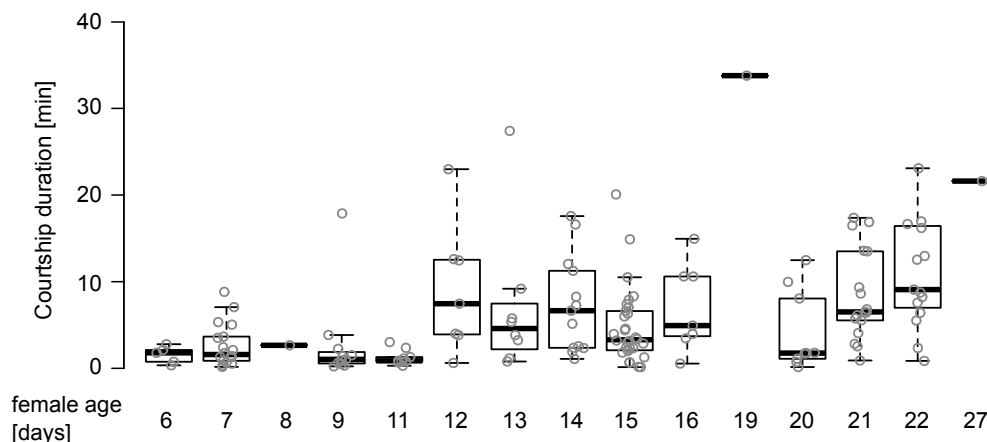


Figure 16 – Courtship duration increases with female age.

The average courtship duration is increased in females that are older than 11 days after hatching from the pupa (Mann-Whitney test, $W = 1525.5$, $N_{\text{females younger than 12 days}}/N_{\text{females older than 11 days}} = 52/161$, $P = 5.811 \times 10^{-12}$).

3.1.4 Lobe length is not associated with the amount of ejaculate in female sperm storage organs

To test whether lobe length influences the amount of ejaculate deposited into the female after copulation, we dissected a random subset of females (54 of stock 1698.01 and 24 of stock 1698.02) in trials with non-modified lobes that revealed a copulation. Neither right lobe length, left lobe length, sum licking duration or female age (days after emerging from the pupa) was significantly associated with ejaculate content in the spermathecae (table 7). However, male adult age and copulation duration had a negative effect. Given that *D. pachea* males become fertile about 13 d after emerging from the pupa (Pitnick 1993), our results indicate an optimal period of male ejaculate transfer at the beginning of their reproductive period. Copulation duration had a negative effect on sperm transfer (table 7), indicating that failed sperm transfer may result in prolonged attempts and longer copulation duration.

variable	F value	P
sum licking duration	1.6841	0.2022
number of licking sequences	0.1107	0.7411
left lobe	0.1139	0.7377
right lobe	1.4739	0.2322
copulation duration	10.94	0.0021
female age	0.5036	0.4822
male age	22.828	0.00003

Table 7 – Linear model, examining the effects of lobe length, sum licking duration, copulation duration and age on spermathecae filling levels. Degrees of freedom: numerator/denominator 38.

3.2 Discussion

3.2.1 Left lobe length affects the chance of a male to copulate

We observed a tendency of females to copulate first with the male that had the longer left lobe when two males courted simultaneously in our trials. These results suggest that a long left lobe might not only stabilize an asymmetric genital complex during copulation (Rhebergen et al. 2016), but also increases the chance of a male to engage into copulation. With our data, we cannot exclude that the sensing of the lobe length by the female occurs just before intromission, while male and female genitalia are contacting each other or if it is used even during courtship before genital contacts establish. Other factors, unrelated to lobe length, can also bias copulation. For example, females might prefer to copulate with males of larger body size or that display particular courtship behaviors. In our study, we found no significant effect of tibia length on copulation success, which was used as an approximation for overall body size. However, the mutation(s) associated with lobe length variation in this stock are unknown. It is possible that one or several alleles associated with lobe length still segregate in this stock, even after 50 generations of inbreeding. If such segregating mutations have pleiotropic effects on other male characters (morphological, physiological or behavioural), these traits are expected to co-vary together with lobe length and the effect of lobe length that we detected might actually be due to the other factors. In trials with artificially introduced lobe length variation (through surgery), males were taken from the selection stock but had the expected wild-type lobe asymmetry. Left lobe length difference was then artificially introduced in those males, so that it would not be expected to co-vary with the relative phenotypic expression of the supposed underlying mutation. In such trials, we observed a trend of the left lobe length being associated with copulation success, but this trend was not significant. Thus, we cannot completely rule out the possibility that left lobe length affects copulation success indirectly via a pleiotropic mutation affecting both, lobe length and other traits.

3.2.2 Male intra-sexual competition is potentially reflected by male courtship intensity

Previous analyses in *D. ananassae* and *D. bipectinata* relate male genital spines to pre-copulatory abilities to achieve a copulation due to increased male intra-sexual competitiveness in so called “scramble competition” or vigorous copulation attempts with females that are

optionally already copulating with another male (Polak and Rashed 2010, Grieshop and Polak 2012). In *D. pachea*, this behavior was not observed and most mounting events of a male resulted in a stable copulation. Once a copulation started, the non-copulating male was never observed to separate the couple. Instead, it continued to display courtship behaviors such as licking, wing vibration or touching the female side in the majority of cases. In addition, male mounting was only observed upon female wing opening and oviscapt protrusion. This indicates that mounting in *D. pachea* is a complex behavior involving both sex partners. Upon mounting, the chance of a *D. pachea* male to engage into copulation thus may largely depend on male-female communication rather than on male male competition.

Total courtship duration was increased in trials where both males courted the female simultaneously compared to trials with only one male courting. This indicates that females potentially require more time to accept one of the males for copulation in cases where two males court simultaneously. Alternatively, a longer courtship duration might indeed rely on male-male competition, causing mutual disturbances in courtship display. We detected a strong association of copulation success with the sum licking duration, which we used as an approximation for overall courtship activity or vigor of each male. We also observed a negative effect of the number of licking sequences on copulation success, indicating that a male has highest chances to copulate if he continuously presents licking behavior at the female abdomen for a prolonged time period. This is achieved by maintaining its position close to the female oviscapt in competition with the other male, suggesting that licking behavior in part reports male-intrasexual conflict.

3.2.3 Potential female benefits gained from mate-choice for males with long left lobes

Female mate choice on male sexual traits was suggested to rely at least in part on the way a sexual trait is displayed or moved (Byers, Hebets, and Podos 2010). This implies that a certain quantity but also accuracy of locomotive activity would matter in courtship and might better reflect overall male quality and “truth in advertising” than a morphological character or ornament alone. Our data suggest that male settling upon mounting the female might be crucial for a successful copulation since we identified a negative effect of failed mounting attempts on copulation success and a positive interaction of failed mounting attempts with female age, possibly indicating that young females are more discriminating compared to older females with respect to male mounting performance. Female mate choice is hypothesized to be based on direct benefits, affecting fecundity and survival of the female, but also on

indirect benefits that relate to genetic quality, fecundity and survival of the progeny (Byers, Hebets, and Podos 2010, Kirkpatrick and Ryan 1991). Left lobe length and male mounting performance might therefore influence female mate-choice through enhancing the quality of male courtship signals and by enhancing the coupling efficiency of male and female genitalia upon mounting.

Alternatively, left lobe length might potentially associate with direct copulation benefits for male and female by ensuring the efficiency of ejaculate transfer during copulation. Males of *D. pachea* produce giant sperm and previous estimates revealed that a *D. pachea* male transmits only about 44 ± 6 sperm cells per copulation (Pitnick and Markow 1994b), while the maximum female sperm storage capacity in the spermathecae was estimated to be much higher and to be about 304 sperm cells (Pitnick and Markow 1994b). Wild-caught *D. pachea* females were found to contain sperm from at least 3-4 males based on spermathecae filling levels (Pitnick and Markow 1994b). As asymmetric lobes stabilize the genital complex (Rhebergen et al. 2016), they might have a positive effect on the amount of sperm transferred per copulation. However, we have not observed any effect of lobe length on ejaculate presence in the spermathecae after copulation. We note that our quantification method was not precise and that sample size was limited. Accurate direct sperm counts requires radio-labeling methods (Pitnick and Markow 1994b), which was not applicable in our experimental setup. In future approaches, improved sperm counts should be applied to test for a correlation between lobe length, female-male copulation complex stability and sperm quantity in female spermathecae.

Based on our data, we note that left lobe length affects the chance of a male to establish genital contacts that lead to a firm complex of female and male genitalia, congruent with previous observations in other insects (Polak and Rashed 2010, Grieshop and Polak 2012, Bertin and Fairbairn 2005, Grieshop and Polak 2014). In particular, the male genital spines in *D. ananassae* and *D. bipectinata* were observed to play a role in pre-copulatory events but had no measurable influence later on with respect to sperm transfer or fecundity (Polak and Rashed 2010, Grieshop and Polak 2012, Grieshop and Polak 2014).

Interestingly, copulation duration negatively affected ejaculate presence in the female. This observation suggests that the couple separates once successful sperm transfer is achieved. However, not all copulations reveal sperm transfer. In occasions of failure the copulation duration may therefore be prolonged to further attempt to mate. Copulation duration varies largely among *Drosophila* species from fractions of a minute to up to about 2 h in *D. acanthoptera* (Acurio et al. 2019, Pitnick 1993). Copulation duration in *D. pachea* is thus com-

paratively long with respect to other species of the genus, pointing to presumably complex copulatory interactions affecting sperm transfer. Future studies must analyze the internal processes of sperm transfer during *D. pachea* copulation to better understand this process and its possible limitations.

Indirect paternal effects on the growth and survival of offspring could potentially play a role in *D. pachea* female choice for males with long left lobes. It has been demonstrated that mate choice based on particular male sexual characters correlates with offspring survival in diverse species (Schantz et al. 1989, Norris 1993, Petrie 1994, Hasselquist, Bensch, and Schantz 1996, Welch, Semlitsch, and Gerhardt 1998, Hoikkala, Aspi, and Suvanto 1998). However, our experiment did not allow us to test for these effects because females were sacrificed after the mating experiment and no progeny was obtained. We assessed ejaculate filling levels instead of the amount of female progeny because *D. pachea* females rarely lay eggs after a single insemination and about four copulations are necessary for a female to start oviposition (Pitnick 1994). To test for indirect effects, future studies should ideally use progeny males from wild caught *D. pachea* females and test if subtle lobe length variation in those males would correlate with offspring survival in single couple crosses. A similar approach was used by Hoikkala, Aspi, and Suvanto (1998), who found that *Drosophila montana* courtship song frequency of wild caught males correlated with the survival rate of the male's progeny.

3.2.4 Age of reproductive activities appear to be non-overlapping in sibling males and females

The amount of ejaculate present in the female spermathecae after a single copulation was negatively affected by the age of the copulating male. Similarly, it was previously found that the number of progeny in single couple crosses (presumably involving multiple copulations) was also dependent on male adult age in *D. pachea* (Jefferson 1977). Males in *D. pachea* need about 10-14 days at 25 °C after emergence to become sexually mature (Pitnick 1993, Pitnick 1994, Jefferson 1977). This is related to adult testis growth and production of giant sperm (Pitnick and Markow 1994b). It was shown that the relatively long time to reach male sexual maturity impacts the proportion of sexually active *D. pachea* adults (operational sex ratio), which is female-biased (Pitnick 1993). Our findings suggest that males potentially have a maximum fertility period at the beginning of their sexual maturity at approximately 13-16 days after emerging from the pupa. The detected reduction of transferred ejaculate in males older than 16 days implies an additional male reproductive limitation.

It was hypothesized that the delay in male sexual maturity might potentially lead to decreased sibling mating in *D. pachea* (Pitnick 1994). In *D. melanogaster*, sibling matings yield fewer progeny compared to crosses with unrelated individuals (Jefferson 1977). In our study, the female was not a sibling of the two males. Courtship durations were shortest in trials with “young” virgin females, between 6 and 11 days. Given that females reach sexual maturity at about 4 days after emerging from the pupa (Pitnick 1993, Jefferson 1977), our observation suggests that young females engage more quickly into copulation compared to older females. Overall, female and male maximum reproductive activities appear to be non-overlapping among siblings of opposite sex and similar age. Such an effect can be relevant in the wild if a cactus rot is colonized by a single previously fertilized female.

4 Timing of development in *Drosophila pachea*

The adult external genitalia of drosophila develop during the pupal stage. We wondered if asymmetric genital development of males *D. pachea* might be correlated with a major timing difference of the overall developmental progress of *D. pachea* with respect to other *Drosophila* species that have symmetric genitalia. In particular, the genital tissue growth mostly occurs in the 6th and 7th developmental stages, therefore we wanted to investigate if these stages were affected by timing changes compared to other species. A second aim was to annotate an exhaustive description of *D. pachea* development under our laboratory conditions, for characterization of other developmental process of interest.

4.1 Results

4.1.1 Durations of *Drosophila pachea* embryonic and larval development

The total duration of the embryonic development in *D. pachea*, measured by time-lapse imaging at 25°C was 32 h 48 min \pm 1 h 13 min (mean \pm standard deviation ; n = 12) (see part 2.3.2, page 62) (figures 17A). The duration until trachea filling was 26 h 48 min \pm 1 h 13 min (mean \pm standard deviation ; n = 12).

The larval development duration was examined on cohorts of synchronised larvae (see part 2.3.1, page 60) by dissection of larval mouth hooks at various developmental time points. Developmental time points are defined as the time spent from the larva hatching to the moment of collection and dissection. As the larval mouth hooks are replaced in each larval molt with variations in their morphology and pigmentation, they have been previously used in *D. melanogaster* to distinguish the three larval instar (Strasburger 1935). We used the same approach in *D. pachea* to determine the developmental stage of the dissected larvae (see part 2.3.3, page 62, and figure 7). The total duration of *D. pachea* larval development on standard *D. pachea* food at 25°C is about 9 days, which corresponds to 216 h. The duration of the first and second instar larva were about 2 days each, and the third instar stage lasted for about 5 days (figure 17A).

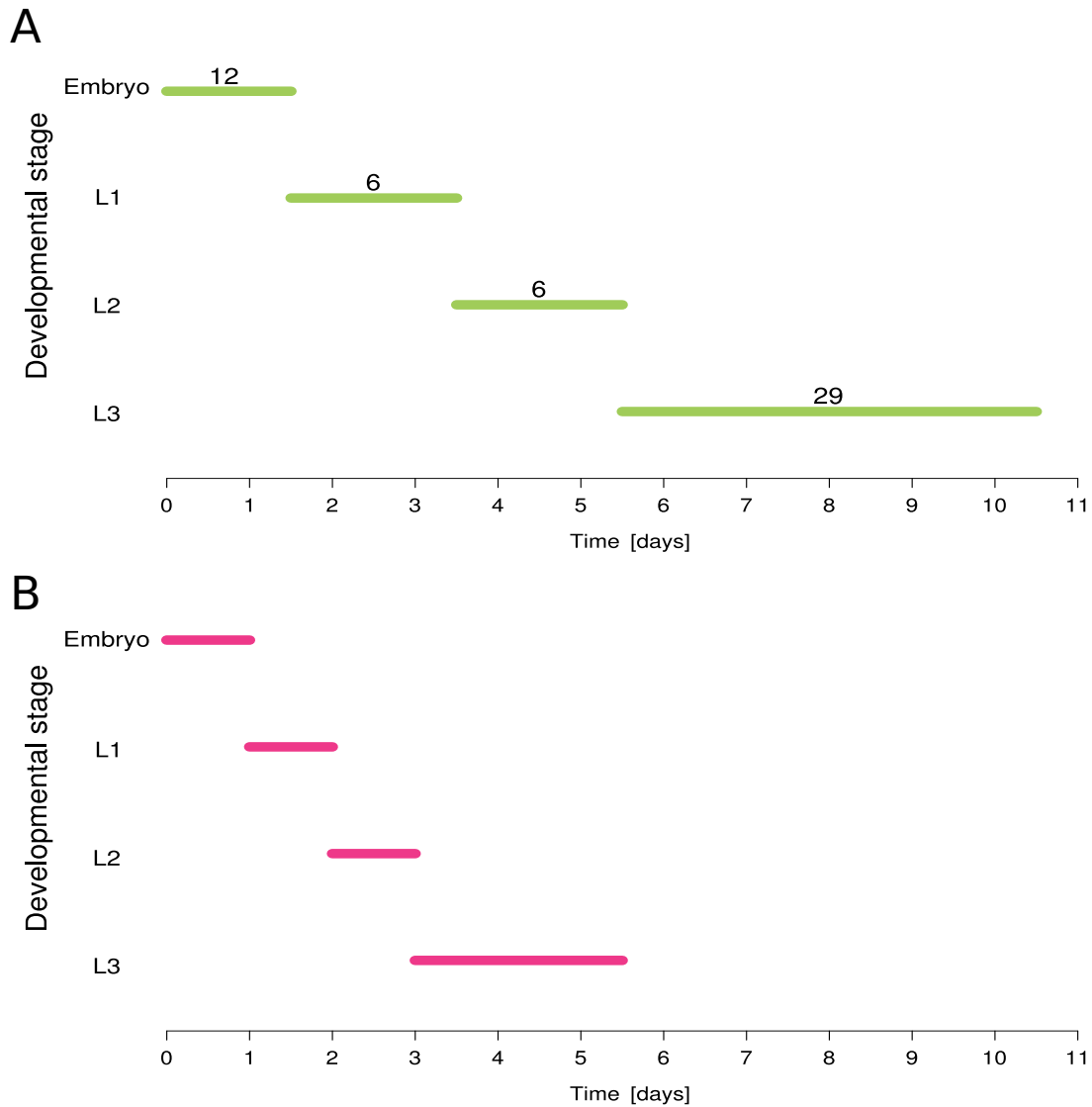


Figure 17 – Duration of the embryonic and larval developmental stages in *D. pachea* and *D. melanogaster*.

A: *D. pachea*, numbers correspond to the number of individuals observed at each stage. Embryonic stage duration was determined by eye on time-lapse monitoring of embryos, from egg laying to larva hatching. Larval stages were determined based on mouth hook morphology of dissected larvae from synchronised cohort, according Strasburger (1935). B: *D. melanogaster*, data was extracted from David and Clavel (1966) (embryonic duration), and Strasburger (1935) (larval stage durations).

4.1.2 The timing of pupal development is conserved up to the pharate adult stage between *D. pachea* and various *Drosophila* species

The beginning of the pupariation was determined as the moment when the larva stopped to move and the anterior spiracles were everted. The pupa then progressively turn from white to brown and the end of the white puparium stage was determined by eye as the moment when the pupa has a brown color. The duration of the white puparium stage at 25°C in *D. melanogaster* is about 80-120 min (Bainbridge and Bownes 1981). The corresponding duration in *D. pachea* at 25°C was approximated on 9 pupae by time-lapse recording (see part 2.3.4, page 63). Similar to the reported observations on *D. melanogaster*, the white pupal stage in *D. pachea* was found to last for about 102 min \pm 41 min (mean \pm standard deviation) in *D. pachea*. This indicates that *D. pachea* pupae from a same synchronised cohort established by collection of white puparium reveal a maximum pupariation age difference of 102 min.

To characterise the pupal development in *D. pachea* and in its close sister species *D. nannoptera* and *D. acanthoptera*, cohorts of synchronised pupae were regularly observed over the course of the pupal development and developmental stages were assigned according the morphological markers established by Bainbridge and Bownes (1981) on *D. melanogaster* (table 8). However, the markers used to characterise stages 8 to 12 are related to eye, wing or body pigmentation. In the case of *D. acanthoptera*, these markers were not convenient as these flies develop black eyes, opposed to most other *Drosophila* species that have red eyes (figure 18). In addition, *D. acanthoptera* is generally less pigmented compared to *D. pachea* and *D. nannoptera* (figure 18) and pigmentation changes were not easily detectable through the pupal case. To overcome these difficulties, the anterior pupal case was partially removed and developmental progress was monitored by time-lapse imaging (see part 2.3.4, page 63).

The overall timing of pupal development was similar among *D. pachea*, *D. nannoptera* and *D. acanthoptera* (figure 19A, B and C, respectively). The duration from the white puparium stage to pharate adult (stages 1 to 7, from 0 h APF to about 55 h APF) was also similar across other *Drosophila* species, including *D. melanogaster* and *D. guttifer* (figure 19D) (Bainbridge and Bownes 1981, Fukutomi et al. 2017) whereas later pupal development from about 55 h APF was prolonged in the nannoptera group species *D. pachea*, *D. nannoptera* and *D. acanthoptera* compared to *D. melanogaster* and *D. guttifer*. This resulted in delayed emerging of the adult of 10 h - 50 h compared to *D. melanogaster*.

Development stage	Description
1	Pupariation : extremity of trachea are everted, pupa does not to move anymore.
2	Clear, white pupa.
3	Light pigmentation, dorsal trachea still visible.
4	Bubbles appear, dorsal trachea is not visible anymore, light pigmentation of the body.
5	Cranial extremity is retracted, distal extremity of wings appeared.
6	Yellow body is visible.
7	Pharate adult. Eyes are not yet pigmented.
8	Eyes disc become a bit yellower that the rest of the body.
9	Orange eyes, transparent wings are visible.
10	Deep red eyes.
11	Bristles are visible on the thorax.
12	Wings are clear grey, clear pigmentation on the body.
13	Wings are completely black, grey pigmentation appeared on the body.
14	Meconium appeared under the form of a dark spot visible through the abdomen.
15	Ecdlosion.

Table 8 – Morphological markers used to examine the developmental stage of pupae, adapted from Bainbridge and Bownes (1981).

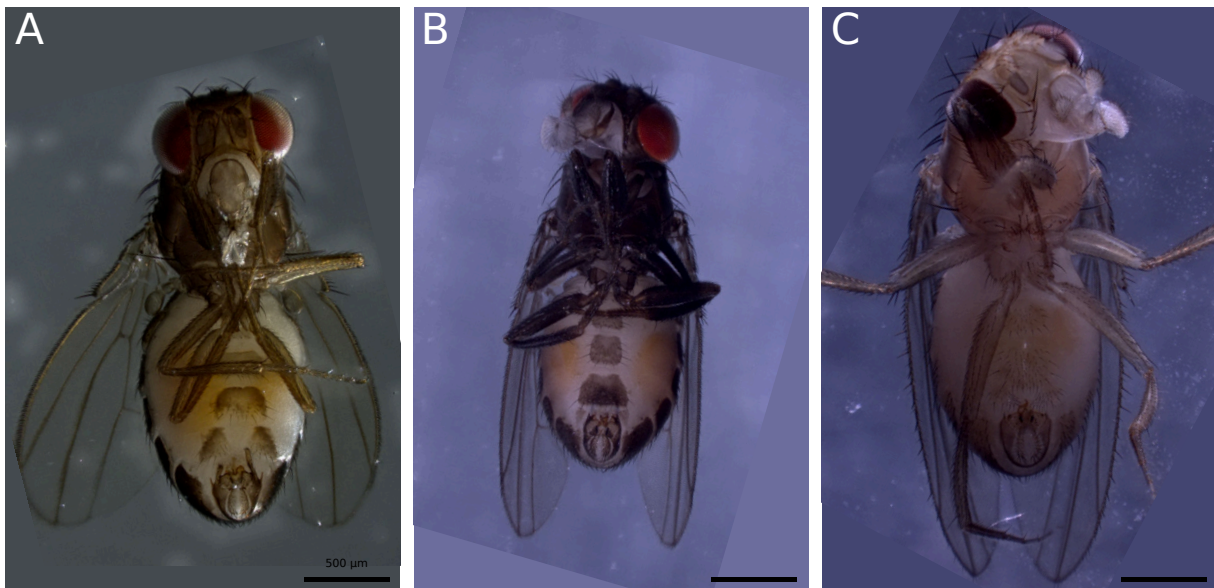


Figure 18 – *D. pachea*, *D. nannoptera*, and *D. acanthoptera* flies display differences in eye and body pigmentation.

A: *D. pachea* male, B: *D. nannoptera* male and C: *D. acanthoptera* male in ventral view. *D. nannoptera* has a black cuticle and red eyes whereas *D. acanthoptera* has a clear brown cuticle and black eyes. *D. pachea* has a brown cuticle and red eyes. Scale bar: 500 μm .

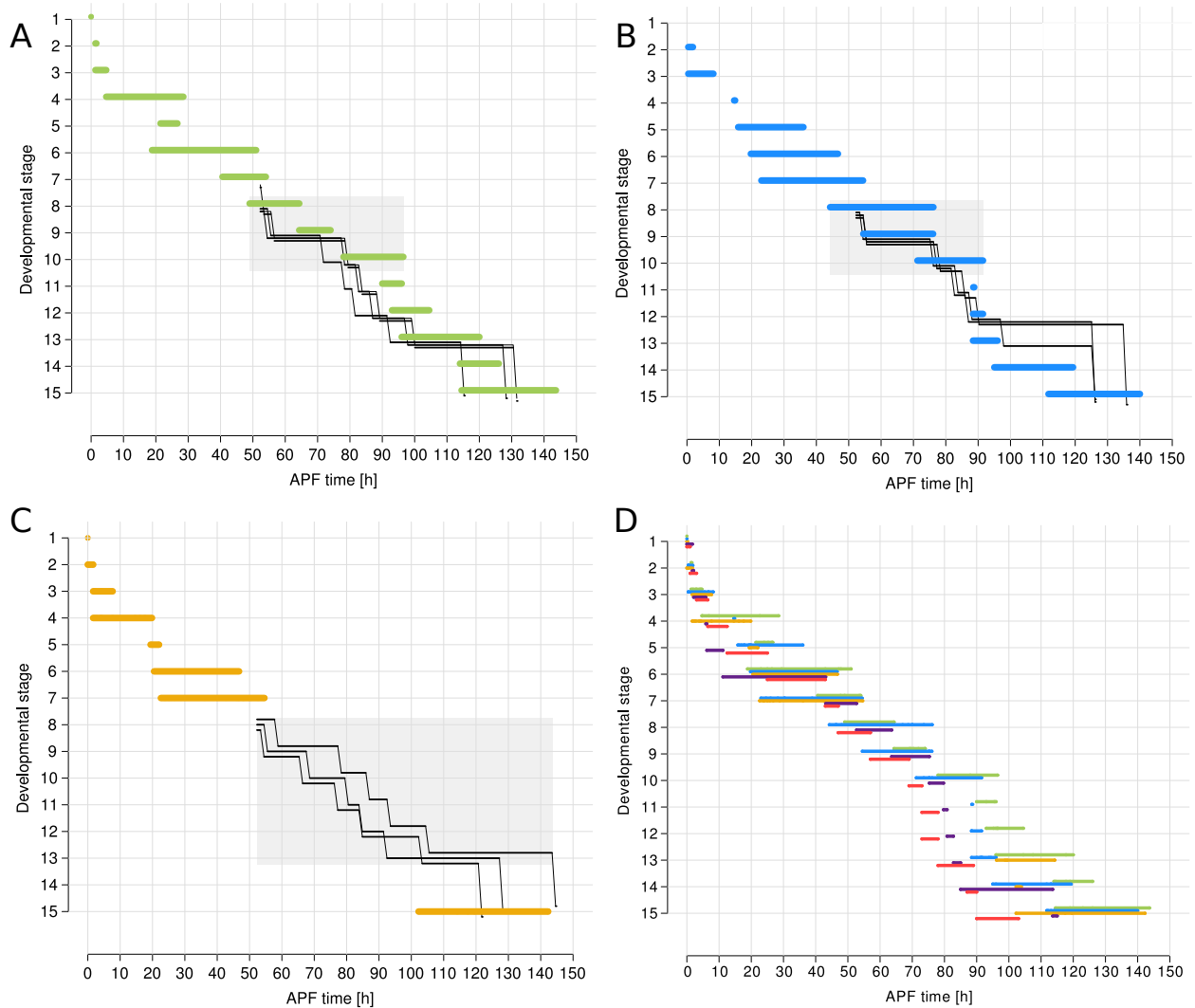


Figure 19 – Timing of the pupal stages in *D. pachea*, *D. nannoptera*, *D. acanthoptera*, *D. melanogaster* and *D. guttifer* at 25°C.

A: *D. pachea* (green), B: *D. nannoptera* (blue) and C: *D. acanthoptera* (yellow). Data shown are a combination of various observations of synchronized cohorts and from time-lapse imaging of developing pupae. Data established based on time-lapse monitoring are indicated by black lines (see part 2.3.4, page 63). Data for stages 13 (black wings) and 14 (meconium) are combined as the meconium was not visible due to orientation of pupae for time lapse acquisition. Grey boxes indicate the time period of eye pigmentation change from clear yellow to the maximum pigmentation (deep red, or black in *D. acanthoptera*). D: combined datasets of *D. pachea* (green), *D. nannoptera* (blue), *D. acanthoptera* (yellow), and for *D. melanogaster* (pink) and *D. guttifer* (purple). Data concerning *D. melanogaster* have been retrieved from Bainbridge and Bownes (1981) and those concerning *D. guttifer*, from Fukutomi et al. (2017).

The development of male genital asymmetry in *D. pachea* becomes apparent at about 24 h APF to 36 h APF (see part 5.2.2, page 113 for the detailed characterization of lobe growth). This period corresponds to the 6th pupal developmental stage and the overall chronological developmental progress appears to be similar between *D. pachea*, *D. nannoptera* and *D. acanthoptera*, but also *D. melanogaster* and *D. guttifera*. At later stages, The global development of *D. pachea* appears to be slower with respect to other species, such as *D. melanogaster*, in which males display symmetric genitalia. However, this corresponds to stages 8-15, when lobe asymmetry is already established. It indicates that the development of the asymmetric genital lobes of male *D. pachea* occurs in the same global developmental context compared to other *Drosophila* species.

Other differences in pupal development between *D. pachea*, *D. nannoptera* and *D. acanthoptera* were observed during the period of eye pigmentation. *D. acanthoptera* has black eyes (figure 18C) and needs about 95 h to reach the maximum eye pigmentation. In contrast, *D. pachea* and *D. nannoptera* require about 45 h (grey boxes, figure 19A, B and C). The prolonged eye pigmentation in *D. acanthoptera* is not due to a slower color change but to a prolonged pigmentation that results in darker eyes in this species.

Stage 15 corresponds to the emergence of the adult fly from the pupal case and is highly variable within each species, however the variance is similar across the species (Levene's test: $F = 0.0973$, $Df = 2$, $p = 0.9077$): *D. pachea* adults emerge between 115 h APF and 145 h APF, *D. nannoptera* adults between 110 h APF and 140 h APF and *D. acanthoptera* adults between 100 h APF and 140 h APF.

4.1.3 The relative timing of pupal stages of *D. pachea* varies between 25°C and 29°C, whereas the total duration does not

Temperature is known to influence the duration of *drosophila* development (David and Clavel 1966, Powsner 1935, James and Partridge 1995). In *D. melanogaster*, the duration of the pupal development from the white puparium stage to the emergence of adults decreases with temperature, from 123.6 h at 16°C to 99.6 h at 25°C and to 85.2 h at 29°C (James and Partridge 1995).

The overall duration of the pupal development of *D. pachea* at 29°C is similar to those observed at 25°C until about 55 h APF, which corresponds to the stage 7 (pharate adult ; table 8) (figure 20). Then, the pupal development is accelerated from stage 8 (begining of eye pigmentation) to stage 13 (end of body and wing pigmentation) at 29°C compared to

25°C. Surprisingly, the development then slows down, leading to a global duration of about 100 h to 145 h at 29°C, which is similar to the developmental duration of 115 h to 145 h at 25°C (figure 20).

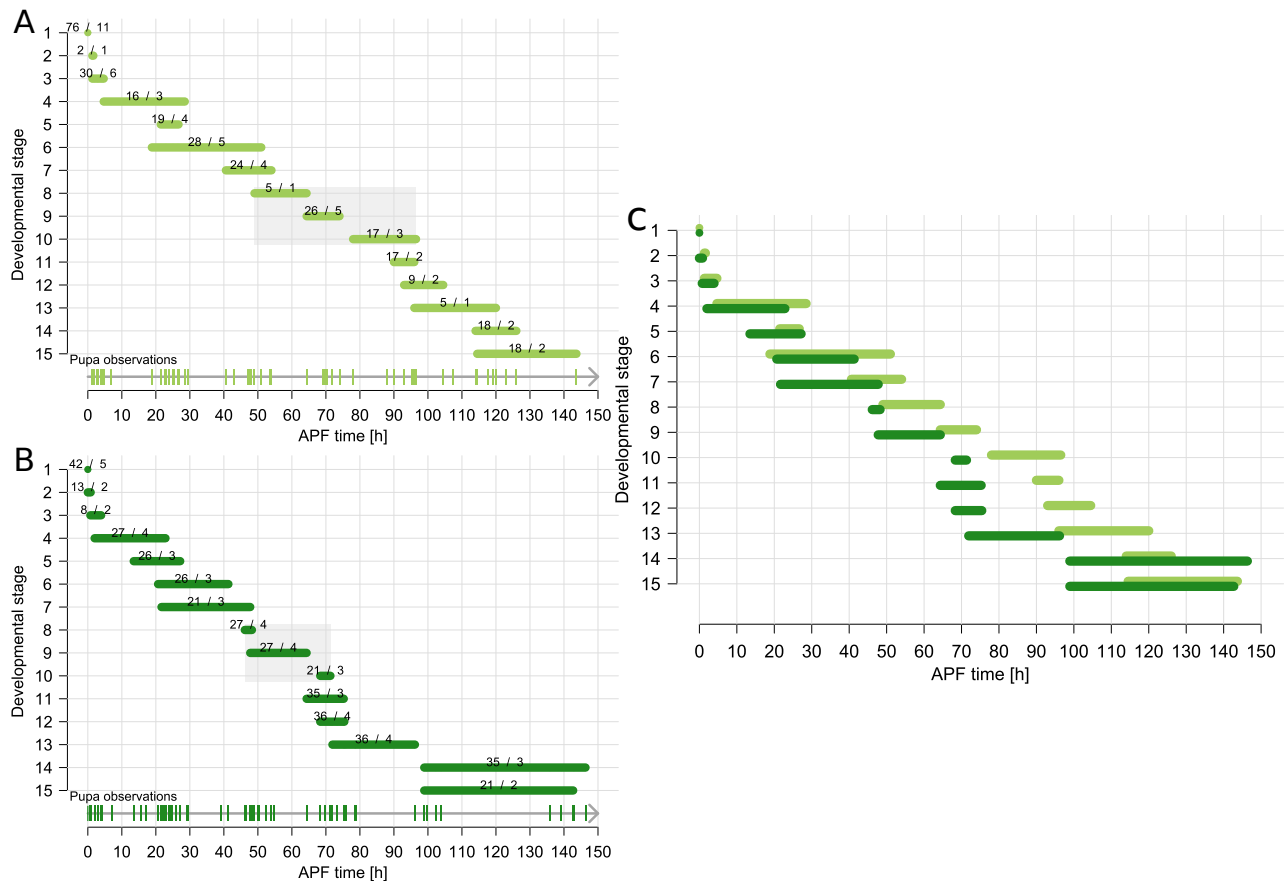


Figure 20 – Progress of pupal development in *D. pachea* at 25°C and 29°C

Synchronised cohorts of pupae at A: 25°C and B: 29°C and observed at various time points as indicated by ticks on the arrow above the x axis. Stages were determined by visual inspection according to Bainbridge and Bownes (1981). First number: number of pupae, second number: number of cohorts. Grey boxes highlight the period of eye pigmentation. C: combined datasets

4.2 Discussion

4.2.1 Conserved overall developmental progress during early pupal stages

The detailed analysis of the timing of pupal stages revealed that the first stages 1st to 7th appear to be rather synchronous among *D. melanogaster* (Bainbridge and Bownes 1981), *D. guttifera* (Fukutomi et al. 2017), and the three closely related species *D. pachea*, *D. acanthoptera* and *D. nannoptera*. Later on, pupal development was more variable between species. This may indicate the existence of some timing constraints on the developmental processes leading to the pharate adult and interspecific variation thereafter. At least a part of this variation could be attributed to the developmental marker used. As the coloration markers are qualitative, it is hard to define precise limits of each stage (ie. eyes turn from yellow to orange and red, following a continuous gradient of pigmentation). A solution to this problem would be to identify a combination of multiple markers for each stage. In the last pupal stage, we observe timing variation between individuals of a same species (up to 30 h between *D. pachea* flies). That variation may depend on environmental factors that we could not control (ie. light/dark illumination status cycle at the moment of pupation or emergence).

The development of male asymmetric genital lobes in *D. pachea* occurs from about 24 h APF to 36 h APF (see part 5.2.2, page 113 for the detailed characterization of lobe growth). This developmental process takes place when the overall pupal developmental progress is conserved between *Drosophila* species. Thus, the genital asymmetry establishment in *D. pachea* is probably not affected through a global developmental timing change compared to other species.

4.2.2 The duration of development varies among *Drosophila* species

The global embryo-to-adult duration of *D. pachea* at 25°C is about 364 - 394 h. This duration is comparatively long but inside the range of the corresponding duration in other *Drosophila* species, that range from 180 h in *D. simulans* (Ashburner et al. 1989), to 457 h in *D. mojavensis* (Markow, Beall, and Matzkin 2009, Matzkin et al. 2011) (table 9, figure 21). The embryonic development of *D. pachea* at 25 °C is about 33 h. The corresponding duration in other *Drosophila* species range from 16 h in *D. sechelia* (Kuntz and Eisen 2014), to 33 h in *D. virilis*. The duration of embryonic development of *D. pachea* is thus long relatively to those of other species (table 10, figure 22).

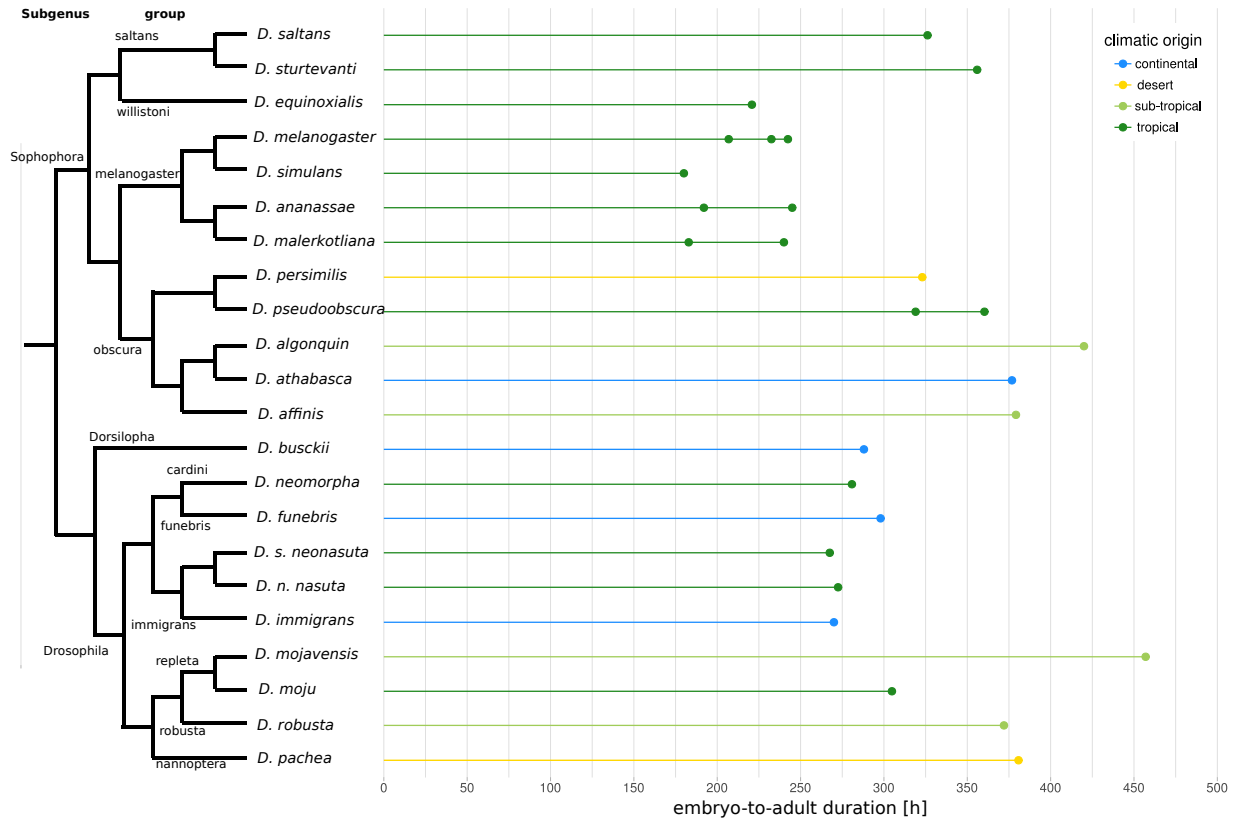


Figure 21 – Embryo-to-adult duration in various *Drosophila* species raised at 25°C.

Data concerning developmental duration and climatic conditions of other species than *D. pachea* was extracted from the literature (see table 9). The cladogram was established according to Yassin (2013) and Lang et al. (2014).

Several parameters might affect the duration of development, such as climate conditions of the corresponding species' habitat. Alternatively, the duration of development might change with genetic distance in a rather clockwise fashion during evolution so that closely related species reveal a more similar duration compared to more distantly related species. To compare such a trends, I plotted developmental duration (embryo-to-adult and embryonic development duration) and habitat characteristics of various *Drosophila* species onto two cladograms that represents the *Drosophila* species phylogeny (figures 21 and 22). The cladogram was generated according to Yassin () and Lang et al. (2014). This qualitative comparison indicates that a genetic component might influence developmental duration, since closely related species indeed also tend to have a very similar duration of development. In contrast, the climate conditions of the species' habitat do not appear to affect the duration of embryo-to-adult development, since it varies largely among species that live in similar environments. Species from the melanogaster group tend to have the shortest developmental

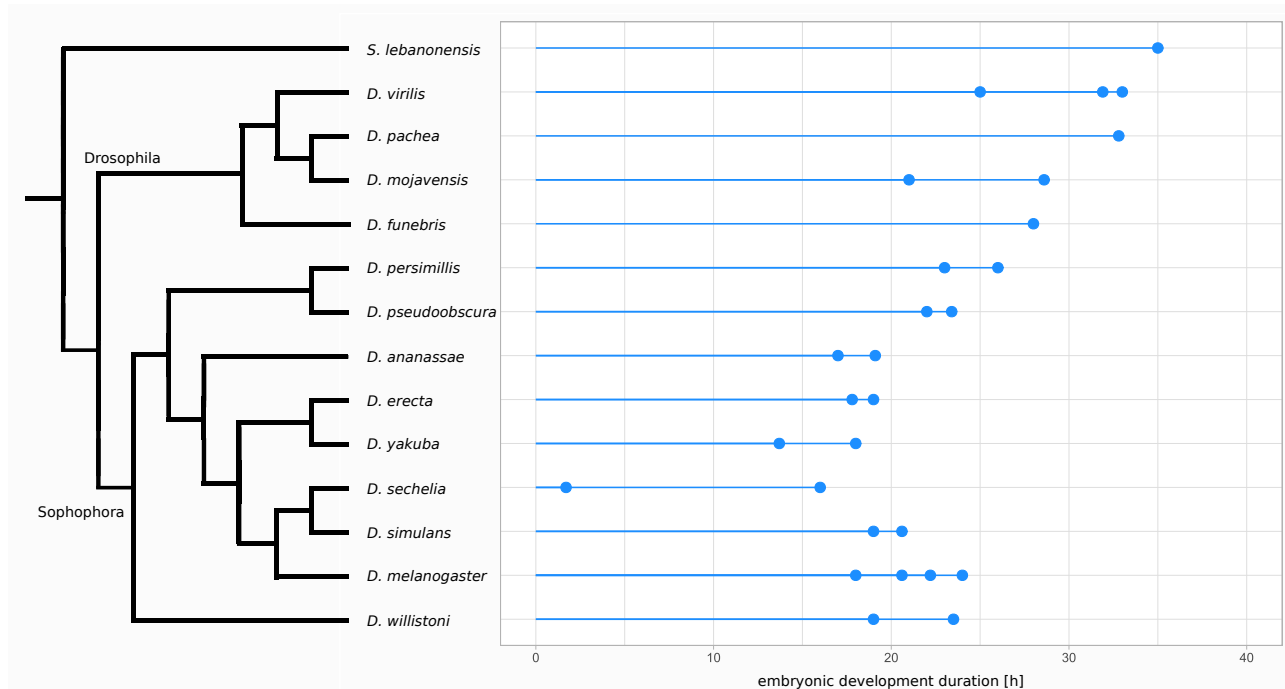


Figure 22 – Durations of the embryonic development in various *Drosophila* species at 22°C- 25°C.

Data concerning other species than *D. packea* was extracted from the literature (see table 10 for references). The data used to establish the cladogram was extracted from Yassin (2013) and Lang et al. (2014).

duration among *Drosophila* species, indicating an acceleration of the overall development in this lineage.

Interestingly, the variations observed in the embryo-to-adult durations between *Drosophila* species mostly coincide with those observed in the embryonic development duration of those species (figures 21 and 22).

D. packea belongs to the nannoptera species group and reveals a longer developmental duration, similarly to species from the robusta group and repleta group (*Drosophila* subgenus) but also to species from the obscura group, willistoni group and saltans group (Sophophora subgenus) (figure 21, table 9). However, we have to keep in mind that the compared species only represent a minority of species with respect to the 1580 described species of the *Drosophila* genus (Bächli, Bernhard, and Godknecht 2020). Thus, climate might have an impact on developmental duration, but is not observed here due to the limited amount of available data.

specie	climate origin	article	food	temp. [°C]	duration [h]
<i>D. affinis</i>	sub-tropical	Fogleman and Wallace 1980	rich	25	379.2
<i>D. algonquin</i>	sub-tropical	Fogleman and Wallace 1980	rich		420.0
<i>D. ananassae</i>	tropical	Moriwaki and Tobari 1975	NA		192.0
		Bharathi et al. 2004	rich		245.0
<i>D. athabasca</i>	continental	Fogleman and Wallace 1980	rich		376.8
<i>D. busckii</i>	continental	Wolfsberg, 1958	NA		288.0
<i>D. equinoxialis</i>	tropical	Krijger, Peters, and Sevenster 2001	rich		220.8
<i>D. funebris</i>	continental	Royes, Robertson, et al. 1964	rich		298.0
<i>D. immigrans</i>	continental	Royes, Robertson, et al. 1964	rich		270.0
<i>D. malerkotliana</i>	tropical	Krijger, Peters, and Sevenster 2001	rich		182.9
		Bharathi et al. 2004	rich		240.0
<i>D. melanogaster</i>	tropical	Krijger, Peters, and Sevenster 2001	rich		206.9
		James and Partridge 1995	rich		242.4
		Bharathi et al. 2004	rich		232.5
<i>D. moju</i>	tropical	Krijger, Peters, and Sevenster 2001	rich		304.8
<i>D. mojavensis</i>	sub-tropical	Markow, Beall, and Matzkin 2009 and Matzkin et al. 2011	rich		457.0
<i>D. n. nasuta</i>	tropical	Bharathi et al. 2004	rich		272.5
<i>D. neomorpha</i>	tropical	Krijger, Peters, and Sevenster 2001	rich		280.8
<i>D. s. neonasuta</i>	tropical	Bharathi et al. 2004	rich		267.5
<i>D. persimilis</i>	desertic	Poulson 1934	NA		323.0
<i>D. pseudoobscura</i>	alpine	Poulson 1934	NA	319.0	
		Marien 1958	rich	360.3	
<i>D. robusta</i>	sub-tropical	Carson 1961	rich	372.0	
<i>D. saltans</i>	tropical	Krijger, Peters, and Sevenster 2001	rich	326.2	
<i>D. simulans</i>	tropical	Ashburner et al. 1989	NA	180.0	
<i>D. sturtevanti</i>	tropical	Krijger, Peters, and Sevenster 2001	rich	355.9	

Table 9 – Embryo-to-adult developmental duration in various *Drosophila* species.

Rich food contains sugar and yeast, whereas poor food does not contain yeast. To ease the comparison, duration has been eventually converted into hours if they had been reported in days. Climate condition of the species habitat were assigned according to the reported collection place. Temp.: temperature.

specie	article	temperature [°C]	embryonic duration [h]
<i>D. ananassae</i>	Kuntz and Eisen 2014	25	17.0
	Markow, Beall, and Matzkin 2009	24	19.1
<i>D. erecta</i>	Kuntz and Eisen 2014	25	19.0
	Markow, Beall, and Matzkin 2009	24	17.8
<i>D. funebris</i>	Lang 2009	22	28.0
<i>D. melanogaster</i>	Kuntz and Eisen 2014	25	18.0
	David and Clavel 1966	25	20.6
	Powsner 1935	25	24.0
	Markow, Beall, and Matzkin 2009	24	22.2
<i>D. mojavensis</i>	Kuntz and Eisen 2014	25	21.0
	Markow, Beall, and Matzkin 2009	24	28.6
<i>D. persimillis</i>	Kuntz and Eisen 2014	25	23.0
	Markow, Beall, and Matzkin 2009	24	26.0
<i>D. pseudoobscura</i>	Kuntz and Eisen 2014	25	22.0
	Markow, Beall, and Matzkin 2009	24	23.4
<i>D. sechelia</i>	Kuntz and Eisen 2014	25	16.0
	Markow, Beall, and Matzkin 2009	24	1.7
<i>D. simulans</i>	Kuntz and Eisen 2014	25	19.0
	Markow, Beall, and Matzkin 2009	24	20.6
<i>D. virilis</i>	Kuntz and Eisen 2014	25	25.0
	Markow, Beall, and Matzkin 2009	24	31.9
	Lang 2009	22	33.0
<i>D. willistoni</i>	Kuntz and Eisen 2014	25	19.0
	Markow, Beall, and Matzkin 2009	24	23.5
<i>D. yakuba</i>	Kuntz and Eisen 2014	25	18.0
	Markow, Beall, and Matzkin 2009	24	13.7
<i>S. lebanonensis</i>	Lang 2009	22	35.0

Table 10 – Duration of the embryonic development in various *Drosophila* species.

Kuntz and Eisen (2014) measured the embryonic duration from cellularisation to trachea filling, whereas David and Clavel (1966), Markow, Beall, and Matzkin (2009), Lang (2009) and Powsner (1935) measured it from oviposition to larval hatching.

Although the habitat characteristics do not appear to affect the developmental duration in *Drosophila*, temperature might still play a role. The duration of embryonic stage, pupal and overall development of *D. melanogaster* at various temperatures has been investigated and a trend was observed that developmental duration decreases when temperature increases (Kuntz and Eisen 2014), James and Partridge 1995, Powsner 1935, Ashburner and Thompson Jr 1978). However, this has not been studied in other *Drosophila* species at larval and pupal stages, except for *D. pachea* pupal stages, where such a trend was not observed and the overall duration was similar at 25 °C and 29 °C. In contrast to *D. melanogaster*, which lives in a wide range of habitats (David and Capy 1988), *D. pachea* is a desert species that lives exclusively on his host plant, the Senita cactus (*Lophocereus schottii*), in the Sonora desert and in Baja California, Mexico (Heed 1982; Markow and O'Grady 2005). The micro climate of the cactus rot pockets in which *D. pachea* live has been monitored over one year by Gibbs, Perkins, and Markow (2003) and it was found that the temperature in the pockets varies from 4.9°C to 42°C. Moreover, *D. pachea* is particularly resistant to heat stress compared to other species (Stratman and Markow 1998). Thus, *D. pachea* may have developed some heat resistance mechanisms or a certain tolerance to daily temperature variations that would buffer the habitat effect on the developmental progress.

Matzkin et al. (2011) tested the impact of nutritional medium on larvae development and found that it affects the developmental duration, in particular in *D. melanogaster* and *D. mojavensis*. In *D. pachea*, the nutritional medium also affects the development duration and survival, in particular at the third larval instar (M. Lang and J. Vidal, unpublished data). As there is no real "standard *Drosophila* food", and recipes vary a lot among reported studies (Lüersen, Röder, and Rimbach 2019), we cannot exclude variations due to food conditions to bias interspecific comparison. In *D. melanogaster*, the larval density was also shown to play on developmental duration, as crowded conditions slowed down larval development due to compromised food conditions and cannibalism (Vijendravarma, Narasimha, and Kawecki 2013). Other factors, such as the the light cycle might affect triggering pupariation (Manning and Markow 1981, Markow 1981). Finally, sex also affects the developmental duration and females tend to have shorter developmental duration than males (Bainbridge and Bownes 1981, Bakker and Nelissen 1963, James and Partridge 1995, Bonnier 1926 Bakker and Nelissen 1963, Bonnier 1926 James and Partridge 1995, Bharathi et al. 2004, Bharathi et al. 2004).

5 Generation of transgenic *D. pachea* expressing DE-cad::GFP, a membrane marker

The genital lobes of *D. pachea* are external in adults, and their development occurs at the posterior end of the male pupa, which is directly observable by microscopy through the skin after removal of the surrounding pupal case. However, to observe the development of such structures *in vivo*, the expression of some fluorescent marker by the fly was mandatory to examine the movement, shape and growth of genital tissues or cells. Thus, we developed a transgenic stock of *D. pachea* expressing a truncated DE-cadherin fused to a GFP to mark the cell membranes. The generation of this new genetic tool in *D. pachea* allowed us to investigate the tissue dynamics underlying the establishment of male genital lobe asymmetry. It also opened the door for future investigations on tissue development in this species.

5.1 Results

5.1.1 The *D. pachea shotgun* homolog shares conserved functional domains with *D. melanogaster*

DE-cadherin is well described in *D. melanogaster* to be localised at the cell membrane and to serve distinct functions in cell adhesion and cell-signalling (Oda et al. 1994, Woods, Wu, and Bryant 1997, Huber et al. 2001, Pacquelet, Lin, and Rørth 2003, Pacquelet and Rørth 2005, Lecuit 2010). The protein has also been fused to GFP in *D. melanogaster*, which then has been widely used to track cells *in vivo* by microscopy (Huang et al. 2009). We aimed to label *D. pachea* cell membranes with a similar approach, but while a stock in *D. melanogaster* exist where the endogenous *shotgun* gene encoding for DE-cadherin is fused to GFP, we rather aimed to overexpress an extra-copy of the encoding *shg* gene, fused to GFP. Furthermore, to ensure that the transgene would be properly located at cell membranes by specific signalling peptides at the N-terminus of the DE-cadherin coding sequence, we initially wanted to make use of the *D. pachea shotgun* homologous gene. However, sequence alignments of the *D. melanogaster* and the *D. pachea shg* homologous coding regions revealed that the start codon of the *shg* gene in *D. melanogaster* was not conserved between the two species. Two putative ATG triplets were found in the *D. pachea* sequence to be in frame with the *shg* coding sequence (CDS) of *D. melanogaster*, at 84 bp upstream of its start codon and 102 bp downstream to it. Thus, we could not unambiguously identify the boundaries of the *D. pachea shg* signalling peptide, expected to be encoded by the first codon triplets of the *shg* CDS. Therefore, we decided to use the functionally characterised *shg* coding sequence

of *D. melanogaster* to derive our transgenic construct (Woods, Wu, and Bryant 1997, Oda et al. 1994, Pacquelet, Lin, and Rørth 2003, Pacquelet and Rørth 2005).

Nonetheless, most of the coding sequence of the *D. pachea shg* homolog could be unambiguously aligned to functional domains annotated in *D. melanogaster shg*. The aligned coding sequence was 4623 bp long (1541 aa), revealing 73.2% nucleotide identity and 77.1% amino-acid identity. All putative protein domains were identified, including the seven cadherin domains, the EGF-like domain, the laminin G-like domain, the transmembrane domain, the β -catenin binding site, as well as parts of the signal peptide, the pro-peptide, the extracellular and the cellular domains (table 11 and figure 23A and B). Thus, the DE-cad encoded by both homologs of *shg* in *D. melanogaster* and *D. pachea* appear to be conserved and probably reveal similarities in protein function and localisation.

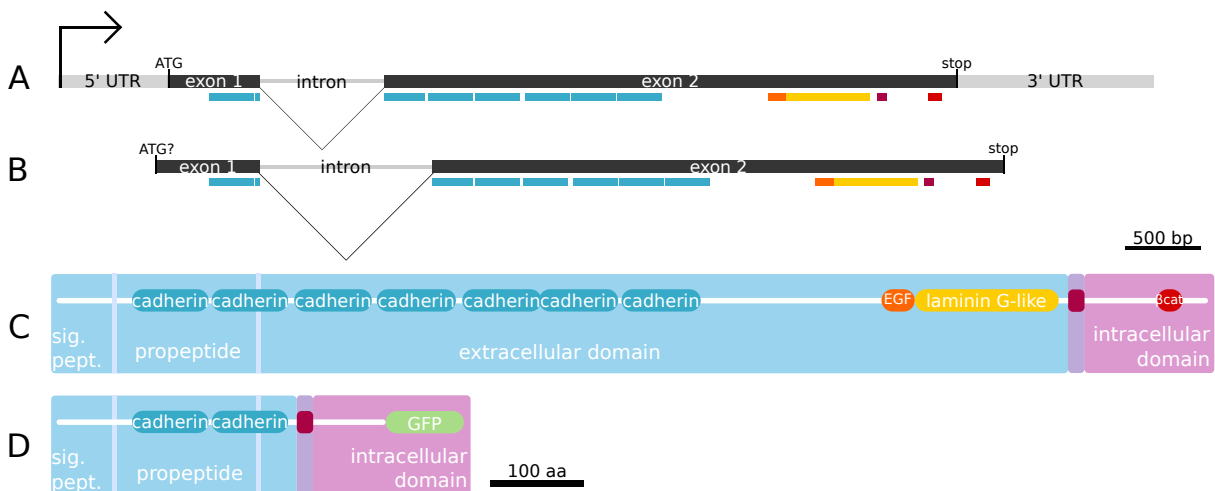


Figure 23 – Annotation of the *shg* gene encoding the DE-Cadherin in *D. melanogaster* and *D. pachea*.

A-B: *Shg* homologous genes in *D. melanogaster* (A) and *D. pachea* (B). The different regions of the genes are indicated. The putative start codon of *D. pachea Shg* is not conserved with *D. melanogaster shg* and the beginning of the coding sequence remains thus uncertain. C: DE-cad protein domains of *D. melanogaster shg* (Oda et al. 1994, protein reference Q24298, available on Uniprot) with seven cadherin domains (blue), a EGF-like domain (orange), a laminin G-like domain (yellow), a transmembrane domain (purple) and a β -catenin binding site (red); the corresponding coding region portions are indicated in A and B with respectively colored lines. Blue background indicates the extracellular part of the protein, purple background the transmembrane domain and pink background the cytoplasmic domain. D: Prediction of the designed truncated DE-cad::GFP fusion protein in transgenic *D. pachea*. Sig. peptide = signal peptide.

domain name	nucleotide position	nucleotide sequence		amino-acid sequence	
		length (bp)	% identity	length (bp)	% identity
CDS	1 to 4624	4623	73.2	1541	77.1
pro-peptide	208 to 783	420	73.1	104	76.4
cadherin 1	213 to 289	297	77.4	99	82.8
cadherin 2	210 to 610	294	75.5	98	77.6
cadherin 3	931 to 1236	306	77.1	102	76.5
cadherin 4	1258 to 1566	309	79.0	103	86.4
cadherin 5	1594 to 1899	306	81.4	102	89.2
cadherin 6	1891 to 2205	315	69.8	105	66.7
cadherin 7	2227 to 2511	285	76.1	95	73.7
EGF-like domain	3259 to 3381	123	69.9	41	80.5
Laminin G-like domain	3385 to 3951	567	76.7	189	81.5
transmembrane domain	3997 to 4059	63	81.0	21	90.5
beta-catenin binding domain	4342 to 4431	90	91.1	30	100

Table 11 – Conservation of *shg* sequence coding for functional domains between *D. melanogaster* and *D. pachea*.

Nucleotide position is given relatively to first nucleotide of the *D. melanogaster* CDS.

5.1.2 Design of the truncated DE-cad::GFP to mark the cell membranes and reduce off-target phenotypes

DE-cadherin has important functions in cell-signalling (Pacquelet, Lin, and Rørth 2003, Pacquelet and Rørth 2005, Lecuit 2010) and the over-expression of this protein as a membrane fluorescent marker might cause general defects in the development of *D. pachea*, due to additionally introduced signalling domains of the transgenic protein. Therefore, we decided to truncate the coding sequence of the transgene in order to keep only sequences that encode essential domains for the correct transmembrane localization while we aimed to remove described signalling domains (see part 2.4.1, page 67 for details on cloning strategy).

Among the different domains of the DE-cad (figure 23A, B and C and table 11), we kept the 5' untranslated region (UTR), the first exon and the 276 first nucleotides of the second exon, coding for the signal peptide, the propeptide and the first two cadherin domains (protein reference Q24298, available on Uniprot; Oda et al. 1994). In addition, we cloned the *shg* coding portion from nucleotide 5865 to 6179, encoding the transmembrane domain and the intra-cellular part of the protein, but not the β -catenin binding site, which is involved both in intra- and extra-cellular signalling via the adherens junctions and the actin cytoskeleton (Pacquelet and Rørth 2005, Lecuit 2010). The structure of the resulting truncated DE-cad::GFP fusion protein is shown in figure 23D. This artificial coding sequence was then cloned downstream of the ubiquitous act-5C promoter (Chung and Keller 1990), resulting in the DE-cad::GFP PiggyBac plasmid (figure 24).

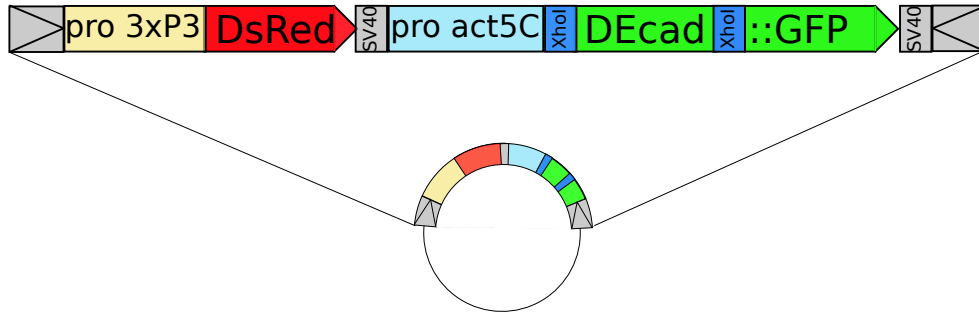


Figure 24 – Simplified map of the DE-cad::GFP PiggyBac plasmid.

The sequence coding for the act5C-DE-cad::GFP membrane marker is indicated (act5C promoter: light blue, DE-cad::GFP: green) as well as those coding for the 3xP3-DsRed selection marker (3xP3 promoter: beige, DsRed: red). The PiggyBac left and right arms are indicated by boxes containing arrows (grey). The XhoI restriction sites (dark blue) and the SV40 sequences are indicated (grey). This plasmids display a ColE1 replication origin and an Ampicilin resistance gene that are not shown.

5.1.3 Transgenic *D. pachea* stocks

From a total of 1709 injected embryos, 14.7 % larvae hatched, 4.3 % pupae formed and 3.5 % adults emerged (60 adults) (table 12). Each 60 adult (G0 flies) was crossed to individuals of the source stock 1698.01_14.2 and 16 of these crosses (26.7 %) revealed transgenic G1 progeny, identified by a red fluorescence in the eye due to the 3xP3-DsRed marker from the integrated PiggyBac vector (table 12). Overall, 0.94 % of injected embryos gave rise to fertile transgenic individuals (table 12). The transformation efficiency in *D. melanogaster* in the experiments of Handler and Harrell (1999) ranged from 0.15 to 0.57 % with 6 to 10 % of the injected embryos that developed and reached sexual maturity. These proportions are thus increased in *D. pachea* compared to the published reference of *D. melanogaster*. Each of the G1 transgenic individuals were then crossed to non-injected virgin adults of opposite sex of stock 1698.01_14.2 to derive a stock (table 13).

	embryos	larvae	pupae	adults	
				total	giving transgenic progeny
n	1709	252	73	60	16
%	100	14.7	4.3	3.5	0.94

Table 12 – *D. pachea* germline transformation efficiency.

Number and percentage of larvae, pupae and adults resulting from the embryo injections.

G0 cross	G1 cross	status
9_B1	9_B1M1	maintained as stock
	9_B1M2	
9_E1	9_E1F1	
	9_E1F2	maintained as stock
	9_E1F3	maintained as stock
	9_E1M1	maintained as stock, transgene insertion mapped, imaged
9_F1	9_F1M1	
9_D2	9_D2F1	maintained as stock, imaged
	9_D2M1	
	9_D2M2	
	9_D2M3	
9_A3	9_A3F1	maintained as stock, transgene insertion mapped, imaged
	9_A3F2	maintained as stock
	9_A3M1	maintained as stock
9_G3	9_G3F1	maintained as stock, transgene insertion mapped, imaged
9_A4	9_A4F1	
9_B4	9_B4F1	
	9_B4F2	maintained as stock
	9_B4F3	maintained as stock
	9_B4F4	maintained as stock
	9_B4F5	maintained as stock
	9_B4F6	maintained as stock
	9_B4F7	
	9_B4F8	maintained as stock
	9_B4F9	maintained as stock, transgene insertion mapped, imaged
	9_B4F10	maintained as stock
	9_B4M1	maintained as stock
9_E4	9_E4F1	
	9_E4M1	maintained as stock
	9_E4M2	maintained as stock
	9_E4M3	maintained as stock
	9_E4M4	
	9_E4M5	
9_F5	9_F5M1	maintained as stock
	9_F5M2	maintained as stock
	9_F5M3	
	9_F5M4	maintained as stock

Table 13 – Crosses and stocks with transgenic *D. pachea*, carrying DE-cad::GFP (continued on the following page).

G0 cross	G1 cross	status
9_D6	9_D6M1	maintained as stock
9_E6	9_E6F1	
	9_E6F2	maintained as stock
9_H6	9_H6F1	
	9_H6F2	maintained as stock
	9_H6M1	
9_H7	9_H7F1	maintained as stock
9_A8	9_A8M1	maintained as stock
9_C8	9_C8F1	maintained as stock
	9_C8M1	
	9_C8M2	maintained as stock

Table 13 – Crosses and stocks with transgenic *D. pachea*, carrying DE-cad::GFP (continued from the previous page).

5.1.4 The DE-cad::GFP is inserted inside putative intergenic regions in four different *D. pachea* stocks

The transgene insertion site was mapped in four stocks 9_E1M1, 9_A3F1, 9_G3F1 and 9_B4F9, used in *in vivo* microscopy experiments (see part 5.1.4, page 108 for details on transgene insertion sites). The insertion sites of the PiggyBac constructs were mapped by inverse PCR (see part 2.5.3, page 74), to amplify parts of the PiggyBac left arm (Handler et al. 1998) and several hundreds of base pairs of the adjacent genomic region. PCR products were sequenced by Sanger sequencing and then aligned to the annotated *D. pachea* genome assembly (Lang and Courtier, in preparation) (figure 25). In all evaluated stocks, the transgene was inserted inside putative intergenic regions (figure 25). In addition, no particular aberrant phenotype was detected in adults from any of the stocks. The mapping of the transgene insertion site of a fifth stock, 9_D2F1, which was used in live-imaging experiments is still ongoing.

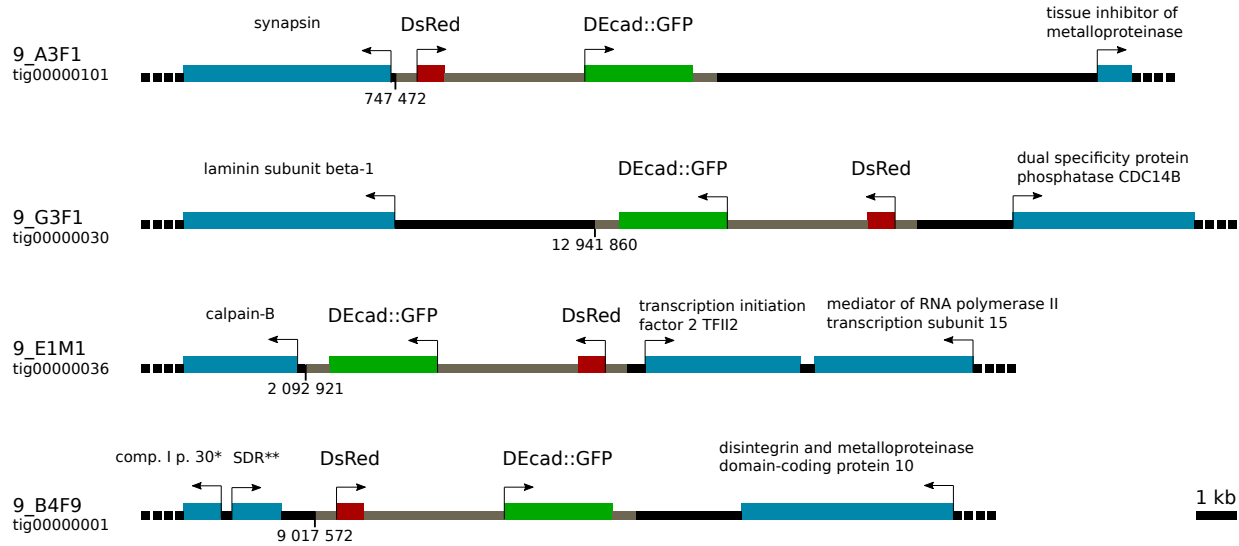


Figure 25 – Localisation of the transgene insertion site in four *D. pachea* stocks. The transgene insertion site was mapped in 9_A3F1, 9_G3F1, 9_E1M1 and 9_B4F9 stocks. The stock name and the contig in which transgene was found are indicated on the left side of the figure. The position of the insertion is indicated for each stock. The DE-cad::GFP, the DsRed and the regions from the transgene are indicated in green, red, and grey respectively. The putative intergenic regions are indicated in black, and predicted genes found at the vicinity of the transgene insertion are indicated in blue. Comp. I p30: complex I intermediate associated protein 30. SDR: dehydrogenase/reductase SDR family protein 7-like.

5.1.5 GFP expression in DE-cad::GFP *Drosophila pachea* is localized at cell membranes

To characterise the localisation of the DE-cad::GFP in our transgenic stocks of *D. pachea*, we compared their fluorescence with those of the *D. melanogaster* DE-cad stock, in which the endogenous DE-cad is fused to GFP (Huang et al. 2009) (see part 2.1, page 48). The GFP fluorescence was investigated with pupae at 24 h APF (as described in part 2.5.4, page 75). The anal plates of the flies constituted a suitable tissue to compare fluorescence localization as they are easy to visualize at the posterior tip of the pupa.

The fluorescence in *D. melanogaster* expressing the DE-cad::GFP is very characteristic of a cell membrane staining where fluorescence is detected at cell boundaries or membranes (figure 26 A). The fluorescence observed in 9_E1M1, 9_A3F1, and 9_G3F1 stocks of transgenic *D. pachea* expressing DE-cad::GFP (figure 26 B, C and D, respectively) revealed a similar pattern to *D. melanogaster* DE-cad::GFP, with GFP expression at the cell membranes. Thus, our DE-cad::GFP construct is indeed located at cell membranes. This fluorescence was found in various other tissues such as male and female genital tissue, male and female anal plates,

legs, or abdominal tissue. Furthermore, the fluorescence is very similar among stocks, indicating that the insertion site of the transgene does not have a detectable effect on DE-cad::GFP intra-cellular localization.

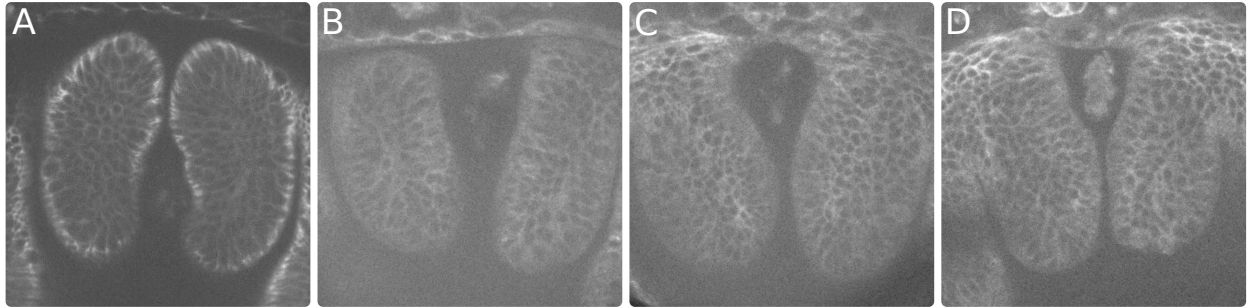


Figure 26 – GFP fluorescence localizes at cell membranes in both the *D. melanogaster* DE-cad::GFP stock (Huang et al. 2009) and *D. pachea* DE-cad::GFP stocks.

Anal plate tissue of pupae at 24 h APF from A: *D. melanogaster* DE-cad::GFP stock, B: *D. pachea* DE-cad::GFP 9_E1M1, C: 9_A3F1 and D: 9_G3F1 stocks. The anal plates are oriented dorsal part up and ventral part down.

5.2 Discussion

5.2.1 The truncated DE-cad::GFP encoded by the transgene localizes at cell membranes in transgenic *D. pachea*

By its role in cell-cell adhesion as well as in cell signalisation (Oda et al. 1994 ; Pacquelet and Rørth 2005), over-expression or mis-expression of DE-cad can lead to severe phenotypes and eventually to lethality (Pacquelet and Rørth 2005). To use the DE-cad::GFP as membrane marker, we designed a truncated form with the aim to stain the cell membranes but without interfering in endogenous DE-cad functions. We did not find any striking off-target phenotype in the transgenic *D. pachea* stocks produced, indicating that the DE-cad::GFP did not present a particular toxicity to the flies. The truncated DE-cad::GFP was expressed in an ubiquitous manner, including male and female developing genitalia, and was correctly located at cell membranes, indicating a conserved function of both the act5C promoter and the signal peptide between *D. melanogaster* and *D. pachea*. Thus, this plasmid constitutes an useful tool for the research community and could probably be used in other *Drosophila* species for live-imaging purposes.

Furthermore, this plasmid has been designed to be easily modified. The DE-cad could be replaced by any other marker of interest by using the flanking XhoI restriction sites, which were introduced during construct cloning.

5.2.2 Generation of transgenic *D. pachea*, a promising new genetic tool

Transgenesis using the PiggyBac approach (Handler et al. 1998) has been done successfully carried-out in several *Drosophila* species, such as in well known model species *D. melanogaster*, but also in *D. simulans*, *D. erecta*, *D. yakuba*, *D. sechellia*, *D. willistoni*, *D. mojavensis*, *D. pseudoobscura* and *D. virilis* (Holtzman et al. 2010). Here, we present transgenic stocks generated in *D. pachea*, establishing this species as a new genetic model and thus opening a door for diverse future studies.

The establishment of transgenic DE-cad::GFP stocks in *D. pachea* allows direct observation of developing tissues *in vivo*, but also enables to carry out laser ablation experiments in order to destroy cell of interest and to monitor the morphological effects in the adult. In addition, mechanical forces that act on tissues can be examined by observing tissue movement after introduction of such incisions. Furthermore, our *D. pachea* transgenic stocks could also

be used for various other purposes to monitor morphogenesis or diverse cell behaviors. As the site of the introduced transgene is not controlled, we generated several stocks that carry the PiggyBac insertion at different locations in the genome. These stocks could be used in forward genetic approaches as a chromosomal marker to map nearby genes.

The generation of future DE-cad::GFP transgenic stocks of the sister species *D. nanoptera* and *D. acanthoptera* would offer another possibility to better compare *in vivo* genitalia development and to find out the changes that occurred in developmental processes leading either to asymmetric genital lobes in *D. pachea*.

Altogether, the successful generation of the transgenic DE-cad::GFP *D. pachea* offers a wide range of possibilities for future studies.

6 How is *D. pachea* male genital lobe asymmetry established during development?

The main objective of my PhD thesis was to characterise asymmetric male genitalia development in *D. pachea* and to investigate the intrinsic growth processes taking place in the developing lobes. This work was done on developing genitalia fixed at various moments of pupal development and *in vivo* with the previously mentioned DE-cad::GFP transgenic stocks of *D. pachea*. Furthermore, male genitalia rotation, which is a conserved developmental process in flies and during which the male genitalia undergo a 360° clockwise rotation, occurs at the pupal stage. As this rotation is always clockwise, it is also an asymmetric morphogenetic process. We investigated the possible functional link between lobe growth and genitalia rotation.

6.1 Results

6.1.1 Asymmetric *Drosophila pachea* lobe growth occurs between 24 h APF and 36 h APF

Several tissue growth differences could account for the different lobe sizes at the left and right sides of *D. pachea* male genitalia. Lobe asymmetry may result from a differential growth timing between lobes, i.e. the long left lobe may start to grow earlier compared to the shorter right lobe. Alternatively, an earlier growth arrest in the right lobe might account for smaller tissue size. The size difference between lobes may also result from difference in mitotic rates, cell sizes, or from differential cell recruitment from neighbouring tissues. To investigate cell proliferation of asymmetric lobe, I performed immuno-fluorescent staining of fixed samples with an anti-PhosphoHistone H3 (PH3) antibody at various developmental time points from 24 h APF to 48 h APF (figure 27).

Lobe growth was first considered to be observed at 24 h APF, by identification of two buds at corresponding ventral tips of the developing genital arch (figure 27). At later time points, this bud appeared to become elongated and increased in cell number until about 36 h APF. Therefore, major cell number increase that constitute the lobes occur between 24 h APF and 36 h APF. To characterise more precisely the cell number increase within the lobes, the number of nuclei was quantified at various developmental time points using Imaris software with an automatic count option (see part 2.5.4, page 2.5.4). The proximal limits of the lobes with respect to the genital arch were defined as a straight line from the lateral border of the

corresponding clasper to the outer limit of the genital arch (figure 27, fourth row, green lines on the schemes). Then, we counted each nucleus stained with DAPI within the lobe tissue. This quantification revealed that lobe growth results from cell number increase between 24 h APF and 36 h APF. The left lobe reaches about 410 nuclei and the right lobe about 220 nuclei (figure 28, blue and red dots, respectively). The increase of cells appeared to saturate after 36 h APF and I used the logistic curve to describe lobe growth (figure 28, blue and red lines correspond to the fit for the left and right lobe, respectively) following the equation:

$$n_{\text{nuclei}} = \frac{\varphi_1}{1 + e^{-(\varphi_2 + \varphi_3 \times \text{age})}}$$

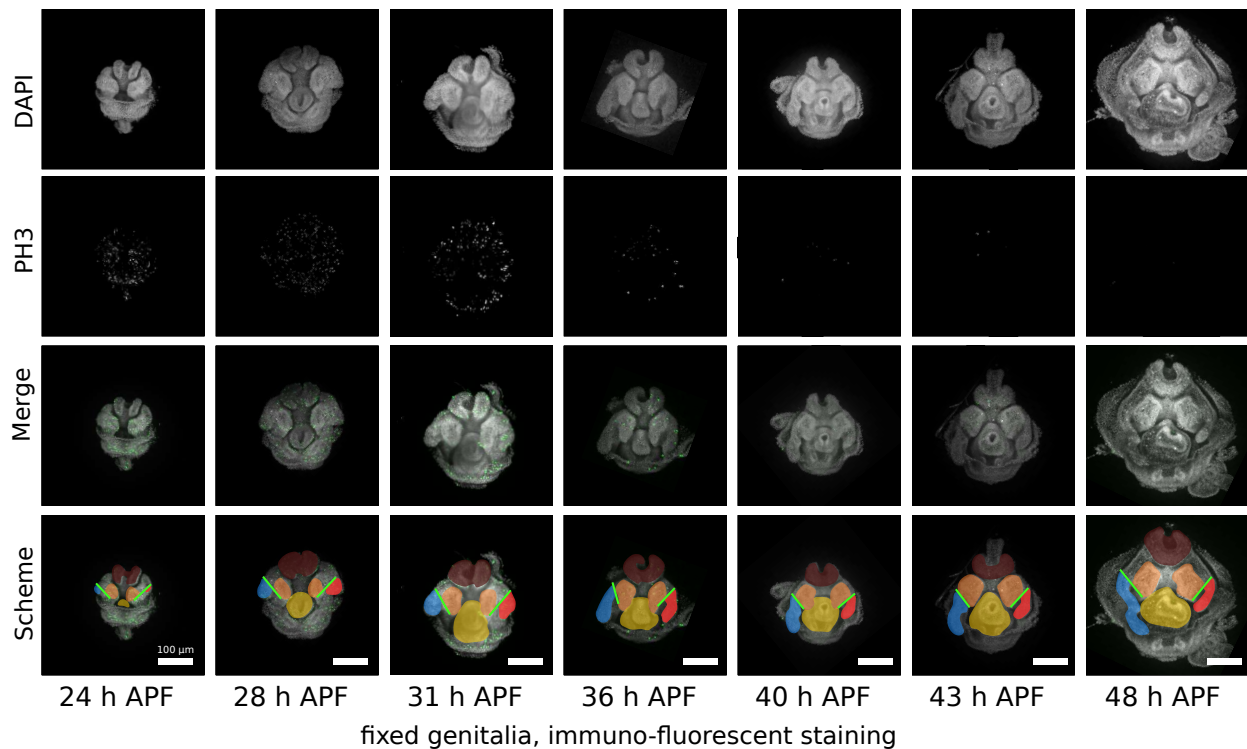


Figure 27 – Immuno-fluorescent staining of developing genitalia at various developmental time points in the wild-type stock 1698.01.

Nuclei were stained with DAPI (grey, first and third rows) and mitotic cells by anti-phospho-histone H3 (green, second and third rows) at various developmental time points ranging from 24 h APF to 48 h APF. The different structures of the developing genitalia are highlighted: anal plates are shown in brown, claspers in orange, phallus in yellow, the left lobe is shown in blue and the right lobe in red (schemes, fourth row). The proximal limits of the lobes, shown by green lines, are defined relatively to the lateral border of the claspers (schemes, fourth row). Scale bar: 100 µm.

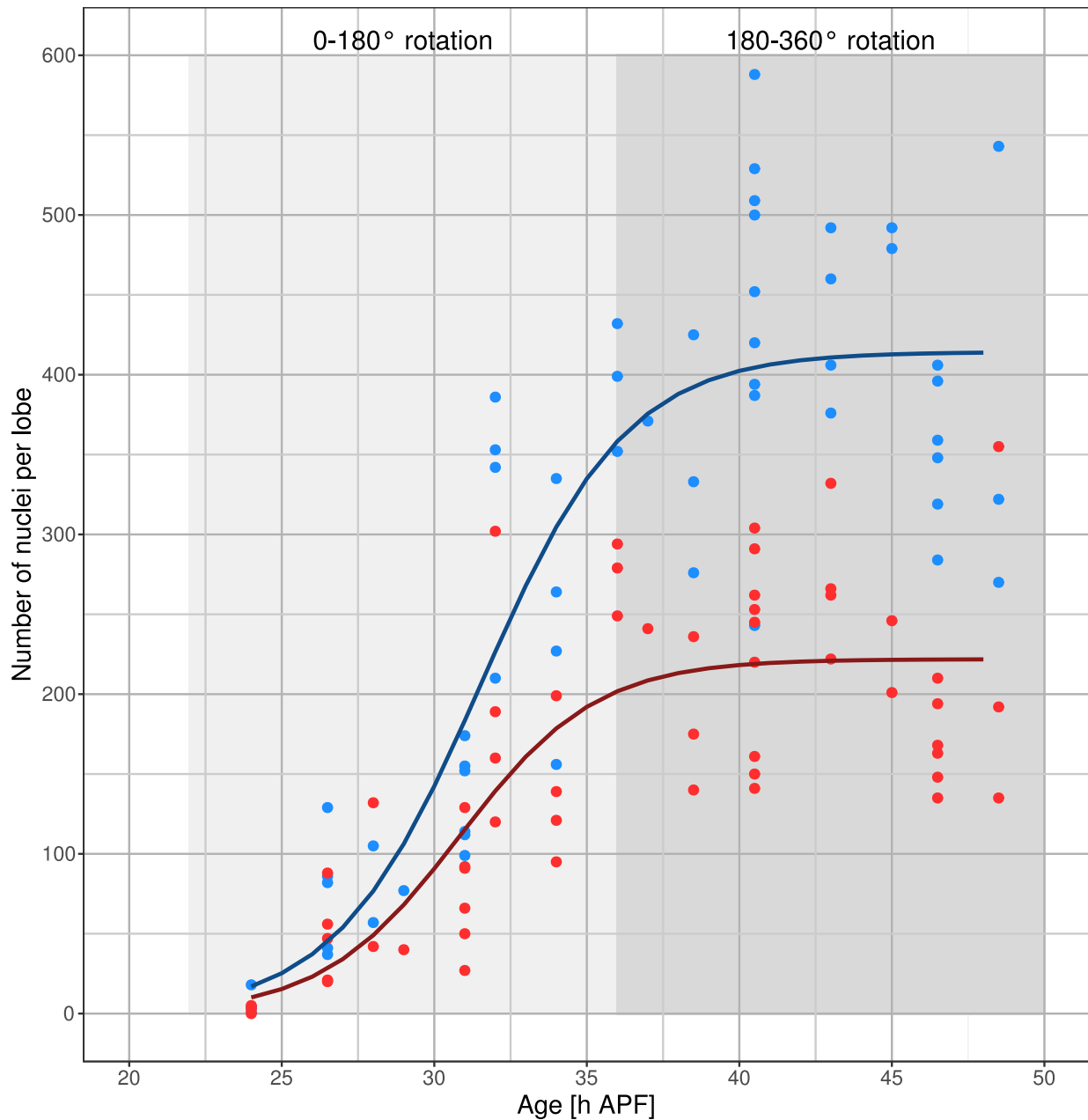


Figure 28 – Quantification of the number of nuclei per lobe at various developmental time points in the 1698;01 wild-type stock.

Quantification was done microscopy data from fixed samples stained with DAPI. The lobe contour was drawn by hand on Imaris software and nuclei were automatically detected and counted in the area. Each dot correspond to the number of nuclei at the left lobe (blue) and right lobe (red). The lines correspond to the logistic regression models fitted on number of nuclei in the left lobe (blue, $\varphi_1 = 414$; $\varphi_2 = -13.17$; $\varphi_3 = 0.4174$) or in the right lobe (red, $\varphi_1 = 222$; $\varphi_2 = -13.75$; $\varphi_3 = 0.4461$).

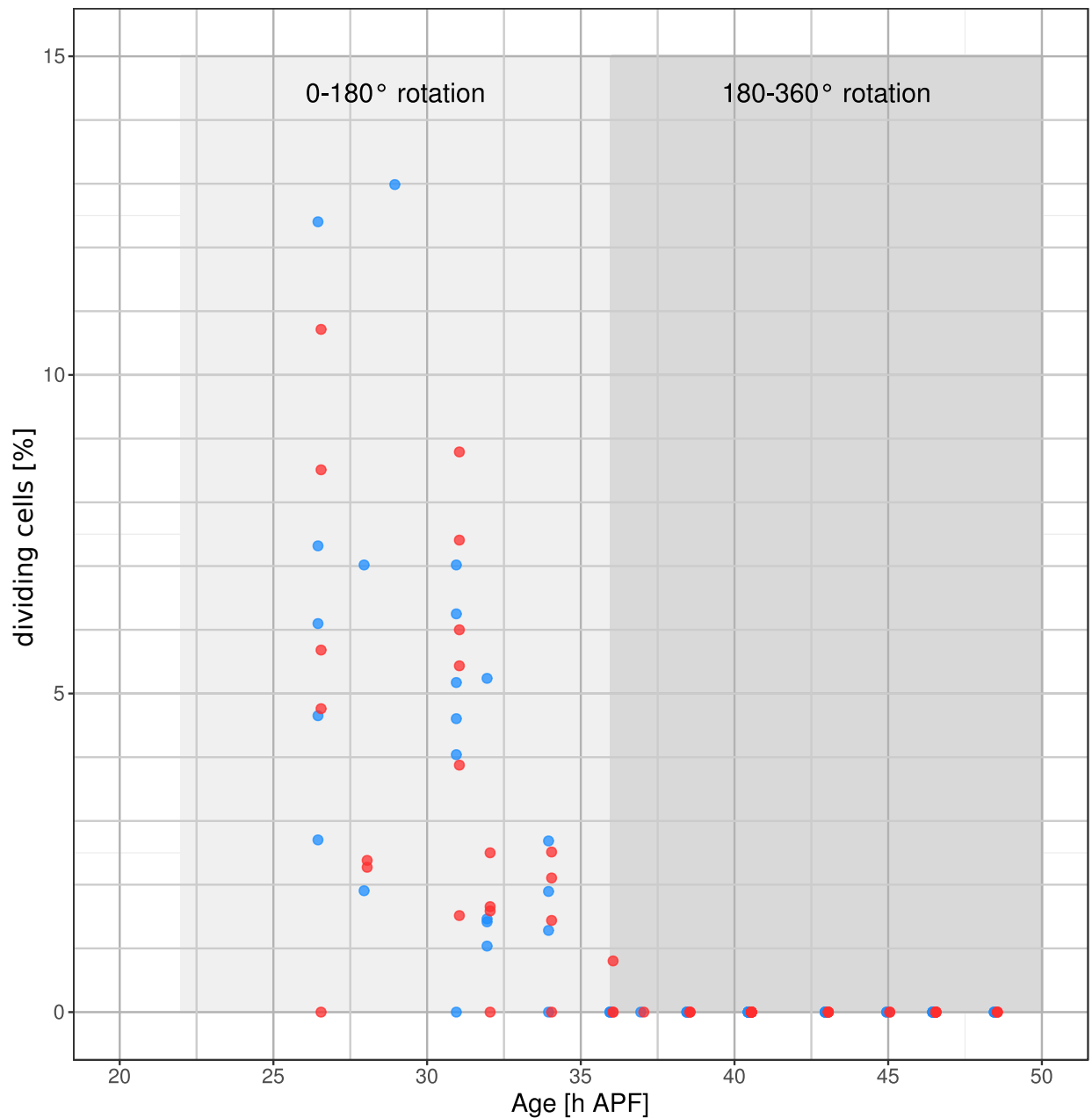


Figure 29 – Proportion of mitotic cells in *D. pachea* male genital lobes at various developmental time points.

Quantification of anti-Ph3 stained nuclei fixed samples stained with anti-phosphohistone H3 (PH3). Each dot correspond to the percentage of mitotic cells in the left lobe (blue) or right lobe (red). The dots have been slightly shifted on the x-axis for a better visualisation.

The best fitting models based on a non-linear least square fit are summarized in table 14. Therefore, the most important difference between the parameters concerns the asymptote of the curve, φ_1 , whereas the growth parameters φ_2 and φ_3 are quite similar between models.

lobe	φ_1	φ_2	φ_3
left	414	-13.17	0.4147
right	222	-13.75	0.4461

Table 14 – The values are those of the best fitting model based on a non-linear least square fit.

Both lobes have similar growth periods, indicating that the lobe asymmetry does not result from an earlier developmental start of the left lobe compared to the right lobe. We can also exclude the possibility that a growth arrest of the right lobe occurs earlier in development compared to the left lobe since growth curves of both lobes tend to saturate at around 36 h APF. Furthermore, lobe growth occurs during the first half of the genitalia rotation (see part 6.1.3, page 118, figure 31) (figure 28, blue dots).

To investigate if the lobe asymmetry resulted from differences in the mitotic rate between left and right lobes, we quantified mitotic cells at various developmental time points (figure 29). We observed the presence of mitotic cells in the entire genital tissue and also in the lobes between 24 h APF and 36 h APF (figure 27). Then, mitosis appears to attenuate in the entire male genitalia tissue (figure 27). From 26 h APF to 36 h APF, the proportion of mitotic cells in left and right lobe varied from 0 - 13% (figure 29), but no difference in mitotic rates was found between the left and the right lobe (Wilcoxon test: $W = 316.5$, $P = 0.7268$). The lobe size difference may thus result either from a short pulse of proliferation that we did not detect on the fixed, immuno-stained samples or this difference may perhaps result from a rather constant cell recruitment from the adjacent genital arch that would not significantly affect tissue growth dynamics, but still result in an increase of cell number.

6.1.2 Differences in male genitalia morphology appear from 24 h APF between *D. pachea* and *D. nannoptera*

Males of the sister species of *D. pachea*, *D. nannoptera* and *D. acanthoptera* do not develop asymmetric lobes. We wanted to compare the development of male genital development in *D. pachea* to corresponding tissues in the sister species in order to delimit the time-period

when developmental differences would occur. For this, we performed pH3 immuno-stainings on fixed and DAPI stained male genital tissues of *D. acanthoptera* and *D. nannoptera* at 24 h APF, 36 h APF and 40 h APF.

As observed in *D. pachea*, the growth of the genital tissue occurs by bulk growth, due to mitotic cells throughout the entire tissue. In *D. pachea* and *D. acanthoptera*, mitotic cells are visible in the whole genital structure up to 36 h APF (figure 30). Focusing on the area where the lobes grow in *D. pachea* and on the corresponding area in *D. nannoptera*, we observe a difference in the tissue shape at 24 h APF and later time points (figure 30, white arrow heads). In *D. pachea*, characteristic lobe buds are visible while the tissue appears to be flat in *D. nannoptera*. At 36 h APF, the male genitalia of *D. pachea* display striking shape differences compared those of *D. nannoptera* and *D. acanthoptera*, that basically do not form lobes. Altogether, these observations indicate that male genital shape differences between *D. pachea*, *D. nannoptera*, and possibly *D. acanthoptera* arise at around 24 h APF, with the outgrowth of the lobes in *D. pachea*.

6.1.3 Genitalia rotation takes place between 24 h APF and 45 h APF in wild-type *Drosophila pachea* whereas it happens about 6 h earlier in a mutant stock

The timing of male genitalia rotation in *D. pachea* was first characterised on dissected pupae from the wild-type stock 1698.01, in which males consistently display a asymmetric lobes. Then, I used males from the selection stock (see part 3.1.1, page 77 for more details) where males genital lobe length is variable (figures 12 and 13).

In the wild-type 1698.01 stock, the rotation occurs from about 23 - 24 h APF to 44 - 45 h APF (figure 31, blue dots) and occur always in clockwise direction as in *D. melanogaster* (Spéder, Ádám, and Noselli 2006, Suzanne et al. 2010, Sato et al. 2015). In the selection stock, the rotation also occurs in clockwise direction but in average rotation starts prematurely compared to the wild-type stock (figure 31, yellow dots). I fitted logistic curves on both datasets, again using non-linear least square fit (figure 31), following the equation:

$$\text{rotation} = \frac{\varphi_1}{1 + e^{-(\varphi_2 + \varphi_3 \times \text{age})}}$$

Parameter φ_1 correspond to the asymptote of the of the curve and should thus correspond to 360 as the maximum rotation angle of the genitalia is 360°. In the model of the wild type-

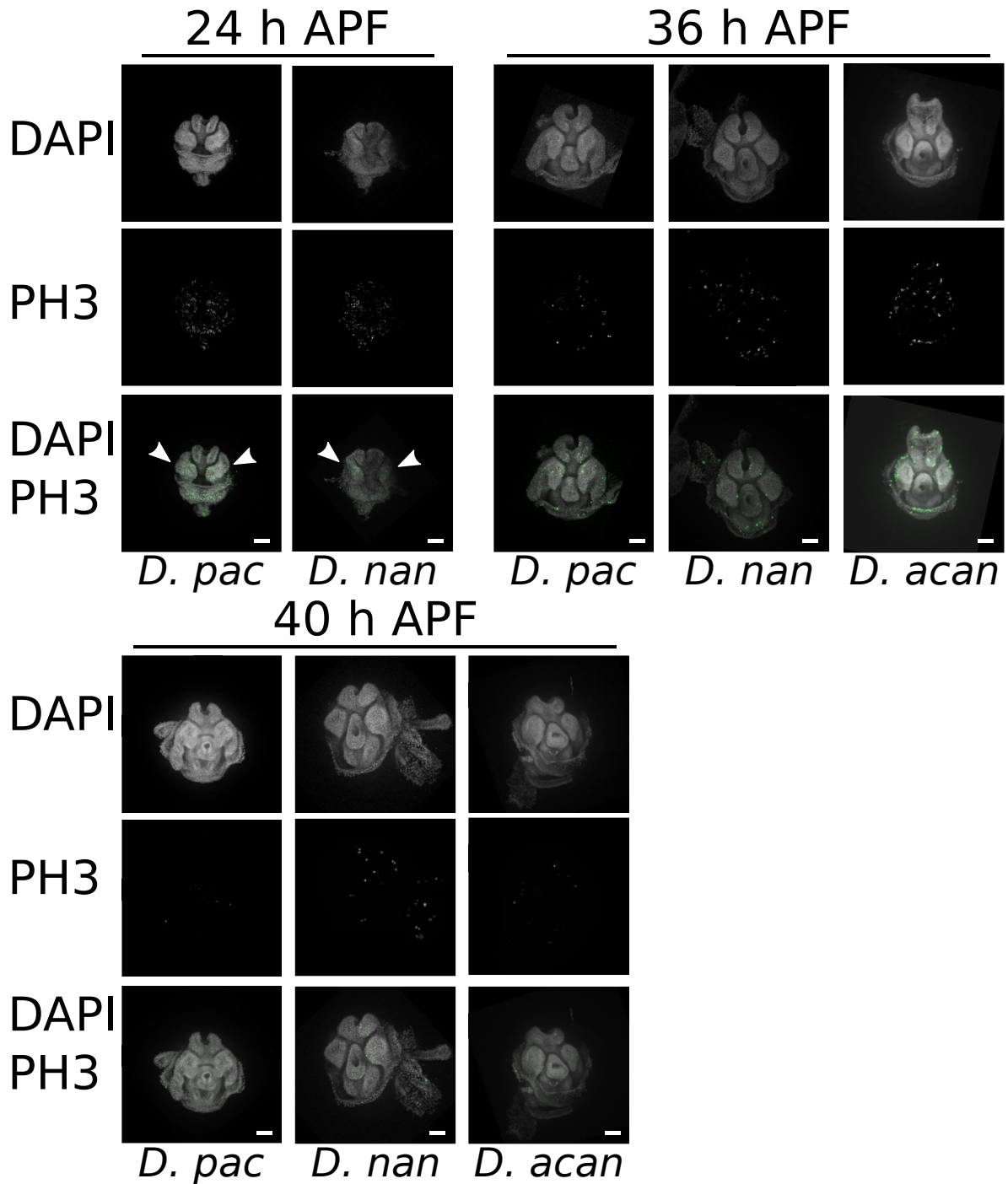


Figure 30 – Immunofluorescent staining of *D. pachea*, *D. acanthoptera* and *D. nannopectera* developing genitalia at various developmental time points.

Nuclei were stained with DAPI (grey, first and third rows) and mitotic cells by anti-phospho-histone H3 (green, second and third rows) at 24 h APF, 36 h APF and 40 h APF in the wild-type stocks 1698.01 in *D. pachea*, nan12 in *D. nannopectera* and acan in *D. acanthoptera*. The anal plates are oriented up and the phallus down. The regions where the lobes develop in *D. pachea* as well as the corresponding region in *D. nannopectera* are indicated by arrow heads. Scale bar: 100 μ m.

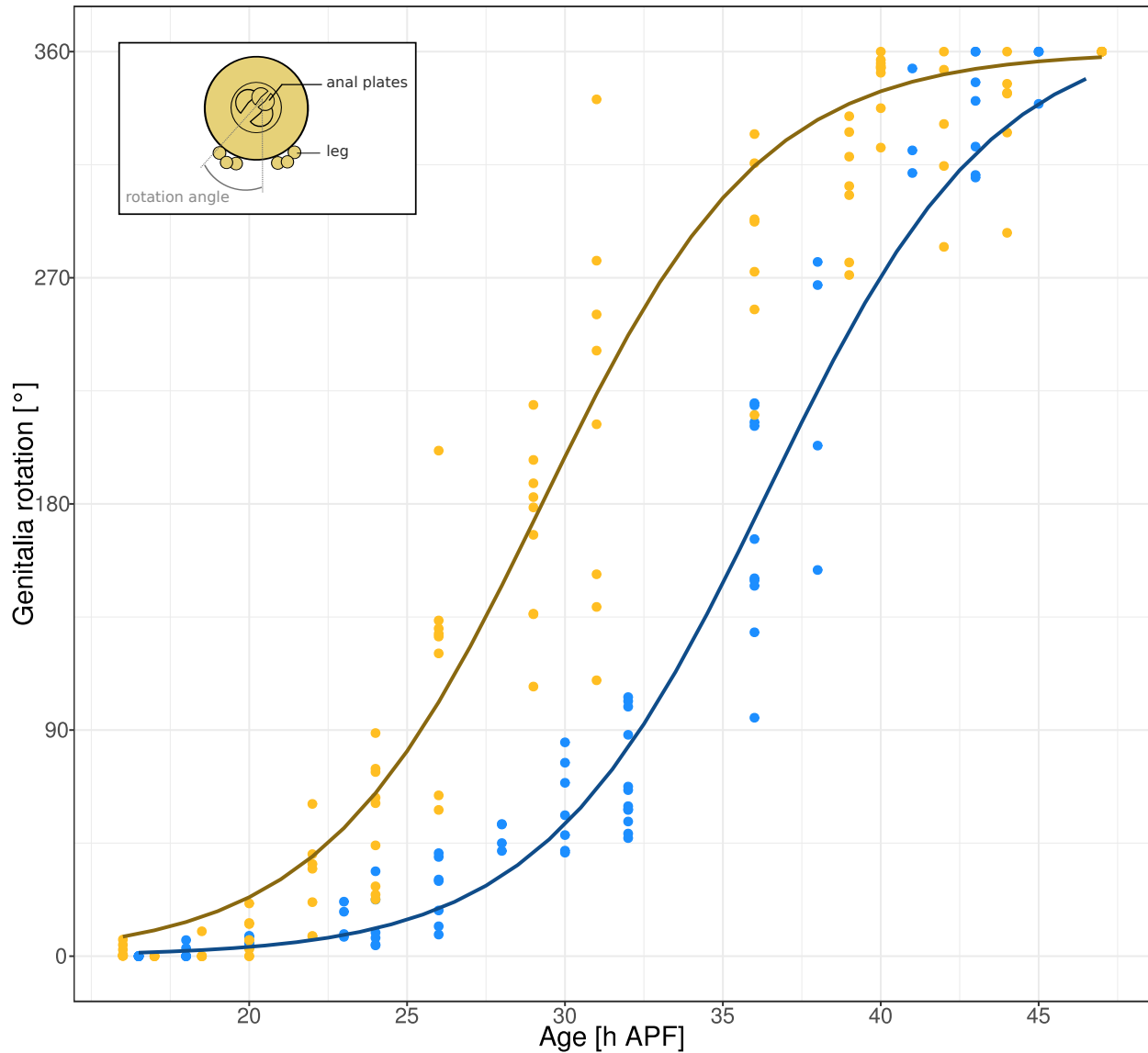


Figure 31 – Characterization of the genitalia rotation timing on fixed samples from selection stock and wild-type stock 1698.01.

Samples were dissected as described in figure 8, page 64, and the angle of genitalia rotation was measured as shown in the sketch. Data of wild-type stock 1698.01 stock are shown in blue and of selection stock in yellow. The lines correspond to logistic models fitted on each dataset (1698.01, $\varphi_1 = 370$; $\varphi_2 = -10.2$; $\varphi_3 = 0.28$; selection stock , $\varphi_1 = 360$; $\varphi_2 = -8.13$; $\varphi_3 = 0.27$).

stock, φ_1 is 370 and not to 360. This is due to the lack of measurements after 45 h APF. The two other parameters, φ_2 and φ_3 , characterise the steepness of the curve ; we note that φ_3 is very similar between the two models whereas φ_2 is greater in the selection stock (-8.13) compared to the wild-type stock (-10.2). This is congruent with the notion that relative rotation velocity (φ_3) is similar between the two stocks but the timing of rotation is shifted (φ_2), occurring about 6 h earlier in the selection stock.

experiment	stock	φ_1	φ_2	φ_3
imaging on dissected tissues	1698.01	370	-10.2	0.28
	selection stock	360	-8.13	0.27
time-lapse imaging	DE-cad::GFP	365	-11.94	0.35

Table 15 – Parameters of the logistic regression models describing genitalia rotation in the wild-type and in the selection stock. The values are those of the best fitting model, based on a non-linear least square fit, characterizing the rotation timing on dissected samples from the wild-type stock 1698.01 or from the selection stock, and from time-lapse imaging on the DE-cad::GFP transgenic stocks.

As the pupae were dissected, our approach did not allow the tracking of the full rotation progress in the same individual, and may thus involve some imprecision with respect to variation in developmental progress between observations due to the synchronisation method (see part 2.3.1, page 60 for more details). However, the development of transgenic *D. packea* expressing the DE-cad::GFP membrane marker in the wild-type genetic background allowed us to follow the entire genitalia rotation process on live pupae by time-lapse microscopy. Of the 20 male pupae analyzed, we observed a full rotation of 14 individuals while premature rotation stop and an arrest of the genitalia morphogenesis occurred in 6 pupae, indicating their death during the time-lapse acquisition. These 6 pupae were excluded from the analysis.

Among pupae monitored by time-lapse imaging, the genitalia rotation started at approximately 24 h APF and ended at 40 - 42 h APF (figure 32). The rotation start is thus similar to what was observed with dissected individuals of stock 1698.01 (figure 32). However, the rotation appeared to be faster during time-lapse acquisition (16 h) compared to the analysis of dissected samples (20 h), also detectable by the logistic curves parameters φ_2 and φ_3 (Table 15) that reveal an accelerated speed of rotation.

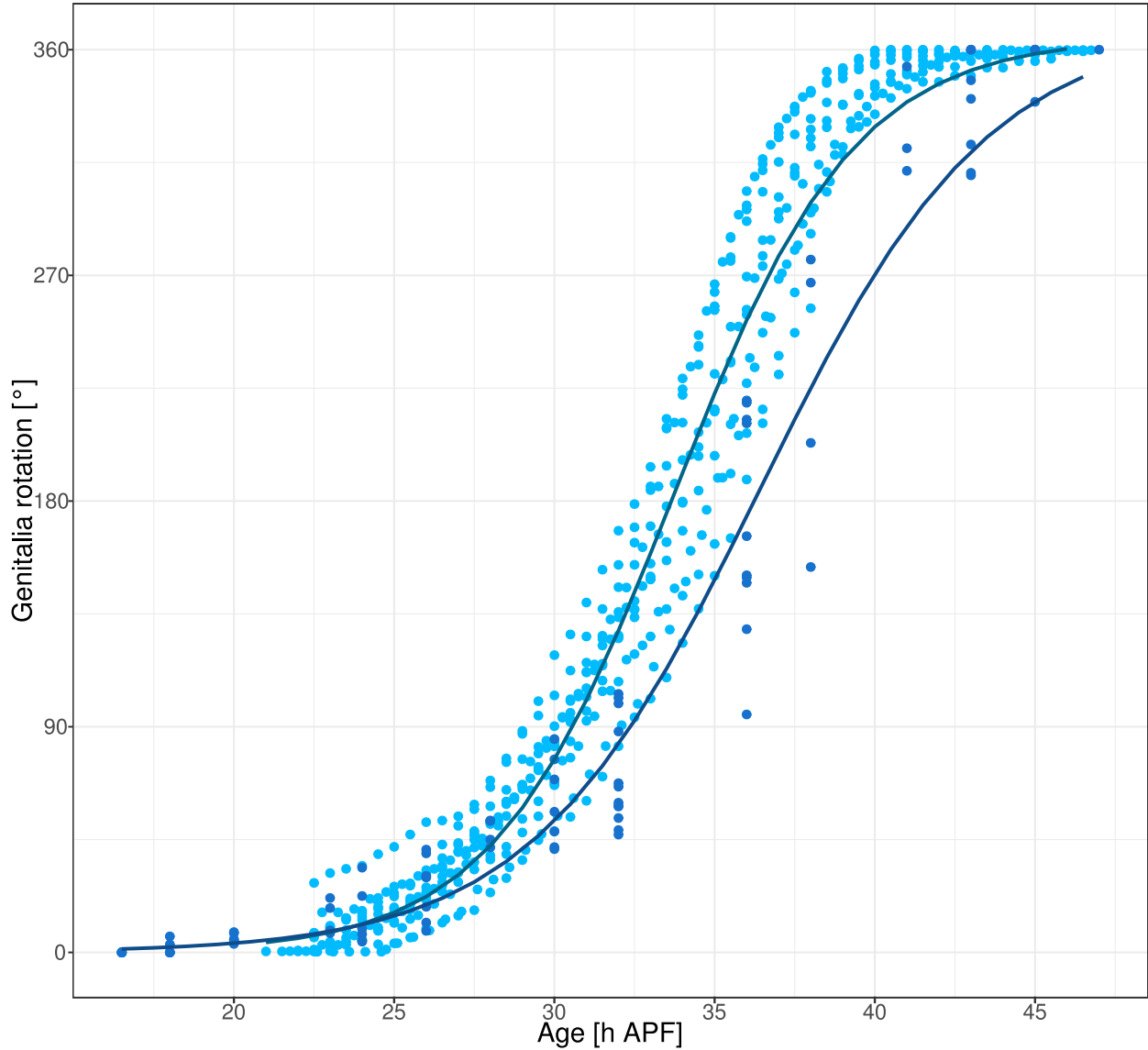


Figure 32 – Characterization of genitalia rotation timing measured on dissected samples from stock 1698.01 (dark-blue) and extrapolated from live-imaging analysis of the *DE-cad::GFP* transgenic stocks (light-blue).

The angle of genitalia rotation was measured as previously described above (figure 31). The lines correspond to the logistic models fitted on each data-set.

6.1.4 The speed of genitalia rotation peaks at 35 h APF, which approximately corresponds to 225° of rotation

The precise timing of the genitalia rotation seems to be important for the correct development of left-right asymmetric lobes. I estimated the rotation velocity throughout the genitalia rotation progress. This speed was estimated from time-lapse analysis by comparing rotation angles between image acquisition time points. Rotation speed increases during the first half rotation and peaks at 35 h APF, which approximately corresponds to 225° of rotation (figure 33). Then, rotation speed decreases until the end of the rotation (figure 33).

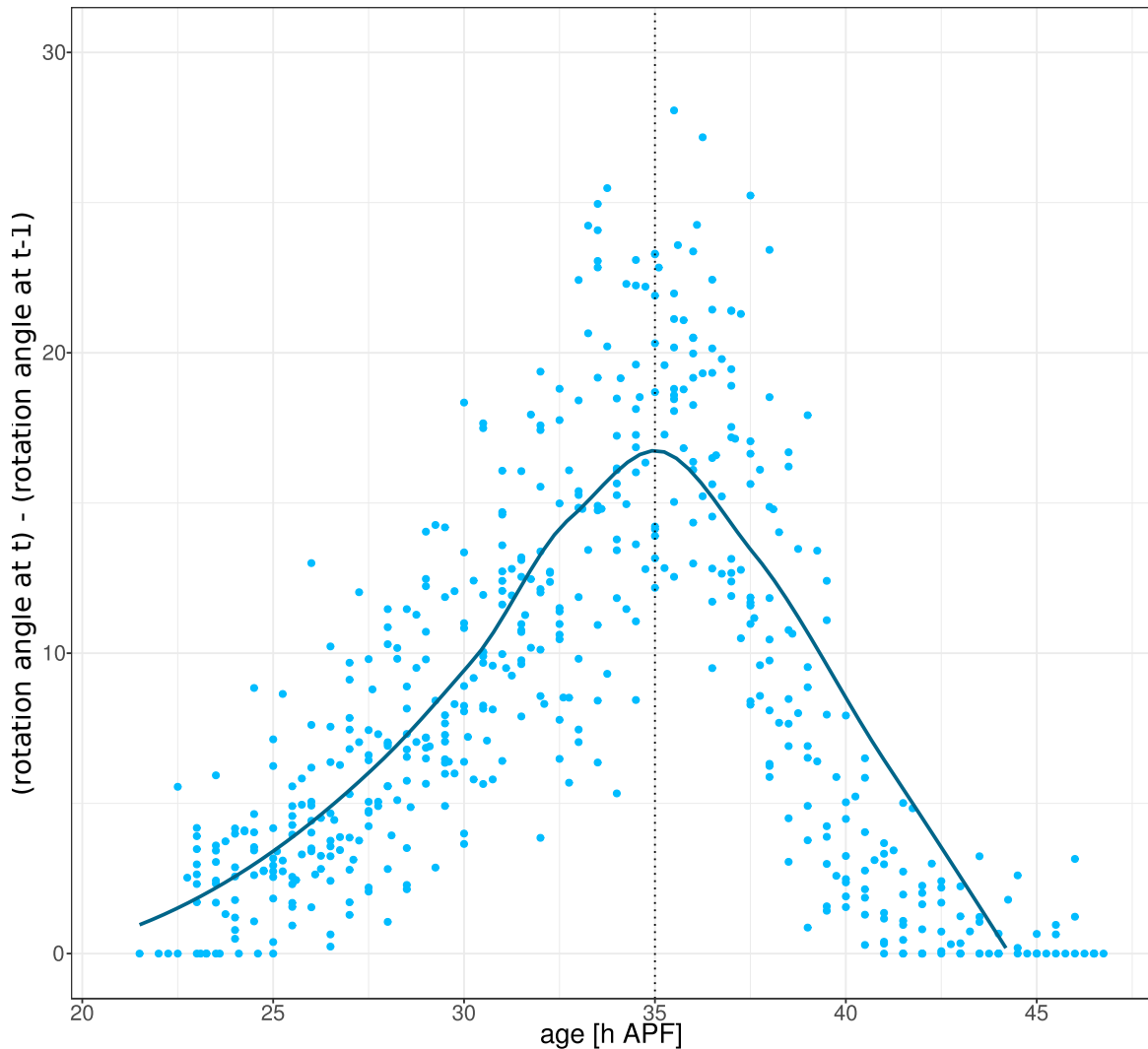


Figure 33 – Genitalia rotation velocity in DE-cad::GFP male pupae.

The line correspond to a regression with the loess method (formula: $y \sim x$).

6.1.5 Live-imaging of developing genitalia reveals possible tissue-tissue interactions and tissue deformation during genitalia rotation

The transgenic *D. pachea* expressing the membrane marker DE-cad::GFP offered us the possibility to monitor both genitalia morphogenesis and the genitalia rotation *in vivo* simultaneously. Therefore, we could monitor the interplay between the two developmental processes. Furthermore, these experiments revealed that during the beginning of the genitalia rotation at 24 h APF, the left lobe primordium appears to be very close to the surrounding, non rotating tissue (figure 34, white arrows). At about 28 h APF, a round shaped cell structure of about 60 cells formed next to the left lobe in the surrounding tissue that could correspond to the reduced A8 segment and/or the A7 segment (figure 34, white dotted line). This structure does not follow the movement of the genitalia rotation and remains at the same location throughout genitalia rotation. However, a change of its shape occurs from 32 h APF to 34 h APF, and the initial round shape turns to an elongated form that appears to be in close contact with the right side of the rotating genitalia. Furthermore, this structure does not appear in live-imaging of developing genitalia in *D. melanogaster* (Suzanne et al. 2010, Sato et al. 2015). When the cell structure disappears between 33 h APF and 35 h APF, the velocity peak of genitalia rotation is detected (see above) and left lobe becomes apparent at the tissue surface in a surmounted position relative to the rest of the posterior pupa (figure 34, white arrowheads). The non-rotating structure is only visible during the period of lobe growth, and could indicate a certain tension of the genitalia surrounding tissue during rotation movement.

At the right side of the developing genitalia, the right lobe primordium also appears to be very close to the surrounding, non rotating tissue from 24 h APF to 30 h APF. From 31 h APF to 34 h APF, the right part of the rotating genitalia gets into contact with the above mentioned non-rotating structure (figure 34, white arrowheads). After the disappearance of the non-rotating structure, between 33 h APF and 35 h APF, the right lobe is visible in our stacks, but it does not surmount the posterior pupal tissue as observed for the left lobe.

In addition, other tissue deformation occurs during genitalia rotation of *D. pachea* that is not observed in *D. melanogaster*. In particular, the anal plates undergo a severe deformation before and at the beginning of the genitalia rotation. At approximately 25 h APF, the two anal plates have a similar bean-shaped structure. The left anal plate is then strongly deformed, in particular at its ventral sided tip that progressively adopts a round shape between 26 h APF and 35 h APF. Later, it recovers a symmetric shape with respect to the right anal plate. This indicates that physical forces act on *D. pachea* genital tissues that

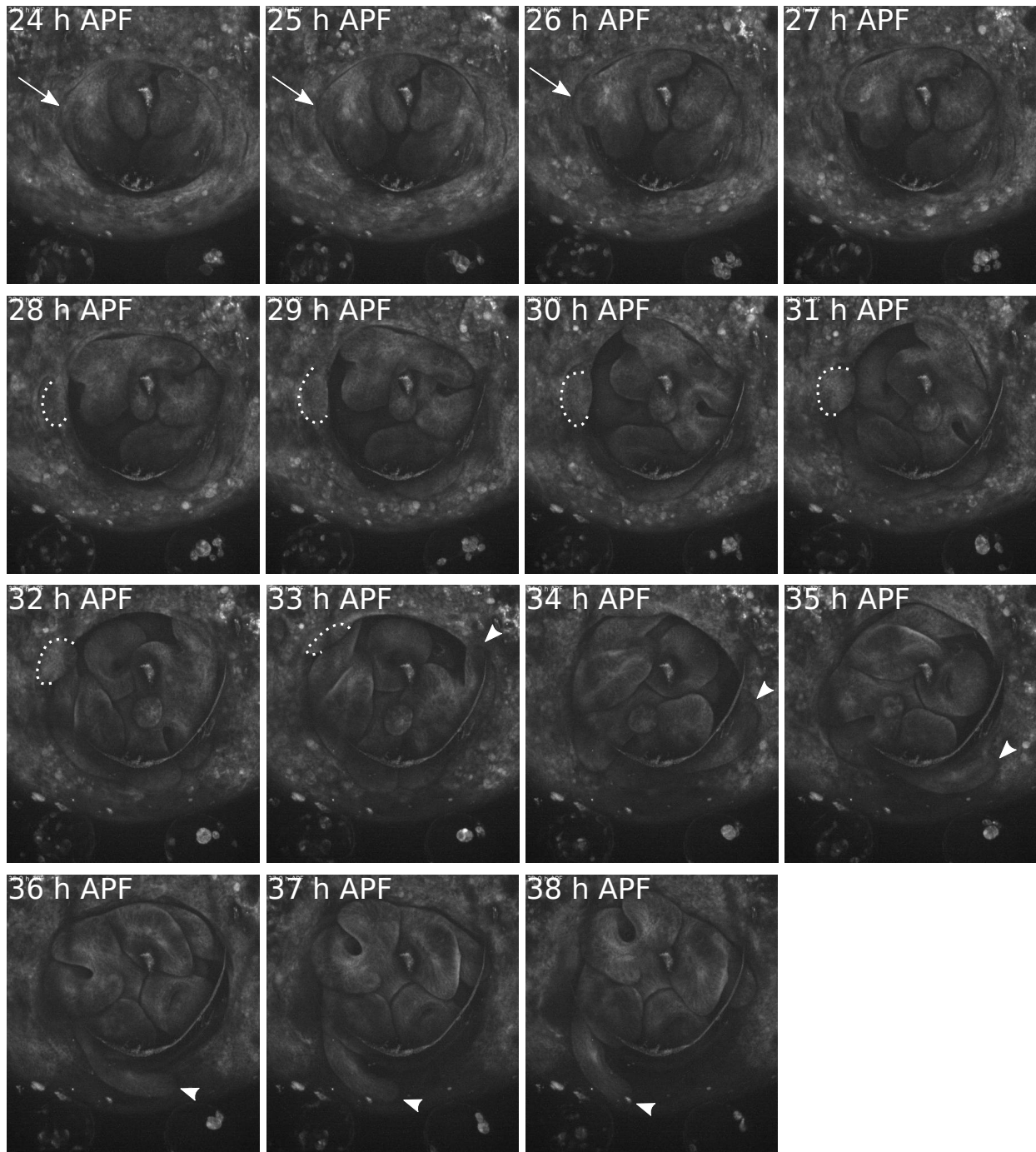


Figure 34 – Time-lapse imaging of developing asymmetric genital lobes during genitalia rotation in transgenic DE-cad::GFP *D. pachea*.

Growth of asymmetric lobes and genitalia rotation were monitored by time-lapse imaging of transgenic *D. pachea* expressing DE-cad::GFP (stock 9_D2F1). Pictures show the projection of image stacks taken each hour from 24 h APF to 38 h APF. The left lobe bud is indicated by arrows. A non-rotating round shaped cell structure is labeled with a white dotted line. The long left lobe appears to surmount the surrounding tissue between 33 h APF and 38 h APF (arrowheads).

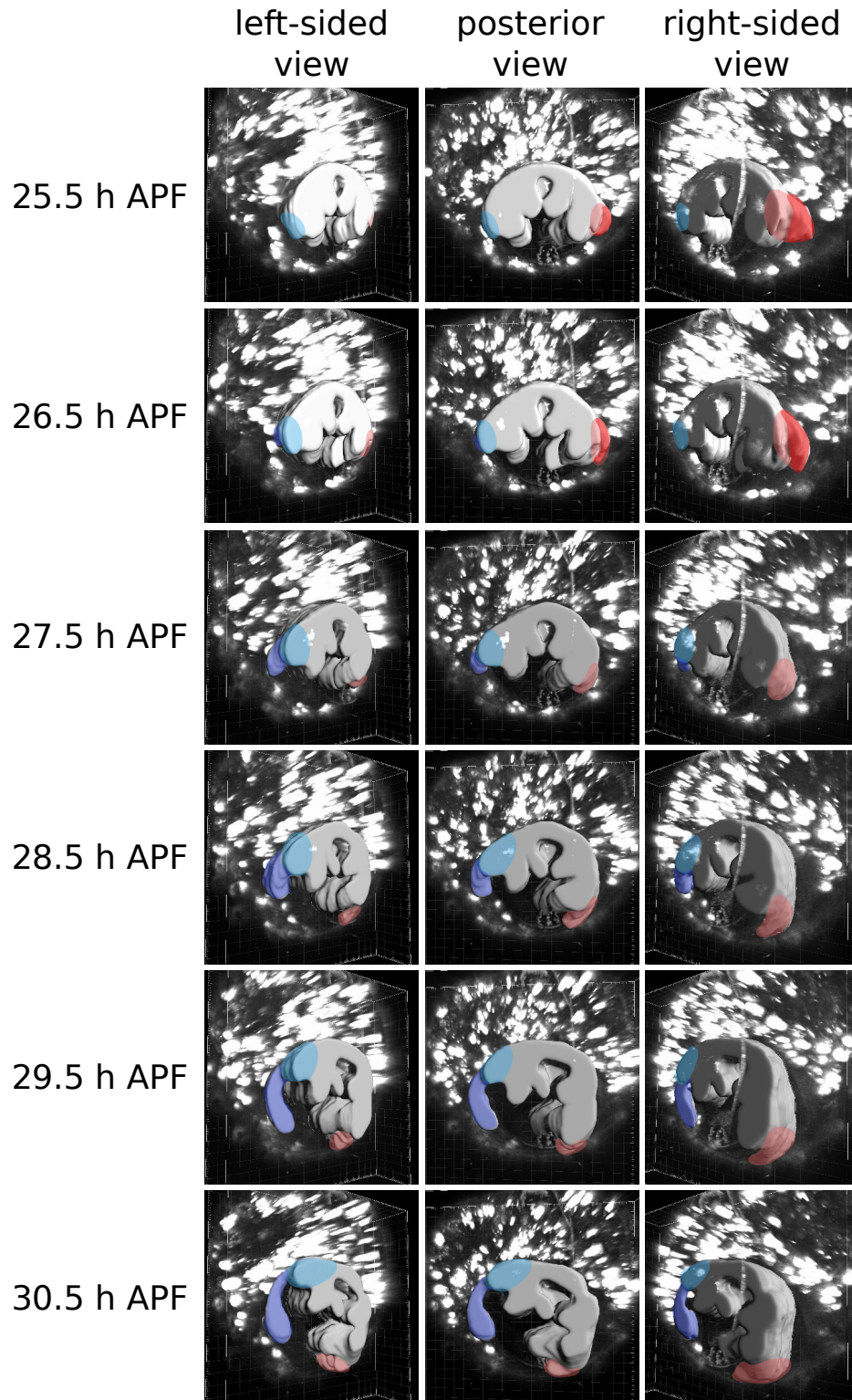


Figure 35 – Three dimensional reconstruction of developing male genitalia in *D. pachea* (continuing on the following page).

The transgenic *D. pachea* expressing the DE-cad::GFP were from stock 9_D2F1. Imaris software images of manually drawn contours of the male genitalia on individual images. The right lobe is highlighted in pink, and the zone of contact between it and the surrounding tissue is in red. The left lobe in light-blue. The non-rotating structure that appear to be close to the left lobe is highlighted in dark-blue.

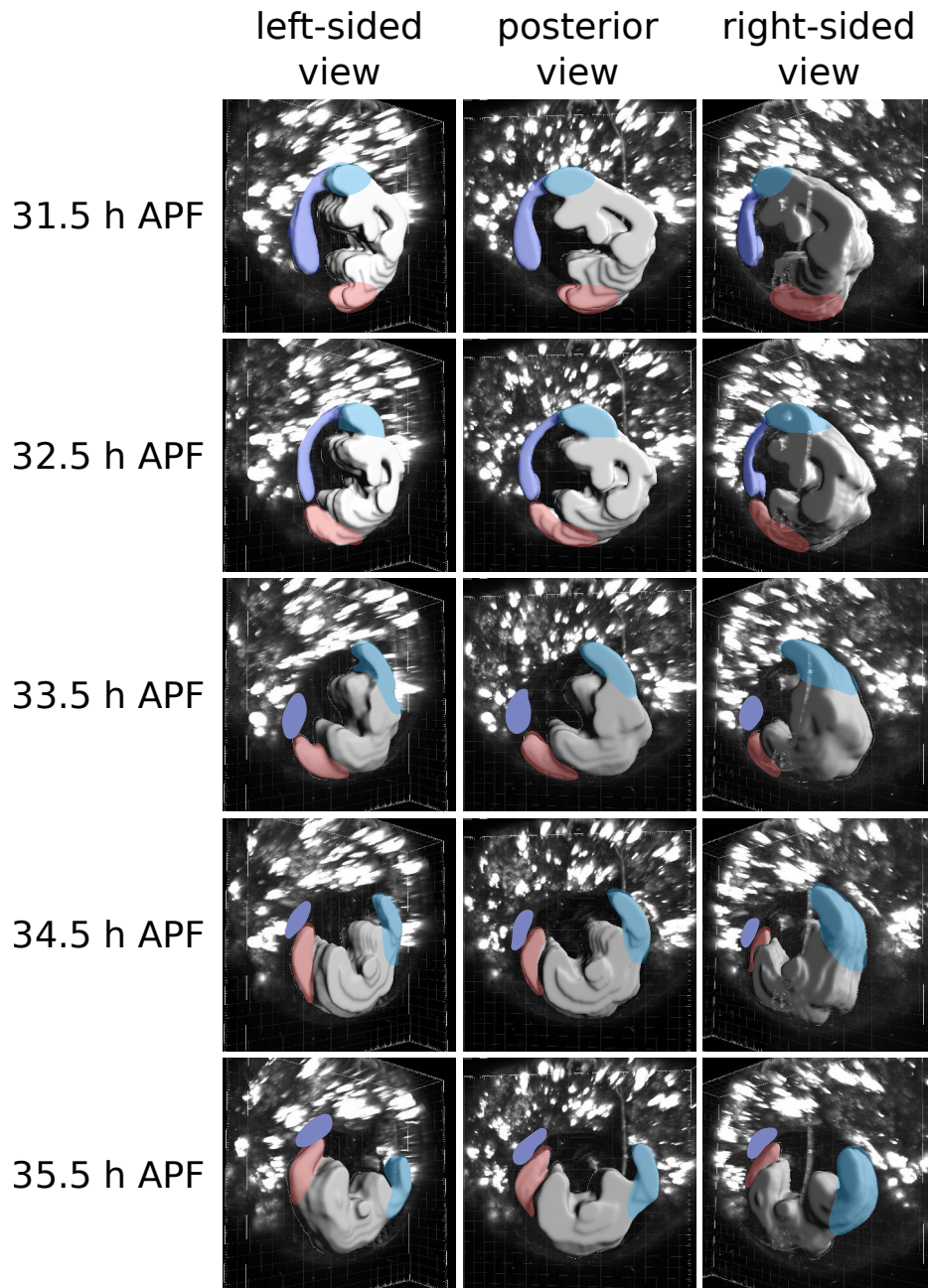


Figure 35 – Three dimensional reconstruction of developing male genitalia in *D. pachea* (continuing from the previous page).

The transgenic *D. pachea* expressing the DE-cad::GFP were from stock 9_D2F1. Imaris software images of manually drawn contours of the male genitalia on individual images. The right lobe is highlighted in pink, the left lobe in light-blue. The non-rotating structure that appear to be close to the left lobe is highlighted in dark-blue.

might be absent or lower in *D. melanogaster* (figure 34, white arrowheads).

To further investigate the potential physical interaction between developing lobes and surrounding tissue, an additional live imaging of developing genitalia at an increased imaging depth of 81 μm , and was carried out, using a magnification of 25X (see part 2.5.4, page 75 for more details). The contours of male genitalia and the outer cell structures were then drawn manually on individual images of the obtained image-stacks and a three-dimensional reconstruction of genital tissue was calculated with Imaris software (figure 35).

The three-dimensional reconstruction of the developing genitalia revealed that the tissue of both lobes seems to be in physical interaction with the surrounding tissue during the genitalia rotation (figure 35). The right lobe appears to be in physical interaction with the non-rotating tissue from 25.5 h APF to 26.5 h APF (figure 35, pink and red), which potentially could result in a rupture of lobe tissue due to the physical pressure imposed by genitalia rotation. The left lobe appears to be close to the above mentioned outer cellular structure at the periphery of the genitalia tissue until 27 h APF. This structure does not follow the genitalia rotation movement (figure 35, left lobe in clear blue, non-rotating structure in dark blue) and a stretched continuous tissue appears until 33 h APF, when the genitalia rotated about 120° and when the distal tip of the peripheral structure gets into contact with the right lobe. After 33 h APF, the shape of the non-rotating structure strikingly changes to a elongated shape and then the structure progressively disappears. This shape change might indicate a rupture of a potential adhesion between this non rotating structure and the left lobe. However, this potential interaction remains to be precisely investigated.

6.2 Discussion

6.2.1 The left-right asymmetric tissue growth does not appear to depend on cell division differences in the left and right lobes

The immunostaining of *D. pachea* male genitalia at various moment during the development revealed that most of the lobe growth occurs between 24 h APF and 36 h APF. The comparison with the developing male genitalia of the closely related species, which does not possess genital lobes, revealed that differences in tissue shape arise at 24 h APF between *D. pachea* and *D. nanoptera*, and are clearly established at 36 h APF. Thus, the changes in the developmental processes underlying tissue shape between these species probably arise during or before this period.

The quantification of the number of nuclei in each lobe shows that the amount of nuclei (cells) progressively increases from 24 h APF to 36 h APF in each lobe and then reach a stable number. The immuno-staining of mitotic cells revealed that lobe growth occurs through 'bulk growth' and not by peripheral growth due to a group of cell at the periphery of the lobe bud (Irvine and Shraiman 2017) and might therefore be potentially mediated via a morphogen gradient, such as *Dpp* in the *D. melanogaster* wing discs. In the wing discs, *Dpp* is expressed in the midline of the tissue, following its proximal-distal axis from which it diffuses. This results in a *Dpp* gradient regulating diverse cell fates in a concentration dependent manner and triggering the bulk growth of the tissue via induction of mitosis throughout the tissue (reviewed in Irvine and Shraiman 2017).

However, the quantification of mitotic cells in each lobe did not reveal differences in mitotic rates between the left and right lobe. Thus, the question of the growth mechanisms acting inside the lobes is still unresolved. Several hypotheses can explain the asymmetric growth such as a pulse or a brief period of mitosis, or a pre-existing slight difference in the size of the tissue giving rise to the lobes. However, none of these events was identified in our time-lapse analysis. Alternatively, the difference in lobe size could result from cell recruitment from the surrounding genital arch tissue. To investigate in more detail the growth mechanisms leading to lobe asymmetry, cell behaviors such as orientation of cell division, apoptosis, cell movements and cell shape changes should be explored more precisely. Also, *ex-vivo* culture of developing genitalia from our transgenic DE-cad::GFP stocks could be envisaged to gain microscopy field depth, as it has been previously done in *D. melanogaster* (Sato et al. 2015),

6.2.2 Premature genitalia rotation in the selection stock is associated with a variable left lobe length of *D. pachea*

In the selection stock in which males have a variable left lobe length, we observe that genitalia rotation occurs about 6 h earlier compared to the 1698.01 wild-type stock. This indicates a potential functional link between genitalia rotation and asymmetric lobe growth. The genitalia rotation potentially controls the size ratio of the left and the right lobe and a premature rotation start could potentially circumvent this effect. Thus, the genitalia rotation might have been co-opted during evolution to trigger left-right asymmetric lobe development in *D. pachea*. The host lab undertakes further investigations on the potential functional link between genitalia rotation direction and lobe asymmetry by using MyoID mutants. In *D. melanogaster*, such MyoID mutants display an inversion of the genitalia rotation direction (Spéder, Ádám, and Noselli 2006). MyoID mutants in *D. pachea* using the CRISPR/Cas9 approach are established to investigate the consequences of genital rotation direction on genital lobe asymmetry.

The mutation(s) responsible for the left lobe length variation of males from the selection stock have not been yet identified. As this variation might be due to the change of the genitalia rotation timing, this mutation might affect either genitalia rotation and lobe growth independently or only the genitalia rotation that would then trigger the development of a left lobe of variable length. Thus, the mutation might affect genes known to impact genitalia rotation, such as MyoIC, which is responsible for a counter-clockwise direction of genitalia rotation in the absence of MyoID function (Petzoldt et al. 2012). Alternatively, genes involved in apoptosis that are essential for correct genitalia rotation might be mutated (Suzanne et al. 2010).

Both on imaging of fixed tissue and on time-lapse imaging, we found that lobe growth occurs from about 24 h APF to 36 h APF. The genitalia rotation was slightly accelerated in samples used in time-lapse imaging experiment compared to the the fixed tissues. The samples used for time-lapse imaging were regularly illuminated with a laser for the image acquisition. Despite of being in a thermostat regulated environment, this illuminations could result in an increase of the temperature of the samples throughout acquisition. As shown in the overall pupal timing characterization in *D. pachea* (see part 4.1.3, page 95), the increase of the temperature tends to increase the speed of the development in early pupal stages. Thus, the acceleration of the genitalia rotation that occurs from about 30 - 32 h APF in live pupae monitored by time-lapse imaging might be an artefact due an increase of the pupa temperature because of the laser illumination.

6.2.3 The developing lobes appear to interact with surrounding non-rotating tissue during the first half of the genitalia rotation

In *Drosophila* species, the genitalia develops from a genital disc composed of three primordia: the female genitalia primordium (derived from the 8th abdominal segment), the male genitalia primordium (derived from the 9th abdominal segment) and the anal primordium (derived from the 10th abdominal segments) (Sánchez and Guerrero 2001, Estrada, Casares, and Sánchez-Herrero 2003). In male pupae, the female genitalia primordium will not develop and will largely be reduced by apoptosis, which is also essential for the rotation of the male genitalia (Suzanne et al. 2010, Benitez et al. 2010, Kuranaga et al. 2011, Macias et al. 2004). The time-lapse imaging of developing genitalia *in vivo* allowed us to monitor the dynamics of the male genitalia development in the context of the genitalia rotation, and the interplay between the genitalia and the surrounding tissues. During the growth between 0° and 120° of genitalia rotation, the developing left lobe seems to be in close contact with a non-rotating cell structure. This could be a tissue deformation that happens during the first half of genitalia rotation. This might indicate a potential adhesion of the lobe with this cell structure and might lead to physical traction and pulling of the left lobe that might result in tissue elongation. The inverse scenario might apply to the right lobe that potentially undergoes physical compression.

To investigate the origin of the non-rotating structure and its potential continuity with the tip of the left lobe, it would be interesting to develop fluorescent markers under the control of specific promoters that are expressed specifically in the 8th abdominal segment (the peripheral surrounding tissue that drives the rotation), or in the 9th abdominal segment (in the male genitalia tissue). The development of a such tool would also be useful to investigate the origin of the cells forming the lobes. In particular, if the non-rotating structure and the tip of the left lobe are connected, a cell recruitment from the non-rotating structure might potentially occur towards the distal tip of the lobe. A complementary approach would be to use laser ablation in the region of contact between the left lobe and the non-rotation structure to investigate physical forces exerted in the tissue and to test if this affects genitalia rotation velocity. Interestingly, genitalia rotation speed peaks at 35 h APR, which corresponds to the disappearing of the non-rotating outer tissue and the surmounting of the lobe over the rest of the posterior pupa. This is in line with our observations of a potential connection between both tissues that breaks during rotation.

Overall, correct timing of genitalia rotation appeared to be an important factor for the establishment of left-right asymmetric genital lobes. I propose a hypothetical model to link

the observations described above (figure 36). This model relies on the existence of a physical interaction between the forming lobes and the surrounding tissue at 24 h APF (figure 36A, red areas). Due to the genitalia rotation, lobe buds are exposed to physical forces, which will lead to tissue compression and rupture at the right lobe and to a stretch of the left lobe, extending it throughout the first half of genitalia rotation. At approximately 180° of genitalia rotation, a break occurs between the left lobe and the surrounding tissue, leading to a decrease of the forces applied on the tissue and a peak of genital rotation speed. This differential interaction of each lobe with the surrounding tissue is caused by the direction of the rotation movement, which is always clockwise. Lobe asymmetry might thus be reversible if the rotation direction changes, since the relative forces acting on genital tissue might also be inverted in direction. In the previously mentioned selection stock where males display variable left lobe lengths and that reveal a premature genitalia rotation, the genitalia rotation perhaps starts before lobe buds become apparent. In this case, there would be decreased interaction between lobe buds and the surrounding tissue to various extents, resulting in variable length of the left lobe (figure 36B). However, this would not explain a constant right lobe length. Future investigations using time-lapse microscopy of individuals that carry the mutation in the selection stock are necessary to shed light on this. Furthermore, the mutation itself should be identified.

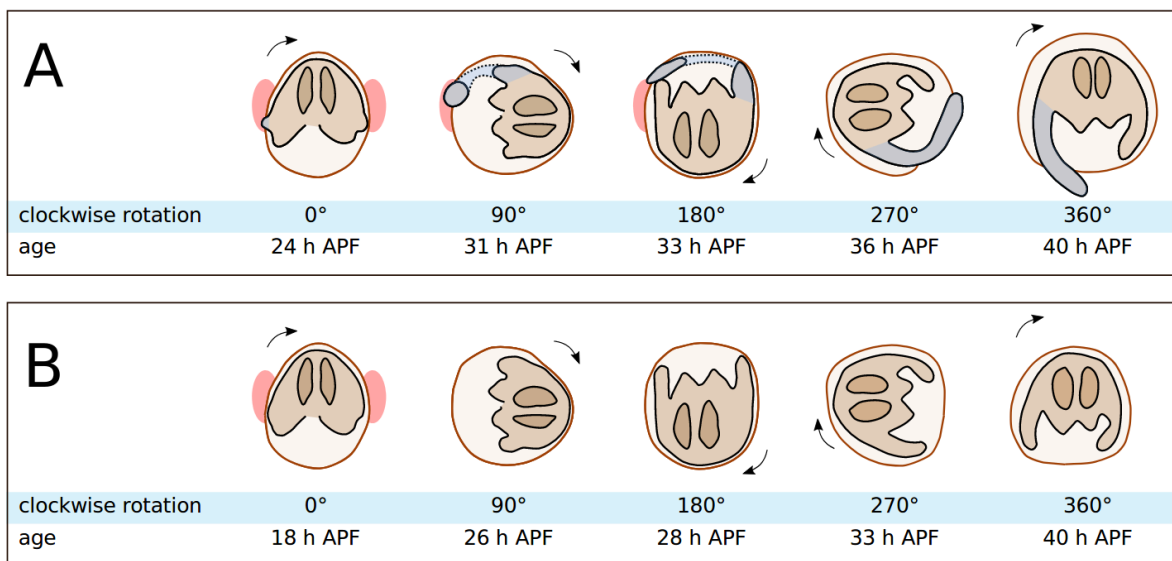


Figure 36 – Hypothetical model explaining the functional link between genitalia rotation and left-right lobe asymmetry establishment.

This model rely on the existence of a physical interaction between lobe buds and surrounding tissues at the beginning of genitalia rotation (red areas). In the case of the wild-type individuals, the rotation would then lead to physical forces shearing the right lobe and extending the left lobe (A). In the case of the mutant displaying symmetrical lobes, the rotation would start before lobe buds are formed, so no physical interaction would be established, leading to symmetrical lobes (B).

Overall, a detailed characterization of potential tissue-tissue interactions of lobes and surrounding tissue is required, including measures of the physical forces that are acting on the genitalia to further test for such a tissue interaction.

7 Conclusions

My thesis was focused on the function of the lobes with respect to reproduction and their establishment during development. In this sense, I tried to uncover ultimate factors (why did they evolve?) and proximate factors (how do they develop and what developmental changes are observed with respect to species that do not develop lobes?) that might have led to the establishment of asymmetric male genital lobes during evolution of *D. pachea*.

The function of the genital lobes of male *D. pachea* during copulation has been previously investigated by the host lab, revealing a function in the stabilization of the complex of female and male genital structures that is formed during copulation (Lang and Orgogozo 2012, Rhebergen et al. 2016). Here, we investigated if the asymmetric genital lobe of males *D. pachea* play a role in pre-copulatory events or at establishment of this genitalia complex. This study reveals that copulation success is indeed correlated with left lobe length. However, the signals by which female detect male left lobe length remains to be uncovered, and could potentially involve visual, tactile, chemical or auditory cues.

To investigate if the effect of the left lobe length on the copulation success was not due to other male characters co-varying with left lobe length due to gene having pleiotropic effects, we conducted experiments with males displaying artificially reduced left lobes by micro-surgery. In these experiments, the left lobe length tended to affect male copulation success but in a weaker, non significant manner, compared to the effect found with non modified males. Thus, we cannot completely exclude that left lobe length indirectly affects the copulation success.

The analysis of courtship behaviors revealed that males *D. pachea* do not display a so called scramble competition for female in which males try to disrupt copulating couples to usurp females (Polak and Rashed 2010, Grieshop and Polak 2012), but intra-sexual competition is reflected by the overall courtship vigor, estimated by male licking behavior.

We found that sperm transfer depends on copulation duration. Surprisingly, longest copulation duration resulted in decreased sperm present in female sperm storage organs. Further investigations remain to be conducted to unravel how the internal transfer of giant sperm occurs in this species.

It has been previously proposed that the difference in age to reach sexual maturity between males and females (Jefferson 1977, Pitnick and Markow 1994b) could be a mechanism to reduce inbreeding. Our study revealed that the age of reproductive activities appear to be

non-overlapping between *D. pachea* males and females. This might contribute to reduce inbreeding in wild specimen.

Altogether, these results indicate that sexual selection potentially drives the evolution towards larger left male genital lobe in *D. pachea* by enhancing the chance of males to engage into copulation.

The second objective of my thesis was to investigate if the development of asymmetric genital lobe was due to an overall timing change in the pupal development compared to those of species with symmetric genitalia. This was achieved by a characterization of the timing of pupal stages in *D. pachea*, but also in closely related species *D. nannopectera* and *D. acanthoptera*. The timing of the first 0 h APF to 50 h APF is conserved between different *Drosophila* species. Lobe growth of *D. pachea* occurs from 24 h APF to 36 h APF, thus this asymmetric developmental processes occurs in a conserved overall developmental context and no timing differences were detected compared to species with symmetric genitalia. Also, the conservation of the timing of the first pupal stages indicates some developmental constraints during this period.

Overall, developmental duration varied among species. At the scale of the *Drosophila* genus, the duration differences tend to increase with phylogenetic distance between groups of species rather than with the climate conditions of the specie's habitat.

The comparison of pupal development at 25°C and 29°C in *D. pachea* revealed that this temperature difference does not affect the overall pupal developmental duration. In other *Drosophila* species, temperature increase results in shorter duration of pupal development (David and Clavel 1966, Powsner 1935, James and Partridge 1995). This might indicate a buffering mechanism of developmental processes with respect to temperature oscillation in *D. pachea*. This species lives in the Sonora desert, known to undergo important diurnal and annual temperature oscillations of up to 35°C difference (Gibbs, Perkins, and Markow 2003).

This work provides an exhaustive estimate of developmental duration in *D. pachea* under laboratory conditions that will be useful for future characterization of any developmental process of interest in this species.

The last objective of my thesis was to characterise the growth processes giving rise to left-right asymmetric genital lobes of *D. pachea*. To do so, we used imaging of fixed genital tissues and *in vivo* imaging of transgenic DE-cad::GFP stocks. Our study revealed that lobe growth is not triggered by a group of cell at the periphery or at the distal tip of the lobes, but occurs

through 'bulk growth' (Irvine and Shraiman 2017). The left and right lobes reach about 410 cells and 220 cells, respectively. No difference in the mitotic rate was detected between the left and the right lobe. Thus, lobe asymmetry may result from cell recruitment from the tissue from the surrounding tissue. The change of cell shape, orientation of cell division or apoptosis could also affect asymmetric lobe growth. These cell behaviors remain to be characterised in detail to unravel more precisely the mechanisms underlying the asymmetric accumulation of cells in the lobes.

Furthermore, lobe growth occurs from 24 h APF to 36 h APF, which correspond to the first half-rotation of the male genitalia. The genitalia rotation was found to occur about 6 h earlier in the selection stock in which males display variable left lobe length, compared to the wild-type stock 1698.01. This indicates a potential functional link between genitalia rotation and establishment of lobe asymmetry. Thus, the genitalia rotation may have been co-opted during evolution to derive the left-right asymmetric genital structures in *D. pachea*.

The *in vivo* imaging of transgenic DE-cad::GFP *D. pachea* stocks revealed the existence of a particular non-rotating structure close to the left lobe, from 28 h APF to 34 h APF. This structure does not appear in *D. melanogaster* (Sato et al. 2015, Suzanne et al. 2010). The characterization of this structure as well as its potential link with asymmetric genital lobe development remains to be done. In particular the origin of interacting tissues, the strength and the nature of this interaction needs to be studied, potentially relying on cell adhesion or evolutionary changes in apoptosis at the onset of genitalia rotation. This could be investigated by a characterization of the mechanical forces acting on genital tissues during genitalia rotation and their potential consequences on lobe morphology.

The generation of transgenics in *D. pachea* opens the door for the development of new genetic tools in this species. Furthermore, the DE-cad::GFP stocks will be useful to investigate lobe growth mechanisms in more detail and could also be used in other developmental studies that rely on a fluorescent cell-membrane marker.

Altogether, the three axis of my thesis revealed new insights on the function and the development of the left-right asymmetric male genital lobes of *D. pachea*.

Bibliography

- Acurio, A. E. et al. (2019). “Repeated evolution of asymmetric genitalia and right-sided mating behavior in the *Drosophila* nannopectera species group”. In: *BMC evolutionary biology* 19.1, pp. 1–14.
- Adachi-Yamada, T. et al. (1999). “Distortion of proximodistal information causes JNK-dependent apoptosis in *Drosophila* wing”. In: *Nature* 400.6740, pp. 166–169.
- Alexander, R. D. (1964). “The evolution of mating behaviour in arthropods”. In: Alexander, R. D., D. C. Marshall, and J. R. Cooley (1997). “Evolutionary perspectives on insect mating”. In: *The evolution of mating systems in insects and arachnids*, pp. 4–31.
- Altschul, S. F. et al. (1990). “Basic local alignment search tool”. In: *Journal of Molecular Biology* 215.3, pp. 403–410.
- Amitin, E. G. and S. Pitnick (2007). “Influence of developmental environment on male-and female-mediated sperm precedence in *Drosophila melanogaster*”. In: *Journal of Evolutionary Biology* 20.1, pp. 381–391.
- Andersson, M. (1982). “Female choice selects for extreme tail length in a widowbird”. In: *Nature* 299.5886, pp. 818–820.
- Antic, D. et al. (2010). “Planar cell polarity enables posterior localization of nodal cilia and left-right axis determination during mouse and *Xenopus* embryogenesis”. In: *PloS one* 5.2, e8999.
- Arnqvist, G. (1998). “Comparative evidence for the evolution of genitalia by sexual selection”. In: *Nature* 393.6687, pp. 784–786.
- Ashburner, M. et al. (1989). *Drosophila. A laboratory handbook*. Cold spring harbor laboratory press.
- Ashburner, M. and J. Thompson Jr (1978). “Laboratory culture of *Drosophila*”. In: *Genetics and biology of Drosophila*.
- Bächli, G., U. Bernhard, and A. Godknecht (2020). *TaxoDros [data base]*. Data retrieved from TaxoDros data base in August 2020.
- Bainbridge, S. P. and M. Bownes (1981). “Staging the metamorphosis of *Drosophila melanogaster*”. In: *Development* 66.1, pp. 57–80.
- Bakker, K. and F. Nelissen (1963). “On the relations between the duration of the larval and pupal period, weight and diurnal rhythm in emergence in *Drosophila melanogaster*”. In: *Entomologia Experimentalis et Applicata* 6.1, pp. 37–52.
- Bateman, A. J. (1948). “Intra-sexual selection in *Drosophila*”. In: *Heredity* 2.3, pp. 349–368.

- Benitez, S. et al. (2010). “Both JNK and apoptosis pathways regulate growth and terminalia rotation during *Drosophila* genital disc development”. In: *International Journal of Developmental Biology* 54.4, p. 643.
- Bertin, A. and D. Fairbairn (2005). “One tool, many uses: precopulatory sexual selection on genital morphology in *Aquarius remigis*”. In: *Journal of evolutionary biology* 18.4, pp. 949–961.
- Bharathi, N. S. et al. (2004). “Correlates of sexual dimorphism for dry weight and development time in five species of *Drosophila*”. In: *Journal of Zoology* 264.1, pp. 87–95.
- Bianconi, E. et al. (2013). “An estimation of the number of cells in the human body”. In: *Annals of human biology* 40.6, pp. 463–471.
- Birch, M. (1970). “Pre-courtship use of abdominal brushes by the nocturnal moth, *Phlogophora meticulosa* (L.) (Lepidoptera: Noctuidae)”. In: *Animal Behaviour* 18, pp. 310–316.
- Birkhead, T. R. and T. Pizzari (2002). “Postcopulatory sexual selection”. In: *Nature Reviews Genetics* 3.4, pp. 262–273.
- Blum, M. and T. Ott (2018). “Animal left–right asymmetry”. In: *Current Biology* 28.7, R301–R304.
- Bohme, W. (1983). “The Tucano Indians of Colombia and the iguanid lizard *Plica plica*: ethnological, herpetological and ethological implications”. In: *Biotropica*, pp. 148–150.
- Bonduriansky, R. (2001). “The evolution of male mate choice in insects: a synthesis of ideas and evidence”. In: *Biological Reviews* 76.3, pp. 305–339.
- Bonnier, G. (1926). “Temperature and time of development of the two sexes in *Drosophila*”. In: *Journal of Experimental Biology* 4.2, pp. 186–195.
- Bradley, R. A. and M. E. Terry (1952). “Rank analysis of incomplete block designs: I. The method of paired comparisons”. In: *Biometrika* 39.3/4, pp. 324–345.
- Brown, N. A. and L. Wolpert (1990). “The development of handedness in left/right asymmetry”. In: *Development* 109.1, pp. 1–9.
- Byers, J., E. Hebets, and J. Podos (2010). “Female mate choice based upon male motor performance”. In: *Animal Behaviour* 79.4, pp. 771–778.
- Carroll, S. B. (2005). *Endless forms most beautiful: The new science of evo devo and the making of the animal kingdom*. 54. WW Norton & Company.
- Carson, H. L. (1961). “Rare parthenogenesis in *Drosophila robusta*”. In: *The American Naturalist* 95.881, pp. 81–86.
- Chapman, T. et al. (2003). “Sexual conflict”. In: *Trends in Ecology & Evolution* 18.1, pp. 41–47.

- Chintapalli, V. R. et al. (2012). “Functional correlates of positional and gender-specific renal asymmetry in *Drosophila*”. In: *PloS one* 7.4, e32577.
- Chougule, A. et al. (2020). “The *Drosophila* actin nucleator DAAM is essential for left-right asymmetry”. In: *PLoS genetics* 16.4, e1008758.
- Chung, Y.-T. and E. B. Keller (1990). “Regulatory elements mediating transcription from the *Drosophila melanogaster* actin 5C proximal promoter.” In: *Molecular and cellular biology* 10.1, pp. 206–216.
- Copetti, D. et al. (2017). “Extensive gene tree discordance and hemiplasy shaped the genomes of North American columnar cacti”. In: *Proceedings of the National Academy of Sciences* 114.45, pp. 12003–12008.
- Core Team, R. (2014). *R: A language and environment for statistical computing. R Foundation for Statistical Computing, Vienna, Austria. 2013.*
- Coutelis, J.-B. et al. (2013). “*Drosophila* left/right asymmetry establishment is controlled by the Hox gene abdominal-B”. In: *Developmental cell* 24.1, pp. 89–97.
- Coutelis, J. et al. (2008). “Left–right asymmetry in *Drosophila*”. In: *Seminars in cell & developmental biology*. Vol. 19. 3. Elsevier, pp. 252–262.
- Coutelis, J.-B. et al. (2014). “Diversity and convergence in the mechanisms establishing L/R asymmetry in metazoa”. In: *EMBO reports* 15.9, pp. 926–937.
- Cowin, S. C. (2004). “Tissue growth and remodeling”. In: *Annu. Rev. Biomed. Eng.* 6, pp. 77–107.
- Danchin, E. et al. (2018). “Cultural flies: Conformist social learning in fruitflies predicts long-lasting mate-choice traditions”. In: *Science* 362.6418, pp. 1025–1030.
- Darwin, C. (1859). *On the origin of species, 1859.*
- David, J. R. and P. Capy (1988). “Genetic variation of *Drosophila melanogaster* natural populations”. In: *Trends in Genetics* 4.4, pp. 106–111.
- David, J. R. and M.-F. Clavel (1966). “Essai de définition d’une température optimale pour le développement de la *Drosophile*”. In: *CR Acad. Sci. Paris* 262D, pp. 2159–2162.
- Davison, A. et al. (2016). “Formin is associated with left-right asymmetry in the pond snail and the frog”. In: *Current Biology* 26.5, pp. 654–660.
- Dobzhansky, T. (1937). “Genetics and the origin of species Columbia Univ”. In: *Press, New York.*[*Google Scholar*].
- Dufour, L. (1844). “Anatomie générale des Dipteres”. In: *Ann. Sci. Nat* 1, pp. 244–264.
- Eberhard, W. G. (1985). *Sexual selection and animal genitalia*. Vol. 244. Harvard University Press Cambridge, MA.
- (1991). “Copulatory courtship and cryptic female choice in insects”. In: *Biological Reviews* 66.1, pp. 1–31.

- Eberhard, W. G. (1994). “Evidence for widespread courtship during copulation in 131 species of insects and spiders, and implications for cryptic female choice”. In: *Evolution* 48.3, pp. 711–733.
- (2010a). “Evolution of genitalia: theories, evidence, and new directions”. In: *Genetica* 138.1, pp. 5–18.
- (2010b). “Rapid divergent evolution of genitalia”. In: *The evolution of primary sexual characters in animals*, pp. 40–78.
- Eder, D., C. Aegerter, and K. Basler (2017). “Forces controlling organ growth and size”. In: *Mechanisms of development* 144, pp. 53–61.
- Edward, D. A. and T. Chapman (2012). “Measuring the fitness benefits of male mate choice in *Drosophila melanogaster*”. In: *Evolution* 66.8, pp. 2646–2653.
- Estes, R. D. (1991). “The significance of horns and other male secondary sexual characters in female bovids”. In: *Applied Animal Behaviour Science* 29.1-4, pp. 403–451.
- Estrada, B., F. Casares, and E. Sánchez-Herrero (2003). “Development of the genitalia in *Drosophila melanogaster*”. In: *Differentiation* 71.6, pp. 299–310.
- Fisher, R. A. (1930). *The genetical theory of natural selection*.
- Fogleman, J. C. and B. Wallace (1980). “Temperature-dependent development and competitive ability of three species in the *Drosophila affinis* subgroup”. In: *American Midland Naturalist*, pp. 341–351.
- Fogleman, J. C. and P. B. Danielson (2001). “Chemical interactions in the cactus-microorganism-*Drosophila* model system of the Sonoran Desert”. In: *American Zoologist* 41.4, pp. 877–889.
- Fukutomi, Y. et al. (2017). “Pupal development and pigmentation process of a polka-dotted fruit fly, *Drosophila guttifera* (Insecta, Diptera)”. In: *Development Genes and Evolution*, pp. 1–10.
- Géminard, C. et al. (2014). “The myosin ID pathway and left–right asymmetry in *Drosophila*”. In: *Genesis* 52.6, pp. 471–480.
- Ghiselin, M. T. (2010). “The distinction between primary and secondary sexual characters”. In: *The Evolution of Primary Sexual Characters in Animals*, pp. 9–14.
- Gibbs, A. G., M. C. Perkins, and T. A. Markow (2003). “No place to hide: microclimates of Sonoran Desert *Drosophila*”. In: *Journal of Thermal Biology* 28.5, pp. 353–362.
- Gibson, D. G. et al. (2009). “Enzymatic assembly of DNA molecules up to several hundred kilobases”. In: *Nature methods* 6.5, pp. 343–345.
- González-Morales, N. et al. (2015). “The atypical cadherin *dachsous* controls left-right asymmetry in *Drosophila*”. In: *Developmental Cell* 33.6, pp. 675–689.

- Green, J. E. et al. (2019). “Evolution of ovipositor length in *Drosophila suzukii* is driven by enhanced cell size expansion and anisotropic tissue reorganization”. In: *Current Biology* 29.12, pp. 2075–2082.
- Grieshop, K. and M. Polak (2012). “The precopulatory function of male genital spines in *Drosophila ananassae* [Doleschall](Diptera: Drosophilidae) revealed by laser surgery”. In: *Evolution: International Journal of Organic Evolution* 66.8, pp. 2637–2645.
- (2014). “Evaluating the post-copulatory sexual selection hypothesis for genital evolution reveals evidence for pleiotropic harm exerted by the male genital spines of *Drosophila ananassae*”. In: *Journal of evolutionary biology* 27.12, pp. 2676–2686.
- Grimes, D. T. and R. D. Burdine (2017). “Left–right patterning: breaking symmetry to asymmetric morphogenesis”. In: *Trends in Genetics* 33.9, pp. 616–628.
- Handler, A. M. and R. A. Harrell (1999). “Germline transformation of *Drosophila melanogaster* with the piggyBac transposon vector”. In: *Insect Molecular Biology* 8.4, pp. 449–457.
- (2001). “Transformation of the Caribbean fruit fly, *Anastrepha suspensa*, with a piggyBac vector marked with polyubiquitin-regulated GFP”. In: *Insect Biochemistry and Molecular Biology* 31.2, pp. 199–205.
- Handler, A. M. et al. (1998). “The lepidopteran transposon vector, piggyBac, mediates germ-line transformation in the Mediterranean fruit fly”. In: *Proceedings of the National Academy of Sciences* 95.13, pp. 7520–7525.
- Hasselquist, D., S. Bensch, and T. von Schantz (1996). “Correlation between male song repertoire, extra-pair paternity and offspring survival in the great reed warbler”. In: *Nature* 381.6579, pp. 229–232.
- Heed, W. B. (1982). “The origin of *Drosophila* in the Sonoran Desert”. In: *Ecological genetics and evolution: the cactus-yeast-Drosophila model system/edited JSF Barker, WT Starmer*.
- Heed, W. B. and H. W. Kircher (1965). “Unique sterol in the ecology and nutrition of *Drosophila pachea*”. In: *Science* 149.3685, pp. 758–761.
- Hernández-Hernández, T. et al. (2011). “Phylogenetic relationships and evolution of growth form in Cactaceae (Caryophyllales, Eudicotyledoneae)”. In: *American journal of botany* 98.1, pp. 44–61.
- Hill, G. E. (1991). “Plumage coloration is a sexually selected indicator of male quality”. In: *Nature* 350.6316, pp. 337–339.
- Hoikkala, A., J. Aspi, and L. Suvanto (1998). “Male courtship song frequency as an indicator of male genetic quality in an insect species, *Drosophila montana*”. In: *Proceedings of the Royal Society of London. Series B: Biological Sciences* 265.1395, pp. 503–508.
- Holtzman, S. et al. (2010). “Transgenic tools for members of the genus *Drosophila* with sequenced genomes”. In: *Fly* 4.4, pp. 349–362.

- Horn, C. and E. A. Wimmer (2000). “A versatile vector set for animal transgenesis”. In: *Development genes and evolution* 210.12, pp. 630–637.
- Hozumi, S. et al. (2006). “An unconventional myosin in *Drosophila* reverses the default handedness in visceral organs”. In: *Nature* 440.7085, pp. 798–802.
- Huang, J. et al. (2009). “Directed, efficient, and versatile modifications of the *Drosophila* genome by genomic engineering”. In: *Proceedings of the National Academy of Sciences* 106.20, pp. 8284–8289.
- Huang, X., J. T. Warren, and L. I. Gilbert (2008). “New players in the regulation of ecdysone biosynthesis”. In: *Journal of Genetics and Genomics* 35.1, pp. 1–10.
- Huber, A. H. et al. (2001). “The Cadherin cytoplasmic domain is unstructured in the absence of β -Catenin, a possible mechanism for regulating cadherin turnover”. In: *Journal of Biological Chemistry* 276.15, pp. 12301–12309.
- Huber, B. A. (2010). “Mating positions and the evolution of asymmetric insect genitalia”. In: *Genetica* 138.1, pp. 19–25.
- Huber, B. A., B. J. Sinclair, and M. Schmitt (2007). “The evolution of asymmetric genitalia in spiders and insects”. In: *Biological Reviews* 82.4, pp. 647–698.
- Irvine, K. D. and B. I. Shraiman (2017). “Mechanical control of growth: ideas, facts and challenges”. In: *Development* 144.23, pp. 4238–4248.
- James, A. C. and L. Partridge (1995). “Thermal evolution of rate of larval development in *Drosophila melanogaster* in laboratory and field populations”. In: *Journal of Evolutionary Biology* 8.3, pp. 315–330.
- Jefferson, M. C. (1977). “Breeding biology of *Drosophila pachea* and its relatives”. In: Joly, D., A. Korol, and E. Nevo (2004). “Sperm size evolution in *Drosophila*: inter- and intraspecific analysis”. In: *Genetica* 120.1-3, pp. 233–244.
- Juan, T. et al. (2018). “Myosin1D is an evolutionarily conserved regulator of animal left–right asymmetry”. In: *Nature communications* 9.1, pp. 1–12.
- Kahn, A. T., B. Mautz, and M. D. Jennions (2010). “Females prefer to associate with males with longer intromittent organs in mosquitofish”. In: *Biology Letters* 6.1, pp. 55–58.
- Kicheva, A. et al. (2007). “Kinetics of morphogen gradient formation”. In: *Science* 315.5811, pp. 521–525.
- Kirkpatrick, M. and M. J. Ryan (1991). “The evolution of mating preferences and the paradox of the lek”. In: *Nature* 350.6313, pp. 33–38.
- Kokko, H. and M. D. Jennions (2014). “The relationship between sexual selection and sexual conflict”. In: *Cold Spring Harbor Perspectives in Biology* 6.9, a017517.
- Krijger, C. L., Y. C. Peters, and J. C. Sevenster (2001). “Competitive ability of neotropical *Drosophila* predicted from larval development times”. In: *Oikos* 92.2, pp. 325–332.

- Kuntz, S. G. and M. B. Eisen (2014). “Drosophila Embryogenesis Scales Uniformly across Temperature in Developmentally Diverse Species”. In: *PLoS Genetics* 10.4. Ed. by C. Desplan, e1004293.
- Kuranaga, E. et al. (2011). “Apoptosis controls the speed of looping morphogenesis in Drosophila male terminalia”. In: *Development* 138.8, pp. 1493–1499.
- Lande, R. (1981). “Models of speciation by sexual selection on polygenic traits”. In: *Proceedings of the National Academy of Sciences* 78.6, pp. 3721–3725.
- Lang, M. (2009). “Comparative analysis of the transcription factor *adf-1* and its binding sites in the *adh* genomic regions of drosophilidae”. PhD thesis. Universitat de Barcelona.
- Lang, M. and V. Orgogozo (2012). “Distinct copulation positions in *Drosophila pachea* males with symmetric or asymmetric external genitalia”. In: *Contributions to Zoology* 81.2.
- Lang, M. et al. (2014). “Radiation of the *Drosophila* nannoptera species group in Mexico”. In: *Journal of evolutionary biology* 27.3, pp. 575–584.
- Lang, M. et al. (2012). “Mutations in the neverland Gene Turned *Drosophila pachea* into an Obligate Specialist Species”. In: *Science* 337.6102, pp. 1658–1661.
- Langerhans, R. B., C. A. Layman, and T. J. DeWitt (2005). “Male genital size reflects a tradeoff between attracting mates and avoiding predators in two live-bearing fish species”. In: *Proceedings of the National Academy of Sciences* 102.21, pp. 7618–7623.
- Lebreton, G. et al. (2018). “Molecular to organismal chirality is induced by the conserved myosin 1D”. In: *Science* 362.6417, pp. 949–952.
- Lecuit, T. (2010). “ α -Catenin mechanosensing for adherens junctions”. In: *Nature Cell Biology* 12.6, pp. 522–524.
- Lecuit, T. and L. Le Goff (2007). “Orchestrating size and shape during morphogenesis”. In: *Nature* 450.7167, pp. 189–192.
- Lecuit, T. and P.-F. Lenne (2007). “Cell surface mechanics and the control of cell shape, tissue patterns and morphogenesis”. In: *Nature reviews Molecular cell biology* 8.8, pp. 633–644.
- Lecuit, T. and L. Mahadevan (2017). *Morphogenesis one century after On Growth and Form*.
- Lefèvre, B. M. (2017). “Epandrial lobe asymmetry in *Deosophila pachea*, development and sexual selection (Master 2 thesis)”. In:
- Lefèvre, B. M. et al. (2020). “A primary sexual trait involved in courtship in insects: Male genital lobe morphology affects the chance to copulate in *Drosophila pachea*”. In: *bioRxiv*.
- LeGoff, L. and T. Lecuit (2016). “Mechanical forces and growth in animal tissues”. In: *Cold Spring Harbor perspectives in biology* 8.3, a019232.
- Leonard, J. L. and A. Córdoba-Aguilar, eds. (2010). *The evolution of primary sexual characters in animals*. Oxford ; New York: Oxford University Press. 537 pp.

- Levin, M., A. J. S. Klar, and A. F. Ramsdell (2016). *Introduction to provocative questions in left-right asymmetry*.
- Levin, M. et al. (1995). “A molecular pathway determining left-right asymmetry in chick embryogenesis”. In: *Cell* 82.5, pp. 803–814.
- Levin, M. et al. (2002). “Asymmetries in H⁺/K⁺-ATPase and cell membrane potentials comprise a very early step in left-right patterning”. In: *Cell* 111.1, pp. 77–89.
- Ludwig, W. (1932). *Das Recht-Links-Problem im Tierreich und beim Menschen:(Mit e. Anh.: Rechts-Links-Merkmale der Pflanzen. Mit 143 Abb.)*. Vol. 27. Heidelberg.
- Lüersen, K., T. Röder, and G. Rimbach (2019). “Drosophila melanogaster in nutrition research—the importance of standardizing experimental diets”. In: *Genes & Nutrition* 14.1, pp. 1–5.
- Macias, A. M. et al. (2004). “PVF1/PVR signaling and apoptosis promotes the rotation and dorsal closure of the Drosophila male terminalia”. In:
- Manjón, C., E. Sánchez-Herrero, and M. Suzanne (2007). “Sharp boundaries of Dpp signalling trigger local cell death required for Drosophila leg morphogenesis”. In: *Nature Cell Biology* 9.1, pp. 57–63.
- Manning, M. and T. A. Markow (1981). “Light-dependent pupation site preferences in Drosophila. II. Drosophila melanogaster and Drosophila simulans”. In: *Behavior genetics* 11.6, pp. 557–563.
- Marien, D. (1958). “Selection for developmental rate in Drosophila pseudoobscura”. In: *Genetics* 43.1, p. 3.
- Markow, T. A. (1981). “Light-dependent pupation site preferences in Drosophila: Behavior of adult visual mutants”. In: *Behavioral and neural biology* 31.3, pp. 348–353.
- Markow, T. A., S. Beall, and L. M. Matzkin (2009). “Egg size, embryonic development time and ovoviviparity in Drosophila species: Ovoviviparity in Drosophila species”. In: *Journal of Evolutionary Biology* 22.2, pp. 430–434.
- Markow, T. A. and P. O’Grady (2005). *Drosophila: a guide to species identification and use*. Elsevier.
- Markow, T. A. and P. M. O’Grady (2007). “Drosophila biology in the genomic age”. In: *Genetics* 177.3, pp. 1269–1276.
- Matsuda, H. and P. A. Abrams (1999). “Why are equally sized gametes so rare? The instability of isogamy and the cost of anisogamy”. In: *Evolutionary Ecology Research* 1.7, pp. 769–784.
- Matzkin, L. M. et al. (2011). “Dietary protein and sugar differentially affect development and metabolic pools in ecologically diverse Drosophila”. In: *The Journal of nutrition* 141.6, pp. 1127–1133.

- Mautz, B. S. et al. (2013). “Penis size interacts with body shape and height to influence male attractiveness”. In: *Proceedings of the National Academy of Sciences* 110.17, pp. 6925–6930.
- Mayr, E. (1963). “Animal species and evolution.” In: *Animal species and evolution*.
- Michiels, N. K. (1998). “Mating Conflicts and Sperm Competition in Simultaneous”. In: *Sperm competition and sexual selection*, p. 219.
- Miller, E. H. (2010). “Genitalic traits of mammals”. In: *JL Leonard and A. C órdoba-Aguilar, eds. The evolution of primary sexual characters in animals. Oxford Univ. Press, Oxford, UK*, pp. 471–493.
- Møller, A. P. (1993). “Fluctuating asymmetry and sexual selection”. In: p. 13.
- Monier, B. et al. (2015). “Apico-basal forces exerted by apoptotic cells drive epithelium folding”. In: *Nature* 518.7538, pp. 245–248.
- Moreno-Garcia, M. and C. Cordero (2008). “On the function of male genital claspers in *Stenomacra marginella* (Heteroptera: Largidae)”. In: *Journal of Ethology* 26.2, pp. 255–260.
- Moriwaki, D. and Y. Tobari (1975). *Drosophila ananassae*. In “*Handbook of Genetics*”(RC King, ed.) Vol. 3.
- Muller, M. N. and R. Wrangham (2002). “Sexual mimicry in hyenas”. In: *The Quarterly review of biology* 77.1, pp. 3–16.
- Mullis, F. et al. (1986). *PCR a practical approach*.
- Naganathan, S. R. et al. (2014). “Active torque generation by the actomyosin cell cortex drives left–right symmetry breaking”. In: *Elife* 3, e04165.
- Namigai, E. K., N. J. Kenny, and S. M. Shimeld (2014). “Right across the tree of life: the evolution of left–right asymmetry in the Bilateria”. In: *Genesis* 52.6, pp. 458–470.
- Nelson, C. M. et al. (2005). “Emergent patterns of growth controlled by multicellular form and mechanics”. In: *Proceedings of the National Academy of Sciences* 102.33, pp. 11594–11599.
- Norris, K. (1993). “Heritable variation in a plumage indicator of viability in male great tits *Parus major*”. In: *Nature* 362.6420, pp. 537–539.
- Oda, H. et al. (1994). “A *Drosophila* homolog of cadherin associated with armadillo and essential for embryonic cell-cell adhesion”. In: *Developmental biology* 165.2, pp. 716–726.
- Okumura, T. et al. (2015). “Class I Myosins Have Overlapping and Specialized Functions in Left-Right Asymmetric Development in *Drosophila*”. In: *Genetics* 199.4, pp. 1183–1199.
- Pacquelet, A., L. Lin, and P. Rørth (2003). “Binding site for p120/ δ -catenin is not required for *Drosophila* E-cadherin function in vivo”. In: *Journal of Cell Biology* 160.3, pp. 313–319.

- Pacquelet, A. and P. Rørth (2005). “Regulatory mechanisms required for DE-cadherin function in cell migration and other types of adhesion”. In: *The Journal of cell biology* 170.5, pp. 803–812.
- Palmer, A. R. (2004). “Symmetry breaking and the evolution of development”. In: *Science* 306.5697, pp. 828–833.
- (2005). “Antisymmetry”. In: *Variation*. Elsevier, pp. 359–XXIV.
- (2016). “What determines direction of asymmetry: genes, environment or chance?” In: *Philosophical Transactions of the Royal Society B: Biological Sciences* 371.1710, p. 20150417.
- Pascual, A. et al. (2004). “Brain asymmetry and long-term memory”. In: *Nature* 427.6975, pp. 605–606.
- Patterson, J. T. and M. R. Wheeler (1942). “Description of new species of the sub-genus *Hirtodrosophila* and *Drosophila*.” In: *University of Texas Publications* 4213, pp. 69–109.
- Perkin, A. (2007). “Comparative penile morphology of East African galagos of the genus *Galagoides* (family Galagidae): implications for taxonomy”. In: *American Journal of Primatology: Official Journal of the American Society of Primatologists* 69.1, pp. 16–26.
- Petrie, M. (1994). “Improved growth and survival of offspring of peacocks with more elaborate trains”. In: *Nature* 371.6498, pp. 598–599.
- Petzoldt, A. G. et al. (2012). “DE-Cadherin regulates unconventional Myosin ID and Myosin IC in *Drosophila* left-right asymmetry establishment”. In: *Development* 139.10, pp. 1874–1884.
- Pitnick, S. (1993). “Operational sex ratios and sperm limitation in populations of *Drosophila* *pachea*”. In: *Behavioral Ecology and Sociobiology* 33.6.
- (1994). “Sexual selection and sperm production in *Drosophila*.” In:
- Pitnick, S. and W. B. Heed (1994). “New species of cactus-breeding *Drosophila* (Diptera: Drosophilidae) in the nannoptera species group”. In: *Annals of the Entomological Society of America* 87.3, pp. 307–310.
- Pitnick, S. and T. A. Markow (1994a). “Large-male advantages associated with costs of sperm production in *Drosophila* *hydei*, a species with giant sperm.” In: *Proceedings of the National Academy of Sciences* 91.20, pp. 9277–9281.
- (1994b). “Male gametic strategies: sperm size, testes size, and the allocation of ejaculate among successive mates by the sperm-limited fly *Drosophila* *pachea* and its relatives”. In: *The American Naturalist* 143.5, pp. 785–819.
- Pitnick, S., T. A. Markow, and G. S. Spicer (1995). “Delayed male maturity is a cost of producing large sperm in *Drosophila*”. In: *Proceedings of the National Academy of Sciences* 92.23, pp. 10614–10618.

- Pitnick, S., T. A. Marrow, and G. S. Spicer (1999). “Evolution of multiple kinds of female sperm-storage organs in *Drosophila*”. In: *Evolution* 53.6, pp. 1804–1822.
- Ploog, D. W. and P. D. MacLean (1963). “Display of penile erection in squirrel monkey (*Saimuri sciureus*)”. In: *Animal behaviour* 11.1, pp. 32–39.
- Polak, M. and A. Rashed (2010). “Microscale laser surgery reveals adaptive function of male intromittent genitalia”. In: *Proceedings of the Royal Society B: Biological Sciences* 277.1686, pp. 1371–1376.
- Poulson, D. F. (1934). “Times of development of the two races of *Drosophila pseudoobscura*”. In: *Journal of Experimental Zoology* 68.2, pp. 237–245.
- Powsner, L. (1935). “The effects of temperature on the durations of the developmental stages of *Drosophila melanogaster*”. In: *Physiological Zoology* 8.4, pp. 474–520.
- Rhebergen, F. T. et al. (2016). “*Drosophila* pachea asymmetric lobes are part of a grasping device and stabilize one-sided mating”. In: *BMC evolutionary biology* 16.1, p. 176.
- Rogulja, D. and K. D. Irvine (2005). “Regulation of cell proliferation by a morphogen gradient”. In: *Cell* 123.3, pp. 449–461.
- Royes, W. V., F. W. Robertson, et al. (1964). “The nutritional requirements and growth relations of different species of *Drosophila*.” In: *Journal of experimental zoology* 156, pp. 105–135.
- Sánchez, L. and I. Guerrero (2001). “The development of the *Drosophila* genital disc”. In: *Bioessays* 23.8, pp. 698–707.
- Sato, K. et al. (2015). “Left–right asymmetric cell intercalation drives directional collective cell movement in epithelial morphogenesis”. In: *Nature communications* 6.1, pp. 1–11.
- Schantz, T. von et al. (1989). “Female choice selects for a viability-based male trait in pheasants”. In: *Nature* 337.6203, pp. 166–169.
- Schilthuisen, M. (2013). “Something gone awry: unsolved mysteries in the evolution of asymmetric animal genitalia”. In: *Animal Biology* 63.1, pp. 1–20.
- (2015). *Nature’s Nether Regions: What the Sex Lives of Bugs, Birds, and Beasts Tell Us about Evolution, Biodiversity, and Ourselves*. Penguin.
- Schilthuisen, M. and B. Gravendeel (2012). “Left-right asymmetry in plants and animals: a gold mine for research”. In: *Contributions to Zoology* 81.2, pp. 75–78.
- Schilthuisen, M. et al. (2007). “Sexual selection maintains whole-body chiral dimorphism in snails: Sexual selection and chiral dimorphism”. In: *Journal of Evolutionary Biology* 20.5, pp. 1941–1949.
- Schneider, C. A., W. S. Rasband, and K. W. Eliceiri (2012). “NIH Image to ImageJ: 25 years of image analysis”. In: *Nature methods* 9.7, pp. 671–675.

- Song, H. et al. (2010). “Planar cell polarity breaks bilateral symmetry by controlling ciliary positioning”. In: *Nature* 466.7304, pp. 378–382.
- Spéder, P., G. Ádám, and S. Noselli (2006). “Type ID unconventional myosin controls left–right asymmetry in *Drosophila*”. In: *Nature* 440.7085, pp. 803–807.
- Spéder, P. and S. Noselli (2007). “Left–right asymmetry: class I myosins show the direction”. In: *Current opinion in cell biology* 19.1, pp. 82–87.
- Spieth, H. T. (1952). *Mating behavior within the genus Drosophila (Diptera)*. American Museum of Natural History.
- Spradling, A. C. and G. M. Rubin (1982). “Transposition of cloned P elements into *Drosophila* germ line chromosomes”. In: *Science* 218.4570, pp. 341–347.
- Sreng, L. (1993). “Cockroach mating behaviors, sex pheromones, and abdominal glands (Diptera: Blaberidae)”. In: *Journal of Insect Behavior* 6.6, pp. 715–735.
- Stern, C. (1941a). “The growth of testes in *Drosophila*. I. The relation between vas deferens and testis within various species”. In: *Journal of Experimental Zoology* 87.1, pp. 113–158.
- (1941b). “The growth of testes in *Drosophila*. II. The nature of interspecific differences”. In: *Journal of Experimental Zoology* 87.1, pp. 159–180.
- Strasburger, E. H. (1935). *Drosophila melanogaster meig.* Springer.
- Stratman, R. and T. Markow (1998). “Resistance to thermal stress in desert *Drosophila*”. In: *Functional Ecology* 12.6, pp. 965–970.
- Streichan, S. J. et al. (2014). “Spatial constraints control cell proliferation in tissues”. In: *Proceedings of the National Academy of Sciences* 111.15, pp. 5586–5591.
- Sulston, J. E. et al. (1983). “The embryonic cell lineage of the nematode *Caenorhabditis elegans*”. In: *Developmental biology* 100.1, pp. 64–119.
- Sun, S. and K. D. Irvine (2016). “Cellular organization and cytoskeletal regulation of the Hippo signaling network”. In: *Trends in cell biology* 26.9, pp. 694–704.
- Suzanne, M. et al. (2010). “Coupling of apoptosis and L/R patterning controls stepwise organ looping”. In: *Current Biology* 20.19, pp. 1773–1778.
- Taniguchi, K. et al. (2011). “Chirality in planar cell shape contributes to left-right asymmetric epithelial morphogenesis”. In: *Science* 333.6040, pp. 339–341.
- Thornhill, R. (1983). “Cryptic Female Choice and Its Implications in the Scorpionfly *Harpobittacus nigriceps*”. In: *The American Naturalist* 122.6, pp. 765–788.
- Throckmorton, L. H. (1975). “The phylogeny, ecology, and geography of *Drosophila*”. In: *Handbook of Genetics* 3, pp. 421–469.
- Tingler, M. et al. (2018). “A conserved role of the unconventional myosin 1d in laterality determination”. In: *Current Biology* 28.5, pp. 810–816.

- Turner, H., D. Firth, et al. (2012). “Bradley-Terry models in R: the BradleyTerry2 package”. In: *Journal of Statistical Software* 48.9.
- Vandenberg, L. N. and M. Levin (2013). “A unified model for left–right asymmetry? Comparison and synthesis of molecular models of embryonic laterality”. In: *Developmental biology* 379.1, pp. 1–15.
- Vijendravarma, R. K., S. Narasimha, and T. J. Kawecki (2013). “Predatory cannibalism in *Drosophila melanogaster* larvae”. In: *Nature communications* 4.1, pp. 1–8.
- Vilela, C. R., G. Bächli, et al. (1990). “Taxonomic studies on Neotropical species of seven genera of Drosophilidae (Diptera).” In: *Mitteilungen der Schweizerischen Entomologischen Gesellschaft* 63.Suppl.
- Wang, Y. and V. Riechmann (2007). “The role of the actomyosin cytoskeleton in coordination of tissue growth during *Drosophila* oogenesis”. In: *Current biology* 17.15, pp. 1349–1355.
- Warren, J. T. et al. (2001). “Woc (without children) gene control of ecdysone biosynthesis in *Drosophila melanogaster*”. In: *Molecular and cellular endocrinology* 181.1, pp. 1–14.
- Welch, A. M., R. D. Semlitsch, and H. C. Gerhardt (1998). “Call duration as an indicator of genetic quality in male gray tree frogs”. In: *Science* 280.5371, pp. 1928–1930.
- Wheeler, M. R. (1949). “Taxonomic studies on the Drosophilidae.” In: *University of Texas Publications* 4920, pp. 157–195.
- Wickler, W. (1966). “Ursprung und biologische Deutung des Genitalprasentierens männlicher Primaten”. In: *Zeitschrift für Tierpsychologie* 23.4, pp. 422–437.
- Woods, D. F., J. W. Wu, and P. J. Bryant (1997). “Localization of proteins to the apico-lateral junctions of *Drosophila* epithelia”. In: *Developmental genetics* 20.2, pp. 111–118.
- Yassin, A. (2013). “Phylogenetic classification of the Drosophilidae Rondani (Diptera): the role of morphology in the postgenomic era”. In: *Systematic Entomology* 38.2, pp. 349–364.
- Yuan, S. and M. Brueckner (2018). “Left–right asymmetry: myosin 1D at the center”. In: *Current Biology* 28.9, R567–R569.

Annexes

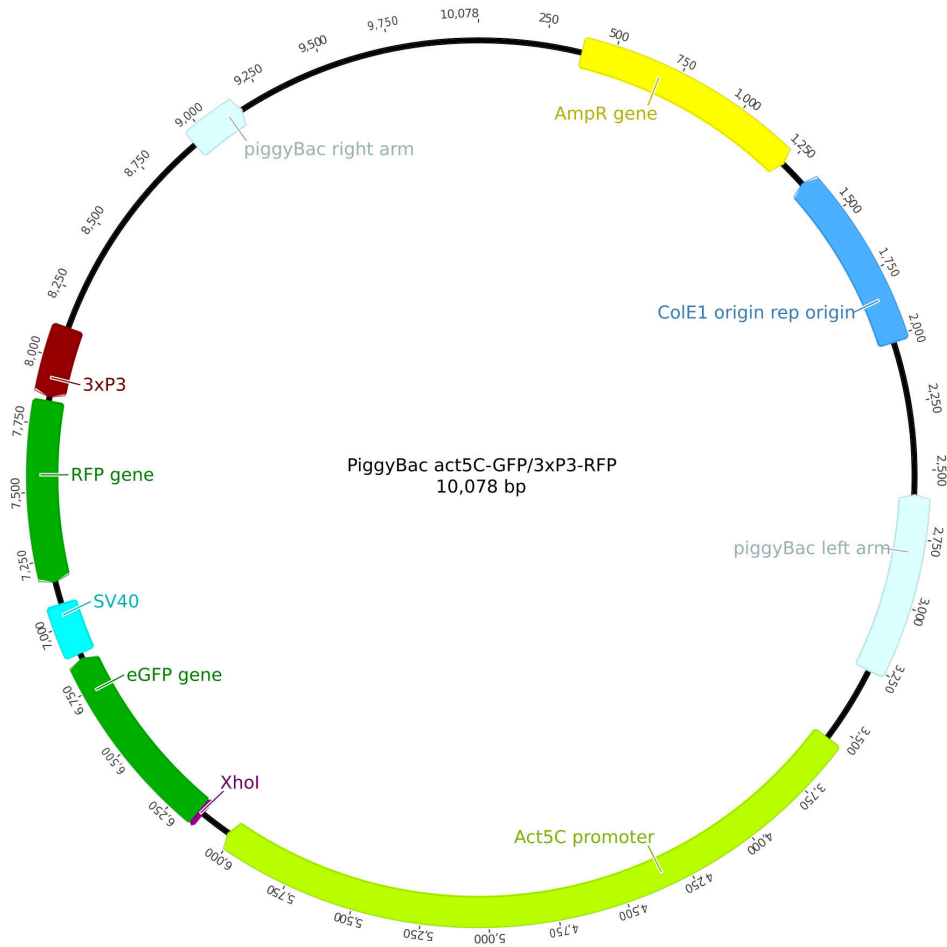
Oligonucleotides

oligonucleotide ID	oligonucleotide sequence (from 5' to 3')	Tm [°C]
p-DE-cad-5'UTR_#1_F	AAATGAGTGAATGCTTTGTGAA	57.56
p-DE-cad-ex1_R	CCGACTGTACCAAGCTGTA	59.19
F1_F	TATAAACACATGTACATATGTATGTTTTGGCATAACAATGAGTAGTTG	68.18
F1_R	TGCTCACCATCTCGAGGGTGGCGGTACCGTTGAG	77.69
F2_F	TACCGCCACCCTCGAGATGGTGAGCAAGGGCGAG	79.60
F2_R	TACTGAGAGTGCACCATATGCGGTGTGAAATACCGCAC	74.68
F3_F	CGGAGGAGGCCATGGTGGCGACCGGTGGATC	79.37
F3_R	TGCTCACCATCTCGAGGGTGGCGGTACCGTTGAG	77.69
F4_F	CCTGCAGGTCGACCACTCGAGTGTTCATTGTGTTTTTGC	76.89
F4_R	CAATGATGAAAAATGATGGCGGCTTAATTG	64.96
F5_F	GCCATCATTTTTTCATCATTGCGATCATCGTATG	67.50
F5_R	TTGGGAGCTCTCCATACTCGAGCACATCGTCCACGGTTGTG	79.03
F6_F	GGTTACGGCACTAGAGCGGCCGCAATTCTATATTCTAAAAACACAAATGATACTCTCAAAA	62.91
F6_R	TCGAGGGTGGCGGTACCGTT	68.50
F7_F	AACGGTACCGCCACCCTCGA	68.50
F7_R	TACCGTCGACCTCGAGAGATCTGATCCAGACATGATAAGATACATTGATGAGTTTGGACAAAC CACAAC TAGAA	67.85
m_DE-cad_3'UTR_R	CGGCTGGCGAAGATTCTCA	62.27
#1_backbone_R	AAAACATACATATGTACATGTGTTTATAGTGGGTTTATTAG	64.61
#1_frag_1_F	CATGTACATATGTATGTTTTGGCATAACAATGAGTAGTTG	66.53
act5C_F2	TTCAGTTTCTTGGCTTATTCA	55.88
m-DE-cad-5'UTR_F	TGTTGCATTGTGTTTTTGCTTTTGAATTGA	65.00
DsRedForw1	AGAGTCGACGGTACGATCCATAATTCGAGCTCGCCCGG	77.42
eGFP_F	GGACGACGGCAACTACAA	60.11
eGFP_R	TTCACCTTGATGCCGTTCTT	60.38
mCherry_F	CCCCGTAATGCAGAAGAAGA	59.94
#11_InvPCR_F1	CGGCGACTGAGATGCCTAAAT	66.60
#11_InvPCR_R1	GCGGTAAGTGTCACTGATTTTGAAC TATAA	67.50
#11_InvPCR_F2	CGCGCTATTTAGAAAAGAGAGCAATATTT	68.40
#11_InvPCR_R2	GACCGCGTGAGTCAAAATGA	66.60

PiggyBac plasmid maps⁴

PiggyBac plasmids

PiggyBac act5C-GFP 3xP3-RFP



Annotations

Annotations	Position (bp)
PiggyBac right arm	8948 - 9165
act5C promoter	3555 - 6022
eGFP	6152 - 6871
RFP	7840 - 7166
3xP3	8116 - 7851
PiggyBac left arm	8948 - 9165

Sequence

TGGTGCACCTCTCAGTACAATCTGCTCTGATGCCGCATAGTTAAGCCAGCCCCGACACCCGCCAACCCCGCTGACGCGCC
CTGACGGGCTTGCTCGCTCCCGGCATCCGCTTACAGACAAGCTGTGACCGTCTCCGGAGCTGCATGTGTACAGAGTTTT

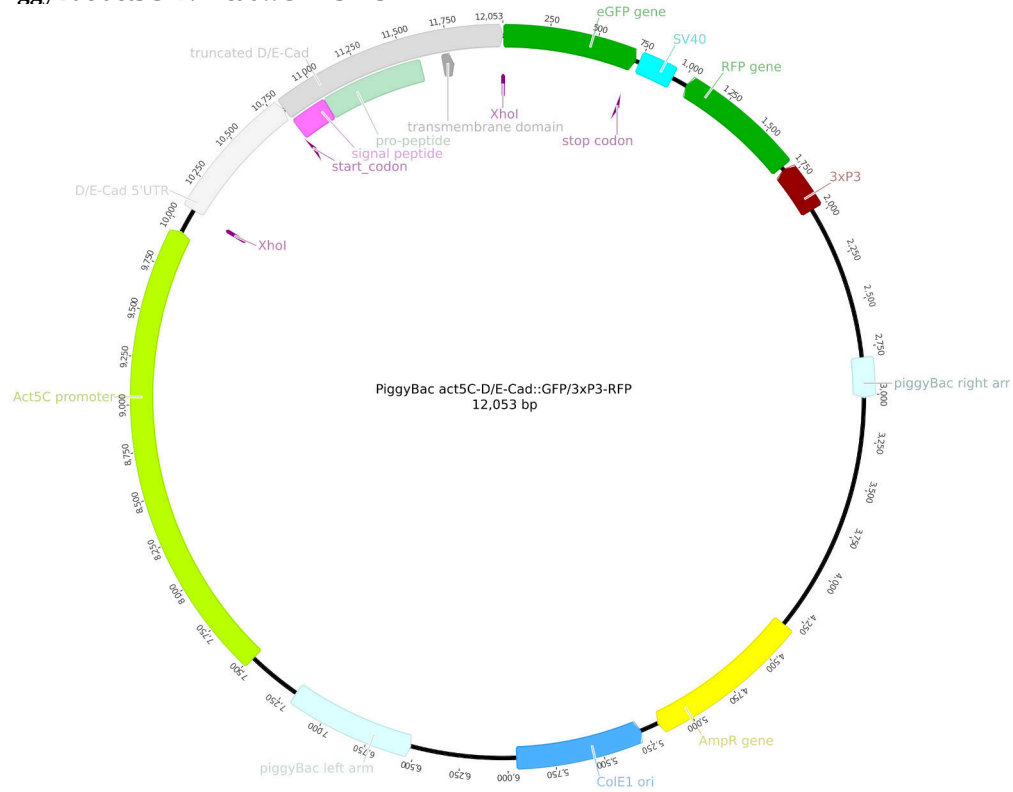
⁴The following plasmids are derived from a modified versions of pBac[3xP3-EGFP afm] plasmid (Horn and Wimmer 2000) and pBAC-ECFP-15xQUAS_TATA-mcd8-GFP-SV40 (Addgene 104878, gift from Christopher Potter). See part 2.4.1 "Cloning strategy", page 67 for details.

CACCGTCATCACCGAAACGCGCGAGACGAAAGGGCCCTCGTGATACGCCTATTTTTATAGGTTAATGTCATGATAATAATG
GTTTTCTTAGACGTCAGGTGGCACTTTTTCGGGGAAATGTGCGCGGAACCCCTATTTGTTATTTTTCTAAAATACATTCAAA
TATGTATCCGCTCATGAGACAATAACCTGATAAATGCTTCAATAATATTGAAAAAGGAAGAGTATGAGTATTCACATT
TCCGTGTCCGCTTATTCCTTTTTTTCGGGCATTTTGCCTTCCCTGTTTTTGCCTCACCCAGAAACCGTGGTGAAGTAAAA
GATGCTGAAGATCAGTTGGGTGCACGAGTGGGTACATCGAACTGGATCTCAACAGCGGTAAGATCCTTGAGAGTTTTCG
CCCCGAAAGACGTTTTTCCAAATGATGAGCACTTTTAAAGTTCTGCTATGTGGCGCGGTATTATCCCGTATTGACGCCGGG
AAGAGCAACTCGGTCGCCGCATACACTATTCTCAGAATGACTTGGTTGAGTACTCACCAGTACAGAAAAGCATCTTACG
GATGGCATGACAGTAAGAGAATTATGCAGTGTGCCATAACCATGAGTGATAACACTGCGGCAACTTACTTCTGACAAC
GATCGGAGGACCGAAGGACTAACCGCTTTTTTGCACAACATGGGGGATCATGTAACCTCGCCTTGATCGTTGGGAACCGG
AGCTGAATGAAGCCATACCAAACGACGAGCGTGACACCAGATGCCGTGATGCAATGGCAACAACGTTGCGCAAACTATTA
ACTGGCAACTACTTACTCTAGCTTCCCGCAACAATTAATAGACTGGATGGAGCGGATAAAGTTGACGAGCACTTCT
GCGTCCGGCTTCCGGCTGGCTGGTTTTATTGCTGATAAATCTGGAGCCGGTGAGCGTGGGTCTCGCGGTATCATTCGAC
CACTGGGGCCAGATGGTAAGCCCTCCCGTATCGTAGTTATCTACACGACGGGAGTCAGGCAACTATGGATGAACGAAAT
AGACAGATCGCTGAGATAGGTGCTCCTACTGATTAAGCATTTGGTAACCTGTACAGCAAGTTTACTCATATATACTTAGAT
TGATTTAAACTTCATTTTTAATTTAAAAGGATCTAGGTGAAGATCCTTTTTGATAATCTCATGACCAAAATCCCTAAC
GTGAGTTTTCGTTCCACTGAGCCTCAGACCCCGTAGAAAAGATCAAAGGATCTTCTTGAGATCCTTTTTTCTGCGCGTA
ATCTGCTGCTTGCAAAACAAAAAACACCGCTACCAGCGGTGGTTTTGTTGCGGATCAAGAGCTACCAACTCTTTTTCC
GAAGGTAACCTGCTTACGACAGCGCAGATACCAAATACTGTCTTCTAGTGTAGCCGTAGTTAGGCCCACTTCAAGA
ACTCTGTACACCCCTACATACCTCGCTGCTGCTAATCCTGTACCAGTGGCTGCTGCCAGTGGCGGATCGTCTT
ACCGGTTGGACTCAAGACGATAGTTACCGGATAAGGCGCAGCGGTGGGCTGAACGGGGGTTCTGTCACACAGCCAG
CTTGAGCGCAACGACTACACCAACTGAGATACCTACAGCCTGAGCATTGAGAAAAGCGCCACGCTTCCCGAAGGGAGAA
AGGCGGACAGGTATCCGGTAAGCGGACGGGTCCGAACAGGAGCGCACGAGGGAGCTTCCAGGGGAAACGCTGGTAT
TTTTATAGTCTCTGCGGTTTCGCCACTTGCAGCTTGCAGTTCGATTTTTGTGATGCTCGTCAGGGGGCGGAGCCTATG
GAAAACGCGCAGCAACGCGGCTTTTTACGGTTCTGCTTTTTGCTGGCTTTTTGCTCACATGTTCTTCTGCGTTAT
CCCTGATTTCTGTGGATAACCGTATTACCGCTTTGAGTGTGCTGATACCGCTCGCCGACGCGAACGACCGAGCGCAGC
GAGTCAGTGTGAGCGGAAAGCGGAGAGCGCCAAATACGCAACCGCTCTCCCGCGCGTTGGCCGATTCATTAATGAC
CTGGCAGCAGAGTTTCCCGACTGAAAGCGGCGAGTGTGCGCAACGCAATTAATGTGAGTTAGCTCACTCATTAGGCAC
CCCAGGCTTACACTTTATGCTTCCGGCTCGTATGTTGTGTGGAATTTGTGAGCGGATAACAATTTACACAGGAAACAGC
TATGACCATGATTACGAATTCGAGCTCGGTACCCGGGATCCTCTAGAGTGTGACGCTCGCGGCACTTGGTTTTGCCATTCT
TTAGCGCGCTCGGCTCACACAGCTTGGCCACAATGTGGTTTTTGTCAAACGAAGATCTATGACGTTTAAAGTTTAG
GTCGAGTAAAGCGCAATCTTTTTTAAACCTAGAAAAGATAGTCTGCGTAAAATTGACGCATGCATTTTGAATAATGTCT
CTCTCTTCTAAATAGCGCAATCCGTCGCTGTGCATTTAGGACATCTCAGTCGCGCTTGGAGCTCCCGTGAGGCGTGC
TTGTCAATCGGTTAAGTGTCACTGATTTGAACTATAACGACCCGCTGAGTCAAAAATGACGCATGATATCTTTTACGTC
ACTTTAAGATTTAACTCATAAGATAATTATATTGTTATTTTCACTTACTTACGTGATAACTTATTATATATATATTT
TCTTGTATAGATATCGTACTAATATATAATAAAATGGGTAGTTCTTTAGACGATGAGCATATCTCTCTGCTCTCTG
CAAAGCGATGACGAGCTTGTGGTGAGGATTTGACAGTGAATATCAGATCACGTAAGTGAAGATGACGTCAGAGCGA
TACAGAAGAAGCGTTTATAGATGAGGTACATGAAGTGCACCAACGTCGAAGCGGTAGTGAATATTAGACGAAACAAATG
TTATTGAACAACAGGTTCTTCAATGGCTTCTAACAGAACTTTGACCTTGCCACAGAGGACTATTAGAGGTAAGAATAAA
CATTTGTTGGTCAACTTCAAAGTCCACGAGCGGTAGCCGAGTCTCTGCACTGAACATTTGTGATCTGTGTGAACGGTGGT
TTCACGCTTCAAAGTGGTGATTTTGTGCTGACGACTCTAGATCGGCTCGCGGACTGACGGTGTGAAGCACCAGCG
TACGTTCCACCCCGTCAACCCCTTGTGTGATGTGCGGACCCCTACGCCCAACTGAGAGAATCAAAGGTTACCC
CAGTTGGGCACTACTCCGAAAACCGCTTCTGACCTGGGAAAACGTAAGCCCCGGGCACTCCGCTGAGGTTGCCGCC
GGGCTTCCGTGTGTCGTCAGTACTGATCGCATGCAATTTATATTCTAAAAACAAAAATGATACTTTCAAAAAAAAT
CATGAATGGCATCAACTCTGAATCAAATCTTTCAGATGCACCTACTTCTCATTTCCACTGTACATCATTTTTCCAGAT
CTCGCTGCCGTGTTATGTGGCCCAAAACCAAGACACGTTTTATGGCCATTAAGCTGGCTGATCGTCCGCAACACCAAA
TACATAATGAATATGTACATTCGAGAAAGAAGCGATCAAAGAAGCGTCTTCGGGCGGAGTAGGAGAATGCGGAGGAGA
AGGAGAAGAGCTGATCTAGTATCTCTCCACAATCCAATGCCAAGTACCAACTGGCCATATTCGGAGCAATTTGAAGCC
AATTTCCATCGCCTGGCGATCGCTCCATTTCTGGCTATATGTTTTTACCCTTACCCGGGCAATTTTCAAAGACTCGTC
GGCAAGATAAGATTGTGTCACCTGCTCTCTCTTCAATTTGTGCAAGAATGCTGAGGAATTTCCGGATGACGTCGGCGAG
TATTTTGAAGAATGAGAATAATTTGTATTTATACGAAAATCAGTTAGTGAATTTTCTACAAAAACATGTTATCTATAGA
TATAATGGCAATGATGATACTGATGATATTTAAGATGATGCCAGCAAAAGGCTTGAATTTCTGCGCTTTTTGCGGAA
CGCAGTGCATGTGCAATTTGTTTTTTTTGGAATATTCATTTTTCGGACTGTCCGCTTTGATTTTCACTTTCTGGCTTATT
CAAAAAGCAAAGTAAAGCCAAAAAGCGAGATGGCAATACCAATGCGGCAAAACGCTAGTGAAGGAAAGGGTGGCGG
GCAGCGAAAGGAAAGGGTGGGGCGGGGCTGGCGGGTCTGTGGCTGGCGCGACGTCACCGACGTTGGAGCCACTCTTT
GACCATGTGCGGTGTGTGATTTATTCGCTGCTCGCCACTCGCCGTTGTTTTTTCTTTTTATGCTGCGCTCTCTCTAG
CGCATCTCGCTTACGCATGCTCAACGACCGCATGTTGCCGTTTTCTTTTTATGCGCTCATTTTGGCTGAAATAGGCAAT
TATTTAAACAAAGATTAGTCAACGAAAACGCTAAAATAAATAAGTCTACAATATGGTTACTTATTGCCATGTGTGTGAC
CAAACGATAGCAACAAAGCAACAACACAGGTGGCTTCCCTCTTCTACTTTTTGTTTGAAGCCGCGTGGCAGCAAGAC
GGCAGACCGGCAACGCAATTAACGCTGACAAAAGAGCAGACGAATTTTGGCGAAAACATCAAGGCGCTGATACGAAT

GCATTTGCAATAACAATTGCGATATTTAATATTGTTTATGAAGCTGTTTGACTTCAAAACACACAAAAAATAAAAA
CAAATTAATTTGAAAGAGAAATTAGGAATCGGACGCTTATCGTTAGGGTAACAACAAGAAATGCTTACTGAGTCACAGCCTC
TGGAAAACCTGCCGAAGCCAGAGAGAGAGAAAAAGAGGGAGAGCAGCTTAGACCCGATGTGCTTGTGTGTGAGGCGTC
TCTCTCTTCGTCTCTGTTGCGCAACCGCATAGACTGCCTGAGAAAAATCGATTACCTATTTTTTATGAATGAATATTTGC
ACTATTACTATTCAAACTATTAAGATAGCAATCACATTTCAATAGCCAAATACTATAACCACCTGAGCGATGCAACGAAAT
GATCAATTTGAGCAAAAATGCTGCATATTTAGGACGGCATCATATAGAAAATGCTTCTGTGTGTACTTTTCTCTCGTC
TGGCAGCTGTTTCGCCGTTATTGTTAAAAACCGCTTAAGTTAGGTGTGTTTTCTACGACTAGTGAATGCCCTACTAGAAG
ATGTGTGTTGCACAAAATGTCCTGGAATAACCAATTTGAAGTGCAGATAGCAGTAAACGTAAGCTAATATGAATATTTAT
TTAACTGTAATGTTTTAATATCGCTGGACATTAATAAAACCACATAAAACACATGTACATATGTATGTTTTGGCATA
CAATGAGTAGTTGGGGAAAAATGTGTAAAAGCACCGTGACCATCACAGCATAAAGATAACCAGCTGAAGTATCGAATAT
GAGTAACCCCAAATGAAATCACATGCCGCAACTGATAGGACCCATGGAAGTACACTCTTTCATGGCGATATACAAGACAC
ACACAAGCACGAACACCCAGTTGCCGAGGAAATTTCTCCGTAATGAAAACCAATCGGCGAACAAATTCATACCCATATAT
GGTAAAAGTTTTGAACGCGACTTGAGAGCGGAGAGCATGCGGCTGATAAGGTTTTAGCGCTAAGCGGGCTTTATAAAAAC
GGGTGCGGGACAGTTTTTCATATCACTACCGTTGAGTTTCTGTGTGTGTGGATACTCTCCCGACACAAAAGCCGCTC
CATCAGCCAGCAGTCGTCTAATCCAGAGACCCGGATCCAGATAGATCTCAACGGTACCGCCACCTCGAGATGGTGAAG
AAGGGCAGGAGGCTGTTACCGGGGTGTGCCATCTGTTGCTGAGCTGGACGGCGAGCTAAACGGCCACAAGTTACGCGT
GTCCGGCGAGGGCGAGGGCGATGCCACCTACGGCAAGCTGACCTGAAGTTTCATCTGCACCACCGGCAAGCTGCCCGTGC
CTTGGCCACCCTCGTGACCACCTGACCTACGGCGTGCAGTGTCTCAGCCGCTACCCCGACCACATGAAGCAGCAGCAG
TTCTTCAAGTCCGCGATGCCGAGGCTACGTCCAGGAGCGCACTCTTCTTCAAGGACGACGGCAACGAAAGCCGCTC
CGCCGAGGTGAAGTTCCAGGGCGACACCTGGTGAACCGCATCGAGCTGAAGGGCATCGACTTCAAGGAGGACGGCAACA
TCTTGGGGCACAAGCTGGAGTACAACACAGCCACAACCTCTATATCATGGCCGACAAGCAGAGAAGCGGCATCAAG
GTGAACTTCAAGATCCGCCACAACATCGAGGACGGCAGCGTGCAGCTCGCCGACCACTACCAGCAGAACACCCCATCGG
CTACGATACGCGTACGGCGCCCTAGGAATGGGGTACGCTTAGAGGGCCCGGTGGAGTGGCGGCCCTCGGCGCGCTCGT
ATCACATGGTCTGCTGGAGTTGCTGACCGCCGCGGGATCACTCTCGGCATGGACGAGCTGTACAAGTAAAGCGGCCG
GACTCTAGATCATAATCAGCCATACCACATTTGTAGAGGTTTTACTTGTCTTAAAAAACCTCCACACCTCCCTGAAAC
CTGAAACATAAAATGAATGCAATTTGTTGTTGTTAACTTGTATTGAGCTTATAATGGTTACAAAATAAAGCAATAGCAT
CACAAATTTCAAAAATAAAGCATTTTTTTCACCTGCATCTAGTTGTGGTTTTGTCCAAACTCATCAATGTATCTTAAAGCT
TATCGATACGCGTACGGCGCCCTAGGAATGGGGTACGCTTAGAGGGCCCGGTGGAGTGGCGGCCCTCGGCGCGCTCGT
ACTGTTCCACGATGGTGTAGTCTCGTTGTGGAGGTGATGTCCAGCTTGTGTGCGTCTTGTAGGCGCGGGCAGCTGC
ACGGGCTTCTTGGCCATGTAGGTGCTTGTACCTCGGCGTCTGAGTGGCCGCGCTTCCAGCTTACGCTCATCTTGAT
CTCCTCCCTTTCAGGGCGCGCTCCTCGGGTACATCCGCTCGGTGGAGGCTCCAGCCATGGTCTTCTTTCGATACCGG
GGCGCTCGGAGGGGAAGTTGGTGCCGCGCAGCTTACCTTGTAGATGAACTCGCCGCTCTGCAGGGAGGAGTCTGGGT
ACGGTCAACACGCGCCCTCCTCGAAGTTTCATACGCGCTCCCACTTGAAGCCCTCGGGGAAGGACAGCTTCAAGTAGT
GGGATGTCCGCGGGTGTCTCACGTAGGCTTGGAGCCGACTGGAAGTGAAGGGACAGGATGTCCAGGCGAAGGGCA
GGGGCCCGCTTGGTCACCTTACGCTTGGCGGTCTGGGTGCCCTCGTAGGGCGGGCCCTCGCCCTCGCCCTCGATCTCG
AACTCGTGGCCCTTACAGGAGCCCTCCATGCGCACCTTGAAGCGCATGAACTCCTTGTATGACGCTCTCGGAGGAGCCAT
GGTGGGACCGGTGGATCCCGGGCCCGGTACCGTGCAGCTTAGCGGTACCCCGATTGTTTAGCTTGTTCAGCTGCGCT
TGTTTATTGCTTAGCTTTCGCTTAGCGACGTGTTCACTTTGCTTGTGTTGAATGAAATGTGCTCCGATGACCTGCAGTAG
CTCTATTTATACCTCGGCGGTGAGGGTTCGAAATCGATAAGCTTGGATCCTAATTGAATTAGCTCAATTGAATTAGTCT
TCTAATTGAATTAGATCCCGGGCGAGCTCGAATTAACCATTTGTGGGAACCGTGCATCAAAACAAAGCGAGATACCGGA
AGTACTGAAAAACAGTCGCTCCAGGCCAGTGGGAACATCGATGTTTTGTTTTGACGGACCCCTTACTCTCGTCTCATATA
AACCGAAGCCAGCTAAGATGGTATACTTATTATCATCTTGTGATGAGGATGCTTCTATCAACGAAAGTACCGGTAAACCG
CAAATGGTTATGTATTATAAATCAAATAAAGCGGAGTGGACACGCTAGACCAAATGTGTTCTGTGATGACCTGCAGTAG
GAAGACGAATAGGTGGCTATGGCATTATTGTACGGAATGATAAACATTTGCCATGATAAATCTTTTTATTATATACAGCC
ATAATGTACAGTAGCAAGGAGAAAAGGTCCAAAGTCCGAAAAAATTTATGAGAAACCTTTACATGAGCCTGACGTCATCG
TTTTATGCGTAAGCGTTTAGAAGCTCTACTTTGAAGAGATATTTGCGCGATAATATCTCTAATATTTTGCCAAATGAAGT
GCCGTGATCAGATGACAGTACTGAAGAGCCAGTAATGAAAAACGTACTTACTGTACTTACTGCCCTCTAAAAATAA
GGCGAAAAGGCAAAATGCATCGTGCAAAAAATGCAAAAAAGTTATTTGTCGAGAGCATAAATTTGATATGTGCGCAAGTTGT
TTCTGACTGACTAATAAGTATAATTTGTTCTATATGTATAAGTTAAGCTAATTACTTATTTTATAATACAACATGACT
GTTTTTAAAGTACAAAATAAGTTTATTTTTGTAAAAGAGAGAAATGTTTAAAAGTTTTGTTACTTTATAGAGAAAATTTG
AGTTTTTGTTTTTTTTTAATAAATAAATAAACAATAAATAAATTTGTTGTTGAATTTATATAGTATGTAAGTGAATA
TAATAAAAACCTAATATCTATTCAAATTAATAAATAAACCCTGATATACAGACCGATAAACAACATGGCTCAATTTTACGC
ATGATTAATCTTTAACGTACGTCAAAATATGATTATCTTTCTAGGGTTAAATAATAGTTTCTAATTTTTTTTTATTTACGC
CTGCTGCTGTAATACCGTATATCTCAACGCTGTCTGTGAGATTGTGCTATTTCTAGCCTTTTTTAGTTTTTCGCTCATCGA
CTTGATATTTGTCGACACATTTTCGTCGATTTGCGTTTTGATCAAAAGACTTGAAGCAGAGACAGCTTAACTCACTGTTCAA
ATTTGATCCATATTAACGATATCAACCCGATGCGTATATGGTGCCTAAAATATAATTTTTAACCCCTTATACTTTGCACT
CTGCTTAAACGCTTTCGTGACAGAGTAACTCATGTTTTCTTTTTTGGATAAAAACCTCTACTGAGTTTGACCTCATAT
TAGACCCTCACAAGTTGCAAAAACGTGGCATTTTTTACCAATGAAGAATTTAAAGTTATTTTTAAAAAATTTTATCACAGAT
TTAAAGAAGAACCAAAAATAAATTTTCAACAGTTTAACTGACAGTTAATCAACGTGTACACAGACGCGTGGCAGAA
AAACACGACGCCGACGTTGGCTAAAATTTAAATCAACTTGTGTTATAGTACAGGATTTGCCGCTCAACGTTGCTTC

TCAAAAGTTGAAGACCAACAAGTTTACGGACTATTAATTATTTGATTTTGCCCCACTTCATTTTGTGGGATCACAAT
 TTTGTTATATTTTAAACAAGCTTGGCACTGGCCGTCGTTTTACAACGTCGTGACTGGGAAAACCCCTGGCGTTACCCAAC
 TTAATCGCCTTGCAGCACATCCCCCTTTCGCCAGCTGGCGTAATAGCGAAGAGGCCCGCACCGATCGCCCTTCCCAACA
 GTTGCAGCCTGAATGGCGAATGGCGCCTGATGCGGTATTTCTCCTTACGCATCTGTGCGGTATTTACACCCGATA

PiggyBac act5C-D/E-cad::GFP 3xP3-RFP



Annotations

Annotations	Position (bp)
PiggyBac right arm	7199 - 6521
act5C promoter	7488 - 9955
D/E-cad 5' UTR	10084 - 10808
truncated D/E-cad	10809 - 12054
GFP	7 - 726
RFP	1695 - 1021
3xP3	1971 - 1706
PiggyBac left arm	2803 - 3020

Sequence

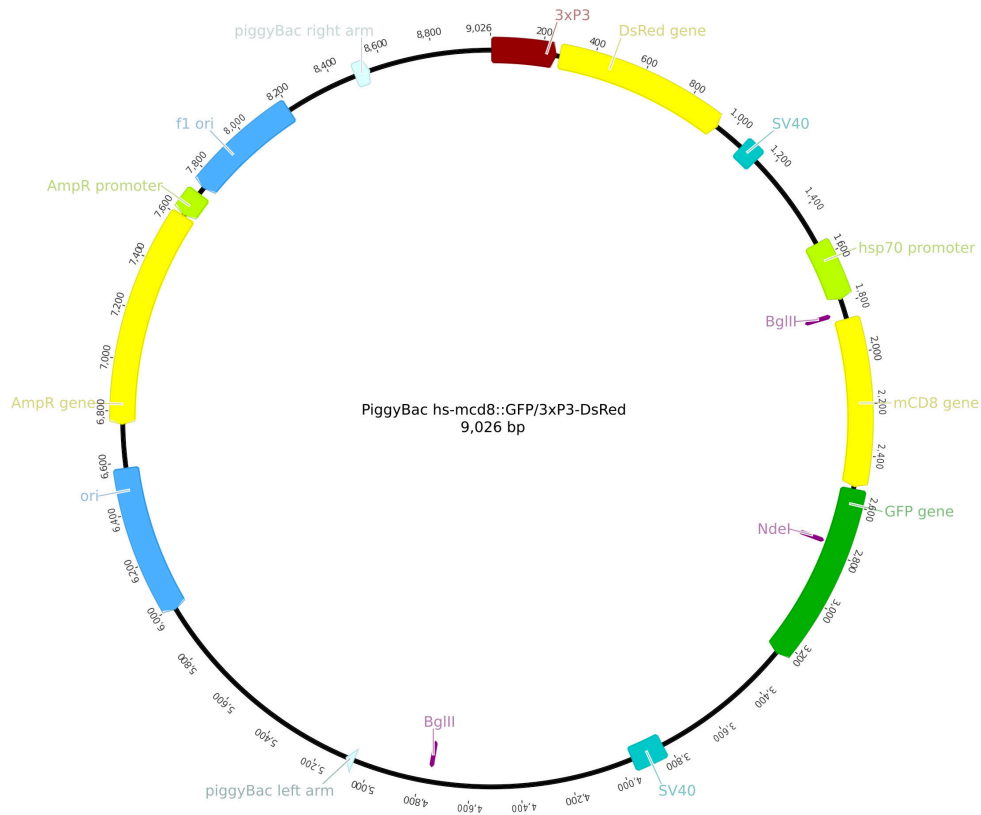
CTCAGATGGTGTAGCAAGGGCGAGGAGCTGTTACCGGGGTGGTGCCATCCTGGTCGAGCTGGACGGCGACGTAAACGG
 CCACAAGTTTCAGCGTGTCCGGCGAGGGCGAGGGCGATGCCACCTACGCAAGCTGACCCCTGAAGTTCATCTGCACCACCG
 GCAAGCTGCCCGTGCCTGGCCACCCCTCGTGACCACCTGACCTACGGCGTGCAGTGCTTCAGCCGCTACCCCGACCAC
 ATGAAGCAGCAGACTTCTTCAAGTCCGCCATGCCCGAAGGTACGTCCAGGAGCGCACCATCTTCTTCAAGGACGACGG
 CAACTACAAGACCCGCGCCGAGGTGAAGTTCGAGGGCGACACCTGGTGAACCGCATCGAGCTGAAGGGCATCGACTTCA

AGGAGGACGGCAACATCCTGGGGCACAAGCTGGAGTACAACACAGCCACAACGCTCTATATCATGGCCGACAAGCAG
AAGAACGGCATCAAGGTGAACCTCAAGATCCGCCACAACATCGAGGACGGCAGCGTGCAGCTCGCCGACCACTACCAGCA
GAACACCCCATCGGGCAGCGCCCGTGTCTGCCGACAACACTACCTGAGCACCCAGTCCGCCCTGAGCAAAGACC
CCAACGAGAAGCGCATCACATGGTCTGTGGAGTTCTGTGACCGCCGCGGGATCACTCTCGGCATGGACGAGCTGTAC
AAGTAAAGCGGCCGACTCTAGATCATAATCAGCCATACCACATTTGTAGAGGTTTACTTGTCTTAAAAAACCTCCCA
CACCTCCCCCTGAACCTGAAACATAAAATGAATGCAATTGTTGTTGTTAACTTGTATTGAGCTTATAATFGGTTACAA
ATAAAGCAATAGCATCACAAATTTACAAATAAAGCATTTTTTTTCACTGCATTCTAGTTGTGGTTTTGTCCAAACTCATCA
ATGTATCTTAAAGCTTATCGATACGGCTACGGCGCCCTAGGAATTGGGGTACGCTCAGAGGCGCCGGTGGAGTGGCGGC
CCTCGGCCGCTCGTACTGTTCCACGATGGTGTAGTCCCTCGTTGTGGGAGGTGATGTCAGCTTGTAGTCCGTTCTGTAG
GCGCCGGCAGCTGCACGGGCTTCTTGGCCATGTAGGTGGTCTTGACCTCGGCGTGTAGTGGCCGCGCTCTCAGCTT
CAGCTCATCTTGTACTCGCCCTCAGGGCGCCGTCGCGGTACATCCGTCGCTGGAGGCTCCAGCCCATGGTCT
TCTTCTGCATTACGGGGCCGTCGGAGGGGAAGTTGGTCCCGCAGCTTACCTTGTAGATGAACTCGCGCTCTGCAGG
GAGGAGTCTGGGTACGGTACCACGCGCCGCTCGAAGTTCATCAGCGCTCCCACTTGAAGCCCTCGGGGAAGGA
CAGCTTCAAGTAGTCGGGGATGTCGGCCGGGTCTTACGTAGGCCCTTGGAGCCGTAAGCTGGAACCTGAGGGACAGGATGT
CCCAGGCAAGGGCAGGGGCGCCCTTGGTCACTTACGTTGGCGGTCTGGGTGCCCTCGTAGGGGCGCCCTCGCC
TCGCCCTCGATCTGAACTCGTGGCCGTTACGAGGCCCTCCATGCGCACCTTGAAGCGCATGAACCTCTTGTAGCAGTC
CTCGGAGGAGGCCATGGTGGCGACCGGTGGATCCCGGGCCGCGGTACCGTCGACTCAGCGGTACCCCGATTGTTTAGC
TTGTTACGCTGCGCTTGTATTGCTTAGCTTTCGTTAGCTTTCGTTAGGACGTTTCACTTGTCTGTTGAAATGAATTTGCTGCT
CCGTAGACGAAGCCCTCTATTTATACTCCGGCGGTGAGGGTTCGAAATCGATAAGCTTGGATCCCTAATTTGAATTTAGCT
CTAATTTGAATTTAGTCTCTAATTTGAATTTAGATCCCGGGCAGCTCGAATTAACCATTTGTGGAAACCGTGCATCAAA
ACGGGAGATACCGAAGTACTGAAAAACAGTCCCTCCAGGCCAGTGGGAACATCGATGTTTTGTTTTGACCGACCCCTTA
CTCTCGTCTCATATAAACCGAAGCCAGCTAAGATGGTATACTTATTATCATCTTGTGATGAGGATGCTTCTATCAACGAA
AGTACCGGTAAACCGCAAATGGTTATGTATTATAATCAAACTAAAGCGGAGTGGACACGCTAGACCAAATGTGTTCTGT
GATGACCTGCAGTAGGAAGACGAATAGGTGGCTATGGCATTATTGTACGGAATGATAAACATTTGCTGCATAAATTTCTT
TTATTATATACAGCCATAATGTCAGTAGCAAGGGAGAAAAGTCCAAAGTCGCAAAAAATTTATGAGAAACCTTTACATG
AGCTGACGTCATGTTTTATGCGTAAGCGTTTTAGAAGCTCTACTTTGAAGAGATATTTGCCGATAAATCTCTAATAT
TTTGCCAAATGAAGTGCCTGGTACATCAGATGACAGTACTGAAGAGCCAGTAATGAAAAACGTACTTACTGTACTTACT
GCCCTCTAAAAAAGGGCAAAGGCAAATGCATCGTGCAAAAATGCAAAAAAGTTATTTGTCGAGAGCATAAATTTGAT
ATGTGCCAAAGTTGTTTCTGACTGACTAATAAGTATAATTTGTTTCTATTATGTATAAGTTAAGCTAATTTACTTATTTTA
TAATACAACATGACTGTTTTTAAAGTACAAAATAAGTTTATTTTTGTAAAAGAGAGAATGTTTAAAAGTTTTGTTACTTT
ATAGAAGAAATTTTGAGTTTTTGTTTTTTTTTAATAAATAAATAAACAATAAATAAATTTGTTTGTGAATTTATTATAGT
ATGTAAGTGAATAATAAAAACCTAATATCTATTCAAATTAATAAATAAACCTCGATATACAGCCGATAAAAACAT
GCGTCAATTTTACGATGATTAATCTTTAACGTACGTCAAAATATGATATATCTTTCTAGGGTAAATAAAGTTTCTAAT
TTTTTATTATTACAGCTGCTGCTGTAATACCGTATATCTCAACGCTGTCTGTGAGATTGTCGATTTCTAGCCTTTTTAG
TTTTTCGCTCATCGACTTGATATTTGTCGACACATTTTCGTCGATTTGCGTTTTGATCAAAGACTTGAGCAGAGACCGT
TAATCAACTGTTCAAATTTGATCCATATTAACGATATCAACCCGATGCGTATATGGTTCGTAATAATATTTTTTAAACCT
CTTATACTTTGACTCTGCGTTAATACGCTTTCGTTACAGACGTAATCATGTTTTCTTTTTTGGATAAAAACCTCTACTG
AGTTTACCTCATATTTAGACCTCACAAAGTTGCAAAAGTGGCATTTTTTTACCAATGAAGAATTTAAAGTTATTTAAAA
AATTTATCATCAGATTTAAAGAAGAACCAAAAATTAATTTATTTCAACAGTTAATCGACCAGTTAATCAACGTGTACAC
AGACGCGTGGCAAAAAACAGCAGCCGACGTTGGCTAAAATTTAATAAACAACCTTGTGTTATAGTCAGCGATTGTC
CGTCCAACGTTTCTCAAAGTTGAAGACCAAAAGTTTACGGACACTATTAATTTATTTGATTTTTGCCCACTTCTATT
TTGTGGGATCACAATTTTGTATATTTTAAACAAAGCTTGGCACTGGCCGTCGTTTTTACAACGTCGTCGACTGGGAAAAC
CTGCGTTTACCCTAATCGCCTTGCAGCACATCCCCCTTTTCGCCAGTGGCGTAATAGCGAAGAGCCCGCACCGAT
CGCCCTTCCCAACAGTTGCGCAGCCTGAATGGCGAATGGCGCTGATGCGGTATTTTCTCCTTACGCATCTGTGCGGTAT
TTCACACCGCATATGGTGCATCTCAGTACAATCTGCTGTGATGCGGCATAGTTAAGCCAGCCCGACCCGCCAACAC
CCGCTGACGCGCCCTGACGGGCTTGTCTGCTCCCGCATCCGCTTACAGACAAGCTGTGACCGCTCTCCGGGAGCTGCATG
TGTGAGGTTTACCCTCATCACCGAAACGCGCAGACGAAAGGGCTCGTGATACGCCATTTTTTATAGGTTAATGT
CATGATAAATAATGGTTTTCTTAGACGTCAGGTGACACTTTTTCGGGAAATGTGCGCGGAACCCCTATTTGTTTTATTTTTCT
AAATACATTTCAAATATGTATCCGCTCATGAGACAATAAACCTGATAAATGCTTCAATAAATAATGAAAAAGGAAGAGTATG
AGTATTTCAACATTTCCGCTGTCGCCCTTATTTCCCTTTTTTGGCGCATTTTGCCTTCTGTTTTTGTCTCACCGAAGACGCT
GGTAAAGTAAAGATGCTGAAGATCAGTTGGGTGCACGAGTGGGTTACATCGAACTGGATCTCAACAGCGGTAAGATCC
TTGAGAGTTTTTCGCCCCGAAGACGTTTTTCCAATGATGAGCACTTTTTAAAGTCTGCTATGTGGCGGATTTATCCCGT
ATTGACGCGGGCAAGAGCAACTCGGTCGCGCATACACTATTCTCAGAATGACTTGGTTGAGTACTCACCAAGTCAAGCA
AAAGCATCTTACGGATGGCATGACAGTAAGAGAAATTAAGCAGTCTGCCATAACCATGAGTGATAAAGTCTGCGGCAACT
TACTTCTGACAACGATCGGAGGACCGAAGGAGCTAACCGCTTTTTGCAACAACATGGGGGATCATGTAACCTGCGCTTGT
CGTTGGGAACCGGAGCTGAATGAAGCCATACCAACGACGAGCGGTGACACCAGATGCCTGTAGCAATGGCAACAACGTT
GCGCAAATTTAACTGGCGAACTACTTACTAGCTTCCCGCAACAATAAATAGACTGGATGGAGGCGGATAAAGTTG
CAGGACCACTTCTGCGCTCGGCCCTTCCGGCTGGCTGGTTTTATGCTGATAAATCTGGAGCCGGTGGAGGTTGGTCTCGC
GGTATCATTTGACGACTGGGGCCAGATGGTAAGCCCTCCCGTATCGTAGTTATCTACAGACGGGAGTCAAGCAACTAT
GGATGAACGAAATAGACAGATCGCTGAGATAGGTGCCCTACTGATTAAGCATTTGGTAACTGTCAGACCAAGTTTACTCAT

ATATACTTTAGATTGATTTAAACTTCATTTTAAATTTAAAAGGATCTAGGTGAAGATCCTTTTGGATAATCTCATGACC
AAAAATCCCTTAACGTGAGTTTTTCGTTCCACTGAGCGTCAGACCCCGTAGAAAAGATCAAAGGATCTTCTTGGATCCTTT
TTTTCTGCGCGTAATCTGCTGCTTGCAAAACAAAAACCACCGCTACCAGCGGTGGTTTGTTTGCCGGATCAAGAGCTAC
CAACTCTTTTTCCGAAGTAACCTGGCTTCAGCAGAGCCAGATACCAATACTGTCTTCTAGTGTAGCCGTAGTTAGGC
CACCCTTCAAGAATCTGTAGCACCGCTACATACCTCGCTCTGCTAATCTGTTACCAGTGGCTGCTGCCAGTGGCGA
TAAGTCGTGCTTACCAGGTTGGACTCAAGACGATAGTTACCAGGATAAGCGCGAGCGGTCCGGCTGAACGGGGGGTFCGT
GCACACAGCCAGCTTGGAGCGAACGACCTACACCGAAGTACGATACCTACAGCGTGAAGAAAGCGCCACGCTT
CCGAAGGGAGAAAAGCGGACAGGTATCCGGTAAGCGGCAGGGTCGGAACAGGAGAGCGCACGAGGGAGCTTCCAGGGGG
AAACGCTTGGTATCTTTATAGTCTGTGCGGTTTCGCCACCTGACTTGAAGCGTGAATTTTGTGATGCTCGTCAGGGG
GGCGGAGCTATGGAAAAACGCCAGCAACCGGCCTTTTTACGGTTCCTGGCCTTTTGTGGCCTTTTGTCCACATGTTT
TTTCTGCGTATCCCTGATTCTGTGGATAACCGTATACCCTTTGAGTGAAGTATACCGCTCGCCGAGCCGGAAC
GACCGAGCGCAGCGAGTCACTGAGCGAGGAAGCGGAAGAGCGCCCAATACGCAAAACCGCTTCCCCGCGGTTGGCCGA
TTCATTAATGCAGTGGCAGCAGGTTTCCGACTGGAAAGCGGCAGTGAAGCGCAACGCAATTAATGTGAGTTAGCTC
ACTCATTAGGCACCCAGGCTTTACACTTATGCTTCCGGCTGTAATGTTGTTGGAAATTTGAGCGGATAACAATTTCA
CACAGAAACAGCTATGACCATGATTACGAATTCGAGCTCGGTACCCGGGATCCTCTAGAGTGCAGCTCGCGGACTT
GGTTTGGCATTCTTAGGCGCGCTCGCTCACACAGCTTGGCCACAATGTGGTTTTTGTCAAACGAAGATTTCTATGACGT
TTTTAAAGTTTAGTTCAGTAAAGCGCAATCTTTTTAAACCTAGAAAAGATAGTCTGCGTAAAAATGACGCATGCATTC
TTGAAATATGCTCTCTTTCTAAATAGCGCGAATCCGTCGTGTGCATTTAGGACATCTCAGTCGCGCTTGGAGCTC
CCGTGAGCGGTGCTTGTCAATGCGGTAAAGTGTCACTGATTTTGAACATAACGACCGGTGAGTCAAAATACGCAATGAT
TATCTTTTACGTGACTTTTAAAGATTTAACTCATAAGATAATTAATTTGTTATTTTCAATGTTTACTTACGTGATACTTAT
TATATATATATTTCTTGTATAGATATCGTGACTAATATATAATAAAATGGGTAGTTCTTTAGACGATGACCATATCCT
CTCTGCTCTTCTGCAAAGCGATGACGAGCTTGTGGTGGAGTCTGACAGTGAATATCAGATCACGTAAGTGAAGATG
ACGTCAGAGCGATACAGAAGAAGCGTTTATAGATGAGGTACATGAAGTGCAGCAACGTCGAAGCGGTAGTGAATATTA
GACGAACAAAATGTTATTTGAACAACAGGTTCTTCAATGGCTTCTAACAGAATCTTGACCTTGCCACAGAGGACTATTAG
AGGTAAAGATAAACATTTGTTGGTCAACTTCAAAGTCCAGGCGTAGCCGAGTCTCTGCACTGAACATTTGTGAGATCTG
TGTGAACGTTGGTTTCAACGCTTCAAAGTGGTGAATTTTGAAGTGCAGACTCTAGATCGCGCTCGCGCGACTGACGGTC
GTAAGCACCCGCTACGTGTCCACCCCGGTCAACAACCCCTTGTGTCAATGTCGGCGACCCCTACGCCCCAACTGAGAGAAC
AATCGCGGAGGAGAAGGAGAACGACTACTCCCGAAAACCGCTTCTGACCTGGGAAAACGTCGAAGCCCGGGGCTCGCT
GAGGGTTGCCGCGGGGCTTCCGTTGTGTCGCTGACTGATCGCATGCAATTTCTATATTTAAAAACACAAATGATACT
TCTAAAAAAAATCATGAATGGCATCAACTCTGAATCAAATCTTTCAGATGCACCTACTTCTCATTTCCTGTCACAT
CATTTTTCCAGATCTCGTGCCTGTTATGTGGCCACAAACCAAGACAGCTTTTATGGCCATTAAGCTGGCTGATCGCT
GCCAAACACAAAATACATAATGAATATGTACACATTCGAGAAAGAGCGATCAAAGAAGCGTCTTCGGGCGGAGTAGGAG
AATCGCGGAGGAGAAGGAGAACGACTGATCTAGTATCTCTCCACAATCCAATGCAACTGACCAACTGGCCATATTTCGGA
GCAATTTGAAGCCAATTTCCATCGCTGGCGATCGCTCCATTTCTGGCTATATGTTTTTACCCTTACCAGGGGCCATTT
TCAAAGACTCGTCGGCAAGATAAGATTGTGCTACTCGTGTCTCTTTCATTGTGCAAGAAATGCTGAGGAATTTCCGCA
TGACGTCCGCGAGTATTTTGAAGAATGAGAATAATTTGTATTTATACGAAAATCAGTTAGTGAATTTTCTACAAAAACA
TGTATCTATAGATAAATTTTGTGCAAAATATGTTGACTATGACAAAGATTTGATGATATACCTTTAATGTATTTCTCAT
TTTTCTATGTATTTATAATGGCAATGATGATACTGATGATATTTTAAAGATGATGCCAGACCAAAAGGCTTGAATTTCTG
GTCTTTTGCCGAACGCAGTGCATGTGCAATTTGTTTTTTTGGAAATATTCAATTTTCCGACTGTCCGCTTTGATTTTCA
TTCCTGGCTTATTTCAAAGCAAGATAAGTAAAGCCAAAAAGCGAGATGGCAATACCAATGCGGCAAAACGGTGTGGAAGG
AAAGGGGTGCGGGGCGAGCGGAAGGAGGGTGGGGCGGGGCTGTCGGGCTGGGCGGCGACTCCAGCGTTG
GAGCCACTCCTTTGACCATGTGTGCGTGTGTGATTAATTCGTGTCTCGCCACTCGCCGTTGTTTTTTCTTTTTATGCT
CGCTCTCTCTAGCCCATCTCGCTTACGCATGCTCAAGCACCAGCATGTTGCCGTTTCTTTTATGCGTATTTTGGCT
CGAAATAGGCAATTAATTAACAAGATTAGTCAACGAAAACGCTAAAAATAAATAAGTCTACAATATGGTTACTTATTG
CATGTGTGTCAGCAACGATAGCAACAAAAGCAACAACACAGGTGGCTTTCCCTCTTTCATTTTTGTTTGAAGCCG
GTGCGAGCAAGACGGCAGCAGCCGCAACGCAATTACGCTGACAAAGAGCAGACGAAGTTTTTGGGCAAAAACATCAAGGC
GCTGATACGAATGCATTTGCAATAACAATTCGATATTTAATATTGTTTATGAAGCTGTTGACTTCAAACACACAAA
AAAAAAAATAAAACAAATTTTGAAGAGAATTAGGAATCGGACGCTTATCGTTAGGGTAACAACAAGAAATGCTTACT
GAGTCAAGCCTCTGGAAACTGCCGCAAGCCAGAGAGAGAGAAAAAGGGGAGAGCAGCTTAGACCGCATGTGCTTG
TGTGTGAGGCGTCTCTCTCTCTGTTGCGCAACGCATAGACTGCACTGAGAAAATCGATTACCTATTTTTTATG
AATGAATATTTGCACTATTAATTAACCTATTAAGATAGCAATCACATTCATAGCCAAATACATACACCTGAGC
GATGCAACGAAATGATCAATTTGAGCAAAAATGCTGCATATTTAGGACGGCATCATTATAGAAATGCTTCTGTGTGTA
CTTTTCTCTGCTGCGAGCTGTTTCCGCTTATTTGTTAAAACCGGCTTAAAGTTAGGTGTGTTTTTCTACGACTAGTGAAT
GCCCTACTAGAAGATGTGTGTTGCACAAAATGTCCTTGAATAACCAATTTGAAGTGCAGATAGCAGTAAACGTAAGCTA
ATATGAATATTAATTAACGTAAATGTTTAAATATCGCTGGACATTAATAAACCCACTATAAACACATGATACATATG
ATGTTTTGGCATAACAATGAGTGTGGGGAAAAAATGTTGTAAGAGCACCCTGACCATCACAGCATAAAGATAACAGCTG
AAGTATCGAATATGATAACCCCAAAATGAATCACATGCGCAACTGATAGGACCCATGGAAGTACTCTTCATGGCGG
ATATACAAGACACACACAGCAGCAACCCAGTTGCGGAGGAAATTTCTCGTAAATGAAAACCAATCGCGCAACAAT
CATACCATATATGGTAAAGTTTTGAACGCGACTTGAAGCGGAGAGCATTTGCGGTGATAAGGTTTTAGCGCTAAGCG
GGTTTTATAAAACGGGCTGCGGGACAGTTTTTCAATCACTACCGTTTTGAGTCTTGTGTGTGGATACTCTCCCG

ACACAAAGCCGCTCCATCAGCCAGCAGTCGTCTAATCCAGAGACCCGGATCCAGATAGATCTCAACGGTACCGCCACC
TCGAGTGTTCATTTGTGTTTTTGTCTTTGAAATGAGCGGTTGTCTCGCGCGTCGATCGCAGTTTCAAATCGGTGTGGCT
CCGCAGCTTCGTTGTAAGTCGACAATAAAGCGATCGAAGTGAAGAAAATACGTTTTGCGATCTTTTTATTATAAATAA
TTGCCAGAAAGTACAAGTTCACAACGAAATACCATCGAAAAGTGCCTTTTTACAAAAGTCGTTGGTAACACACATACC
AACGCAGCGAACCGAACACACGCACACAATGCGCGCGCTTGGCGGTGTGCGTGTAAACACTTTTTTACCTGGTCTTAC
CTGTTTGGCGGTGCGAAAGAGAGAGGGCAACAGAAACGAGAAAGAGAGTGCCTAACGCGGACGAGTGAAGATAAAGTGA
ACGAAAATATCAGCCAGAGCAGCTGCACCGAAATCGGAATAAGTCAGTTAACAATCAGGGCGCGCACTGTACGAGTTCGA
TTCGATTGATAATTTAGCGGTTGCCATGAAAATGCAGTCCAACAACCGGTACTGAGAGAAAACGAAACAAGAAGA
AGAGTGCAAAATAGAATAGAATAAAAAAGAAGTGGAAAGTAGAAGTGGCAACACAAAACAAAAGTAAAAGGTGTGTGAGTGA
AATAATACTGGGTGATTCACGAAGAAGTGCTCAAAGTGTGCGGTTGAAAAAAGAGAGTCTGCGATGGCGGATCGCCG
CTAGAGAGTATGTCCACCAGTGTCCAGCGAATGCCAGAAGTACCCTGCATCAATATGTGCGCGACCCCGCAGGCCGG
CCACCTAAATCCCGCCAGCAACAGACGCCAGCAGCACAAGCGAAAATGCGCGCACTTGGCAGGCGACTAATCCCCG
CGAGACTCCTCTGGGCGTTATCGTGGCCATCAGCCTTCTGTACCCGCGCTCGCACTTCACTCGCCGCGGACAAAAAC
TTTTCCGGCGACAATCGTAAGCCCGCCTTCAAAAACTCGCGCGGATACGCTCCTAAGGTCAAAGAGGAGCAGCCCGAAAA
CACCTACGTTCTCACCGTAGAGCCGTCGACCCTGATCCCGACCAGGTCATTCGATACAGCATCGTCCAGTCGCGGTTCCG
AGCGACCCAAAGTTCTTATCAATCCCAGCACGGCGTAATCTTACCACCCACACATTCGATCGTGACGAGCCGATCCAC
GAGAAGTTCGCTTTCGTACCCGTCAGGCCACGGATAATGGTCTGCCCCACTGGACGACGTTTGCACCTTCAACGTTAC
CATCGAGGACATCAACGACAATGCACCCGCTTCAACAAGGCGCGCTACGACGAATCCATGTGCGAAAATGCCAGCCCG
ACGCGGTGTTGATGACTATCAGCGCCAGTGAATTCGACGATGGCAACAACAGTTTGGTCAATACGAGATTCCTGCGGGAG
CGGACTTTCACTTCAAGATTGACAAGGAGTCGGTATTATCTACTGAAACGACCGATTGACAAGAGACCCGGCCA
ATCGTATGCGATAATCGTGCGGGCATATAACGTAGTGCAGATCCGCCACAGGATGCACAAATCGAAGTGCAGCATCCGGG
TGGTGGAGTCTCAATTAAGCCGCATCATTTTTCATCATTCGATCATCGTATGCCTCGCGCTACTGTGATCATCCTG
TTGGCAGTGGTGGTGCAGAAAAGCAGAAGAATGGCTGGCACGAAAAGGACATCGACGACATTCGCGAGACGATCATTA
TTACGAGGACGAGGTGGCGGCGAGCGGGACACGGACTATGATCTGAATGTCTGCGCACCCAGCCCTTCTACGAGGAGA
AGCTGTACAAGATCCTCATGCGTTACAGGGGAACATGCGCGACCCCAACGACATACCCGACATCGCCGACTTCTGGGC
GACAAGAAGGAGAACTGCGACCCGGATGTGGCGCCACAACCGTGGACGATGTG

PiggyBac hs-mCD8::GFP 3xP3-DsRed



Annotations

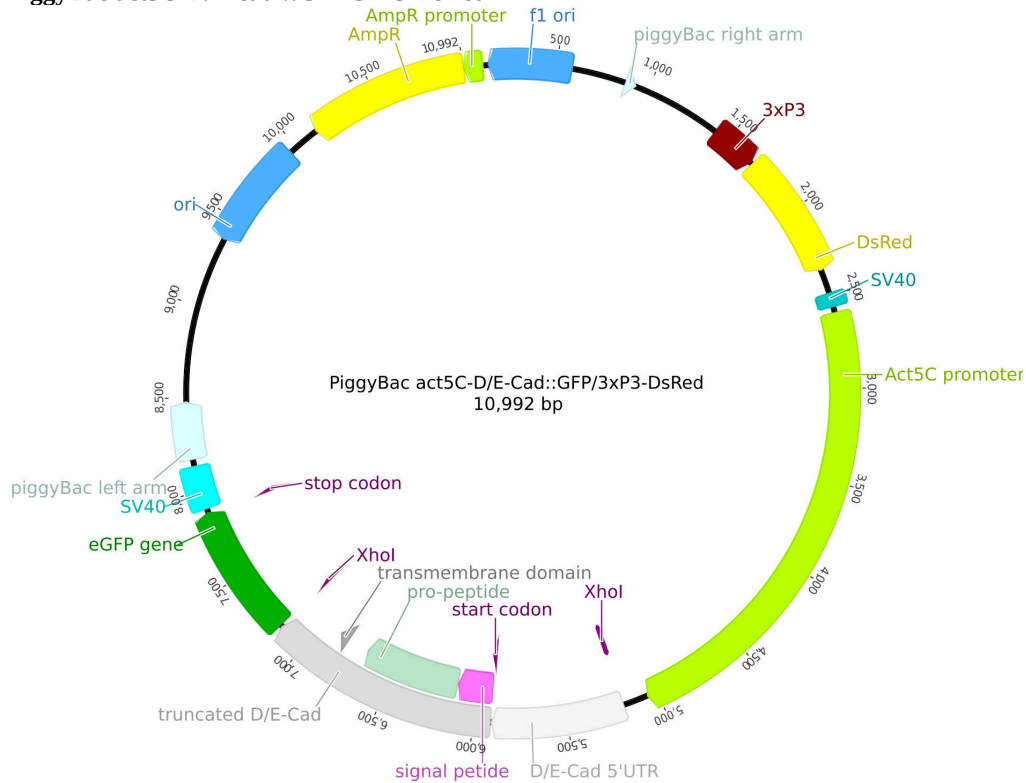
Annotations	Position (bp)
PiggyBac right arm	8485 - 8547
3xP3	1 - 255
DsRed	266 - 946
hs promoter	1549 - 1787
mCD8	1863 - 2528
GFP	2535 - 3251
PiggyBac left arm	5065 - 5099

Sequence

TAATTCGAGCTCGCCCGGGATCTAATTCAATTAGAGACTAATTCAATTAGAGCTAATTCAATTAGGATCCAAGCTTATC
GATTTCTGAACCTCGACCGCCGAGTATAAATAGAGCGCTTCGTCTACGGAGCGACAATTCAATTCAAAACAGCAAAGT
GAACACGTCGCTAAGCGAAAGCTAAGCAAATAAACAAGCGCAGCTGAACAAGCTAAACAATCGGGGTACCGCTAGAGTCCG
ACGGTACGATCCACCGGTCCGACCACATGGTGCCTCCCTCAAGAACGTCATCAAGGAGTTTCAAGTGCCTTCAAGTGC
TGGAGGGCACCGTGAACGGCCACGAGTTTCGAGATCGAGGGCAGGGCCGAGGGCCGCCCTACGAGGGCCACAACACCGTG
AAGCTGAAGGTGACCAAGGGCGGCCCTGCCCTTCGCTGGGACATCCTGTCCCCCAGTTCCAGTACGGCTCCAAGGT
GTACGTGAAGCACCCCGCGACATCCCGGACTACAAGAAGCTGTCCCTCCCGAGGGCTTCAAGTGGGAGCGCGTATGA
ACTTCGAGGACGGCGCGTGGTACCGTGACCCAGGACTCCTCCCTGCAGGACGGCTGTTCATCTACAAGTGAAGTTC
ATCGCGTGAACCTTCCCTCCGACGGCCCGTAAATGCAGAAGAAGACCATGGGCTGGGAGGCTCCACCGAGCGCTGT
CCCCCGCAGCGCGTGTGAAGGGCGAGATCCACAAGGCCCTGAAGCTGAAGGACGGCGCCACTACCTGGTGGAGTTCA
AGTCCATCTACATGGCCAAAGAAGCCCGTGCAGCTGCCCGCTACTACTACGTGGACTCCAAGCTGGACATCACCTCCAC
AACGAGGACTACACCATCGTGGAGCAGTACGAGCGCACCGAGGGCCGCCACCACCTGTTCCTGTAGCGGGCGGACTCTA
GATCATAATCAGCCATACCACATTTGTAGAGGTTTACTTGTCTTAAAAAACCTCCACACCTCCCCCTGAACCTGAAAC
ATAAAATGAATGC AATTTGTTGTTAACTTGTATTATGTCAGCTTATAATGGTTACAAATAAAGCAATAGCATCACAAT
TTCACAAATAAAGCATTTTTTTTCACTGCACCGGTTACGGCACTAGAGCGGCCGCCACCAGCGGTACAGTGTCACTGGGTC
GTGGGTAATCGCTTATCCTCGGATAAACAATTATCCTACGGGTAATCGCTTATCCGCTCGGGTAATCGCTTATCCTCGG
GTAATCGCTTATCCTTGGGTAATCGCTTATCCTCGGATAAACAATTATCCTCAGGGTAATCGCTTATCCGCTCGGGTAA
TCGCTTATCCTCGGGTAATCGCTTATCCTTGGGTAATCGCTTATCCTCGGATAAACAATTATCCTCAGGGTAATCGCTT
ATCCGCTCGGGTAATCGCTTATCCTCGGGTAATCGCTTATCCTTTCAGTTGGGACTCAGTGAAGGAGACCTGAATTCCT
GCAGCCGAGCGGAGACTCTAGCGAGCGCCGAGTATAAATAGAGCGCTTCGTCTACGGAGCGACAATTCAATTCAAAAC
AAGCAAAGTGAACCGTCCGTAAGCGAAAGCTAAGCAAATAAACAAGCGCAGCTGAACAAGTAAACAATCTGCAGTAAA
GTAAAGTTAAAGTGAATCAATTAAGAATAAACAGCAACAGTAAATCAACTGCAACTACTGAAATCTGCCAAGAAGTA
ATTATGAATACAAGAAGAGAAGTCTGAATAGGAATTTGGGAATTCGTTAACAGATCGGGGATCAATTCGTTAACAGAT
CTGGGGCCCGGGTTCGAGCAAAATGGCCTCACCGTTGACCCGCTTTCTGTGCTGAACTGTGTGCTGGGTGAGTTCGA
TTATCCTGGGGAGTGGAGAAGCTAAGCCACAGGACCCGAACCTCGAATCTTTCCAAAGAAAATGGACGCCGAACCTGGT
CAGAAGTGGACCTGGTATGTGAAGTGTGGGGTCCGTTTCGCAAGGATGCTTTGGCTCTTCCAGAACTCCAGCTCCAA
ACTCCCCAGCCACCTTCGTTGCTATATGGCTTCACTCCCAACAAGATAACGTGGGACGAGAAGCTGAATTCGTCGA
AAGTGTTCCTGCCATGAGGGACACGAATAATAAGTACGTTCTCACCTGAACAAGTTCAGCAAGGAAAACGAAGGCTAC
TATTTCTGCTCAGTCATCAGCAACTCGGTGATGACTTCAGTTCTGTGCTGCCAGTCTTCAGAAAGTGAATCTACTAC
TACCAAGCCAGTGTGCGAACTCCCTCACCTGTGCACCTACCGGACATCTCAGCCCCAGAGACCAGAAGATTGTCGGC
CCCGTGGCTCAGTGAAGGGACCGGATTGGACTTCGCTGTGATATTTACATCTGGGCACCCTTGGCGGAACTCGCTG
GCCCTTCTGCTGTCTTGTATCATCTCATCTGTACCACAGCCGCGGATCCATGAGTAAAGGAGAAGAACTTTTCAC
TGGAGTTGTCCCAATCTTGTGTAATTAGATGGTGTATTAATGGGCACAAATTTCTGTGCTAGTGGAGAGGGTGAAGGTG
ATGCAACATACGGAAAACCTTACCTTAAATTTATTTGCACTACTGAAAACTACCTGTTCATGGCCAACTTTGCACT
ACTTTAATTTATGGTGTCAATGCTTTTCAAGATACCCAGATCATATGAAACAGCATGACTTTTCAAGAGTGCCATGCC
CGAAGGTTATGTCCAGGAAAGAACTATATTTTTCAAAGATGACGGGAACATAAAGACACAGTGTGAAGTCAAGTTTGAAG
GTGATACCTTGTTAATAGAATCGAGTTAAAAGGTATTGATTTTAAAGAAGATGGAAACATCTTGGACACAAATTTGGAA
TACAATAAATCACTACACAATGTATACATCATGCGAGACAAACAAAAGAAATGGAATCAAAGTTAACTTCAAATTTAGACA
CAACATTTAAGATGGAAGCGTTCAACTAGCAGACCATATCAACAAAATACTCCAATTTGGCGATGGCCCTGTCTTTTAC
CAGACAACCATTACCTGTCCACACAATCTGCCCTTTCGAAAGATCCCAACGAAAAGAGAGACCACATGGTCTCTTTGAG
TTTGTAACTACTGATCTAATTTGTTGTGATTTTATGATTTCCAACCTATGGAATGATGAATGGGAGCAGTGGTGGGA
ATGCCTTTAATGAGGAAAACCTGTTTTGCTCAGAAGAAATGCCATCTAGTGTGATGAGGCTACTGCTGACTCTCAACAT
TCTACTCTCCAAAAAAGAGAGAAGGTAGAAGACCCCAAGGACTTTCTTCAGAAATGCTAAGTTTTTTGAGTCAATGC
TGTGTTTGTAAATAGAATCTTTGCTTGTCTTTGCTATTTTACCAACCAAGGAAAAGCTGCACTGCTATACAGAAAATTA
TGGAAAAATTTTGTATAGTGTGCTTACTAGAGATCATAATCAGCCATACCACATTTGTAGAGGTTTTACTTGTCTTT

TGTATATCGAGGTTTATTTATTAATTTGAATAGATATTAAGTTTTATTATATTTACACTTACATACTAATAATAAATTC
 ACAAACAATTTATTTATGTTTATTTATTTATTTAAAAAACAACAACTCAAATTTCTTCTATAAAGTAACAAAACTTTT
 ATCGAATTCCTGCAGCCCGGGGATCCACTAGTTCAGTGTCCACAATGGTTAATTCGAGCTCGCCCGGGGATCTAAT
 TCAATTAGAGACTAATTC AATTAGAGCTAATTC AATTAGGATCCAAGCTTATCGATTTCGAACCTCGACC GCGGAGTA
 TAAATAGAGGCGCTTCGTCTACGGAGCGACAATTC AATTC AACAAGCAAAGTGAACACGTCGCTAAGCGAAAGCTAAGC
 AAATAACAAGCGCAGCTGAACAAGCTAACAATCGGGGTACCGCTAGAGTCGACGGTACGATCCA

PiggyBac act5C-D/E-cad ::GFP 3xP3-DsRed



Annotations

Annotations	Position (bp)
PiggyBac right arm	874 - 936
3xP3	1416 - 1670
DsRed	1681 - 2361
act5C promoter	2590 - 5057
D/E-cad 5' UTR	5186 - 5910
truncated D/E-cad	5911 - 7156
GFP	7162 - 7881
PiggyBac left arm	8172 - 8480

Sequence

ACTCTTCCTTTTTCAATATATTGAAGCATTATCAGGGTTATTGTCTCATGAGCGGATACATATTTGAATGTATTTAGA
 AAAATAACAATAGGGGTTCCGCGCACATTTCCCGAAAAGTGCCACCTAAATTGTAAGCGTTAATTTTTGTTAAAAAT
 TC GCGTTAAATTTTTGTTAAATCAGCTCATTTTTAACAATAGGCCGAAAATCGGC AAAATCCCTTATAAATCAAAGAA
 TAGACCGAGATAGGGTTGAGTGTGTTCCAGTTTGGAAACAAGAGTCCACTATTAAAGAACGTGGACTCCAACGTCAAAGG
 GCGAAAACCGTCTATCAGGGCGATGGCCACTACGTGAACCATCACCTAATCAAGTTTTTTGGGGTCGAGGTGCCGTA

AAGCTAAATCGAACCTAAAGGGAGCCCCGATTTAGAGCTTGACGGGAAAGCCGGCAACGTGGCGAGAAAGGAA
GGGAAGAAAGCGAAAGGAGCGGGCGCTAGGGCGCTGGCAAGTGTAGCGGTACGCTGCGCGTAACACCACACCCGCGC
GTTAATGCGCCGTACAGGGCGCGTCCCATTCGCCATTCAGGCTGCGCAACTGTTGGGAAGGGCGATCGGTGCGGGCCT
CTTCGCTATTACGCCAGCTGGCGAAAGGGGATGTGCTGCAAGGCGATTAAGTTGGGTAACGCCAGGGTTTTCCAGTCA
CGACGTTGTAACGACGGCCAGTGAGCGCGCTCGTTCATTCACGTTTTTGAACCCGTGGAGGACGGGCGAGCTCGCGG
TGCAATATGTTTTACAGCGTGTAGGAGCAGATGAAGATGCTCGACAGCTGCAGAACCGCAGCTAGATTAACCCTAGA
AAGATAATCATATGTGACGTACGTTAAAGATAATCATGTGTAATAATGACGCATGTGTTTTATCGGTCTGTATATCGAG
GTTTTATTATTAATTTGAATAGATATTAAGTTTTATTATATTACACTTACATAATAATAAATTCACAAACAATTT
ATTTATGTTTTATTATTTATTAATAAAAAACAAAACTCAAAATTTCTTATATAAAGTAACAAAACTTTTATCGAATTCCT
GCAGCCCGGGGATCCACTAGTTCTAGTGTCCACAAATGGTTAATTCGAGCTCGCCCGGGGATCTAATTCAAATAGAGA
CTAATTCAAATAGAGCTAATTCAAATAGGATCCAAGCTTATCGATTTCGAACCCCTCGACCGCGGAGTATAAATAGAGG
GCTTCGCTACGGAGCGCAATTCAAATCAACAAGCAAAGTGAACACGTCGCTAAGCGAAAGCTAAGCAATAAACAAG
CGCAGCTGAACAAGCTAAACAATCGGGTACCCTAGAGTCGACGGTACGATCCATAATTCGAGCTCGCCCGGGGCTA
ATTCAAATAGAGCTAATTCAAATAGAGCTAATTCAAATAGGATCCAAGCTTATCGATTTCAAGCCCTCGACCGCGGAG
TATAAATAGAGGCGCTTCGCTACGGAGCGCAATTCAAATCAACAAGCAAAGTGAACACGTCGCTAAGCGAAAGCTAA
GCAATAAACAAGCGCAGCTGAACAAGCTAAACAATCGGGTACCCTAGAGTCGACGGTACGATCCACCGTCCGCCACC
ATGGTGCCTCCTCAAGAAGCTCATCAAGGAGTTCATGCGCTTCAAGGTGCGCATGGAGGGCACCCTGAACGGCCACGA
GATTCGAGATCGAGGGCGAGGGCGGGCCCGCTACGAGGGCCACAACCCGTGAAGCTGAAGGTGACCAAGGGCGGCC
CCCTGCGCTTCGCTGGGACATCCTGTCCCCCAGTTCCAGTACGGCTCAAGGTGTACGTGAAGCACCCTCGCCGACATC
CCCGACTACAAGAAGCTGTCTTCCCCGAGGGCTTCAAGTGGGAGCGCGTGAACCTTCGAGGACGGCGGCTGGTGAC
CGTACCCAGGACTCCTCCTGCAGGACGGCTGCTTCATCTACAAGTGAAGTTCATCGGCTGAACCTCCTCCCTCCGACG
GCCCCGTAATGCAGAAGAAGCATTGGGCTGGGAGGCTCCACCGAGCGCTGTACCCCGCGCAGGGCTGTGAAGGGC
GATTCACAAGGCCCTGAAGCTGAAGGACGGCGGCCACTCCTGGTGGAGTTCAGTCCATCTACATGGCCAAAGAGCC
CGTGCAGCTGCCCGGCTACTACTACGTGGACTCCAAGCTGGACATCACTCCACAACGAGGACTACACCATCGTGGAGC
AGTACGAGCGCACCAGGGCCGCCACCACCTGTCTGTAGCGGGCGGACTCTAGATCATAATCAGCCATACCACATTT
GTAGAGTTTTACTGTCTTAAAAACCTCCACACCTCCCCCTGAACCTGAAACATAAAATGAATGCAATTTGTTGTTGT
TACTTGTTTATTCGAGCTTATAATGGTTACAAATAAAGCAATAGCATCACAAATTCACAAATAAAGCATTTTTTCAC
TGCAACCGTTACGGCACFAGAGCGGCCCGCAATTCATATTCTAAAAACACAATGATACTTCTAAAAAAAATCATGA
ATGGCATCAACTCTGAATCAAACTTTGCGAGATGCACCTACTTCTCATTTTCCACTGTACATCATTTTTCCAGATCTCGC
TGCTGTTATGTGGCCACAACAAGACAGCTTTTATGGCCATTAAGCTGGTGTATCGTCCGCAACACCAATACAT
AATGAATATGTACACATTCGAGAAAGAAGCGATCAAGAAGCGTCTTCGGCGGAGTAGGAGAATGCGGAGGAGAAGGAG
AACGAGCTGATCTAGTATCTCCACAATCCAATGCCAATGACCACTGGCCATATTCGGAGCAATTTGAAGCCAAATTT
CCATCGCCCTGGCGCATCGTCCATTCCTTGGCTATATGTTTTTACCCTTACCCTGGGGCCATTTTCAAGACTCGTCCGCA
GATAAGATTGTGTCACTCGCTGTCTCTCTCATTTGTGCGAAGAATGCTGAGGAATTTGCGGATGACGTGCGGAGTATTT
TGAAGAATGAGAATAATTTGTATTTATACGAAAATCAGTTAGTGGAAATTTTACAAAACATGTTATCTATAGATAATT
TTGTGCAAAATATGTTGACTATGACAAAAGTTGTATGTATATACCTTTAATGTATTTCTCATTTTTCTTATGTATTTATA
TGGCAATGATGATACTGATGATATTTAAGATGATGCCAGACAAAAGGCTTGAATTTCTGCGCTTTTTGCGCAACGCAG
TGCAATGTCATTTGTTTTTGGAAATATTCATTTTCGAGCTGTCCGCTTGTGATTTTCAATTTTCAATTTTCAAAA
AGCAAAGTAAAGCCAAAAGCGAGATGGCAATACCAATGCGGCAAAAAGGCTAGTGAAGGAAAGGGGTGCGGGCAGC
GGAAGGAAAGGGTGGGGCGGGGCTGGCGGGGTCTGTGCTGGGCGGACGTCACCGAGTTGGAGCCACTCCTTTGACCA
TGTGTGCGTGTGTATTTATTCGTGTCTCGCCACTCGCCGTTGTTTTTTCTTTTTATGCTGCGCTCTCTCTAGCGCCA
TCTCGTTACGCATGCTCAACGCACCGCATGTTGCCGTTTCTTTTATGCGTCAATTTGGCTCGAAATAGGCAATATTT
AAACAAAGATTAGTCAACGAAAACGCTAAAATAAATAAGTCTACAATATGGTACTTATGGCATGTGTGTCAGCAAC
GATAGCAACAAAAGCAACAACACAGGTGGCTTCCCTCTTCACTTTTTGTTTGAAGCCGCTGCGAGCAAGACGGCAC
GACCGCAACGCATTTACGCTGACAAAGAGCAGACGAGTTTTGGCGAAAACATCAAGCGCCTGATACGAATGCATT
TGCAATAACAATTCGATATTTAATATGTTTTATGAAGCTGTTTGTACTTCAAAACACACAAAAAAAATAAAACAAAT
TATTTGAAAGAGAATTAGGAATCGGACGCTTATCGTTAGGTAACAACAAGAAATGCTTACTGAGTCACAGCCTCGGAA
AATGCGCGCAAGCCAGAGAGAGAGAGAAAAAGGGGAGAGACGCTTAGACCCCATGTGCTTGTGTGAGGCGCTCTCT
CTTCGCTCTGTGTCGCAACGCATAGACTGCCTGAAAAATCGATTACCTATTTTTTATGAATGAATATTTGCACTAT
TACTATTCAAAATATTAAGATAGCAATCACATTCATAGCCAAATCTATACCACCTGAGCGATGCAACGAAATGATCA
ATTTGAGCAAAAATGCTGCATATTTAGGACGGCATCATATAGAAAATGCTTCTGTGTGTACTTTTTCTCTGCTGTCGCA
GCTGTTTTGCGGTTATTTGTTAAACCGGCTTAAAGTTAGGTGTGTTTTCTACGACTAGTGAATGCCCTACTAGAAGATGTG
TGTGTCACAAAATGTCCTGGAATAACCAATTTGAAGTGCAGATAGCAGTAAACGTAAGCTAATATGAATATATTTAAC
TGTAATGTTTTAATATCGCTGGACATTACTAATAAACCCACTATAAACACATGTACATATGTATGTTTTGGCATACAATG
AGTAGTTGGGGAATAATGTGTAAGACCCGTGACCATCACAGCATAAAGATAACCGCTGAAGTATCGAATATAGATA
ACCCCAAAATGAATCACATGCCGCAACTGATAGGACCCATGGAAGTACACTCTTCAATGGCGATATACAAGACACACACA
AGCACGAACCCAGTTGCGGAGGAAATTTCTCGTAATGAAAACCAATCGGCGAACAATTCATACCAATATATGTTAA
AAGTTTTGAACGCGACTTGAGAGCGGAGAGCATTGCGGCTGATAAGGTTTTAGCGCTAAGCGGGCTTTATAAACCGGCT
CGGGACAGTTTTCATATCACTACCGTTTGTGTTCTGTGCTGTGGATACTCTCCCGACACAAGCCGCTCCATCA
GCCAGAGTCGTCTAATCCAGAGACCCCGGATCCAGATAGATCTCAACGGTACCGCCACCCTCGAGTGTGTCATTGTTT

TTTGCTTTTGAATTGAGCGGTTGTCTCGCGCGTGCATCGCAGTTTCAAATCGGTGTGGCTCCGCAGCTTCGTTGTAAGT
CGACAATAAAGCGATCGAAGTGAAAGAAAATACGTTTTTGCATCTTTTTATTTAAATAATTCGCCAGAAAGTACAAGT
TCACAACGAAATACCATCGAAAAGTGCCTTTTTACCAAAAGTCGTTGGTAACACACATACCAACGCAGCGAACCGAAACCA
CACGCACACAAATGAGCGCGCTTGGCGGTGTGCGTGTAAACCACTTTTTTACCTGGTCTTACCTGTTTGCCTGCGAAAGA
GAGGAGGCAACAGAAACGGAGAAAGAGAGTGCCCAAGCGGACGAGTAAAGATAAAAAGTGAACGAAAATATCAGCCAGAG
CAGTGCACCGAAATCGGAATAAGTCAGTTAAACAATCAGGGCGCGACTGTACGAGTTCGATCTATTTGATAAATTATTGA
GCGGTTGCCATGAAAATGCAGTCCAAACAAACCGTACACTGAGAGAAAACGAAAACAAGAAGAAGAGTGCAAAATAGAATAGA
ATAAAAAGAAGTGAAGTAGAAGTGGCAACACAACAAAAGTAAAAGGTGTGTGAGTGAATAAATACTGGGTGATTCA
CGAAGAAGTGCTCAAAAAGTGTTCGCGTTGAAAAAAGAGAGTCTGCGATGGCGGATCGCCGCTAGAGAGATGTCCACCA
GTGTCCAGCGAATGTCCAGAAGCTACCCTGCATCAATATGTGCGGACCCCGCAGGCGGCGCACCTAAATCCCGCCAG
CAACAGACGCACCAGCAGCACAAGCGAAAATGCGCGACCTTGGCAGGCGACTAATCCCGCGAGACTCCTCCTGGGCGT
TATCGTGGCCATCAGCCTTCTGTACCCCGCCCTCGCACTTCACTCGCCGCGGACAAAACTTTTCCGGCGACAATCGTA
AGCCCGCTTCAAAAACCTGCGCCGATACGCTCCTAAGTCAAAGAGGAGCAGCCGAAAACACTACGTTCTCACCGTA
GAGCCCGTCGACCCTGATCCCGACCAGGTCATTCGATACAGCATCGTCCAGTCGCGCTTCGAGCGACCAAGTTCTTTAT
CAATCCAGCAGGGCGTAATCTTACCACCCACACATTCGATCGTGACGAGCGGATCCACGAGAAGTTCGTTCTCGTCA
CCGTCAGGCCACGGATAATGGTCTGCCCCACTGGAGCAGCTTTGCACCTTCAACGTTACCATCGAGGACATCAACGAC
AATGACCCCGCTTCAACAAGGCGCGCTACGACGAATCCATGTCCGAAAATGCCAGCCGACGCGGTGGTGTACTAT
CAGCGCAGTGCAGTTCGACGATGGCAACAACAGTTTGGTCAATAACGAGATTCGCGGGAGCGCGACTTTCAGTACTTCA
AGATTGACAAAGGATCGGGTATTATCTACCTGAAAACCGGATTTGACAAGAGACCCGCAATCGTATGCGATAATCGTG
CGGGCATATAACGTAGTGCAGATCCGCCACAGGATGCACAAATCGAAGTGCAGTCCGGGTGGTGGAGTCTCAATTA
GCCGCCATCATTTTTTCATCATTGCGATCATCGTATGCCTCGCGCTACTGCTGATCATCTCTGTTGGCAGTGGTGGTGCAGA
AAAAGCAGAAGAATGGCTGGCAGAAAAGGACATCGACGACATTCGCGAGACGATCATAAATACGAGGACGAGGGTGGC
GGCAGCGGGACCGGACTATGATCTGAATGTCTGCGCACCCAGCCCTTCTACGAGGAGAAGCTGTACAAGATCTCA
TGCGTTACAGGGAAATGCGCGACCCCAACGACATACCCGACATCGCCGACTTCTGCGGACAAAGAAGGAGAAGTGGC
ACCGGGATGTGGGCGCCACAACCGTGGACGATGTGCTCGAGATGGTGAGCAAGGGCAGGAGCTGTTACCCGGGTGGT
CCATCCTGGTTCGAGTGGACGGCAGCTAAACGGCCACAAGTTCAGCGTGTCCGGCGAGGGCGAGGGCGATGCCACCTA
CGGCAAGCTGACCTGAAGTTCATCTGCACCACCGGCAAGCTGCCCGTGCCTGGCCACCCCTCGTGACCACCCCTGACCT
ACGCGTGCAGTGTTCAGCCGCTACCCCGACACATGAAGCAGCAGCAGTTCCTTCAAGTCCGCCATGCCCGAAGCTAC
GTCCAGGAGCGCACCATCTTCTCAAGGACGACGGCAACTACAAGACCCGCGCGAGGTGAAGTTCGAGGGCGACACCT
GGTGAACCGCATCGAGTGAAGGGCATCGACTTCAAGGAGGACGGCAACATCCTGGGGCACAGCTGGAGTACAACATACA
ACAGCCACAACTGCTATATCATGGCCGACAAGCAGAAGAACGGCATCAAGGTGAACCTCAAGATCCGCCACAACATCGAG
GACGGCAGCGTGCAGTCCGCGACCACTACCAGCAGAACCCCCATCGCGGACGGCCCGTGTGCTGCCCGACAACCA
CTACCTGAGCACCCAGTCCGCCCTGAGCAAAAGACCCCAACGAGAAGCGCGATCACATGGTCTGCTGGAGTTCGTTACCG
CCGCGGGATCACTCTCGGCATGGACGAGCTGTACAAGTAAAGCGGCGGACTCTAGATCATAATCAGCCATACCACAT
TTGTAGAGTTTTACTTGTCTTAAAAAACCCTCCACACCTCCCCCTGAACCTGAAACATAAAATGAATGCAATTGTGTGTT
GTTAACTTTGTTTATGTCAGCTTATAATGGTTACAATAAAGCAATAGCATCACAAATTTCAAAAATAAAGCATTTTTTTT
ACTGCATCTAGTTGTGGTTTGTCCAAACTCATCAATGTATCTTATCATGTCTGGATCAGATCTCTCGAGGTCGACGGTA
TCGATAAGCTTGTATCTATAACAAGAAAATATATATAAATAAGTTATCACGTAAGTAGAACATGAAATAACAATATAA
TTATCGTATGAGTTAAATCTTAAAAGTCAGTAAAAGATAATCATGCGTCATTTTGACTCACGGGTGCTTATAGTTCAA
AATCAGTGCACCTTACCGCATTGACAAGCAGCGCTCAGGGAGCTCCAAGCGCGACTGAGATGTCTAAATGACAGCG
ACGGATTCCGCTATTTAGAAAAGAGAGCAATATTTCAAGAATGCATGCGTCAATTTTACGCGACTATCTTTCTAGGG
TTAATCTAGCTGCATCAGGATCATATCGTCCGGTCTTTTTCCCGCTCAGTCATCGCCCAAGCTGGCGCTATCTGGGCAT
CGGGGAGGAAGAAGCCCGTCCCTTTTTCCCGGAGGTTGAAGCGGCATGGAAAAGAGTTTCCGAGGATGACTGCTGTGCA
TTGACGTTGAGCGAAAACGCACGTTTACCATGATGATTCGGGAAGGTGTGGCCATGCACGCTTTAACGGTGAACGTTC
GTTACGGCCACCTGGGATACCAGTTCGTCGCGGCTTTTCCGGACACAGTTCGGATGGTCAGCCGAAAGCGCATCAGCAA
CCCGAACAATACGGCGACAGCCGAACTGCCGTGCCGGTGTGCAGATTAATGACAGCGGTGCGGGCTGGGATATTACG
TCAGCGAGGACGGGTATCTGGCTGGATGCCGAGAAATGGACATGGATACCCCGTGAAGTACCAGCGGGCGCGCTTGG
CGTAATCATGGTCAATAGCTGTTTTCTGTGTGAAATGTTATCCGCTCACAAATTCACACAACATACGAGCCGGAAGCATA
AAGTGAAGCCTGGGCTGCTAATGAGTGAAGTAACTCACATTAATTCGCTTGGCTCACGCGCTTTCCAGTCCGG
AAACCTGTGCTGCAGCTGCATTAATGAATCGGCCAACGCGGGGAGAGCGGTTTGCCTATTGGCGCTCTTCCGCTT
CCTCGCTCACTGACTCGCTGCGCTCGGTCTGGCTGCGGCGAGCGGTATCAGTCACTCAAAGCGGTAATACGGTTA
TCCACAGAATCAGGGGATAACGCAGGAAAGAACATGTGAGCAAAAGCCAGCAAAAGCCAGGAACCGTAAAAAGCGCC
GTTGCTGGCGTTTTTCCATAGGCTCCGCCCCCTGACGAGCATCACAAAAATCGACGCTCAAGTCAGAGGTGGCGAAACC
CGACAGGACTATAAAGATAACAGGCGTTTCCCCCTGGAAGCTCCCTCGTGCCTCTCTGTCCGACCCCTGCCGTTACC
GGATACCTGTCCGCTTTCTCCCTTCGGGAAGCGTGGCGCTTCTCATAGCTCACGCTGTAGGTATCTCAGTTCCGTGTA
GGTCGTTCCGCTCAAGCTGGGCTGTGTGCAGAACCCCGCTTACGCCCAGCGCTGCGCTTATCCGGTAACATATCGCT
TTAGTCCAAACCGGTAAAGACAGCACTTATCGCCACTGGCAGCAGCCACTGTTAACAGGATTAGCAGGAGGATGTA
GGCGGTGCTACAGAGTTCTGAAGTGGTGGCTAACTACGGTACACTAGAAGAACAGTATTTGGTATCTGCGCTCTGCT
GAAGCCAGTACCTTCGGA AAAAGAGTTGGTAGCTCTTGATCCGGCAAAACAACCCGCTGGTAGCGGTGGTTTTTTG
TTTGAAGCAGCAGATTACCGCGA AAAAAGGATCTCAAGAAGATCCTTTGATCTTTTCTACGGGGTCTGACGCTCA

GTGGAACGAAAACACGTTAAGGGATTTTGGTCATGAGATTATCAAAAAGGATCTTCACCTAGATCCTTTTAAATTAAA
AATGAAGTTTAAATCAATCTAAAGTATATATGAGTAAACTTGGTCTGACAGTTACCAATGCTTAATCAGTGAGGCACCT
ATCTCAGCGATCTGTCTATTTTCGTTTCATCCATAGTTGCCTGACTCCCCGTCGTGTAGATAACTACGATACGGGAGGGCTT
ACCACTGCGCCCCAGTGCATGCAATGATACCGCGAGACCCACGCTCACCGGCTCCAGATTTATCAGCAATAAACCAGCCAG
CCGGAAGGGCCGAGCGCAGAAGTGGTCTGCAACTTTATCCGCCTCCATCCAGTCTATTAATTGTTGCCGGGAAGCTAGA
GTAAGTAGTTCGCCAGTTAATAGTTTGCGCAACGTTGTTGCCATTGCTACAGGCATCGTGGTGTACGCTCGTCTGTTGG
TATGGCTTCATTCAGCTCCGGTTCCCAACGATCAAGGCGAGTTACATGATCCCCATGTTGTGCAAAAAAGCGGTTAGCT
CCTTCGGTCCCTCCGATCGTTGTCAGAAGTAAGTTGGCCGAGTGTATCACTCATGGTTATGGCAGCACTGCATAAATCT
CTTACTGTATGCCATCCGTAAGATGCTTTTCTGTGACTGGTGAGTACTCAACCAAGTCATCTGAGAATAGTGTATGCCG
GCGACCGAGTTGCTCTTGCCCGGCGTCAATACGGGATAATACCGGCCACATAGCAGAACTTTAAAAGTGCATCATTTG
GAAAACGTTCTTCGGGGCGAAAACCTCAAGGATCTTACCGCTGTTGAGATCCAGTTCGATGTAACCCACTCGTGCACCC
AACTGATCTTCAGCATCTTTTACTTTTACCAGCGTTTCTGGGTGAGCAAAAACAGGAAGGCAAAATGCCGCAAAAAAGGG
AATAAGGGCGACACGGAATGTTGAATACTCAT

9 **Abstract**

10 **Introduction:** Male genitalia are thought to ensure transfer of sperm through direct physical contact
11 with female during copulation. However, little attention has been given to their pre-copulatory role
12 with respect to sexual selection and sexual conflict. Males of the fruitfly *Drosophila pachea* have a
13 pair of asymmetric external genital lobes, which are primary sexual structures and stabilize the
14 copulatory complex of female and male genitalia.

15 **Results:** We tested for a pre-copulatory role of these lobes with a *D. pachea* stock where males
16 have variable lobe lengths. In 92 mate competition trials with a single female and two males,
17 females preferentially engaged into a first copulation with males that had a longer left lobe and that
18 displayed increased courtship vigor. In 53 additional trials with both males having partially
19 amputated left lobes of different lengths, we observed a weaker and non-significant effect of left
20 lobe length on copulation success. Courtship durations significantly increased with female age and
21 when two males courted the female simultaneously, compared to trials with only one courting male.

22 **Conclusion:** Left lobe length affects the chance of a male to engage into copulation. The
23 morphology of this primary sexual trait may affect reproductive success by mediating courtship
24 signals or by facilitating the establishment of genital contacts at the onset of copulation.

25 keywords: *Drosophila pachea*, primary sexual trait, mating behaviour, mate-competition
26 experiments, genitalia

27 **Introduction**

28 Males and females exhibit different reproduction strategies due to higher energy costs of
29 larger female gametes compared to smaller and more abundant male gametes [1]. This implies
30 male-male intrasexual mate-competition for siring the limited female gametes. In turn, females may
31 optimize reproduction by choosing males that confer survival and fecundity benefits to her and to
32 the offspring. This dynamics has been formalized into genetic models [2, 3] involving female
33 preferences for particular male characters and male mate competition, and can contribute to the
34 rapid evolution of female preferences and male sexual attributes. There is also evidence for male
35 mate-choice and female intra-sexual selection [4–6], showing that traditional sex-roles can change
36 between species and in individuals under diverse conditions. In general, sexual selection implies a
37 sexual conflict whenever male and female reproductive fitness strategies differ [7].

38 Across animals with internal fertilization, genitalia are usually the most rapidly evolving
39 organs [8]. Several hypotheses propose that the evolution of genitalia is based on sexual selection
40 and a consequence of sexual conflict between males and females at different levels of reproduction,
41 including competition of sperm from different males inside the female (sperm competition) [9],
42 female controlled storage and usage of sperm to fertilize eggs (cryptic female choice) [8, 10, 11], or
43 sexually antagonistic co-evolution of aggressive and defensive morphologies and/or behaviors
44 between male and female to control fertilization decisions [12, 13]. Male courtship is well known as
45 a behaviour to attract females before copulation begins, but has also been reported to occur during
46 or even after copulation [14, 15]. It is thought to be a widespread and key aspect of copulation in
47 the cryptic female choice scenario, where males stimulate the female to utilize his own sperm [8,
48 10]. A variety of insect species were reported where males had evolved elaborated male genital
49 structures that are apparently used for courtship throughout copulation to stimulate the female
50 through tapping or other physical stimuli [14, 15].

51 Traditionally, sexual traits are categorized as primary or secondary. Genital structures are
52 considered “primary” when they are directly used for the transfer of gametes during copulation or
53 when they contribute to the complexing of female and male copulatory organs [8, 16]. Other traits
54 that differ between sexes and that are linked to reproduction are considered “secondary” sexual
55 traits. For primary sexual traits, sexual selection is traditionally thought to act during or after
56 copulation [8, 15], while secondary sexual traits can be involved in pre-copulatory mate-choice via
57 visual, auditory or chemical long range signalling [17–25].

58 Primary genitalia could also be possibly involved in pre-copulatory mate choice. Supposing
59 that a particular male genital trait enhances or favours female fecundity, it might become preferred
60 by the female during pre-copulatory courtship or at the moment of genitalia coupling [26–28]. This
61 preference could rely on direct benefits to reduce energy investment or predation risk caused by
62 unsuccessful copulation attempts, or on indirect male genetic quality to be inherited into the
63 offspring generation. Several examples of primary genitalia used in pre-copulatory courtship
64 signalling are known in vertebrates. For example, male and female genital display, swelling, or
65 coloration changes are associated with sexual activity [29–31] and penile display was also observed
66 in lizards [32]. Human male penis size was found to influence male attractiveness to women [33]. In
67 diverse mammalian species, females have also evolved external and visible structures that resemble
68 male genitals, a phenomenon called andromimicry [31, 34, 35]. These structures are likely used in
69 visual signaling, so it is possible that the male analogous parts also do. Furthermore, females of
70 some live-bearing fish species were reported to prefer to mate with males with large gonopodia [36,
71 37]. These cases involve visual stimuli and large genital organs. Only a few studies examined the
72 roles of primary genitalia in invertebrates during courtship or at the onset of copulation before
73 phallus intromission is achieved [26–28, 38, 39]. Longer male external genitalia of the water strider
74 *Aquarius remigis* were associated with higher mating success [28]. In addition, male genital spine
75 morphology of *Drosophila bipectinata* and *Drosophila ananassae* were reported to evolve in

76 response to direct competition among males for securing mates in a so called ‘scramble
77 competition’ scenario [26, 27]. In general, the role of primary sexual traits in establishing
78 copulation or their role during courtship needs further investigation.

79 The fruitfly species *Drosophila pachea* is a promising model to study the evolution of
80 primary sexual traits, especially with respect to the evolution of left-right asymmetry. Male *D.*
81 *pachea* have an asymmetric aedeagus (intromission organ) and a pair of asymmetric external lobes
82 with the left lobe being approximately 1.5 times longer than the right lobe [40–42] (Figure 1). The
83 genital lobes have likely evolved during the past 3-6 Ma and are not found in closely related species
84 [43]. *D. pachea* couples also mate in a right-sided copulation position where the male rests on top
85 of the female abdomen with the antero-posterior midline shifted about 6-8 degrees to the right side
86 of the female midline [41, 42, 44]. Male and female genitalia form an asymmetric complex during
87 copulation and the asymmetric lobes stabilize this genital complex [44]. Furthermore, *D. pachea* is
88 among the *Drosophila* species that produce the longest (giant) sperm [45, 46], and their ejaculates
89 contain in average just about 40 sperm cells [47]. Thus, a particular right-sided mating position
90 could potentially be associated with optimal transfer of giant sperm during copulation [42].

91 The aim of this study was to test if the asymmetric genital lobes of *D. pachea* would have an
92 effect on pre-copulatory mate-choice, in addition to their role in stabilizing the complex of male and
93 female genitalia during copulation. Previously, we found that males originating from one of our *D.*
94 *pachea* laboratory stocks possess short and rather symmetric lobes [41] (Figure 1), while others
95 have the typical size asymmetry. The variability in left genital lobe length that we observed within
96 this fly stock enabled us to test if lobe length might affect pre-copulatory courtship or mate
97 competition. We selected *D. pachea* males with short left lobes and produced a stock with an
98 increased variance of left lobe length. Next, we tested sibling males of this “selection stock” in
99 mate-competition assays for their success to engage first into copulation with a single female. We
100 also tested whether copulation success in our assay would be affected by male courtship vigour.

101 Then, we surgically shortened the length of the left lobe in males that had developed long left lobes,
102 to further test whether left lobe length affects copulation success. Finally, we assessed whether lobe
103 length affects ejaculate allocation into female storage organs.

104 **Results**

105 **Genital lobe lengths differ between *D. pachea* stocks**

106 In our laboratory stock 15090-1698.01, *D. pachea* males display a characteristic left-right
107 size asymmetry of genital lobes with the left lobe being consistently larger than the right lobe
108 (Figure 1A,C, Figure 2 A, Table S4, Additional datafile 3). Similarly, in stock 15090-1698.02, most
109 males reveal larger left lobes, but a few individuals are observed with particularly small lobes that
110 are rather symmetric in length (Figure 1B-D, Figure 2B). We selected for males with short lobe
111 lengths and crossed them with sibling females for 50 generations (Material and Methods). The
112 resulting stock was named “selection stock”. We observed an increased variance of left lobe length
113 compared to the source stock (Levene’s test: selection stock / 15090-1698.02: $DF = 1/147$, $F =$
114 11.506 , $P = 0.0008913$) (Figure 2C, Additional datafile 3). In contrast, the right lobe length differed
115 only marginally among the two stocks (Table S4) and the variances of right lobe lengths were not
116 significantly different among them (Levene’s test, $DF = 1/147$, $F = 0.5164$, $P = 0.4735$).

117 **Male genital left lobe length, male courtship and failed copulation attempts have an effect on** 118 **copulation success**

119 We performed a mate competition assay (Material and Methods) with two males and a
120 single female to test if differences in genital lobe length and courtship behavior may influence the
121 chance of a male to copulate first with a single female. This first engagement into copulation will be
122 referred to as “copulation success”. We filmed courtship and copulation behavior of two males of
123 the selection stock and a single female of stock 15090-1698.01 or 15090-1698.02. We annotated

124 111 trials where both males simultaneously courted the female (Material and Methods) (51 and 60
125 trials with females of stocks 15090-1698.01 or 15090-1698.02, respectively). In particular, we
126 waited for a first copulation to occur, then isolated the non-copulating male and finally the other
127 two specimen once the first copulation had ended. Then, we dissected the genitalia of both males to
128 determine lobe lengths. We examined 54 additional trials with two courting males from the
129 selection stock that had partially amputated left lobes and females of stock 15090-1698.01. This
130 was done to test if other characters might co-vary with left lobe length and could potentially also
131 have an effect on copulation success. We shortened the left lobes of both males in order to be able to
132 neglect possible effects of the caused wound. The relative courtship activity or vigor of the two
133 males in each trial was compared by quantifying periods that each male spent touching the female
134 ovipositor or the ground next to it with the proboscis (mouth-parts), hereafter referred to as “licking
135 behavior” (Material and Methods). We counted the sum duration of these periods (sum licking
136 duration) and the number of licking periods (number of licking sequences). A copulation was
137 considered to take place, once a male had mounted the female abdomen and achieved to settle into
138 an invariant copulation position (Material and Methods).

139 In the majority of trials (130/165), the first mounting attempt of a male resulted in a stable
140 copulation. We did not observe any male behavior that could indicate an attempt of the non-
141 copulating male to directly usurp the female as observed for *D. ananassae* or *D. bipectinata* [26,
142 27]. However, in 35 trials, a total of 51 failed mounting attempts were observed (Material and
143 Methods). These were not proportionally higher among trials with lobe amputated males (9 failed
144 mounting attempts in 7 / 54 trials 13%) compared to unmodified males (42 failed mounting
145 attempts in 28 / 111 trials 25%). Thus, the partial lobe amputation probably did not decrease the
146 ability of a male to mount a female. Only 15/51 failed mounting attempts lasted 8 seconds or longer.
147 Among those, the non-mounted male continued to court the female in 10/15 attempts. However, this
148 was also observed in 131/165 successful mounting attempts and these proportions are not

149 significantly different (χ^2 -test, $\chi^2 : 1.4852$, $df = 1$, $P = 0.2230$). Altogether, mounting failure was not
150 found to be significantly associated with the courtship activity of the other male.

151 Different variables were tested to have an effect on male copulation success by using a
152 Bradley Terry Model [48] (Material and Methods). In trials with unmodified males, copulation
153 success was positively associated with left lobe length and the sum licking duration of the males
154 during courtship (Table 1). The effect of sum licking duration is illustrated when comparing the
155 ratio of sum licking duration and total courtship duration between the copulating and the non-
156 copulating male (Figure 3A). This ratio was higher in the copulating male compared to the non-
157 copulating male. Copulation success was negatively associated with the number of licking
158 sequences and with the number of failed mounting attempts (Table 1). In particular, we identified a
159 positive interaction of failed mounting attempts and female age, indicating that the negative effect
160 of failed mounting attempts is pronounced in young females but not in older females. However, this
161 difference turned out to be based on three outlier observations when comparing the number of failed
162 mounting attempts of either male over female age (Additional datafile 1, Figure S5). Therefore,
163 more observations are required to evaluate this interaction and the effect of failed mounting
164 attempts on copulation success.

165 In trials with males that underwent lobe surgery, left lobe length was not significantly
166 associated with copulation success (Table 2), although a similar positive effect was detected. Thus,
167 we cannot exclude the possibility that left lobe length co-varies with yet another unknown selected
168 trait that reveals an advantage for the male to copulate. Similarly, a non-significant negative effect
169 of the number of licking events on copulation success was observed with those males (Table 2) but
170 a positive significant effect of sum licking duration.

171 **Courtship duration is increased when two males court a female simultaneously**

172 Regardless of the stock for the female used, courtship durations appeared to be longer when

173 both males courted the female simultaneously compared to trials where only one male courted
174 (Mann-Whitney-Wilcoxon test, $W = 1906.5$, $N = 48/165$, $P = 4.7 \times 10^{-8}$) (Figure 3B). We also
175 observed that courtship duration was strikingly increased in females that were older than 11 days
176 (after emerging from the pupa) compared to younger females (Additional datafile 1: Figure S4)
177 (Mann-Whitney test, $W = 660$, females younger than 12 days / females 12 days or older = 33 / 132,
178 $P = 6.333 \times 10^{-10}$). Thus, older females may be less likely to copulate and may also discriminate less
179 between males based on failed mounting attempts (see above).

180 **Lobe length is not associated with the amount of ejaculate in female sperm storage organs**

181 To test whether lobe length influences the amount of ejaculate deposited into the female
182 after copulation, we dissected a random subset of females (54 of stock 15090-1698.01 and 24 of
183 stock 15090-1698.02) in trials with non-modified lobes that revealed a copulation. Neither right
184 lobe length, left lobe length, sum licking duration or female age (days after emerging from the
185 pupa) was significantly associated with ejaculate content in the spermathecae (Table 3). However,
186 male adult age and copulation duration had a negative effect. Given that *D. pachea* males become
187 fertile about 13 d after emerging from the pupa [49], our results indicate an optimal period of male
188 ejaculate transfer at the beginning of their reproductive period. Copulation duration had a negative
189 effect on sperm transfer (Table 3), indicating that failed sperm transfer may result in prolonged
190 attempts and longer copulation duration.

191

192 **Discussion**

193 **Left lobe length affects the chance of a male to copulate**

194 We observed a tendency of females to copulate first with the male that had the longer left
195 lobe when two males courted simultaneously in our trials. These results suggest that a long left lobe
196 might not only stabilize an asymmetric genital complex during copulation [44], but also increases
197 the chance of a male to engage into copulation. With our data, we cannot exclude that the sensing of
198 the lobe length by the female occurs just before intromission, while male and female genitalia are
199 contacting each other or if it is used even during courtship before genital contacts establish. Other
200 factors, unrelated to lobe length, can also bias copulation. For example, females might prefer to
201 copulate with males of larger body size or that display particular courtship behaviors. In our study,
202 we found no significant effect of tibia length on copulation success, which was used as an
203 approximation for overall body size. However, the mutation(s) associated with lobe length variation
204 in this stock are unknown. It is possible that one or several alleles associated with lobe length still
205 segregate in this stock, even after 50 generations of inbreeding. If such segregating mutations have
206 pleiotropic effects on other male characters (morphological, physiological or behavioural), these
207 traits are expected to co-vary together with lobe length and the effect of lobe length that we detected
208 might actually be due to the other factors. In trials with artificially introduced lobe length variation
209 (through surgery), males were taken from the selection stock but had the expected wild-type lobe
210 asymmetry. Left lobe length difference was then artificially introduced in those males, so that it
211 would not be expected to co-vary with the relative phenotypic expression of the supposed
212 underlying mutation. In such trials, we observed a trend of the left lobe length being associated with
213 copulation success, but this trend was not significant. Thus, we cannot completely rule out the
214 possibility that left lobe length affects copulation success indirectly via a pleiotropic mutation
215 affecting both, lobe length and other traits.

216 **Male intra-sexual competition is potentially reflected by male courtship intensity**

217 Previous analyses in *D. ananassae* and *D. bipectinata* relate male genital spines to pre-
218 copulatory abilities to achieve a copulation due to increased male intrasexual competitiveness in so
219 called “scramble competition” or vigorous copulation attempts with females that are optionally
220 already copulating with another male [26, 27]. In *D. pachea*, this behavior was not observed and
221 most mounting events of a male resulted in a stable copulation. Once a copulation started, the non-
222 copulating male was never observed to separate the couple. Instead, it continued to display
223 courtship behaviors such as licking, wing vibration or touching the female side in the majority of
224 cases. In addition, male mounting was only observed upon female wing opening and oviscapit
225 protrusion. This indicates that mounting in *D. pachea* is a complex behavior involving both sex
226 partners. Upon mounting, the chance of a *D. pachea* male to engage into copulation thus may
227 largely depend on male-female communication rather than on male-male competition.

228 Total courtship durations were increased in trials where both males courted the female
229 simultaneously compared to trials with only one male courting. This indicates that females
230 potentially require more time to accept one of the males for copulation in cases where two males
231 court simultaneously. Alternatively, longer courtship durations might indeed rely on male-male
232 competition, causing mutual disturbances in courtship display. We detected a strong association of
233 copulation success with the sum licking duration, which we used as an approximation for overall
234 courtship activity or vigor of each male. We also observed a negative effect of the number of licking
235 sequences on copulation success, indicating that a male has highest chances to copulate if he
236 continuously presents licking behavior at the female abdomen for a prolonged time period. This is
237 achieved by maintaining its position close to the female oviscape in competition with the other
238 male, suggesting that licking behavior in part reports male-intrasexual conflict.

239

240 **Potential female benefits gained from choosing males with long left lobes**

241 Female mate choice on male sexual traits was suggested to rely at least in part on the way a
242 sexual trait is displayed or moved [50]. This implies that a certain quantity but also accuracy of
243 locomotor activity would matter in courtship and might better reflect overall male quality and “truth
244 in advertising” than a morphological character or ornament alone. Our data suggest that male
245 settling upon mounting the female might be crucial for a successful copulation since we identified a
246 negative effect of failed mounting attempts on copulation success and a positive interaction of failed
247 mounting attempts with female age, possibly indicating that young females are more discriminative
248 compared to older females with respect to male mounting performance. Female mate choice is
249 hypothesized to be based on direct benefits, affecting fecundity and survival of the female, but also
250 on indirect benefits that relate to genetic quality, fecundity and survival of the progeny [50, 51].
251 Left lobe length and male mounting performance might therefore influence female mate-choice
252 through enhancing the quality of male courtship signals and by enhancing the coupling efficiency of
253 male and female genitalia upon mounting.

254 Alternatively, left lobe length might potentially associate with direct copulation benefits for
255 male and female by ensuring the efficiency of ejaculate transfer during copulation. Males of *D.*
256 *pachea* produce giant sperm and previous estimates revealed that a *D. pachea* male transmits only
257 about 44 ± 6 sperm cells per copulation [47], while the maximum female sperm storage capacity in
258 the spermathecae was estimated to be much higher and to be about 304 sperm cells [47]. Wild-
259 caught *D. pachea* females were found to contain sperm from at least 3-4 males based on
260 spermathecae filling levels [47]. As asymmetric lobes stabilize the genital complex [44], they might
261 have a positive effect on the amount of sperm transferred per copulation. However, we have not
262 observed any effect of lobe length on ejaculate presence in the spermathecae after copulation. We
263 note that our quantification method was not precise and that sample size was limited. Accurate
264 direct sperm counts requires radio-labeling methods [47], which was not applicable in our

265 experimental setup. In future approaches, improved sperm counts should be applied to test for a
266 correlation between lobe length, female-male copulation complex stability and sperm quantity in
267 female spermathecae. Based on our data, we note that left lobe length affects the chance of a male
268 to establish genital contacts that lead to a firm complex of female and male genitalia, congruent
269 with previous observations in other insects [26–28, 52]. In particular, the male genital spines in *D.*
270 *ananassae* and *D. bipectinata* were observed to play a role in pre-copulatory events but had no
271 measurable influence later on with respect to sperm transfer or fecundity [26, 27, 52].

272 Interestingly, copulation duration negatively affected ejaculate presence in the female. This
273 observation suggests that the couple separates once successful sperm transfer is achieved. However,
274 not all copulations reveal sperm transfer. In occasions of failure the copulation duration may
275 therefore be prolonged to further attempt to mate. Copulation duration varies largely among
276 *Drosophila* species from fractions of a minute to up to about 2 h in *D. acanthoptera* [42, 49].
277 Copulation duration in *D. pachea* is thus comparatively long with respect to other species of the
278 genus, pointing to presumably complex copulatory interactions affecting sperm transfer. Future
279 studies must analyze the internal processes of sperm transfer during *D. pachea* copulation to better
280 understand this process and its possible limitations.

281 Indirect paternal effects on the growth and survival of offspring could potentially play a role
282 in *D. pachea* female choice for males with long left lobes. It has been demonstrated that mate
283 choice based on particular male sexual characters correlates with offspring survival in diverse
284 species [18, 20–23, 53]. However, our experiment did not allow us to test for these effects because
285 females were sacrificed after the mating experiment and no progeny was obtained. We assessed
286 ejaculate filling levels instead of the amount of female progeny because *D. pachea* females rarely
287 lay eggs after a single insemination and about four copulations are necessary for a female to start
288 oviposition [54]. To test for indirect effects, future studies should ideally use progeny males from
289 wild caught *D. pachea* females and test if subtle lobe length variation in those males would

290 correlate with offspring survival in single couple crosses. A similar approach was used by Hoikkala
291 et al. (1998) [53], who found that *Drosophila montana* courtship song frequency of wild caught
292 males correlated with the survival rate of the male's progeny.

293 **Age of reproductive activities appear to be non-overlapping in sibling males and females**

294 The amount of ejaculate present in the female spermathecae after a single copulation was
295 negatively affected by the age of the copulating male. Similarly, it was previously found that the
296 number of progeny in single couple crosses (presumably involving multiple copulations) was also
297 dependent on male adult age in *D. pachea* [55]. Males in *D. pachea* need about 10-14 days at 25° C
298 after emergence to become sexually mature [49, 54, 55]. This is related to adult testis growth and
299 production of giant sperm [47]. It was shown that the relatively long time to reach male sexual
300 maturity impacts the proportion of sexually active *D. pachea* adults (operational sex ratio), which is
301 female-biased [49]. Our findings suggest that males potentially have a maximum fertility period at
302 the beginning of their sexual maturity at approximately 13-16 days after emerging from the pupa.
303 The detected reduction of transferred ejaculate in males older than 16 days implies an additional
304 male reproductive limitation.

305 It was hypothesized that the delay in male sexual maturity might potentially lead to
306 decreased sibling mating in *D. pachea* [54]. In *D. melanogaster*, sibling matings yield fewer
307 progeny compared to crosses with unrelated individuals [55]. In our study, the female was not a
308 sibling of the two males. Courtship durations were shortest in trials with “young” virgin females,
309 between 6 and 11 days. Given that females reach sexual maturity at about 4 days after emerging
310 from the pupa [49, 55], our observation suggests that young females engage more quickly into
311 copulation compared to older females. Overall, female and male maximum reproductive activities
312 appear to be non-overlapping among siblings of opposite sex and similar age. Such an effect can be
313 relevant in the wild if a cactus rot is colonized by a single previously fertilized female.

314 **Conclusion**

315 Longer male left genital lobes potentially enhance the probability of *D. pachea* males to
316 engage into copulation, which is expected to confer a reproductive advantage over males with
317 shorter left lobes. The chance of a male to copulate first with a female was also affected by the
318 relative male courtship activity and potentially by mounting attempt failures, especially for females
319 at the beginning of their reproductive activity. The evolution of left lobe length might not only
320 relate to its previously known function as a stabilizing device during copulation, but also through
321 pre-copulatory mate choice by increasing the chances to copulate and to increase the coupling
322 efficiency of genitalia upon mounting. Lobes do not appear to impact sperm transfer in later
323 copulatory events. In addition, reproductive ages are non-overlapping between the two sexes
324 potentially decreasing the amount of sibling mating in this species.

325 **Material and Methods**

326 **Fly stock establishment and maintenance**

327 Two *D. pachea* stocks 15090-1698.01 and 15090-1698.02 were retrieved from the San
328 Diego Drosophila Species Stock Center (now The National Drosophila Species Stock Center,
329 College of Agriculture and Life Science, Cornell University, USA) (Additional datafile 1: Table
330 S1). Flies were maintained in 25 x 95 mm plastic vials containing 10 mL of standard Drosophila
331 medium (60 g/L brewer's yeast, 66.6 g/L cornmeal, 8.6 g/L agar, 5 g/L methyl-4-hydroxybenzoate
332 and 2.5% v/v ethanol) and a ~ 10 x 50 mm piece of bench protection sheet (Bench guard). As *D.*
333 *pachea* requires 7-dehydrocholesterol for proper development [56–58], we mixed the medium of
334 each vial with 40 µL of 5 mg/mL 7-dehydrocholesterol, dissolved in ethanol (standard *D. pachea*
335 food). Flies were kept at 25°C inside incubators (Velp) with a self-made light installation for a 12 h
336 light: 12h dark photo-periodic cycle combined with a 30-min linear illumination change between

337 light (1080 lumen) and dark (0 lumen). We used males of stock 15090-1698.02 to generate a new
338 stock with increased proportions of males with short genital lobes. For this, we chose 3 males with
339 apparently symmetric (aberrant) genital lobes and crossed them with 3-4 sibling virgin females. We
340 repeated the selection with the progeny for a total of 36 generations. Then, we discarded males with
341 clearly visible asymmetric (wild-type) lobes from the progeny for another 14 generations to derive
342 the final stock (selection stock).

343 **Virgin fly selection**

344 Virgin flies at 0-1 d after emerging from the pupa were CO₂ anaesthetised on a CO₂-pad
345 (INJECT+MATIC Sleeper) under a stereo-microscope Stemi 2000 (Zeiss), separated according to
346 sex and maintained in groups of 20-30 individuals. Males and females were raised until reaching
347 sexual maturity, about 14 days for males and 4 days for females at 25° C [49]. This allowed us to
348 use virgin individuals in each mating experiment. Males were anaesthetised on the CO₂ pad (see
349 above), sorted according to lobe morphology (asymmetric and symmetric lobes) and isolated into
350 single vials at least two days before each mating experiment took place.

351 **Mate-competition assay**

352 We used a single virgin female of wild-type stock 15090-1698.01 or 15090-1698.02 and two
353 sibling males of the selection stock that visually differed in lobe length when inspected with a
354 binocular microscope (Additional datafile 1: Figure S1). This selection was done to increase the
355 average pairwise difference of lobe lengths between the two males. Specimens were introduced into
356 a white, cylindrical mating cell (Additional datafile 1: Figure S2) with a diameter of 20 mm, a depth
357 of 4 mm and a transparent 1 mm Plexiglas top-cover. Optionally, mating cells were concave with a
358 diameter of 20 mm and a depth of 4 mm at the center (Additional datafile 2: trials 1-16). Flies were
359 transferred without CO₂ anaesthesia using a fly aspirator: a 7 mm diameter silicone tube closed at
360 the tip with cotton and a 1000 µL wide bore (3 mm) micro-tip. Movie recordings were started as

361 soon as the chamber was immediately put under the camera (see below).

362 All mating trials were carried out inside a temperature and humidity controlled climate
363 chamber at $25^{\circ}\text{C} \pm 0.1^{\circ}\text{C}$ and $80\% \pm 5\%$ or $60\% \pm 5\%$ (trials 1-15) humidity. We used digital
364 cameras MIRA ZOOM MZ902 (OWL) or DigiMicro Profi (DNT) to record copulation and
365 courtship behaviour. The MIRA ZOOM MZ902 (OWL) camera was mounted on a modified
366 microscope stand (191348, Conrad) equipped with a 8-cm LED white light illumination ring (EB-
367 AE-COB-Cover, YM E-Bright) and a platform to hold four individual cylindrical mating cells
368 (Additional datafile 1: Figure S2). Experiment 16 was filmed with the OWL camera and a concave
369 shaped mating cell that was put on a flat plastic cover on top of the microscope stand. For trials 1-
370 15, we used concave shaped mating cells that were put onto the stand of the DigiMicro Profi (DNT)
371 camera. Data was acquired with the programs Cheese (version 3.18.1)
372 (<https://wiki.gnome.org/Apps/Cheese>) or GUVVIEW (version 0.9.9) GTK UVC (trials 1-15) on
373 an ubuntu linux operating system in webm or mkv format. Up to four trials were recorded in a
374 single movie, which was split after recording and converted into mp4 format with Avidemux 2.6
375 (<http://www.avidemux.org/>) to obtain a single movie per experiment.

376 We waited for a copulation to take place between one of the males and the female (see
377 below). The mating cell was then shortly recovered from the climate chamber in order to remove
378 the non-copulating male with an aspirator and to transfer it into a 2-mL reaction tube filled with
379 70% ethanol. This was performed after the copulating male appeared to have settled into a stable
380 mating posture on the female abdomen, which was controlled by live-imaging. The copulating male
381 and the female were isolated from the mating cell after copulation had ended and were also isolated
382 into single 2-mL reaction tubes filled with 70% ethanol. Optionally, the female was kept alive for
383 12-24 h in a vial containing 5-10 mL grape juice agar (24 gr/L agar, 26 gr/L sucrose, 120 mg/L
384 Tegosept, 20% $\%_v$ grape juice, and 1.5% $\%_v$ ethanol). The presence of eggs on the plate was
385 systematically checked but never observed. Females were finally sacrificed to prepare

386 spermathecae.

387 **Left lobe surgery**

388 Epandrial lobe surgery was done on 5-6 day-old *D. pachea* adult males of the selection stock
389 following Rhebergen et al. (2016). Males were anaesthetised on a CO₂ pad (see above) and then
390 further immobilized with a small copper wire, which was slightly pressed onto the male abdomen.
391 The left epandrial lobe was shortened to various lengths with micro dissection scissors (SuperFine
392 Vannas Scissors, World Precision Instruments). Flies were let to recover for at least 7 days on
393 standard *D. pachea* food at 25° C in groups. No mortality was observed in males that underwent
394 lobe surgery, similar to what was observed by Rhebergen et al. (2016). Partially amputated lobes
395 ranged in length from lacking at least their most distal tip to more reduced stumps whose length
396 approximated the corresponding right lobe.

397 **Adult dissection and imaging**

398 Adults were dissected in water with forceps (Forceps Dumont #5, Fine Science Tool) inside
399 a transparent 25 mm round dissection dish under a stereo-microscope (Zeiss Stemi 2000). Male
400 genitalia were isolated by piercing the abdomen with the forceps between the genital arch and the
401 A6 abdominal segment and thereby separating the genitalia from the abdomen. We also dissected
402 the left anterior leg of each dissected male. Female spermathecae were recovered after opening the
403 ventral abdomen with forceps and removal of the gut and ovaries. The spermathecae were isolated
404 and separated according to left and right sides and immediately examined using a microscope (see
405 below). All dissected tissues were stored in 200 µL storage solution (glycerol:acetate:ethanol, 1:1:3)
406 at 4° C.

407 For imaging, male genitalia were transferred into a dissection dish filled with pure glycerol
408 and examined with a VHX2000 (Keyence) microscope equipped with a 100-1000x VH-Z100W
409 (Keyence) zoom objective at 300-400 fold magnification. Genitalia were oriented to be visible in

410 posterior view. The left and right lateral spines, as well as the dorsal edge of the genital arch were
411 aligned to be visible in the same focal plane. In some preparations, the genital arch broke and lobes
412 were aligned without adjusting the position of the dorsal genital arch. The experiment was
413 discarded from analysis in cases where lobes could not be aligned. Male lobe lengths were
414 measured on acquired images as the distance between the base of each lateral spine and the tip of
415 each lobe (Figure 1c,d) using ImageJ version 1.50d (<https://imagej.nih.gov/ij>). Male legs were put
416 on a flat glycerol surface with the inner side of the tibia facing to the camera. Legs were imaged at
417 200 fold magnification with the VHX 2000 microscope (Keyence) as described above.

418 We prepared the female paired sperm storage organs (spermathecae) at 12 h - 24 h after
419 copulation (54 females from stock 15090-1698.01 and 24 females from stock 15090-1698.02,
420 additional file 2) and examined the presence of ejaculate. *D. pachea* has giant sperm [47], which
421 makes direct sperm counts difficult. Therefore, we determined an apparent average spermathecae
422 filling level per female based on visual inspection, similar to Jefferson (1977) [55]. Female
423 spermathecae were arranged on the bottom of the transparent plastic dissection dish, filled with
424 water. Images were acquired using transmission light in lateral view with the Keyence VHX2000
425 microscope at 400-500 fold magnification. Ejaculate was directly visible inside the transparent
426 spermathecae. Ejaculate filling levels were annotated for each spermatheca separately to match
427 three different categories: 0, 1/6 or 1/3 of its total volume. Then, the average filling level for both
428 spermathecae was calculated for each female.

429 **Annotation of courtship and copulation behaviour**

430 Videos were analysed with the OpenShot Video Editor software, version 1.4.3
431 (<https://www.openshot.org>) to annotate the relative timing of courtship and copulation in our
432 experiments (Additional datafile 1: Figure S3). Data was manually entered into spreadsheets. We
433 annotated the beginning of male courtship as the start of at least three consecutive male courtship
434 behaviours according to Spieth (1952) [59], such as male touching the female abdomen with the

435 forelegs, wing vibration, male following the female, and male licking behavior (see above). We
436 estimated licking behavior throughout courtship of each male in trials where both males courted the
437 female simultaneously. This data was used to approximate male courtship vigor. We calculated the
438 sum duration of all licking events per male and trial and the number of licking sequences. However,
439 this behavior could not be quantified in 7 trials because the males changed positions very fast so
440 that they could not be unambiguously distinguished (Additional datafile 2, Additional datafile 4). In
441 all analysed trials, licking behaviour was observed throughout *D. pachea* courtship from shortly
442 after courtship start (Materials and Methods) to the start of copulation (Additional datafile 1: Figure
443 S3). Both males reached at least once the licking position in all trials (Additional datafile 1, Table
444 S3). This indicates that the female had physical contact with the proboscis of both males before
445 copulation started (Additional datafile 1: Figure S3).

446 The beginning of copulation was defined as the moment when the male mounted the female
447 abdomen. However, we only scored a copulation start if the male also settled into an invariant
448 copulation posture. Upon mounting, the male moves its abdomen tip forth and back along the
449 female oviscape. This behavior lasts for up to about 3 minutes and during this time the male grasps
450 the female wings and abdomen with its legs. This behavior was previously described as settling
451 period and ends with a characteristic right-sided, invariant copulation posture [41, 42, 44]. Any
452 copulation that ended within the first minutes after mounting without settling was considered to be a
453 “failed mounting attempt” (Additional datafile 4). The end of copulation was considered as the
454 moment when male and female genitalia were separated and the male had completely descended
455 with the forelegs from the female abdomen.

456 Copulation duration (Additional datafile 1, Table S3)) was comparable to previous analyses
457 of *D. pachea* copulation durations [41, 44, 47, 55]. We observed that copulation ended upon
458 isolation of the non-copulating male in 3 trials with females of stock 15090-1698.01 and in 4 trials
459 with females of stock 15090-1698.02, probably indicating premature copulation end due to

460 specimen handling . However, the estimates were included into the dataset and had little impact on
461 average copulation duration when comparing mean and median values.

462 **Mate-competition analysis**

463 Our aim was to compare at least 50 mate-competition trials, where both males courted the
464 female simultaneously and where copulation was observed. In total, we carried out 98 and 89 trials
465 with females of stocks 15090-1698.01 and 15090-1698.02, respectively (Additional datafile 1:
466 Table S2). We performed another 62 trials with males that underwent surgical manipulation of the
467 left lobe and females of stock 15090-1698.01 (Additional datafile 1: Table S2). In total, we removed
468 36 trials from the analysis because either copulation was not observed until 1 h after recording
469 started (21 trials), flies escaped, got injured or died inside the mating cell (4 trials) or the dissections
470 of male genitalia failed (11 trials, Additional datafile 1: Table S2). We thus examined 152 trials with
471 unmodified males and 61 trials with males that had undergone genital surgery, (see below,
472 Additional file 1: Table S2). Among those, we observed that both males courted the female
473 simultaneously in 111 and 54 trials, respectively. Statistical assessment with the Bradley Terry
474 Model (see below) further required a complete dataset so that we excluded 20 additional trials with
475 missing values, 19 trials with unmodified males (left lobe length: 2 trials, right lobe length: 2 trials,
476 licking behavior and/or failed mounting attempts: 7 trials, tibia length: 8 trials) and one trial with
477 lobe-modified males (no information on tibia length). In total, we considered 92 trials with
478 unmodified males and 53 trials with lobe-modified males.

479 Data analysis was performed in R version 3.6 [60]. Male copulation success (see above) was
480 evaluated with a Bradley Terry Model [48] using the R package BradleyTerry2 [61]. We
481 incorporated data (Additional datafile 2) into a list with three objects: 1) “contest” with the pairings
482 of males, a trial ID and a factor indicating trials with males that had modified left genital lobes, 2)
483 trial-specific variables “conditions” containing female age, female stock, courtship duration and a
484 factor indicating which male initiated courtship, 3) male-specific predictor variables

485 “male_predictors” with left and right genital lobe lengths, male tibia length, sum licking duration,
486 number of licking sequences and failed mounting attempts (Additional datafile 5). We developed
487 the statistical model (Additional datafile 1, Tables S5-11) by evaluating the effect of different
488 variables on copulation success and by comparing pairs of nested models, using Chi-square tests
489 with the generic anova() function [61].

490 We tested trial specific variables in interaction with all male-specific variables, but only
491 found an interaction of female age with failed mounting attempts in the dataset with unmodified
492 males (Additional datafile 1, Figure S5, Table S8, Table 1). We also tested for interactions between
493 male specific predictor variables but did not find any. The best fitting model for the dataset with
494 unmodified males was: copulation success ~ sum licking duration + number of licking sequences +
495 left_lobe length + failed mounting attempt x female age; and for the trials with lobe modified
496 males: copulation success ~ sum licking duration + number of licking sequences + left lobe length.
497 The male specific variables tibia length (body size approximation) and right lobe length were
498 excluded from the final model.

499 Spermathecae filling levels were evaluated with a linear model using the lm() function:
500 spermatheca filling level ~ left lobe length + right lobe length + sum licking duration + Number of
501 licking sequences + copulation duration + female age + male age, and significance of each variable
502 was evaluated with an F-test using anova().

503 **Declarations**

504 **Ethics approval and consent to participate**

505 “Not applicable” --- This research focuses on invertebrate insects. There are no ethical
506 considerations mentioned for these species according to EU Directive 86/609-STE123.

507 **Consent for publication**

508 "Not applicable"

509 **Availability of data and material**

510 The data sets supporting the results of this article are available in the DRYAD repository,
511 https://datadryad.org/stash/share/jzbHRT070QV55ejT_BxIcopEoG-wVDjRI_HpQK0ergY.

512 **Competing interests**

513 The authors declare no competing financial interests

514 **Funding**

515 This study was supported by the CNRS and by a grant of the European Research Council
516 under the European Community's Seventh Framework Program (FP7/2007-2013 Grant Agreement
517 no. 337579) given to VCO. BL was supported by a pre-doctoral fellowship Sorbonne Paris Cité of
518 the Université Paris 7 Denis Diderot and by a fellowship from the Labex "Who am I?" ("Initiatives
519 d'excellence", Idex ANR-18-IDEX-0001, ANR-11-LABX-0071).

520 **Authors' contributions**

521 ML and BL designed the experiments. BL and DC recorded fly copulation and performed
522 light microscopy analysis of *Drosophila* male genitalia. BL and ML analysed the data. ML, VCO
523 and BL wrote the manuscript. All authors have read and approved the manuscript.

524 **Acknowledgements**

525 We thank Therese A. Markow for discussions. We are very grateful to Alexandre Peluffo for
526 help with the statistical analysis, Claus Lang for technical support and Juliette Royer for dissections
527 of *D. pachea* male genitalia.

528 **References**

- 529 1. Bateman AJ. Intra-sexual selection in *Drosophila*. *Heredity*. 1948;2:349–68.
- 530 2. Fisher RA. *The Genetical Theory of Natural Selection*. Oxford: Clarendon Press. 272 p. 1930.
- 531 3. Lande R. Models of speciation by sexual selection on polygenic traits. *Proceedings of the*
532 *National Academy of Sciences*. 1981;78:3721–5. doi:10.1073/pnas.78.6.3721.
- 533 4. Bonduriansky R. The evolution of male mate choice in insects: a synthesis of ideas and evidence.
534 *Biological Reviews*. 2001;76:305–39. doi:10.1017/S1464793101005693.
- 535 5. Leonard J, Córdoba-Aguilar A. *The evolution of primary sexual characters in animals*. Oxford
536 University Press; 2010.
- 537 6. Edward DA, Chapman T. The evolution and significance of male mate choice. *Trends in Ecology*
538 *& Evolution*. 2011;26:647–54. doi:https://doi.org/10.1016/j.tree.2011.07.012.
- 539 7. Kokko H, Jennions MD. The Relationship between Sexual Selection and Sexual Conflict. *Cold*
540 *Spring Harbor Perspectives in Biology* . 2014;6. doi:10.1101/cshperspect.a017517.
- 541 8. Eberhard WG. *Sexual selection and animal genitalia*. Harvard University Press; 1985.
- 542 9. Birkhead TR, Pizzari T. Postcopulatory sexual selection. *Nat Rev Genet*. 2002;3.
543 doi:10.1038/nrg774.
- 544 10. Thornhill R. Cryptic Female Choice and Its Implications in the Scorpionfly *Harpobittacus*
545 *nigriceps*. *The American Naturalist*. 1983;122:765–88. doi:10.1086/284170.
- 546 11. Eberhard WG. Evolution of genitalia: theories, evidence, and new directions. *Genetica*.
547 2010;138:5–18. <http://www.springerlink.com/content/h37548365611773/export-citation/>.
- 548 12. Arnqvist G. Comparative evidence for the evolution of genitalia by sexual selection. *Nature*.
549 1998;393:784–6. doi:10.1038/31689.
- 550 13. Chapman T, Arnqvist G, Bangham J, Rowe L. Sexual conflict. *Trends Ecol Evol*. 2003;18:41–7.
551 doi:10.1016/S0169-5347(02)00004-6.
- 552 14. Eberhard WG. Copulatory Courtship and Cryptic Female Choice in Insects. *Biological Reviews*.
553 1991;66:1–31. doi:10.1111/j.1469-185X.1991.tb01133.x.
- 554 15. Eberhard WG. Evidence for widespread courtship during copulation in 131 species of insects
555 and spiders, and implications for cryptic female choice. *Evolution*. 1994;48:711–33.
556 doi:10.1111/j.1558-5646.1994.tb01356.x.
- 557 16. Ghiselin MT. The distinction between primary and secondary sexual characters. In: Leonard JL,
558 Córdoba-Aguilar A, editors. *The Evolution of Primary Sexual Characters in Animals*. New York:
559 Oxford University Press; 2010. p. 9–14.
- 560 17. Andersson M. Female choice selects for extreme tail length in a widowbird. *Nature*.
561 1982;299:818–20. doi:10.1038/299818a0.

- 562 18. von Schantz T, Göransson G, Andersson G, Fröberg I, Grahn M, Helgée A, et al. Female choice
563 selects for a viability-based male trait in pheasants. *Nature*. 1989;337:166–9.
564 doi:10.1038/337166a0.
- 565 19. Hill GE. Plumage coloration is a sexually selected indicator of male quality. *Nature*.
566 1991;350:337–9. doi:10.1038/350337a0.
- 567 20. Norris K. Heritable variation in a plumage indicator of viability in male great tits *Parus major*.
568 *Nature*. 1993;362:537–9. doi:10.1038/362537a0.
- 569 21. Petrie M. Improved growth and survival of offspring of peacocks with more elaborate trains.
570 *Nature*. 1994;371:598–9. doi:10.1038/371598a0.
- 571 22. Hasselquist D, Bensch S, von Schantz T. Correlation between male song repertoire, extra-pair
572 paternity and offspring survival in the great reed warbler. *Nature*. 1996;381:229–32.
573 doi:10.1038/381229a0.
- 574 23. Welch AM, Semlitsch RD, Gerhardt HC. Call Duration as an Indicator of Genetic Quality in
575 Male Gray Tree Frogs. *Science*. 1998;280:1928 LP – 1930. doi:10.1126/science.280.5371.1928.
- 576 24. Birch M. Pre-courtship use of abdominal brushes by the nocturnal moth, *Phlogophora*
577 *meticulosa* (L.) (Lepidoptera: Noctuidae). *Animal Behaviour*. 1970;18:310–6.
578 doi:https://doi.org/10.1016/S0003-3472(70)80043-4.
- 579 25. Sreng L. Cockroach mating behaviors, sex pheromones, and abdominal glands (Dictyoptera:
580 Blaberidae). *Journal of Insect Behavior*. 1993;6:715–35. doi:10.1007/BF01201672.
- 581 26. Polak M, Rashed A. Microscale laser surgery reveals adaptive function of male intromittent
582 genitalia. *Proc R Soc B*. 2010;277. doi:10.1098/rspb.2009.1720.
- 583 27. Grieshop K, Polak M. The precopulatory function of male genital spines in *Drosophila*
584 *ananassae* [Doleschall] (Diptera: Drosophilidae) revealed by laser surgery. *Evolution*. 2012;66.
585 doi:10.1111/j.1558-5646.2012.01638.x.
- 586 28. Bertin A, Fairbairn DJ. One tool, many uses: precopulatory sexual selection on genital
587 morphology in *Aquarius remigis*. *Journal of Evolutionary Biology*. 2005;18:949–61.
588 doi:10.1111/j.1420-9101.2005.00913.x.
- 589 29. Ploog DW, MacLean PD. Display of penile erection in squirrel monkey (*Saimiri sciureus*).
590 *Animal Behaviour*. 1963;11:32–9. doi:https://doi.org/10.1016/0003-3472(63)90005-8.
- 591 30. Wickler W. Ursprung und biologische Deutung des Genitalpräsentierens männlicher Primaten.
592 *Zeitschrift für Tierpsychologie*. 1966;23:422–37. doi:10.1111/j.1439-0310.1966.tb01605.x.
- 593 31. Miller EH. Genitalic traits of mammals. In: Leonard J, Córdoba-Aguilar A, editors. *The*
594 *evolution of primary sexual characters in animals*. New York: Oxford University Press; 2010. p.
595 471–93.
- 596 32. Bohme W. The Tucano Indians of Colombia and the Iguanid Lizard *Plica plica*: Ethnological,
597 Herpetological and Ethological Implications. *Biotropica*. 1983;15:148–50. doi:10.2307/2387961.

- 598 33. Mautz BS, Wong BBM, Peters RA, Jennions MD. Penis size interacts with body shape and
599 height to influence male attractiveness. *Proceedings of the National Academy of Sciences*.
600 2013;110:6925–30. doi:10.1073/pnas.1219361110.
- 601 34. Estes RD. The significance of horns and other male secondary sexual characters in female
602 bovids. *Applied Animal Behaviour Science*. 1991;29:403–51. doi:https://doi.org/10.1016/0168-
603 1591(91)90264-X.
- 604 35. Muller MN, Wrangham R. Sexual Mimicry in Hyenas. *The Quarterly Review of Biology*.
605 2002;77:3–16. doi:10.1086/339199.
- 606 36. Kahn AT, Mautz B, Jennions MD. Females prefer to associate with males with longer
607 intromittent organs in mosquitofish. *Biology Letters*. 2010;6:55–8. doi:10.1098/rsbl.2009.0637.
- 608 37. Langerhans RB, Layman CA, DeWitt TJ. Male genital size reflects a tradeoff between attracting
609 mates and avoiding predators in two live-bearing fish species. *Proceedings of the National Academy*
610 *of Sciences*. 2005;102:7618–23. doi:10.1073/pnas.0500935102.
- 611 38. Moreno-García M, Cordero C. On the function of male genital claspers in *Stenomacra*
612 *marginella* (Heteroptera: Largidae). *Journal of Ethology*. 2008;26:255–60. doi:10.1007/s10164-007-
613 0058-8.
- 614 39. Michiels NK. Mating Conflicts and Sperm Competition in Simultaneous. In: Birkhead TR,
615 Møller AP, editors. *Sperm competition and sexual selection*. New York: Academic Press; 1998. p.
616 219–254.
- 617 40. Pitnick S, Heed W. New Species of Cactus-Breeding *Drosophila* (Diptera: Drosophilidae) in the
618 *Nannoptera* Species Group. *Annals of the Entomological Society of America*. 1994;87:307–10.
619 <http://www.nature.com/nature/journal/v440/n7085/full/nature04623.html>.
- 620 41. Lang M, Orgogozo V. Distinct copulation positions in *Drosophila pachea* males with symmetric
621 or asymmetric: External genitalia. *Contributions to Zoology*. 2012;81:87–94.
- 622 42. Acurio A, Rhebergen FT, Paulus SE, Courtier-Orgogozo V, Lang M. Repeated evolution of
623 asymmetric genitalia and right-sided mating behavior in the *Drosophila nannoptera* species group.
624 *BMC Evolutionary Biology*. 2019;19:109. doi:10.1186/s12862-019-1434-z.
- 625 43. Lang M, Polihronakis Richmond M, Acurio AE, Markow TA, Orgogozo V. Radiation of the
626 *Drosophila nannoptera* species group in Mexico. *Journal of Evolutionary Biology*. 2014;27:575–84.
627 doi:10.1111/jeb.12325.
- 628 44. Rhebergen FT, Courtier-Orgogozo V, Dumont J, Schilthuizen M, Lang M. *Drosophila pachea*
629 asymmetric lobes are part of a grasping device and stabilize one-sided mating. *BMC Evolutionary*
630 *Biology*. 2016;16:176. doi:10.1186/s12862-016-0747-4.
- 631 45. Pitnick S, Markow TA, Spicer GS. Delayed male maturity is a cost of producing large sperm in
632 *Drosophila*. *Proceedings of the National Academy of Sciences*. 1995;92:10614–8.
633 <http://www.pnas.org/content/92/23/10614.abstract>.

- 634 46. Pitnick S, Markow T, Spicer GS. Evolution of Multiple Kinds of Female Sperm-Storage Organs
635 in *Drosophila*. *Evolution*. 1999;53:1804–22. doi:10.2307/2640442.
- 636 47. Pitnick S, Markow TA. Male gametic strategies: sperm size, testes size, and the allocation of
637 ejaculate among successive mates by the sperm-limited fly *Drosophila pachea* and its relatives. *The*
638 *American Naturalist*. 1994;143:785–819.
- 639 48. Bradley RA, Terry ME. Rank Analysis of Incomplete Block Designs: I. The Method of Paired
640 Comparisons. *Biometrika*. 1952;39 3/4:324–45. doi:10.2307/2334029.
- 641 49. Pitnick S. Operational sex ratios and sperm limitation in populations of *Drosophila pachea*.
642 *Behavioral Ecology and Sociobiology*. 1993;33:383–91.
- 643 50. Byers J, Hebets E, Podos J. Female mate choice based upon male motor performance. *Animal*
644 *Behaviour*. 2010;79:771–8. doi:https://doi.org/10.1016/j.anbehav.2010.01.009.
- 645 51. Kirkpatrick M, Ryan MJ. The evolution of mating preferences and the paradox of the lek.
646 *Nature*. 1991;350:33–8. doi:10.1038/350033a0.
- 647 52. Grieshop K, Polak M. Evaluating the post-copulatory sexual selection hypothesis for genital
648 evolution reveals evidence for pleiotropic harm exerted by the male genital spines of *Drosophila*
649 *ananassae*. *J Evol Biol*. 2014;27. doi:10.1111/jeb.12524.
- 650 53. Hoikkala A, Aspi J, Suvanto L. Male courtship song frequency as an indicator of male genetic
651 quality in an insect species, *Drosophila montana*. *Proceedings of the Royal Society of London*
652 *Series B: Biological Sciences*. 1998;265:503–8. doi:10.1098/rspb.1998.0323.
- 653 54. Pitnick SS. Sexual selection and sperm production in *Drosophila*. Thesis (Ph. D.)--Arizona State
654 University, 1992. ; 1992.
- 655 55. Jefferson M. Breeding biology of *Drosophila pachea* and its relatives. 1977.
- 656 56. Heed WB, Kircher HW. Unique Sterol in the Ecology and Nutrition of *Drosophila pachea*.
657 *Science*. 1965;149:758–61. doi:10.1126/science.149.3685.758.
- 658 57. Lang M, Murat S, Clark AG, Gouppil G, Blais C, Matzkin LM, et al. Mutations in the neverland
659 gene turned *Drosophila pachea* into an obligate specialist species. *Science*. 2012;337:1658–61.
- 660 58. Warren JT, Wismar J, Subrahmanyam B, Gilbert LI. Woc (without children) gene control of
661 ecdysone biosynthesis in *Drosophila melanogaster*. *Molecular and cellular endocrinology*.
662 2001;181:1–14.
- 663 59. Spieth HT. Mating behavior within the genus *Drosophila* (Diptera). *Bull Am Museum Nat Hist*.
664 1952;99.
- 665 60. R Core Team. R: A language and environment for statistical computing. R Foundation for
666 Statistical Computing, Vienna, Austria. 2013. 2014.
- 667 61. Turner H, Firth D. Bradley-Terry Models in R: The BradleyTerry2 Package. *Journal of*
668 *Statistical Software, Articles*. 2012;48:1–21. doi:10.18637/jss.v048.i09.

669 **Supporting Information**

670 **Additional datafile 1:** Supplementary Figures and Tables, **Figure S1:** Camera device for movie
671 recording, **Figure S2:** Pairwise lobe length differences of males used in the competition mating
672 experiment, **Figure S3:** Courtship and copulation duration in competition mating experiments
673 **Figure S4:** Courtship duration increases with female age, **Figure S5:** Failed copulation attempts
674 compared to female age, **Table S1:** *Drosophila pachea* resources, **Table S2:** Competition mating
675 trials used for courtship analysis, **Table S3:** Courtship duration, licking index and copulation
676 duration in trials where both males courted the female, **Table S4:** Genital lobe lengths in *D. pachea*
677 stocks.

678 **Additional datafile 2:** Measurements of mating behaviour, genital lobe lengths and spermathecae
679 filling levels of individuals used in the competition mating experiments.

680 **Additional datafile 3:** Raw measurements of lobe lengths in different *D. pachea* stocks

681 **Additional datafile 4:** Dataset for male licking behavior and male mounting.

682 **Additional datafile 5:** R list object “PacData”, dataset for Bradley-Terry model fit

683 **Tables**

684 **Table 1: Bradley–Terry (BT) model examining the effects of left lobe length, sum licking**
685 **duration, number of licking sequences and failed mounting attempts on copulation success,** in
686 92 trials with non-lobe modified males. The main effect for “female age” cannot be estimated in the BT
687 model because it is specific to each trial and not to each male. Bolded estimates are significant.

variable	estimate	std. error	z value	P (> z)
sum licking duration	1.224514	0.334856	3.657	0.0003
number of licking sequences	-0.259216	0.127859	-2.027	0.0426
left lobe	0.007471	0.003582	2.086	0.0370
failed mounting attempts	-4.493660	1.834694	-2.449	0.0143
female age	NA	NA	NA	NA
failed mounting attempts x female age	0.295355	0.119397	2.474	0.01337

688 **Table 2: Bradley–Terry (BT) model examining the effects of left lobe length, sum licking**
 689 **duration, and number of licking sequences on copulation success**, in 53 trials with males that had
 690 surgically modified left genital lobes. Bolded estimates are significant.

variable	estimate	std. error	z value	P (> z)
sum licking duration	0.561757	0.256917	2.187	0.0288
number of licking sequences	-0.176035	0.090341	-1.949	0.0513
left lobe	0.009199	0.005090	1.807	0.0707

691 **Table 3: Linear model, examining the effects of lobe length, sum licking duration, copulation**
 692 **duration and age on spermathecae filling levels**. degrees of freedom: numerator / denominator 38

variable	F value	P
sum licking duration	1.6841	0.2022
number of licking sequences	0.1107	0.7411
left lobe length	0.1139	0.7377
right lobe length	1.4739	0.2322
copulation duration	10.94	0.0021
female age	0.5036	0.4822
male age	22.828	0.00003

693 **Figure Legends**

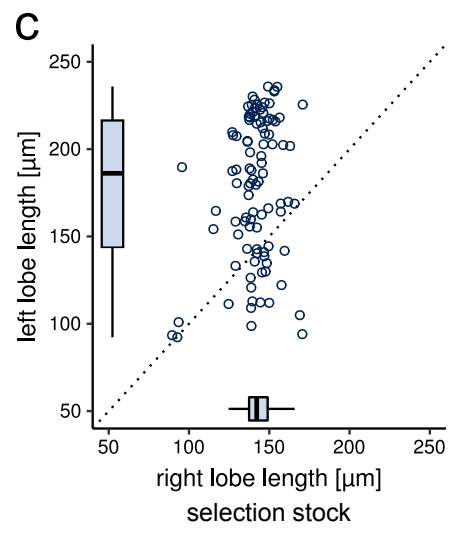
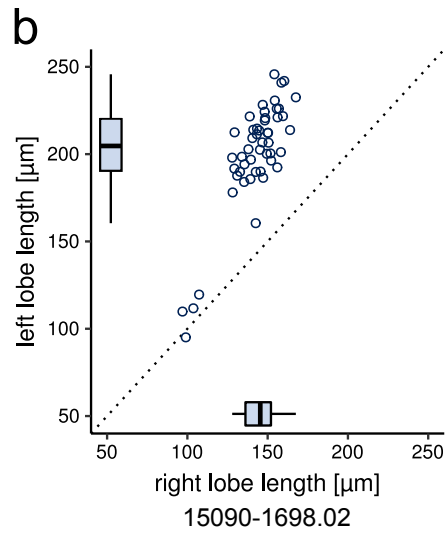
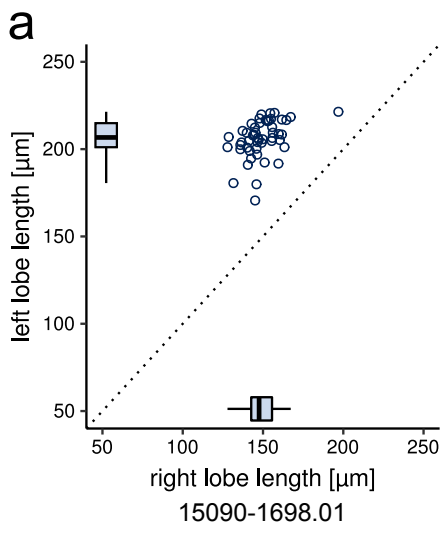
694 **Figure 1: *Drosophila pachea* male genital lobes.** (a) Male of stock 15090-1698.02 in ventral view
 695 and with asymmetric lobes. (b) Male of the selection stock with apparently symmetric lobes. The
 696 scale bars correspond to 200 μ m. (c) Posterior view of a dissected male terminalia of stock 15090-
 697 1698.02 with asymmetric lobes. (d) Posterior view of a dissected male terminalia of the selection
 698 stock; the scale bars correspond to 100 μ m, dots indicate lobe length measurement points.

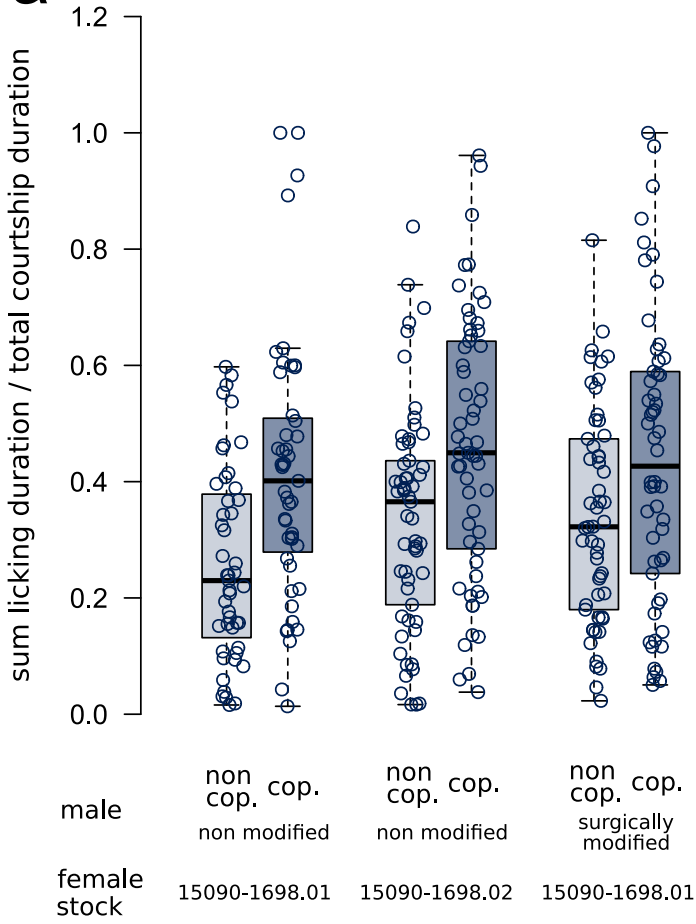
699 **Figure 2: Genital lobe lengths differ between *D. pachea* stocks.** Lengths of the left and right
 700 epandrial lobe lobes are presented for (a) stock 15090-1698.01, (b) stock 15090-1698.02, and (c)
 701 the selection stock. Sibling males of those used in the mating experiment are shown in panel (c).
 702 Each point represents one male. The variance of left lobe length is increased in the selection stock

703 compared to the source stock 15090-1698.02 (Levene's test: selection stock / 15090-1698.02: DF =
704 1/147, F = 11.506, P = 0.0009), while the variance of the right lobe length were not significantly
705 different (Levene's test, DF = 1/147, F = 0.5164, P = 0.4735).

706 **Figure 3: Courtship durations and relative courtship activity.** (a) The ratio of sum licking
707 duration and total courtship duration in each trial shows that the copulating male (cop, grey box-
708 plots) had a higher average sum licking duration compared to the non-copulating male (non-cop,
709 white box-plots). Each point represents one male. (b) The total courtship duration was shorter in
710 trials with only one male displaying courtship signs (one, white box-plots) compared to trials with
711 both males courting simultaneously (both, grey box-plots) (Mann-Whitney-Wilcoxon test, female
712 stock 15090-1698.01, non modified males, W = 385, N = 25/51, P = 0.0053 ; females of stock
713 15090-1698.02, W = 219, N = 16/60, P = 0.0009 ; females stock 15090-1698.01, modified males, W
714 = 62.5, N = 7/54, P = 0.0044). Horizontal bars indicate pairwise comparisons with P-values ** <
715 0.01 or *** < 0.001. Each point represents one mating experiment.





a**b**